Polygenic architecture of growth rate in *Arabidopsis thaliana*

Inaugural-Dissertation

Zur Erlangung des Doktorgrades der Mathematisch-Naturwissenschaftlichen Fakultät der Universität zu Köln

Vorgelegt von

Benedict Wieters

aus Erkelenz, Deutschland

Köln, 2021

Publications

Benedict Wieters, Kim A. Steige, Fei He, Evan M. Koch, Sebastián E. Ramos-Onsins, Hongya Gu, Ya-Long Guo, Shamil Sunyaev, Juliette de Meaux (2021). Polygenic adaptation of rosette growth variation in *Arabidopsis thaliana* populations. PLoS Genetics

Margarita Takou, **Benedict Wieters**, Stanislav Kopriva, George Coupland, Anja Linstädter, Juliette de Meaux (2019). Linking genes with ecological strategies in *Arabidopsis thaliana.* Journal of Experimental Botany 70 (4), 1141-1151

Berichterstatter: Prof. Dr. Juliette de Meaux

Gutachter: Prof. Dr. Tobias Bollenbach

Tag der Disputation: 02.06.2021

Abstract

Understanding the molecular mechanisms that have enabled phenotypic diversification in response to natural selection is one of the greatest challenges in modern biology. Complex traits with a polygenic basis such as growth rate are important for plant performance under natural conditions. However, determining the molecular basis of adaptation in these traits is challenging due to the small effect sizes expected and the population structure between genotypes. My work aimed to characterize the genetic basis of complex phenotypes with a polygenic basis in the model species *Arabidopsis thaliana*.

First, I examined signatures of local growth adaptation in geographically distant populations. Therefore, I measured rosette growth in artificial mimicking latitudinal differences as well as in natural field conditions imposing different levels of competition, for a set of genotypes representative of four major regional populations, including the long separated population of China. Rosette size at the end of the growth phase proved to be the most strongly heritable component of growth rate. All genotypes significantly increased their rosette diameter when light levels were reduced, indicating that environmental plasticity is a predominant source of variation for adjusting plant size to prevailing light conditions. Phenotypic divergence between regional populations indicate that growth rate evolution is generally constrained by stabilizing selection

To understand the genetic basis underlying differences in growth rate, I conducted genome-wide association studies (GWAS). Few loci associated with genetic variation for growth above the Bonferroni confidence level. However, marginally associated variants were significantly enriched among genes with annotated roles in growth and stress responses. Polygenic scores calculated from marginally associated variants confirmed the polygenic basis of growth variation. A meta-analysis of GWAS signals across environmental conditions confirmed the relevance of sub-significant associations. By associating loss-of-function alleles with growth dynamics, I identified and validated that genes related to chloroplast maturation modulate growth under limiting light conditions. To overcome limitations imposed by functional classification in Gene Ontology (GO), I sought to identify genes specifically associated with

growth modifications in response to light or competition, by quantifying differences in gene expression between wild-type plants and mutants in key light signaling genes. The group of genes I identified using this approach showed overlapped significantly with genes whose variants associate with growth variation in the natural population.

Since associations in GWAS can be confounded by population structure, I characterized the genetics of gene expression divergence between regions by quantifying allele-specific expression (ASE) differences within inter-regional F1 hybrids. To do this, I generated inter-population hybrids between genotypes from 4 different regions (Morocco, Sweden, Spain, China). Comparison with differential parental gene expression (*trans*) showed a significant correlation between *cis* and *trans*, indicating that these genetic variants contribute significantly to expression divergence. We used quantitative models to determine the phylogeographic origin of these regulatory variants and document marked inter-regional differences in their functional distribution.

Overall, this work illustrates that the genetic basis of growth adaptation is complex and polygenic. By combining information from a reductionist approach (using mutants), a quantitative genetic approach (using GWAS), and a transcriptomic approach (identifying patterns of ASE evolution), I reveal the molecular targets of natural selection. The overlap between signatures of polygenic selection on *cis*-regulatory variation, the study of phenotypic variation using GWAS, and the experimental identification of regulatory changes associated with growth alterations collectively support the notion that functions related to light perception, hormones, defense/stress, and growth regulation are involved in the local adaptation of plant growth. My work highlights the complex signatures of polygenic adaptation in *A. thaliana*, and pioneers novel innovative approach to overcome the experimental limitations caused by complex genetic architecture, confounding effects of population structure, and detection bias of genetic variants.

Zusammenfassung

Molekularen Mechanismen, die die phänotypische Anpassung als Reaktion auf die natürliche Selektion ermöglicht haben zu verstehen ist eine der größten Herausforderungen der modernen Biologie. Komplexe Phänotypen mit einer polygenen Basis wie die Wachstumsrate sind wichtig für das Überleben von Pflanzen unter natürlichen Bedingungen. Geringe Effekte einzelner Loci und Populationsstruktur machen die Bestimmung der molekularen Basis jedoch herausfordernd. Ziel meiner Arbeit war es, die genetische Basis komplexer Phänotypen mit polygener Basis in der Modellart *Arabidopsis thaliana* zu charakterisieren.

Zunächst untersuchte ich lokale Anpassungen im Wachstum geographisch getrennter Populationen. Dazu habe ich das Wachstum von Rosetten unter künstlichen, sowie natürlichen Bedingungen für eine Reihe von Genotypen gemessen, die repräsentativ für vier große regionale Populationen sind, einschließlich der weit entfernten chinesischen Population. Die finale Größe erwies sich als die am stärksten erbliche Komponente der Wachstumsrate. Alle Genotypen vergrößerten ihren Durchmesser unter reduzierten Lichtverhältnissen signifikant, weswegen ein Großteil der Variation in Pflanzengröße eine Reaktion auf die bestehenden Lichtverhältnisse zu sein scheint. Begrenzte phänotypische Unterschiede zwischen regionalen Populationen deuten darauf hin, dass die Evolution der Wachstumsrate im Allgemeinen durch stabilisierende Selektion eingeschränkt wird.

Um die zugrunde liegende genetische Basis zu verstehen, habe ich Genom-weite Assoziationsstudien (GWAS) durchgeführt. Nur wenige Loci assoziierten mit genetischer Variation für Wachstum oberhalb des Bonferroni-Konfidenzniveaus. Allerdings waren Gene mit annotierten Funktionen im Wachstum und Stressreaktionen signifikant unter marginal assoziierten Varianten angereichert. Daraus berechnete „polygenic scores“ bestätigten die polygene Basis der Wachstumsvariation. Eine Meta-Analyse der GWAS-Signale über Umweltbedingungen hinweg bestätigte die Relevanz der marginal assoziierten Loci. Durch die Assoziation von nicht funktionalen Allelen mit der Wachstumsdynamik konnte ermittelt werden, dass Gene, die mit der Reifung von Chloroplasten zusammenhängen, das Wachstum unter limitierenden Lichtbedingungen modulieren. Ich habe versucht Gene zu

identifizieren, die spezifisch mit Anpassungen des Wachstums an Licht oder Konkurrenz assoziiert sind, um Einschränkungen, die durch funktionale Klassifikation in der „Gene Ontology“ (GO) auferlegt werden zu überwinden. Dafür habe ich die Unterschiede in der Genexpression zwischen Wildtyp-Pflanzen und Mutanten in wichtigen Lichtsignalgenen quantifiziert. Die so identifizierten Gene enthielten signifikant viele Gene, die mit Variationen im Wachstum der natürlichen Populationen assoziiert sind.

Da GWAS durch die Populationsstruktur beeinträchtigt werden können, analysierte ich Gen-Expressions-Unterschiede zwischen den Regionen durch Quantifizierung der allel-spezifischen Expression (ASE) in F1-Hybriden (*cis*). Dazu kreuzte ich Genotypen aus vier verschiedenen Regionen (Marokko, Schweden, Spanien, China). Eine signifikante Korrelation zwischen *cis* und der unterschiedlichen Genexpression der Eltern (*trans)*, deutet darauf hin, dass diese genetischen Varianten signifikant zu Expressionsunterschieden beitragen. Mit quantitativen Modellen, bestimmten wir den geographischen Ursprung dieser regulatorischen Varianten und dokumentierten deutliche funktionelle Unterschiede.

Insgesamt veranschaulicht diese Arbeit die komplexe und polygene genetische Basis von Wachstumsanpassungen. Die Kombination von Informationen aus einem reduktionistischen (unter Verwendung von Mutanten), einem quantitativ-genetischen (unter Verwendung von GWAS) und einem transkriptomischen Ansatz (Identifizierung von Mustern der ASE-Evolution) zeigt molekulare Ziele der natürlichen Selektion auf. Aufgrund von Überschneidungen zwischen *cis*-regulatorischen Signaturen, phänotypischer Variation und regulatorischen Veränderungen, die mit Anpassungen im Wachstum verbunden sind, können Funktionen, die mit Lichtwahrnehmung, Pflanzenhormonen, Abwehr/Stress-Reaktion und Wachstumsregulation zusammenhängen als Regulatoren der lokalen Anpassung des Pflanzenwachstums identifiziert werden.

Meine Arbeit hebt die komplexen Signaturen der polygenen Anpassung in *A. thaliana* hervor und ist ein innovativer Ansatz, um die experimentellen Einschränkungen die durch die komplexe genetische Architektur, störende Effekte der Populationsstruktur und den Nachweis von genetischen Varianten verursacht werden zu überwinden.

Table of Contents

Table of Figures

Index of Tables

Author’s Contribution

This thesis includes several experiments investigating the basis of growth rate adaptation in *Arabidopsis thaliana*. Most of the experiments were collaborative projects, an overview of the contributors is presented in Table 1.

Table 1: Contributions for the experiments presented in this thesis.

The initials mark contributors for the different projects and phases within the project that are presented in this thesis.

Experiment	Study Design	Data collection	Data analysis	Manuscript preparation
Growth rate in HL and LL	**BW**, JdM	**BW**	**BW**, EK, FH, JdM	**BW**, JdM, SR, SY
Mutant verification	**BW**, FG, GS, JdM	FG	**BW**, FG	**BW,** FG
Competition experiments	**BW**, GC, GS, JdM, JE, KS, SM	JE, SM, GC, KS	**BW**	**BW**
RNA-sequencing of light-signalling mutants	**BW**, JdM, KK, UH	KK	**BW**, FH	**BW**, JdM
ASE in F1-hybrids	**BW**, JdM, MT	**BW**, KB	**BW**, FH, JdM, MT	**BW**, JdM, MT

Benedict Wieters (BW), Evan Koch (EK), Franziska Geuchen (FG), Fei He (FH), Gero Carus (GC), Gregor Schmitz (GS), Jennifer Escher (JE), Juliette de Meaux (JdM), Kirsten Bell (KB), Konstantin Kerner (KK), Kim A. Steige (KS), Margarita Takou (MT), Simon Mitreiter (SM), Sebastian Ramos-Onsins (SR), Shamil Sunyaev (SY)

Abbreviations

AIC	Akaike information criterion
ASE	Allele-specific expression
BM	Biomass
CAPS	Cleaved Amplified Polymorphic Sequences
CD	Competition plants sampled during the day
CE	Central Europe
CH	China
CN	Competition plants sampled at night
COP1	CONSTITUTIVE PHOTOMORPHOGENIC 1
D	Diameter in December in the 1st field experiment
df	Degrees of freedom
FDR	False discovery rate
FS	Final Size
Fst	Fixation index
FT	Flowering Time
glm	Generalized linear model
GO	Gene Ontology
GxE	Genome x Environment interaction
GWAS	Genome-wide association study
H	Final Plant Height
H^2	Broad-sense heritability
HD	High density condition
HL	High light condition

HLN	High light plants sampled at night
ID	Intermediate density condition
LD	Low density condition
LL	Low light condition
LLN	Low light plants sampled at night
LOF	Loss-of-function
MAF	Minor allele frequency
NE	Northern Europe
PCA	Principal component analysis
PCR	Polymerase chain reaction
PhyB	phytochrome B
QTL	Quantitative Trait Locus
R: FR	Red: Far Red Light Ratio
SAS	Shade avoidance syndrome
SL	Slope
SNP	Single Nucleotide Polymorphism
SP	Spain
SPA	SUPRESSOR OF PHYA
spa1234	SPA1-SPA4 quadruple mutant
WE	Western Europe
WT	Wild Type

1 Introduction

Understanding the molecular mechanisms that allowed phenotypic diversification in response to natural selection is one of the major challenges of modern biology (Thornton *et al.*, 2007; Barrett & Hoekstra, 2011). The link between fitness, phenotypes and their underpinning genes needs to be elucidated. To this end, my work aimed at characterizing the genetic basis of complex phenotypes with a polygenic basis.

1.1 Polygenic basis of adaptation

Alleles of various effect sizes contribute to adaptation

The alleles that contribute to the local adaptation of plant performance can have effect sizes ranging from large effect alleles, which visibly impact adaptive phenotypes down to alleles of infinitesimal effects that cannot be identified individually. When adapting to a new fitness optimum, the initial adaptive steps are often achieved by the quick fixation of few mutations of large effect (Orr, 2002). Mutations that are quickly fixed by selection tend to leave a distinctive signature by creating regions of low nucleotide variation (i.e. a selective sweep). These rare large-effect alleles are likely to contribute to rapid changes to a distant new optimum, but they are less useful when adapting to subtle shifts of optima (Barghi et al. 2020). In addition, if selection proceeded only by the fast fixation of large effect mutations, adaptive variation would be rapidly exhausted and populations would stop responding to selection after a few generations. Many studies, however, show that this is not the case: there is hardly any limit to the supply in adaptive mutations (Barton & Keightley, 2002). Even for distant fitness optima there are often mixtures of large shifts via selective sweeps, followed by polygenic adaptation to create small adjustments towards the trait optimum (Csilléry *et al.*, 2018; Stetter *et al.*, 2018). For traits with a veritably polygenic architecture, it has even been argued that virtually all expressed genes can be relevant to observed phenotypes, because of high biological complexity and inter-connectivity of gene expression networks (Boyle *et al.*, 2017; Wray *et al.*, 2018; de Miguel *et al.*, 2020).

In this context, I asked the following question: can we understand the molecular basis of polygenic adaptation.

Detection of signatures of polygenic adaptation

Evolutionary adaptation after an environmental change can lead to rapid adaptation via frequency shifts at many potentially causal variants (Pritchard & Di Rienzo, 2010). For polygenic traits with large numbers of loci, selection is modest and manifests as frequency shifts across many loci with alleles shifting in the same direction (Berg & Coop, 2014). Genome-wide association studies (GWAS) can help identifying many loci that are associated with variation in a given trait and estimating allelic effects at these loci (Korte & Farlow, 2013; Berg & Coop, 2014). One problem of association mapping is, that the discovered SNPs only explain a fraction of the heritability ("missing heritability"), because many SNPs with small effects are not detected (Manolio *et al.*, 2009; Barghi *et al.*, 2020).

Signals of allele frequency changes and effect size knowledge from GWAS can be combined to identify traits with a polygenic adaptation signature when comparing to an empirical null model based on neutral sites (Berg & Coop, 2014). Common single-nucleotide polymorphisms (SNPs) with effect sizes well below genome-wide statistical significance can account for most of the ‘‘missing heritability’’ of many traits (Yang *et al.*, 2010; Shi *et al.*, 2016).

Population structure is major caveat in the detection of associations

In practice, the detection of polygenicity via subtle signals aggregated over many loci identified in GWAS results is extremely sensitive to systematic biases introduced by population structure (Berg *et al.*, 2019; Sohail *et al.*, 2019). Especially comparisons across traits and study populations require careful correction of population structure (Novembre & Barton, 2018). Common SNPs with signatures of selection on fitness tend to affect other traits as well, without necessarily having anything to do with the trait itself (ascertainment bias) (Novembre & Barton, 2018). Another caveat for genome scans is the multiple testing correction, which further reduces the sensitivity, making the detection of signatures of polygenic adaptation quite challenging (Barghi *et al.*, 2020).

In the study of traits in humans, GWAS is the most widely used tool to discover genetic associations, especially since experiments are harder to conduct with humans (Visscher *et al.*, 2017). The study of polygenic adaptation in plant systems is one potential way to deal with several of the issues, since common garden experiments with clonal individuals are a big advantage when studying plants compared to humans. For example, polygenic adaptation scans developed in humans were applied to inbred maize populations with an incorporation of relatedness to better account for confounding effects due to population structure (Josephs *et al.*, 2019). In maritime pine, a variable degree of polygenicity was identified for five fitness-related traits, including growth rate (de Miguel *et al.*, 2020). Provided population structure is correctly taken into account, it should thus be possible to use signatures for polygenic adaptation of growth to identify its molecular basis.

1.2 Plant growth rate is a complex trait with relevance for fitness

Growth is a complex trait

The growth rate of a plant is a crucial component of individual fitness, as it reflects the resource acquisition and conditions reproductive output (Mitchell-Olds, 1996; Wilson *et al.*, 2007). Several examples of genetic variation of plant growth rate in *A. thaliana* have been documented with a diverse genomic basis (Bac-Molenaar *et al.*, 2015; Vasseur *et al.*, 2018; Hanemian *et al.*, 2019). Despite its complex architecture, plant growth rate can be severely influenced by single genes, as demonstrated for dwarfism in alpine populations (González & Inzé, 2015; Luo *et al.*, 2015a). Still, most growth-related traits are characterized by a polygenic architecture with many underlying variants (Mckown *et al.*, 2014; Sohail *et al.*, 2019; de Miguel *et al.*, 2020). Growth rate can quantify the resource acquisition of different genotypes across environments making it an important indicator of plant performance.

Growth is important for fitness

The vegetative growth phase of a plant is important for fitness, since it is the life history trait that is expressed between germination and flowering and, hence, seed dispersal (Debieu *et*

al., 2013). Although life history traits are more directly linked to fitness, they are strongly dependent on external cues like photoperiod and temperature (Koornneef *et al.*, 2004; Takou *et al.*, 2019). Nonetheless, growth rate is also highly impacted by internal and external cues and relies on functions at different levels of plant organization (Hanemian *et al.*, 2019). Genes related to pathogen resistance are involved in the modulation of trade-offs between resistance and growth (Todesco *et al.*, 2010; Vetter *et al.*, 2012). Trade-offs are also introduced by physiological costs, which constrain the allocation between growth and defense traits (Davila Olivas *et al.*, 2017; Züst & Agrawal, 2017). Still, the growth rate can be measured in a wide variety of environments, even if there are cues missing that are crucial for life history traits.

The growth response to the environment is plastic

All plants can adjust their growth rate plastically. Plasticity describes the immediate adjustment of the phenotype to respond to environmental differences (Chevin & Lande, 2010). In drought conditions or at lower temperatures plant growth can be slower as a consequence of resource limitations (Körner, 2015; Bac-Molenaar *et al.*, 2016). In the Brassicaceae *Boechera stricta,* conditions with warm temperatures increase above and below-ground biomass and result in a higher growth allocation to roots (Salmela *et al.*, 2016). Under light limitation plant rosettes grow to larger diameters to maximize light uptake (Hornitschek *et al.*, 2012; Ballaré & Pierik, 2017). These responses can actively contribute to maintain fitness under challenging conditions, without having to evolve genetically fixed adaptations (Pigliucci, 2005).

Growth mediates the response to light quality

The shade-avoidance syndrome (SAS) is a well described plastic response to limited light conditions, that is characterized by a redirection of the development towards internode extension, resulting in longer leaves that might escape the shade (Smith, 1982). The distance and size of neighboring plants determine the extent of light limitation and the light input for photosynthesis. Shade is perceived by the reduced light quantity, but also by the Red: Far Red light ratio (R: FR) and can also result in several phenotypic adjustments, among them petiole elongation, upward leaf movement, altered leaf size and structure, inhibition of

branching, acceleration of flowering and differences in photosynthetic and respiratory metabolism (Smith, 1982; Ballaré & Pierik, 2017).

The R to FR part of the spectrum can be perceived by phytochromes, which mediate many light-regulated processes, such as seed germination and the shade-avoidance response (Chen *et al.*, 2004). Phytochrome B (PhyB) is part of an interconnected network controlling growth in response to light and temperature, where one branch involves CONSTITUTIVE PHOTOMORPHOGENIC 1 (COP1) and SUPPRESSOR OF PHYA-105 1 (SPA1), SPA2, SPA3 and/or SPA4 which interact with COP1 and enhance its activity (Legris *et al.*, 2017). COP1 is a RING E3 ligase targeting a number of proteins involved in the growth response to light (photomorphogenesis) for degradation, which is needed to inhibit hypocotyl growth (Osterlund *et al.*, 2000). *Cop1* and *spa1/spa3/spa4* mutants show reduced hypocotyl growth in the dark (Deng *et al.*, 1992; Laubinger & Hoecker, 2003) and a significantly impaired SAS (Rolauffs *et al.*, 2012).

Overall, the light perception via phyB can promote morphological and anatomical changes that increase plant fitness (Casal & Mazzella, 1998). Activated phyB under sunlight conditions can promote the formation of thicker and mechanically more resistant stems with improved water conductivity compared with plants under shade (Ballaré & Pierik, 2017). Limited light (low R: FR ratio) can down-regulate defense responses in shade-intolerant species and lead to increased susceptibility to insect herbivores and microbial pathogens of various lifestyles (Ballaré, 2014; Ballaré & Pierik, 2017). Foraging for light through the growth response is often prioritized over plant immune responses when shading and pathogens occur together (Ballaré, 2014). Therefore, the present light regime can seriously impact plant fitness and the response to light limitation is expected to stand under strong selection.

The growth response can determine the outcome of competition

Ruderal species, such as the model plant *Arabidopsis thaliana* (L.) Heyhn have specialized to disturbed habitats. When a new habitat patch is colonized, the population census size is small, but generation after generation, plant density will increase with the age of the

population. As a result, ruderal species get exposed to increasing levels of intra- or inter-specific plant-plant competition.

Detection of limited light caused by neighboring plants above-ground can result in rosette size differences, where the optimal phenotypic strategy depends on the competitor species identity (Baron *et al.*, 2015). The competitor species also influences the below-ground competition, which results in reduced biomass and a re-direction of allocation between root and shoot biomass (Cahill, 2003). Below- and above-ground competition show some fundamental differences:

Below-ground the total size of the root system of an individual determines the resource acquisition (Van Gelderen *et al.*, 2018). Root growth and the ability of *A. thaliana* to reach the fruiting phase and produce seeds are negatively impacted, depending on the density of intra-specific competitors (Masclaux *et al.*, 2010; Muñoz-Parra *et al.*, 2017). Above-ground it is not the total size of the leaf system, but the height compared to the competitors, since a plant that is slightly taller can avoid light limitation, while the inferior competitors are highly limited (Van Gelderen *et al.*, 2018).

Competitive ability can also interact with other traits, like the water-use efficiency (i.e. rate of carbon fixation to water loss) (Campitelli *et al.*, 2016). In *A. thaliana,* stomatal size variation is negatively correlated with water-use efficiency and both air humidity and the local probability of spring drought severity (Mojica *et al.*, 2016; Dittberner *et al.*, 2018). The genetic variation for stress tolerance appears to be part of a trait syndrome, because it is often reported to coincide with variation in life history (Takou *et al.*, 2019). Trade-offs between growth rate and development change with latitude, demonstrating, that the resource allocation is not identical throughout the range of *A. thaliana* (Debieu *et al.*, 2013; Glander *et al.*, 2018).

1.3 Local adaptation in *Arabidopsis thaliana*

Local adaptation suggests a diversity of ecological specializations within *A. thaliana*

A. thaliana is a well suited system for the study of local adaptation, since it has the widest geographic range in the *Arabidopsis* genus and grows in very different habitats (Clauss & Koch, 2006; Novikova *et al.*, 2016). Natural populations have mostly been found in temperate climates throughout Europe, from the North of Scandinavia to the South of Spain, from Western Europe over the Balkans, to Central Asia & China in the East, and parts of Africa (Hoffmann, 2005; He *et al.*, 2007; 1001 Genomes Consortium, 2016; Durvasula *et al.*, 2017). It is also naturalized in North America and Argentina (Stock *et al.*, 2015; Kasulin *et al.*, 2017; Exposito-Alonso *et al.*, 2018a). This exceptionally wide distribution range can be linked to dispersal by humans and is only limited by very low spring or autumn temperatures, or by high temperature in regions of low precipitation (Hoffmann, 2002; Lee *et al.*, 2017).

Genetic variation of *A. thaliana* is shaped by climate

The genomic information on the populations has helped to demonstrate that the last glacial period determined the current distribution of genetic variation (Koch, 2019a). The African individuals harbor the greatest variation and the deepest history in *A. thaliana* and after the last glacial maximum populations have spread from ice age refugia in local “relict” populations towards Northern latitudes, experiencing successive bottlenecks (Durvasula *et al.*, 2017; Lee *et al.*, 2017). The native African populations harbor the greatest variation in sub-Saharan Africa, but also populations from North Africa show a clear differentiation from the European population (Durvasula *et al.*, 2017). As a result, regional diversity is highest in Africa and lowest in Scandinavia, while it also follows a longitudinal gradient in Eurasia (1001 Genomes Consortium, 2016; Zou *et al.*, 2017). The Chinese population in the Yangtze River basin has adapted to a very different climate in genes related to the vegetative phase length and diverged about 60,000 years ago with limited gene flow (Zou *et al.*, 2017).

Climatic variations create signatures of local adaptation

Despite a history of gene flow between regions, local adaptation of *A. thaliana* populations has been documented throughout its range (Fournier-Level *et al.*, 2011; Hancock *et al.*, 2011; Agren & Schemske, 2012; Savolainen *et al.*, 2013; Weigel & Nordborg, 2015; Lee *et al.*, 2017). Field experiments and correlation analyses with climate parameters identified

associations with fitness variation in the field and enrichment of non-synonymous SNPs associating with environmental variance (Hancock *et al.*, 2011; Lasky *et al.*, 2014). Furthermore, alleles associating with local fitness increase were more prevalent in populations closer to the field sites (Fournier-Level *et al.*, 2011). Therefore, much of the variation observed in this species is involved in the optimization of plant performance to local environmental conditions.

Growth rate is at the center of development trait combinations that underpin local adaptation in *A. thaliana*

Flowering time is the best studied developmental trait in plants, especially in *A. thaliana*. There are elevated levels of variation in flowering time in this species, which follow climatic clines, at both the regional and species levels (Méndez-Vigo *et al.*, 2011; Montesinos-Navarro *et al.*, 2011; Debieu *et al.*, 2013; Li *et al.*, 2014; Sasaki *et al.*, 2015). Earlier flowering time is favored in warmer climates, a pattern that has also been documented in many other species (Austen *et al.*, 2017; Whittaker & Dean, 2017).

The analysis of co-variation between environmental and phenotypic variance consolidated evidence for the adaptive distribution of flowering time (van Heerwaarden *et al.*, 2015). However, much of the flowering time variation measured in the lab does not manifest as variation in flowering phenology under natural conditions in the field (Wilczek *et al.*, 2009; Brachi *et al.*, 2010; Hu *et al.*, 2017). This is because the control of flowering is tightly dependent on the prevailing environmental conditions. This has two implications. First, flowering time expressed in natural common garden conditions can be deviating (Brachi *et al.*, 2010). Second, the adaptive relevance of flowering time is dependent on the timing of seedling establishment, and therefore on another developmental trait: seed dormancy (Donohue, 2002; Wilczek *et al.*, 2009). Seed dormancy, the delay of germination during unfavorable environmental conditions, is also a crucial developmental trait. It has a strong fitness advantage before the warm season, but can be disadvantageous if it delays plant growth before winter (Donohue, 2002; Donohue *et al.*, 2005; Chiang *et al.*, 2013). Seed dormancy and its major quantitative trait locus (QTL) DOG1 show signals of local adaptation

towards strong dormancy in Southern regions, to escape dry and hot summers (Kronholm *et al.*, 2012; Kerdaffrec *et al.*, 2016; Postma & Ågren, 2016). Both flowering time and dormancy are life history traits that determine the maternal environment the seeds experience during their maturation, impacting life history traits expressed by the next generation (Chiang *et al.*, 2013; He *et al.*, 2014; Postma & Ågren, 2015). Light, temperature, nutrient and water availability have all been identified as significant environmental factors influencing the maternal inheritance of seed dormancy (Footitt *et al.*, 2013; He *et al.*, 2014; Morrison & Linder, 2014; Kerdaffrec *et al.*, 2016). As a result, flowering time and seed dormancy can evolve as a syndrome, defining distinct life history strategies that have diversified across environments (Chiang *et al.*, 2013; Vidigal *et al.*, 2016; Marcer *et al.*, 2018). The interlacing of these two traits and their sensitivity to environmental conditions, makes investigations of the adaptive relevance of their variation particularly challenging.

Much less is known about growth rate. Growth rate describes the transformation of the plant between the seedling stage and its reproduction. It is thus a fundamental component of life-history adaptation (Takou *et al.*, 2019). At the same time, it is a continuous trait that integrates the effect of individual physiological and morphological traits. As such, the molecular basis of growth variation can be further revealed by the analysis of gene expression variation. Understanding the molecular basis of growth rate variation is thus expected to shed new light on plant adaptation. At the same time, studying this complex trait enables us to explore the current limitations of methods aiming at the detection of local adaptation, such as polygenic architecture, environmental plasticity and population structure.

1.5 Aims of the thesis

The aim of this thesis is to pioneer multivariate approaches to elucidate the molecular basis of complex trait adaptation in plants. In particular, I focused on three questions:

1) Is there local adaptation of growth rate in *A. thaliana*?

To answer this question I investigated growth rate in response to the light regime & intra-specific competition. Association signals identified by GWAS were investigated for patterns of

polygenic adaptation.

2) What is the genetic basis of associations to growth rate?

Gene ontology enrichments were used to elucidate the functional basis. To improve the functional characterization of gene sets, I used gene expression differences of mutants in light-signaling genes, to annotate genes in the genome whose expression variation associates specifically with a modification of plant growth.

3) Is there gene expression variation between populations?

I extended the two first approaches with an investigation of patterns of adaptation in regional gene expression differences during the exponential growth phase. Combining analyses of natural variation, mutant analyses and gene expression studies, I identify several molecular processes that are expected to have played an important role in the process of adaptation to regional environmental conditions in *A. thaliana*.

2 Material & Methods

2.1 Analysis of the growth response to light and density

The growth response was measured in five experimental conditions. The response to light quality was measured in two light conditions, the response to intra-specific conditions in three independent experiments.

2.1.1 Plant Material & Genotype information

2.1.1.1Growth under different light conditions

For phenotypic analyses of growth rate variation, I chose 278 genotypes of *Arabidopsis thaliana* originating from 220 locations distributed throughout 4 regions (Northern Europe, Western Europe, Spain and Central-Eastern China, Table 22, Figure 1). These lines were chosen based on a principle component analysis (PCA) which confirmed that genotypes within these regions formed distinct genetic clusters (Figure 2), whose specific evolutionary history has been previously documented (Kronholm *et al.*, 2012; 1001 Genomes Consortium, 2016; Zou *et al.*, 2017; Fulgione *et al.*, 2018).

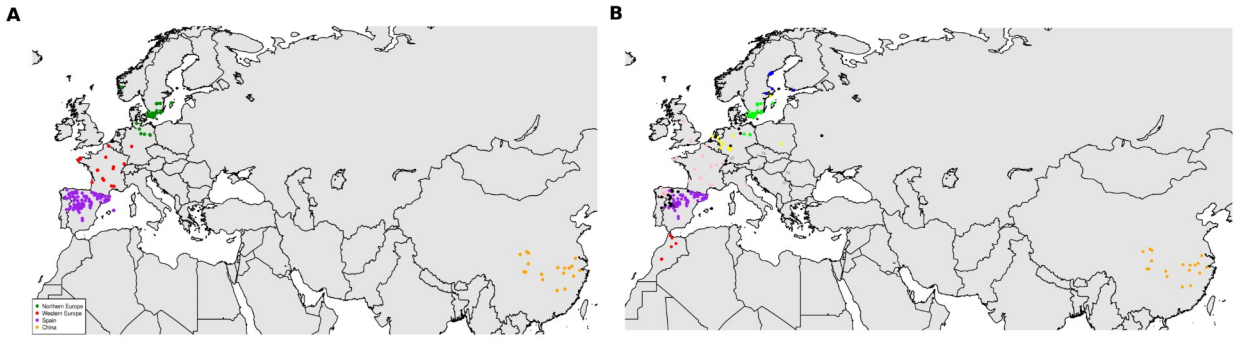

Figure 1: Genotype origin map.

Each dot represents the sampling point of a genotype. A) Genotypes in the HL and LL experiment. The genotypes were assigned to Northern Europe (green), Western Europe (red), Spain (purple) and China (orange). B) Genotypes in the different competition experiments. The genotypes were assigned to the 1001 Genomes groups Northern Sweden (blue), Southern Sweden (green), Germany (yellow), Western Europe (pink), Central Europe (grey), Spain (purple), admixed (black), Africa (red) and Asia (orange).

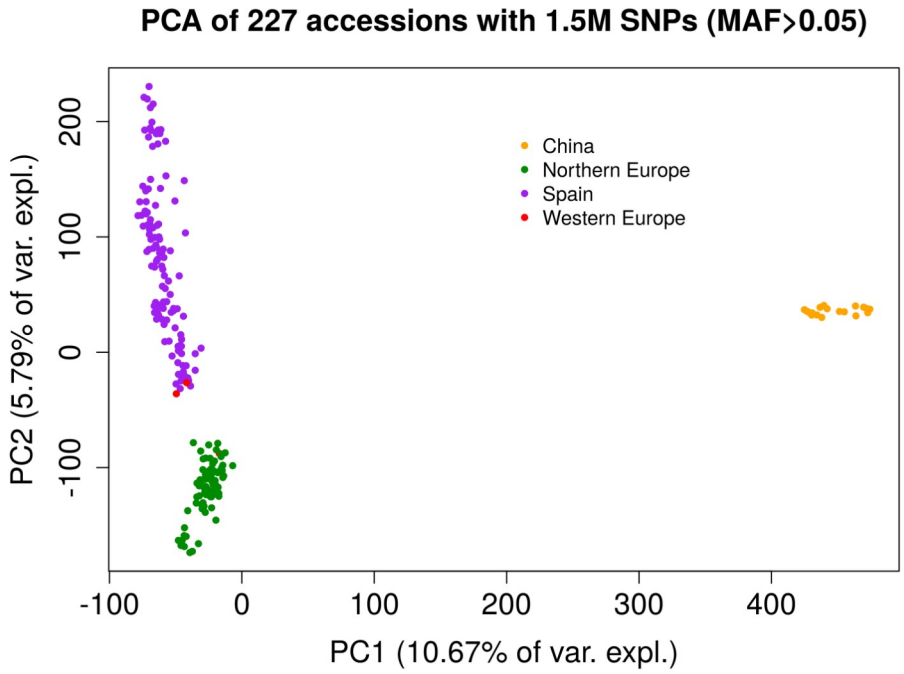

Figure 2: Principal component analysis of 227 genotypes.

The PCA is based on 1.5 millions SNPs with a minor allele frequency larger than 0.05. The first two principle components explain about 16 % of the variance between the genotypes. Regions: China (orange), Northern Europe (green), Spain (purple), Western Europe (red).

2.1.1.2 Intra-specific competition

In total, 348 *A. thaliana* accessions from 22 countries (details in Table 22, Figure 1B) with the majority of the genotypes coming from Sweden (126 genotypes), Spain (97), France (52), Germany (23) and China (19) were included for the first two experiments on intra-specific competition in controlled conditions and the field. The genotypes were part of the 1001 Genomes Project (1001 Genomes Consortium, 2016) and the genomic information was downloaded from http://1001genomes.org/.

The accessions were clustered into nine regions using the regions assigned from the 1001 Genomes Project (1001 Genomes Consortium, 2016). The groups are: Admixed (29 genotypes), Asia (19), Central Europe (22), Germany (17), North Sweden (22), South Sweden (101), Spain (73) and Western Europe (65).

For above-ground competition, 318 *A. thaliana* accessions from four regions were chosen (Table 22), with accessions from Sweden (122), Germany (25), France (50) and Spain (96). The genotypes were selected to have a large overlap with the other experiments, especially with growth in different light conditions.

To increase the number of genotypes, 52 more accessions, predominantly from France, were sequenced, using Illumina TruSeq (Illumina, USA) at the Cologne Center for Genomics (CCG, accessions in Table 23). The fastq files from sequencing were trimmed using trimmomatic (Version 0.36, (Bolger *et al.*, 2014)), mapped using Burrows-Wheeler Aligner (BWA, Version 0.7.12, (Li & Durbin, 2009)) and gVCFs were called using HaplotypeCaller from GATK (Version 4.0.3.0, (McKenna *et al.*, 2010)). Genotypes were called from the gVCF using the GenotypeGVCFs function from GATK and the resulting vcf files were merged using the vcf-merge function from vcftools (version 0.1.15, (Danecek *et al.*, 2011)).

For estimating a SNP matrix, missing data was imputed using BEAGLE (version 5.1, (Browning, 2019). The resulting matrix was transformed with the vcftools –012 option and read into R (version 3.6.3, (R-Development-Core-Team, 2008)).

2.1.2 Experimental Set-up

2.1.2.1Growth under different light conditions

Seeds were stratified for three days at 4 °C in the dark on wet paper, and six replicate seedlings per genotype were replanted, each in one 6x6 cm round pots containing soil (“Classic” from Einheitserde) mixed with perlite. Growth was measured in a nested design under two light regimes, high light (HL) and low light (LL), in the same chamber but in successive independent trials. Plants were grown in a temperature-controlled walk-in growth chamber (Dixell, Germany) set at 20 °C during the day and 18 °C during the night, and watered once a week. For each light regime, pots were randomized within three blocks of eight trays with 7x5 cm pots, with one replicate of each genotype in each block. Trays were randomized and the rows in the trays were rotated every two to three days to account for variability within the chamber. The plants were exposed to light for 12 h with LEDs (LED Modul III DR-B-W-FR lights by dhlicht) set to 100% intensity of blue (440 nm), red (660 nm)

and white (HL conditions) or 30% of red and blue plus 100% of white light (LL conditions), followed by a 10 min far-red light pulse to simulate sunset (40% intensity at 735nm). The total measured light intensity was 224 +/- 10 µmol/m²s in HL and 95 +/- 7 in LL. These two light regime mimic latitudinal differences in natural light intensity (Figure 3).

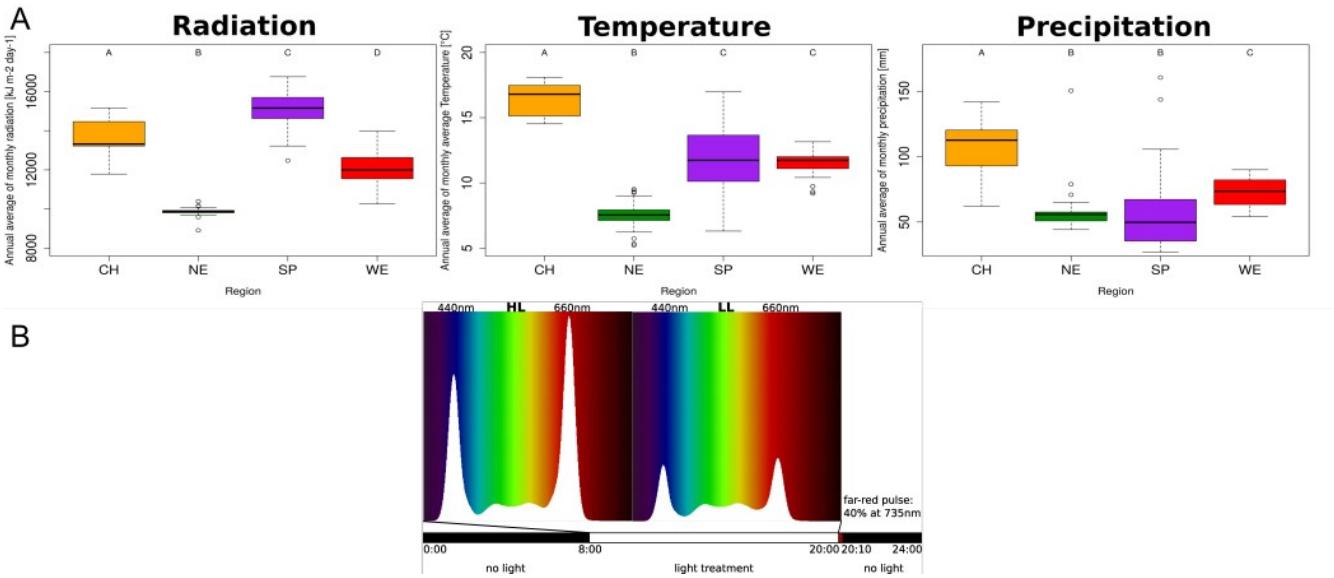

Figure 3: Climatic variation between regions.

A) Annual average of the monthly radiation (left), monthly average temperature (center) and monthly precipitation (right) estimates for the sampling location of each genotype from Worldclim2 data (estimate per ~1km²). Boxplots with different letters are significantly different according to Tukey's HSD ($p < 0.05$). Region information: China (CH, 20 unique locations), Northern Europe (NE, 46 unique locations), Spain (SP, 120 unique locations) & Western Europe (WE, 15 unique locations). B) Experimental set-up in the growth chamber with the light-spectrum and intensity in HL (left) and LL (right). The bottom bar represent the timing of the light.

2.1.2.2 Intra-specific competition

The intra-specific competition was investigated in three separate experiments.

Genetic variation of biomass production under controlled conditions with varying plant density

The first experiment to investigate the density effect on diverse *A. thaliana* accessions was conducted by Gero Carus and Dr. Kim Steige (Carus, 2017). The 384 accessions were grown in one replicate at either low density (LD, 5 plants per pot) or at high density (HD, 100 plants per pot) with VM soil (Einheitserde, Germany). The plants were grown in a walk-in growth chamber with 14 hours of light (50% blue light at 440 nm, 50% red light at 660 nm and 80

white light at 4000k) and a humidity of 60%. For stratification of the seeds, the chamber was set to 4 °C for 3 days and afterwards set to 20 °C during the day and 18 °C during the night. The plants were watered 1-2 times per week with 20-30 ml water per pot. Additionally, all plants were fertilized with Hakaphos Blau Fertilizer (Compo, Germany) every 2 weeks.

Below-ground competition in Cologne 2016-2017

The first field experiment was designed to investigate variation in below-ground competitive ability and conducted in the Cologne experimental garden from September 2016 to March 2017 by Simon Mitreiter and Dr. Kim Steige (Mitreiter, 2017).

In total, 348 *A. thaliana* genotypes from 22 countries were grown in LD (5 seeds per pot) or HD (100 seeds per pot) with two replicates each. The seeds were sown into 9 cm pots filled with construction sand, topped with a 2-3 mm thin layer of VM soil (Einheitserde, Germany) and put into trays of 24 pots with a randomized block design. The nutrient scarcity of this soil limited plant growth and maximized competition for below-ground resources. Because of the nutrient and water limitations in sand the competition was considered as predominantly below-ground, since growth was so severely limited, that rosettes did not overlap. Seeds were germinated in the greenhouse under hoods for a week and subsequently put outside into a fenced, plastic foil-covered patch in the greenhouse garden of the Botanical Institute of the University of Cologne (50.93 °N, 6.94 °E) on the 22nd September 2016. Temperature data for 5 cm above the ground was downloaded from the German Meteorological Office (https://opendata.dwd.de/climate_environment/), for the weather station in Cologne Stammheim (50.99 °N, 6.98 °E, ~7 km from the field site). The temperatures during the experiment are plotted in Figure 4.

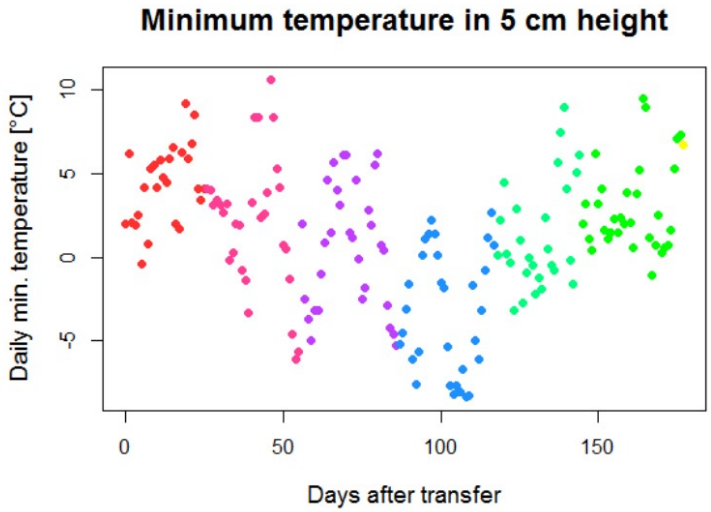

Figure 4: Daily Minimum Temperature during the below-ground competition field experiment.

Temperature records are from the weather station in Köln Stammheim. Data points are colored according to the month of measurement: October (red), November (magenta), December (purple), January (blue), February (lime), March (green), April (yellow). Figure from (Mitreiter 2017).

The plants were watered 12 days after the transfer to prevent dehydration of the young seedlings in the sand substrate and, again, 174 after transfer to prevent drought damage. Slug pellets were applied and the plants were sprayed with the insecticide Confidor® (Bayer, Germany) at 48 and 74 days after transfer to avoid pests. Since the plants started to display signs of severe starvation stress, they were fertilized 152 days after transfer with Wuxal® Super NPK 8-8-6 liquid fertilizer (Wuxal, Germany) to complete their life cycle, but this was after the analyzed growth measurements.

Above-ground competition in Cologne 2017-2018

The second field experiment was designed to investigate above-ground competition and conducted in the Cologne experimental garden from September 2017 to April 2018 by Jennifer Escher and Dr. Kim Steige (Escher, 2018).

To investigate the effect of different strength of intra-specific competition on *A. thaliana*, three different conditions (no, intermediate and high competition) were assessed: 1) one focal plant

growing alone (no competition, LD), 2) one focal plant growing with four neighbors at a distance of 1 cm (high competition, HD) and 3) one focal plant with four neighbors at a distance of 2 cm (intermediate competition, ID). For each accession and treatment four replicates were included and the competing plants were from the same genotype as the focal plant. Seeds were sown into 8 cm round pots with VM soil (Einheitserde, Germany) using a plastic template for the pots to ensure equal positioning of the seeds. Seeds were sown within one week and directly placed outside with plastic covers until germination (same location as the below-ground competition experiment). The pots were randomized in block design with one block for each replicate, consisting of 40 trays with 24 pots. In total 3768 plants were used in this experiment. After two weeks, covers were removed and redundant seedlings were weeded out. For the first six weeks plants were watered as necessary to keep them from drying out. Plants were grown outside, from September until May. The minimum temperature 5 cm above the ground in Cologne Stammheim is plotted in Figure 5.

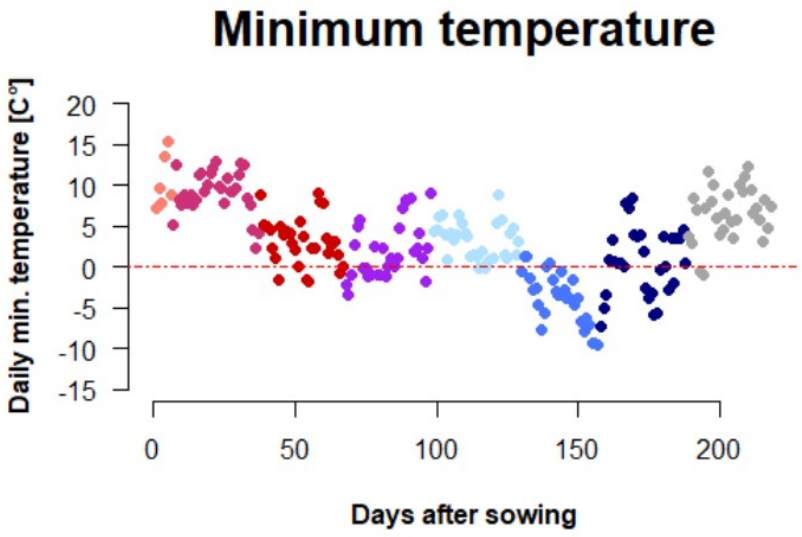

Figure 5: Daily Minimum Temperature during the above-ground competition field experiment.

Temperature records are from the weather station in Köln Stammheim. Data points are colored according to the month of measurement: September (salmon), October (magenta), November (red), December (purple), January (light blue), February (blue), March (dark blue), April (grey). Figure from (Escher 2018).

2.1.3 Data collection & phenotypic measurements

2.1.3.1Growth under HL and LL conditions

Individual plants were photographed approximately bi-weekly with a Canon EOS 5D Mark III digital camera until days 46 (8 weeks) and 89 (13 weeks), for those grown under the HL and LL regimes, respectively. I only measured diameter for one time point per week, but included additional measurements if it was necessary to fit the logistic curves. Flowering time was measured as days to first flower opening. For genotypes without a flowering individual by the end of the experiment, a flowering time value of 59 or 90 days (last date that flowering was scored) was assigned to HL and LL plants, respectively. Since only 37% of the plants in the experiment flowered, I also used flowering time data from the 1001 Genomes project, where flowering was scored at 10 and 16 °C for 177 genotypes (1001 Genomes Consortium, 2016). A measure of the diameter of each plant (defined as the longest distance between two leaves) was extracted at least once a week with ImageJ (v.1.50b, (Rasband, 2012)). In a preliminary experiment conducted by Lucas Aschenbrenner on a subset of 17 genotypes, we used Rosette Tracker, an ImageJ tool (De Vylder *et al.*, 2012), to show that diameter correlated positively with rosette area under both light regimes (HL $r= 0.83$, $p<3.2E-5$, LL $r= 0.56$, $p<0.0186$) (Aschenbrenner, 2017). We confirmed that plant diameter accurately predicts rosette area on this larger data set ($r= 0.929$, $p<2.2E-16$ in HL). Rosette diameter was therefore used to determine the increase in rosette area over time. To capture a signal of the stress-response to high light irradiation, in HL the plants were scored for red leaf coloration after 27 days, by counting the number of leaves that turned red.

2.1.3.2 Intra-specific competition

Genetic variation of biomass production under controlled conditions with varying plant density

The fresh and dry weight of the above-ground biomass was measured 21, 27, 33 and 39 days after sowing. For estimation of the fresh weight, the leaf material was weighed on a AC 210 P precision scale (Sartorius, Germany) with an accuracy of 0.1 mg. For measurements one plant per pot was removed, so the density decreased slowly as the experiment proceeded.

After the fresh weight measurements the plants were dried for five days at 60 °C in a dry cabinet Dry Line 53 (VWR International, USA). In addition, germination rate was estimated after eight days, by counting the seedlings in each pot and dividing it by the number of seeds (5/100). Hypocotyl length was scored after 15 days, to quantify variation in seedling growth. The time of bolting was measured as days after sowing. After 80 days all plants that did not bolt were vernalized at 4 °C to induce flowering. After six weeks at lower temperature, the plants were returned to the previous conditions and bolting was scored as days after vernalization.

Below-ground competition in Cologne 2016-2017

Germination rate was scored using pictures taken with a Canon EOS 5D digital camera and analyzed using ImageJ (Rasband, 2012). Rosette diameter was measured each month (39, 69, 99, 129 and 159 days after transfer) for three plants per pot. Bolting was scored as the day of the first plant per pot bolting, since the plants within each pot all bolted within three days.

Above-ground competition in Cologne 2017-2018

For each phenotypic measurement, only the focal plant was measured. Pots with no or low germination in the competitors (< 3) were excluded, as competition would differ otherwise. Rosette diameter of the focal plant was measured for each focal plant during the growth period from October to March. The first two measurements (after 25 and 39 days) were documented in photos with a Canon EOS 5D Mark III digital camera and analyzed with the program ImageJ (version 1.51d, (Rasband, 2012)). After that, the plants were measured by hand once a month (after 52, 79, 107, 134 and 163 days). After 115 days, the plants started the production of flowering stems (bolting) and first bolting time was measured in January. Flowering time was measured when the first flower was opened. Bolting and flowering time was scored every second day for the focal plant. Final height was assessed once plants stopped flowering, by measuring the total size of the focal plant from bottom to top with a regular 30 cm ruler. Focal and competing plants were sampled separately to get an estimate of the fitness traits number of siliques and number of branches. These phenotypic traits are

not analyzed in depth here, because the measurement of the dried plant material was not reliable.

2.1.4 Statistical analysis of experimental data

2.1.4.1 Growth under HL and LL conditions

All following analyses were conducted using R (version 3.6.3) (R-Development-Core-Team, 2008), and function names refer to those in the R package mentioned unless otherwise noted. The nested design of our analysis allowed me to conduct the analysis in successive steps. First, I extracted three parameters that together provided a comprehensive description of individual rosette growth. For this, rosette diameter measurements over time (our input phenotype) were modeled as a three-parameter logistic growth using the drm function from the drc package in R (Ritz *et al.*, 2015). The three following growth parameters were extracted: final size (FS, largest estimated rosette diameter in cm), slope (SL, factor of magnification in the linear phase) and t50 (inflection point; time at which growth is maximum and half of FS has been reached, which quantifies the duration of the rosette area growth phase in number of days). For each parameter, a genotypic mean correcting for block, tray and position effect was computed with a generalized linear model with a Gaussian error distribution and the following model: parameter~accession+block+tray/(row+col)+error. Genotypic means in HL and LL were extracted separately, because light treatments had to be performed in separate trials. To quantify the plasticity of growth to the light regime of each genotype, I correlated genotypic means in LL against HL and extracted the residuals. Genome by Environment (GxE) estimates thus quantify the deviation of the response of a given genotype from the mean response of all genotypes for the respective parameter. The estimate increases with the magnitude of growth plasticity induced by a decrease in light intensity (Figure 34). Broad-sense heritability (H^2) was determined for each trait in each environment as previously reported (Dittberner *et al.*, 2018). Briefly, genetic and environmental variances were estimated using the lme function from the nlme package (Pinheiro *et al.*, 2018), with the block as fixed and genotype as random effect and heritability was determined as the ratio of genetic variance over the total variance. The heritability of GxE

could not be estimated, because plasticity was calculated on the basis of genotypic means, and the heritability calculation requires variation within a genotype to estimate environmental variance. For this reason, I also computed trait pseudo-heritability, which is based on the genome-wide association study (GWAS) mixed model (see below) and allowed us to estimate the proportion of the observed phenotypic variance that is explained by genotypic relatedness for all traits (Korte & Farlow, 2013).

To assess the correlation of phenotypic traits with climatic variables, I investigated solar radiation estimates, temperature, precipitation, humidity and wind speed with 2.5-min grid resolution (WorldClim2 database, (Fick & Hijmans, 2017), accessed on March 20, 2018) and soil water content (Trabucco & Zomer, 2010). I estimated the mean over the putative growth season for each genotype in addition to the annual averages, following (Dittberner *et al.*, 2018). Because of the strong correlations between climatic variables, I conducted principal component analyses (PCAs) to combine the data. I analyzed annual average radiation separately and combined the other variables into the PCAs: growing season data, variables related to precipitation and to temperature. Raw climatic data and the principle components (PCs) are in Table 24 and the loadings of the PCA are in Table 25.

Regional differences in mean growth parameters were tested with a multivariate analysis, using the manova function, the matrix of growth parameters (genetic means) or plasticity and the following model: growth~ population*light regime. Significance levels were determined by the Pillai test. For univariate analysis, I used GLMs to test the effect of population of origin on the genotypic means. A Gaussian distribution was taken for error distribution, and the dispersion parameter was estimated by the glm function. Group means were compared with the glht function (which performs general linear hypothesis testing) and plotted on boxplots using the cld function, both of the multcomp package (Hothorn *et al.*, 2017).

Pairwise trait correlations within and across populations were calculated with the cor.test function (Pearson’s product-moment correlation), and p-values were established using the lmekin function in R, which includes a kinship matrix of individuals (see below) and thus corrects for population structure (after Glander et al. 2018). I used the corrplot function from

the corrplot package to plot correlations (Wei & Simko, 2017). Plots were modified using inkscape version 0.92.3 (inkscape.org) (The Inkscape Team, 2007). Significance levels were adjusted for false-discovery rates with the function p.adjust.

2.1.4.2 Plant growth variation in response to density

For further analysis of density in controlled conditions the biomass after 39 days in high and low density and the bolting time were chosen, because they were the measurements at the end of the growth phase. This experiment included no replicates, thus heritabilities could not be estimated and the raw measurements were taken as genotypic value. GxE was estimated with a generalized linear model (glm) (Trait~Treatment) and a negative binomial error distribution.

For the below-ground competition, 13% of the high-density pots displayed a low germination (less than 50% of the seeds germinated) and 48 genotypes had to be removed, leaving 320 genotypes for analysis. Because of biomass loss I could not use a model of growth, because the logistic growth model did not converge for the diameter data. Therefore, I focused on the diameter measured in December, because heritability was highest for this time point. To get some estimate of the growth dynamic, the difference between diameter in December and November was calculated, as well as the maximum diameter measured for each plant.

Genotype means for below-ground competition traits were estimated with a glm (Trait~Genotype+Replicate+Germination).Trait was the input phenotype, Genotype the genetic background, Replicate the biological replicate (1 or 2) and Germination the germination rate, estimated as germinated plants after 7 days divided by 5 (in LD) or 100 (in HD). For all traits in this experiment a Gaussian error distribution was used. For further analyses I focused on FS and final height, since they had a high heritability and could be used to estimate the plant size at the end of growth.

Genotype means for above-ground competition traits were estimated using a glm (Trait~Genotype+Block/Tray), where Trait was the input phenotype, Genotype the genetic background, Block the biological replicate (1-4) and Tray the tray number within a block. For diameter measurements, FS, t50, final height, height at flowering and the number of silique a

negative binomial error distribution was used. For the remaining traits the data was fitted with a Gaussian error distribution. GxE of genotypic means was estimated with a glm(Trait~Treatment) and a Gaussian error distribution, except for bolting time in above-ground competition, where a poisson distribution was more accurate.

For the above-ground competition, the logistic growth model of diameter measurements was applied to get estimates of FS, slope and t50 in the different density treatments. In this experiment few models did not converge, if this was the case the corresponding plant was removed from the data (8 of 713 plants in HD and 6 of 730 plants in ID did not converge, every genotype still had more than 2 replicates).

2.1.5 Genome-wide association studies

Genomic data were available for 231 of the 278 genotypes included in the phenotypic analysis, i.e. for 84 genotypes from Northern Europe (NE, predominantly Sweden), 3 from Western Europe (WE), 119 from Spain (SP) and 15 from China (CH) (1001 Genomes Consortium, 2016; Zou *et al.*, 2017). Chinese genotypes were excluded from the GWAS because of their limited number (15 genotypes) and their strong genetic divergence (Zou et al. 2017). In total, the growth parameters of 203 and 201 genotypes grown under HL and LL, respectively, were used for the GWAS. For biomass, 267 genotypes in HD and 235 in LD were used for GWAS. GWAS for diameter in below-ground competition was performed with 272 genotypes in HD and 259 genotypes in LD. For GWAS of traits in above-ground competition, 242, 230 and 232 genotypes were used for LD, HD and ID of FS. For final height, 231, 216 and 214 genotypes were used for LD, HD and ID.

Genome-wide association studies were conducted using the method from (Korte & Farlow, 2013). The corresponding GWAS package was downloaded from https://github.com/arthurkorte/GWAS. Single Nucleotide Polymorphisms (SNPs) with minor allele frequency below 5% or with more than 5% missing data were removed from the genotype matrix, resulting in a matrix of 1,448,192 SNPs, produced with vcftools (--012 recode option) (version 0.1.15, Danecek et al. 2011). A kinship matrix was computed with the emma.kinship function (Kang *et al.*, 2010; Korte & Farlow, 2013). For each growth parameter,

genotypic means were used as phenotype measurements. I performed GWAS across the European sample of genotypes but also within region (Spain and Northern Europe). For each SNP, the script output delivered p-values, which were Bonferroni corrected for multiple testing, and effect sizes. For each trait, I estimated a pseudo-heritability, the proportion of the observed phenotypic variance that is explained by the estimated relatedness (e.g. kinship matrix, (Korte & Farlow, 2013)). To identify candidate genes underpinning significant GWAS associations, I extracted genes within 10 kb up- and downstream of the SNP. For candidate gene identification, I only describe genes with an annotated function that can be linked to growth, but for enrichment analyses all genes in proximity were used. Additionally, I downloaded an annotation of loss-of-function (LOF) variants (Monroe *et al.*, 2018) and performed a GWAS association following the procedure described above except that the SNP data set was replaced with the LOF data set, which assigned one of two states (functional or LOF), for each genotype and each of the 2500 genes with known LOF alleles.

In addition, overlaps between GWAS associations of different phenotypes were compared in a meta-analysis of these GWAS results using METAL (Willer *et al.*, 2010). This tool estimates weighted Z-scores for effects that are in the same direction in several GWAS. To do this, I created input tables with information from each individual GWAS and grouped them into all GWAS on density traits (ALL), all traits in HL and LL (HLLL), GWAS in low density including FS in HL and LL (NODENS), high density GWAS genes (HIDENS) and their GxE (GXE). Then, I executed the METAL software with default settings on these sets to identify sets of genes related to growth in general (ALL, NODENS), or in response to density (NODENS, HIDENS, GXE). This resulted in a list of SNPs with their effect direction for each trait and a Z-score of effect sizes with a p-value for significance. The identified SNPs were used for a GO enrichment using the fisher test and the elim procedure in the topGO function (Alexa *et al.*, 2006; Alexa & Rahnenfuhrer, 2019) as described in (He *et al.*, 2016). I removed tandem duplicated genes within a 10-gene sliding window. For this, all TAIR10 genes were aligned against each other by using BLAST (version 2.9.0, available at https://blast.ncbi.nlm.nih.gov), then, the duplicated genes were selected as genes with an e-value <1E-30. Finally, tandem

duplicated genes identified within a 10-gene distance were filtered out to avoid inflated functional enrichments.

Smile plots to investigate effect size symmetry within populations

To investigate the association between effect size and allele frequency, GWAS were performed for the traits FS, t50 and SL in HL and LL within NE (85 individuals) and SP (115 individuals). The effect sizes (beta) for SNPs with a p-value < 0.001 were selected for plotting and the frequency of the phenotype-increasing allele was plotted for each SNP per trait and region.

Co-variance between environment and population structure effects

The phenotyping of mutants in the identified LOF gene AT2G17750 (NEP1-interacting protein, NIP1) was carried out within the Bachelor Thesis of Franziska Geuchen under my supervision (Geuchen, 2021).

A first characterization was conducted of T-DNA mutant lines for the gene AT5G15700 (RPOTmp). RPOTmp is interacting with NIP1, by fixing it to the thylakoid membrane (Azevedo *et al.*, 2008). We chose this approach, since there were no T-DNA insertion lines for NIP1. Three different RPOTmp LOF lines were ordered from NASC (The Nottingham Arabidopsis Stock Centre) and ABRC (Arabidopsis Biological Resource Center): SAIL_914_C09 (Sessions *et al.*, 2002), SALK_206574 (Alonso *et al.*, 2003) and GABI_286E07 (Kleinboelting *et al.*, 2012). The lines were checked for the transposons using polymerase chain reaction (PCR). To do this, DNA was extracted using the NucleoSpin Plant II Kit (Macherey-Nagel, Germany) and a PCR with primers specific to the respective transposon (Table 2) was conducted (Table 3). Primers specific to the gene were used as a positive control in the PCR, water instead of DNA was used as a negative control.

Table 2: Primer sequences that were used for the PCRs.

The table shows the primer sequences, whether they bind specifically to the gene or a T-DNA insertion ("Specific to") and if they work as forward or reverse primers ("Orientation"). All the primers could be used with an annealing temperature of 60 °C. The first three primers were suggested by GABI-KAT, therefore they miss some information.

Primer	Orientation	Specific to	Primer sequence
1		T-DNA GABI-KAT	ATATTGACCATCATACTCATTGC
2		Gene	TCAAGGTAATGTGCATAAGTTGCT
3		Gene	TAGTAAAGAGACTTTGGGCCGTTA
4	Forward	T-DNA SAIL	AGTCGTGTCTTACCGGGTTG
5	Forward	T-DNA SAIL	GCCTACATACCTCGCTCTGC
6	Reverse	Gene	TCCTCTTCGGCTACACTCGT
7	Reverse	T-DNA SALK	CTCGTCCTGCAGTTCATTCA
8	Forward	T-DNA SALK	CTGGCGTAATAGCGAAGAGG
9	Reverse	Gene	CCATTTGAGAGGAGGAACCA
10	Forward	Gene	GGCTTAAGAAAGCAAGGGTTT
11	Forward	Gene	CTGTTTATGCTTGGCTGCAA

Table 3: PCR cycles.

The steps of the PCR with their respective temperature, duration and number of repetitions.

Steps	Temperature [°C]	Time [mm:ss]	Number of passes
Denaturation	95.0	2:00	1
Denaturation	95.0	0:25	34
Annealing	60.0	0:30	34
Elongation	72.0	0:30	34
Elongation	72.0	5:00	1

After PCR, a gel electrophoresis was performed. According to the PCR-results the genotypes were classified as Wild Type (WT, Col-0), non-mutant (no T-insertion) and mutant (T-DNA insertion).

For phenotyping, the plants were grown in HL and LL conditions as described before and their diameter was measured for 16 replicates for 43 days in HL and 85 days in LL. A second

characterization was conducted of 12 RNA interference lines of NIP1, called CATMA2a16430-[2581-2592] (Hilson *et al.*, 2004). These lines and the Col-0 WT were grown in the same conditions as the first experiment. Five replicates in HL and ten in LL were measured until day 53. The RNAi plants were genotyped by performing a BASTA resistance test, since the vector that was used to create these lines contained a BASTA resistance gene. Since all the 180 plants had to be tested separately in case of segregating lines, this method was a quick and easy alternative to the traditional PCR and gel electrophoresis. For the test, a 0.2 % BASTA solution was prepared with 0.0005 % Silwet® Gold (Spiess-Urania, Germany) and applied to one leaf per plant. After a week, the plants whose leaf stayed green, should be transgenic plants, since they appear to have a BASTA resistance gene. The growth parameters of the diameter measurements were analyzed as described before for the T-DNA mutant lines, the growth response of the RNAi-lines was analyzed for day 46 in HL and day 53 in LL conditions with the same model.

2.1.6 Validation of the polygenic signal

2.1.6.1 Investigation of polygenic scores

In humans, where population structure and environmental variation are correlated, insufficient correction of the genetic associations caused by shared ancestry has been shown to create spurious associations (Berg *et al.*, 2019; Sohail *et al.*, 2019). Even though environmental variance is much better controlled in common garden experiments including kinship as a covariate, association tests can still be confounded by genetic relatedness (Fustier *et al.*, 2019). This is of particular concern when many trait/SNP associations are below the Bonferroni significance threshold. The rate of false positive was not excessively inflated by genomic differentiation between regions, because GWAS performed within regions (Northern Europe or Spain, Figure 38 & 39) had similar p-value distributions than GWAS performed on the complete phenotypic dataset. Nevertheless, I used two additional approaches to confirm the polygenic basis of traits.

First, I examined whether phenotypic variation could be predicted by polygenic scores derived from sub-significant GWAS hits, with p<10E-4. To this end and for each trait, we calculated

genotypic means, performed GWAS, as described above, and computed polygenic scores following (Berg & Coop, 2014). SNPs with a significant association with the phenotype were pruned to remove SNPs standing in strong linkage disequilibrium with plink version 1.90 (Purcell & Chang, 2019), following (Sohail *et al.*, 2019). The plink -clump function was set to select SNPs below a (GWAS) p-value threshold of 10E-4, start clumps around these index SNPs in windows of 1 Mb, and remove all SNPs with $p < 0.01$ that are in LD with the index SNPs. The SNP with the lowest p-value in a clump was retained for further analysis. Briefly, input files, including allele frequencies for all SNPs, all SNPs with GWAS p-values lower than 10E-4 and their effect size estimates were created with a custom R script. Each genotype was defined as its own population (genotypes from Spain and Northern Europe were grouped in regions). Scripts were downloaded from https://github.com/jjberg2/PolygenicAdaptationCode. The pipeline was run with default parameters, and polygenic scores (Z-scores) were estimated. I used two approaches to validate the biological relevance of GWAS associations. I took two replicates to compute the polygenic scores and correlated it with the phenotype of the third replicate. Additionally, I used 80% of the genotypes and used the resulting GWAS association to compute a polygenic score for the remaining genotypes. Correlation were calculated with the R function cor.test (Pearson's product-moment correlation).

Second, I investigated functional enrichment among all genes in *A. thaliana* with a ranking based on the GWAS results of the different traits or the differentiation index (Fst) between Northern Europe and Spain. If the polygenic signal was due to insufficient correction for population structure, I hypothesized that similar functions would be enriched among genes with high Fst and genes with low GWAS p-values. Fst values for each gene were calculated with the F_ST.stats function of the PopGenome library for genotypes from Spain and Northern Europe (Pfeifer *et al.*, 2014). Negative Fst values were set to zero. To assign a single GWAS p-value for each gene, either the lowest p-value of SNPs within the gene was assigned for each trait, or, if no SNP was within the gene, I assigned the p-value from the physically closest SNP (Korte & Farlow, 2013).

Enrichments were tested as previously described (He *et al.*, 2016). The genes were ranked either by Fst or by p-value in GWAS and tested with the Kolmogorov-Smirnov statistic. To call a GO enrichment significant, I chose p= 0.008 as a significance threshold. This conservative threshold was determined as the 0.01% quantile of the p-value distribution when GO enrichments were tested for 1000 random sets of the same number of SNP. To assess similarity between traits in Gene Ontology (GO) enrichments, I calculated graph-based similarity with the GOSemSim package (Yu *et al.*, 2010). A distance matrix was estimated with average connectivity between the GO terms. The clustered GO categories were then plotted as a dendrogram with the plot.phylo function from the ape package (version 5.3) (Paradis *et al.*, 2004). GO categories enriched at p-value below 0.001 were highlighted. The distribution of enriched GO categories was evaluated by visual inspection.

2.1.6.2 Testing for adaptation or maladaptation

For population genetics analyses, one genotype was chosen at random whenever plants were sampled in the same location, acquiring a total of 220 genotypes. As a proxy for the genomic load imposed by deleterious mutations, the number of derived non-synonymous mutations per haploid genome has been proposed (Simons & Sella, 2016). This approach was not possible here because the genomes of individuals from China and Europe were sequenced in different labs, and the depth and quality of sequencing varied too much to make a fair comparison. Instead, I used two data sets that together cataloged LOF alleles after controlling as much as possible for heterogeneity in sequencing quality: one that included European genotypes (Monroe *et al.*, 2018) and a more recent data set that included Chinese genotypes (Xu *et al.*, 2019). As an estimate of the individual burden of deleterious mutations, I counted the number of LOF alleles for each individual and tested whether individuals with a larger number tended to have a lower growth rate using the Spearman rank correlation.

To search for footprints of adaptive evolution, I computed an Fst value between Spain and Northern Europe for each SNP in the GWAS analysis using the R-package hierfstat and the basic.stats function (Goudet, 2005). Negative Fst values were set to zero, and the quantile

function was used to calculate the 95th percentile. The Fst distribution of SNPs associated with any GWAS (p<10E-4) was compared to the genome-wide distribution with a Kolmogorov-Smirnov test. I also computed the likelihood that its 95th percentile was greater than the 95th percentile of 10 000 random samples of an equally large set of SNPs. To compare the phenotypic differentiation of traits, Qst values for the phenotypic traits were estimated as previously described (Dittberner *et al.*, 2018). Briefly, Qst was estimated as VarB / (VarW + VarB), where VarW is the genotypic variance within and VarB between regions.

These variances were estimated with the lme function of the nlme package (Pinheiro *et al.*, 2018), with the block as fixed and population/genotype as random effect. I extracted the intercept variance for VarB and the residual variance for VarW. Since replicates were taken from the selfed progeny of each genotype, VarB and VarW are broad-sense genetic variance components. To reveal signatures of local adaptation, the Qst of each trait was compared to the 95th percentile of the Fst distribution (between Spain and Northern Europe) (Whitlock & Guillaume, 2009; Leinonen *et al.*, 2013).

To verify that outlier Qst values were unlikely to arise randomly, I permuted phenotypic data by randomizing genotype labels and verified that the difference between observed Qst and 95th percentile of Fst was significantly greater than for randomized Qst, following (Dittberner *et al.*, 2018). In a second approach, I used a multivariate normal distribution to generate phenotypic divergence based on the kinship matrix to generate an expected Qst distribution (Koch, 2018). Finally, I applied the over-dispersion test (Qx test), which compares polygenic scores computed for associated versus random SNPs (null model), in a process similar to a Qst/Fst comparison, but assuming that each population is composed of the selfing progeny of one genotype (Berg & Coop, 2014). A Qx significantly larger than the Qx computed for the null model indicates that polygenic trait prediction is more differentiated than expected from the kinship matrix and can be taken as an indication that the trait has evolved under divergent selection, either within or between regions (Berg & Coop, 2014).

2.2 Defining genes and molecular function with mutants of the light signaling pathway

We investigated whether studying molecular variation in growth conditions representative of the ecological function of genes allowed a better interpretation of GWAS data. To this end, we compared gene expression between WT plants (Col-0) and 8 mutants of genes in the light signaling pathway in collaboration with Dr. Konstantin Kerner and Prof. Dr. Ute Höcker. These genes have a significant effect on plant growth, and this effect depends on the situation of plant-plant competition, which is known to vary in natural settings. I used the gene expression data of this collection of mutants to identify sets of genes that associate with changes in plant growth in the environments that were used for characterizing genetic variation in plant growth in this thesis. Since the Gene ontology categorization is not reflecting ecological importance, I wanted to test whether the genes relevant for phenotypes of interest contribute dis-proportionally to the polygenic basis of growth.

2.2.1 Plant material and experimental setup

The mutants and their phenotype (after (Legris *et al.*, 2017)) are summarized in Table 4.

Table 4: Plant material used for gene expression variance in mutants of the light-signaling pathway.

Information on name of the accession, the name of the knocked-out gene (Mutated gene), its function and the observed phenotype under darkness and light conditions. Etiolation is the phenotype in darkness/limited light with elongated hypocotyl and petioles. De-etiolation is the change of this phenotype to the normal growth in light conditions with darker leaves without extended petiole elongation.

Name	Mutated gene	Gene function	Mutant phenotype
Col-0	Wild type	-	Etiolated in darkness/high far-red light; de-etiolated in light conditions
cop1-4	CONSTITUTIVE PHOTOMORPHOGENIC 1	Forms complex with SPA and is involved in degradation of HY5	Constitutive de-etiolated (light) phenotype

spa1234	SUPRESSOR OF PHYA 1,2,3,4	Forms complex with COP1 and is involved in degradation of HY5	Constitutive de-etiolated (light) phenotype
hfr1	ELONGATED HYPOCOTYL 5	Transcription factor, inducing light phenotype	Constitutive etiolated (shade) phenotype
phyB-9	PHYTOCHROME B	red/far-red light receptor	Constitutive etiolated (shade) phenotype

The plants were grown with four replicates in three experimental conditions: HL with and without competition and LL. The HL and LL conditions were as described in 2.1.1. The competition was as described in the HD condition in the above-ground competition field experiment (2.2.1). Furthermore, plant material was collected at day and night in HL and night in LL, resulting in 5 “environments” (HL, day, single plants; HL, night, single plants; HL, day, competition; HL, night, competition; LL, night, single plants). In total, 140 plants were grown in 5 conditions as summarized in Figure 6.

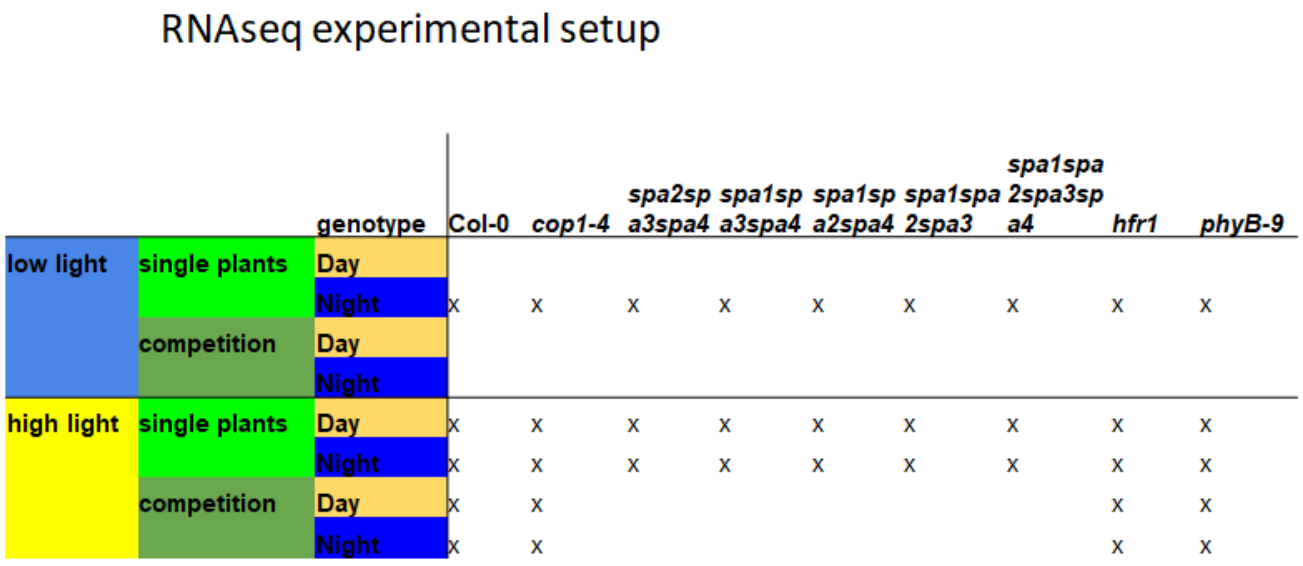

Figure 6: Experimental conditions for RNA expression of mutants in light-signaling genes.

The plants were grown with 5 replicates in low light or high light, with single plants or competition and sampled at night and/or day. The genotypes are as described in Table 4. The x at the environment- genotype combination marks, if the combination was included in the experiment. The study of copy-specific effect of spa knock-outs is not included in the thesis.

Here, I focused on a subset of these genotypes. I only investigated the Wild type (Col-0), mutants with an altered light perception (*phyb*) and mutants with an impacted shade avoidance response (*cop1 & spa* quadruple mutants (*spa1spa2spa3spa4* or *spa1234*). The study of copy-specific effect of *spa* is not included in this thesis. Expected phenotypes in response to light and competition environment are summarized in Figure 7.

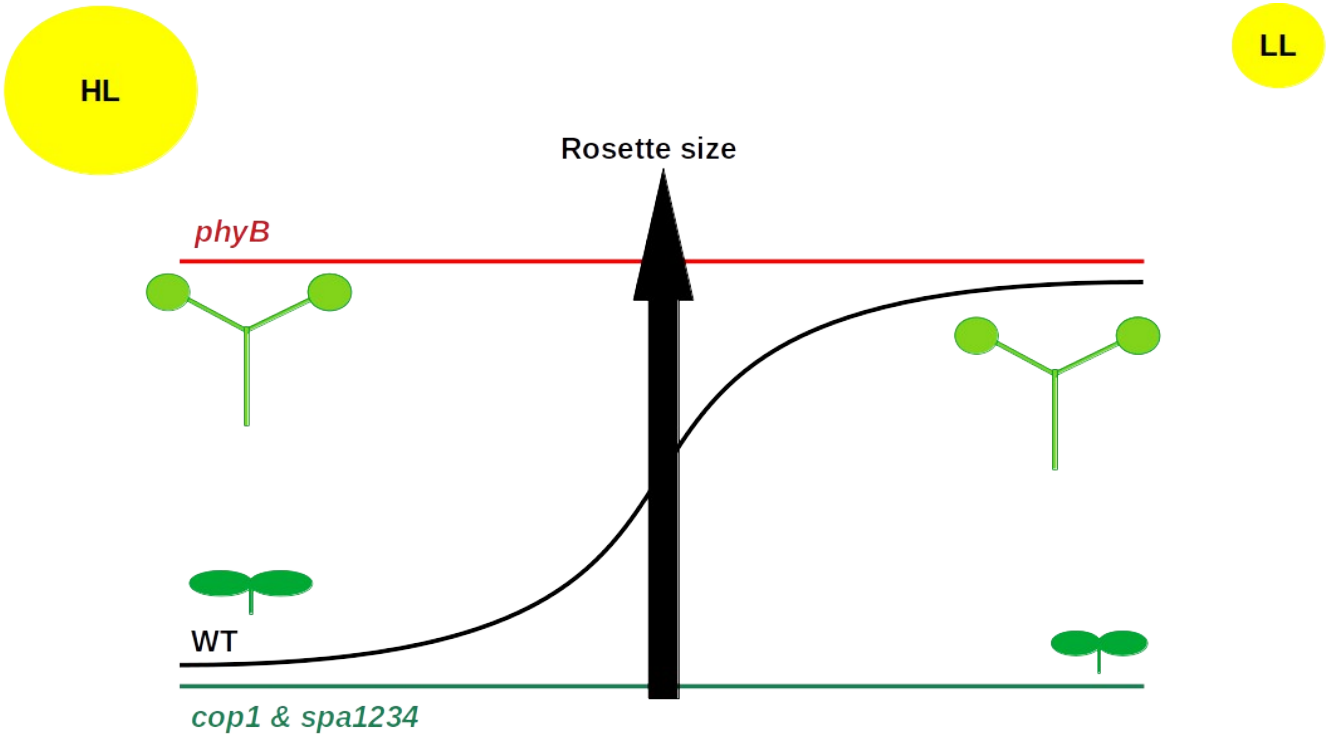

Figure 7: Illustration of the phenotypes based on genetic background.

The observed rosette sizes of the genetic backgrounds are illustrated with the lines for *phyB* (red), WT (black) and *cop1+spa1234* (green). Phenotypes in HL are on the left side and phenotypes in LL and under competition are on the right side. The drawings of plants illustrate the phenotypes for shade avoidance (top) and growth in light (bottom).

Leaf material of 3-4 adult leaves was harvested after 21 days (average t50 in HL), either two hours before (“Night”) or four hours after the lights were turned on (“Day”).

2.2.2 Sample preparation, RNA sequencing and data processing

RNA was extracted using the RNeasy Mini Kit (Qiagen, USA). RNA sequencing was performed by Novogene (China) on the Illumina NovaSeq 6000 platform (Illumina, USA).

Samples were only sequenced when they met the minimum requirements of a RNA Integrity Numer (RIN, from Bioanalyzer, Agilent, USA) of 6.3 or more and a purity (260/280, from Nanodrop, Thermofischer Scientific, Germany) of 1.8 or more. These criteria were reached for all samples.

The mapping and quality control was performed by Dr. Fei He. Sequence quality was checked with FastQC. The first 3 bp and unpaired reads were discarded with Trimmomatic v0.36 (Bolger *et al.*, 2014). The transcriptomes were mapped to the TAIR10 *A. thaliana* reference genome (arabidopsis.org) with STAR v2.5.3 (Dobin *et al.*, 2013) using standards settings. Read counts of the genes were estimated with htseq-count (Anders *et al.*, 2015) after filtering for a mapping quality of at least 20% with samtools v1.5 (Li *et al.*, 2009).

To assess the RNA mapping quality for each gene a median coverage ratio was calculated. To do this, the depth of each nucleotide in each expressed transcript was divided by the median coverage of the gene across all samples. If this ratio was below 0.5, the depth for that gene was half or lower compared to the other samples and was considered a gene with low mapping quality in that sample. To get an estimate across the genome, the proportion of genes with low mapping quality was estimated for each sample. Samples with a proportion of 30% or more genes with low mapping quality were excluded from further analysis.

2.2.3 Analysis of responsive genes and functional enrichment

To identify genes that are important for the growth phenotype in a given environment, I first identified genes whose expression depends on the genetic background within a growth environment. As described in Figure 7, the mutants can show mismatching phenotypes compared to the WT. I investigated patterns of differential gene expression between genetic backgrounds to identify genes that are underlying these mismatches. To identify genes that are differentially expressed, I used DESEQ2 (Version 1.30.1) (Love *et al.*, 2014).

First, I compared the genotypes with matching environment (in HL: WT to *cop1 & spa1234*; in LL and competition: WT to *phyB*) and removed genes that were differentially expressed between these groups, since they are not responsible for the phenotypic difference in growth.

Then, I compared the expression of the reduced set in the WT to the mismatching mutant (in HL: *phyB*; in LL and competition: *cop1 & spa1234*) to identify genes with a significantly different expression related to the difference in growth phenotype.

The different categories might share some important genes related to growth. To check the overlap between genes in these categories, I plotted the overlap in gene identities using the upset function (Conway & Gehlenborg, 2019), which creates visualization plots of intersections between complex data. Furthermore, to assess the functions of the genes identified for each environment, I performed a GO enrichment of these genes as described before (2.1.5).

Trait-specific gene sets were identified with the GWAS described before. I used the results from 9 GWAS for the HLLL experiment for the traits FS, t50 and SL in HL, LL and the GxE and for 18 GWAS for the competition experiments for FS, Height, Diameter and Height in LD, ID and HD and the GxE. Additionally, I included the markers identified in the meta-analysis, which describe common signals across sets of traits.

To identify genes associated with the phenotypes, I considered all genes within +-10kb around moderately associated SNPs for each GWAS (p<1E-4). Tandem duplicates were removed as described before (2.1.5). The GWAS genes were filtered to only include genes that were expressed in the RNA-seq experiment. To estimate the overlap of genes identified with GWAS of individual traits and the genes identified with RNA-seq, I performed hypergeometric tests in R using the phyper function. To control for multiple testing, I used the false-discovery rate (FDR) in the p.adjust function in R.

2.3 *Cis*-regulatory divergence in F1-hybrids

Allele-specific expression (ASE) in crosses of *A. thaliana* genotypes between different regions and their parents was used to estimate the contribution of *cis*- and *trans*-regulatory divergence in gene expression.

2.3.1 Plant material and experimental setup

In total, 24 genotypes from four geographic regions were used to disentangle regional difference in growth (Table 5).

Table 5: Gentoypes used as parents for *cis*-regulatory divergence.

Information on the assigned name (M for Morocco, C for China, S for Sweden and E for Spain, with genotype numbers 1-6), Genotype name, numeric ID, population and location.

Name	Genotype	ID	Population	Latitude	Longitude
M1	IFr0	22002	Morocco	33.550	-5.175
M2	Elh2	35616	Morocco	31.472	-7.406
M3	Bab0	22008	Morocco	35.043	-5.024
M4	Taz0	22005	Morocco	34.092	-4.103
M5	Arb0	18513	Morocco	31.419	-7.526
M6	Zin9	18515	Morocco	35.453	-5.427
C1	Hwc-61	2204174	China	30.525	114.471
C2	Gwx-11	2204177	China	32.725	105.122
C3	Jjgs-30	2204161	China	26.755	114.310
C4	Ctl-62	2204176	China	29.823	106.056
C5	Zla-62	2204170	China	30.054	119.924
C6	Hnzjj-75	2204239	China	29.412	110.442
S1	Fjä1-5	6020	Sweden	56.06	14.290
S2	EkS-2	9369	Sweden	57.678	14.999
S3	Liarum	8241	Sweden	55.947	13.821
S4	T510	6109	Sweden	55.793	13.123
S5	Fly2-1	6023	Sweden	55.751	13.371
S6	Puk-1	9436	Sweden	56.163	14.681
E1	Se-0	6961	Spain	38.333	-3.533
E2	IP-Pan-0	9568	Spain	42.760	-0.230
E3	IP-Coc-1	9535	Spain	42.310	3.190
E4	Ts-5	6971	Spain	41.719	2.9306
E5	Evs-0	9845	Spain	40.480	-3.960
E6	IP-Pal-0	9567	Spain	42.340	1.300

I planned to cross each genotype to 2 genotypes from every other population in both directions (each genotype as seed donor/maternal plant), but some combinations did not work. In total, 79 F1 plants were generated, of which 67 were sequenced at least once (Table 26). Additionally, all 24 parental genotypes were sequenced, leading to 247 hybrid sequences and 127 sequences of the parents. The number of sequenced parents and hybrids is summarized in Figure 8.

	M	C	S	E
M	29			
C	42	32		
S	38	55	32	
E	40	48	4	33

Figure 8: Crossing scheme and sequenced transcriptomes.

The first column and row show the genotype origin (M for Morocco, C for China, S for Sweden and E for Espana/Spain). The diagonal (dark grey) shows sequences of the parents, the other numbers are the transcriptomes of crosses between genotypes from the regions in the first column/row).

In order to get the transcriptomes, the plants were grown in a randomized block design in HL conditions as described above. After 21 days (the average t50 in HL), 3-4 adult leaves were sampled per plant. For a first run in 2019, the material was immediately frozen in liquid nitrogen and transferred to -80°C afterwards. After RNA-quality issues in the samples after storage times longer than three months, we changed this protocol for a second run in 2020: Instead of freezing the leaves in liquid nitrogen, they were put into tubes with 1 ml of RNAlater (ThermoFischer, Germany) and were stored at -20°C.

2.4.2 RNA extraction and sequencing

RNA and DNA were extracted using the AllPrep DNA/RNA Mini Kit (QIAGEN, USA). For the first experiment, the DNA was used to test if the samples were the expected hybrids using a restriction enzyme digestion and Cleaved Amplified Polymorphic Sequences (CAPS) markers that were designed to be specific for either parental genotype. We used custom primers to amplify DNA around regions with different restriction enzyme cut sites between populations. The primers were designed to have a population cut site for either parent as control. The combinations of primers for specific crosses and the primer sequences are in Table 6. The amplified area was digested and visualized with a 0.8% agarose gel. A hybrid between the populations would show all 4 possible bands (2 fragments per population), while the parents only show 2 fragments. Thus, we could confirm that all the samples were crosses between the two populations, by heterozygosity at the site.

Table 6: Primer for CAPS digestion.

Each row shows a primer used for digestion, with name, parents that can be distinguished with the primer and restriction enzyme that was used and the sequences.

Primer_left	Primer_right	Parent1	Parent2	Restriction Enzyme	Sequence_left	Sequence_right
CEMS_Pvu_left	CEMS_Pvu_right	C	M, E, S	PvuII	CTTGAAACATTGAAGCTGGAGA	TGCAATGCTTCTATTTCGGA
MES_Eco_left	MES_Eco_right	M	E, S	EcoRI	TTCTGCCATTGGAGAAGCTC	TTGTCACACCAACGGCATG
SS_Pvu_left	SS_Pvu_right	S1	S4	PvuII	TGTGAATGAAACCTCTCTGCTG	GGCAAATCAGGAAGCGTTCT
EE5_Pvu_left	EE5_Pvu_right	E5	E2	PvuII	AACTTGGAGATTCGCCCGAT	GACAAAGCGACCCGTAGTTC
EE4_Eco_left	EE4_Eco_right	E4	E5	EcoRI	TTGAAGGCGATGGTGTTTCC	AACATGCTCGCTTGAACCAG
SE_Alu_left	SE_Alu_right	S	E	AluI	ACAAGTTGGGCCGAAATTAG	TTGTCCACAAGATCTCTAAA

RNA quality and quantity were checked with a Qubit 4 Fluorometer (Thermofisher Scientific, Germany) and a 2100 Bioanalyzer (Agilent, USA). Whole transcriptome sequencing for 374 plants was performed in 12 subsequent batches at the Cologne Center for Genomics (CCG, Table 26).

2.4.3 Allele specific expression analysis

Read processing

After FastQC quality check (www.bioinformatics.babraham.ac.uk/projects/fastqc/), the FastX-toolkit was used for sequence trimming and filtering. Low-quality nucleotides were removed from the 3' ends of the sequences (fastq_quality_trimmer -Q 33 -t20 -l 50). Sequences were reverse-complemented by fastx_reverse_complement, and 5' ends were cut following the parameter described above, before being reverse-complemented back to the original direction of reads. Reads with less than 90% bases above quality threshold (fastq_quality_filter -Q 33 -q 20 -p 90), and paired-end reads with a single valid end were removed.

Verifying the identity and integrity of each transcriptome

Given that a large number of samples were collected in 12 different trials, sample mislabeling can happen. To verify that samples were not mislabeled, we mapped each transcriptome to the Col-0 reference genome (TAIR10) using STAR with default parameters (Dobin *et al.*, 2013) and called SNPs using samtools (Li *et al.*, 2009). In parallel, all parental genomes were mapped to Col-0 (TAIR10) using BWA (Li & Durbin, 2009). We removed all sites with PHRED scores below 20, thereby excluding all multi- or poorly mapped reads. We used the function mpileup in bcftools to call SNPs for each parental genome and each transcriptome (Li *et al.*, 2009). On the basis of the parental genome, we predicted the SNP expected to be heterozygote in each F1 transcriptome and used this expectation to assign parental genome to each hybrid (and parental transcriptome). Of all samples, four did not match their predicted parents and were discarded. To test the integrity of each sequenced transcriptome library and ensure that differences in cDNA retro-transcription or RNA stability were not confounded with estimates of gene expression differences, we quantified variance in coverage across each transcript using a custom script. Most transcripts showed uniform coverage over 95% of annotated transcribed positions (Figure 35).

Read-mapping to each parental genome

We developed a pipeline that allowed identifying the reads specific of each parental allele while minimizing biases introduced by mapping to a unique reference genome. For this, we generated a pseudo-reference genome specific of each parent and mapped each

transcriptome twice, one to each of its parental pseudo-reference genome. First, whole-genome DNA short-read sequences of all parental genotypes were first downloaded from the SRA and EBI databases and mapped to the Col-0 reference genome (TAIR10) with the BWA MEM algorithm (Li & Durbin, 2009). Subsequently, SNPs were called with GATK (version GATK4.11, (Poplin *et al.*, 2017). With a custom R script, we filtered out indels, sites with SNP calling quality below 50, sites with more than 2 alleles and heterozygous sites (parental strain are expected to be 100% homozygotes), a pseudo-reference genome was created for each parent by replacing each polymorphic site in the Col-0 reference genome (TAIR10) by the variant identified in the parent. Transcriptome samples collected from F1 hybrids were mapped twice independently, once against each of the two parental pseudo-reference genomes with the same procedure. We then removed all sites with PHRED scores below 20, and called SNPs using bcftools, thereby generating two vcf files, one for transcript mapping to the first parent and one for transcript mapping to the second mapping (Li *et al.*, 2009). For allele-specific read-counts in the F1 hybrids, we counted reads of the allele of each parent based on the read depth index DP4 given at each variable position of the corresponding vcf file. This approach allowed maximizing the number of reads that can be counted and effectively prevented that biases in read mapping would inflate the count of one allele relative to the other. Since transcripts often contained multiple SNPs, we extracted allele counts for the SNP whose allelic ratio was the median among the ratios measured for all the SNPs of the gene.

To identify genes with *cis*-regulatory variation, we searched for genes with a significant change in ASE in at least one cross. For this, we used the glm function implemented in R, with the matrix of allele counts as dependent variable, and the identity of the F1 as independent variable, including the tray and the sequencing batch as co-variates and assuming a quasibinomial distribution of error. In this way, the effect of covariates tray and sequencing batch could be accounted for while estimates of allelic expression differences were extracted. We note that tray and sequencing batch had a significant effect on allele counts for only 1% and 0.5% of expressed genes. Fold-change differences in gene expression were estimated with a glm(readcount= 1, family= quasibinomial) for each F1. This

model tests whether the read counts are at equal proportion. Genes that were significantly different from an equal proportion were considered as ASE genes.

We identified four matrices depicting the expected pattern of ASE for each phylogenetic origin (ancestral in Africa, derived in China, derived in Spain or derived in Sweden). These matrices assigned a 1 to crosses where the allele counts were expected to show a significant departure from equal expression, and 0 otherwise (Figure 9). The phylogenetic origin of *cis*-regulatory change was inferred by maximum likelihood, competing the four models that tested the fit each to the matrix of contrasts given phylogeographic origin to the distribution of allelic expression difference in the set of 1-6 replicates of each of 10-12 F1 genotypes for each regional contrast.

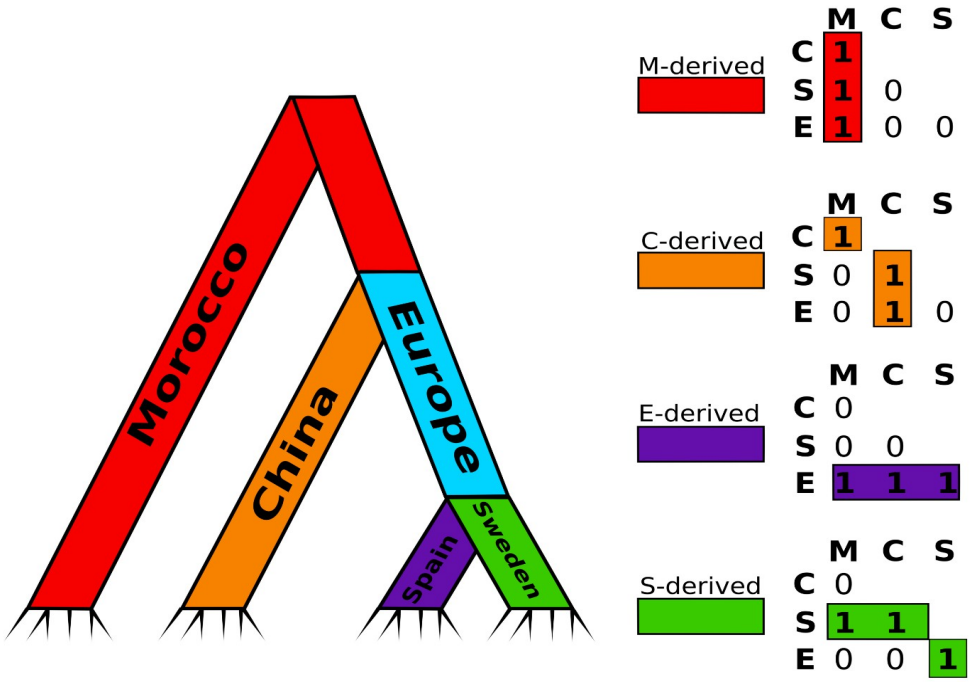

Figure 9: Estimation of regional differences in allele-specific expression (ASE).

The expected phylogeny of the genotypes is presented on the left, with Morocco as the most ancestral branch (red), followed by China (orange) and Europe (blue), which is split into Spain (purple) and Sweden (green). Region-specific ASE was estimated by comparing the different pairs of crosses. For genes with ASE specific to Morocco (M-specific), the allelic ratio was significantly different between Morocco and all other regions (marked with 1), but not significantly different between the other regions (marked with 0). The same comparison was conducted for all regions for each gene to identify which region explains the observed ASE best.

Contribution of *cis*-regulation to gene expression differences between parental lines

Transcriptome samples were collected for each parental genotype in the same experiment as the F1 transcriptome. Transcriptome sequence reads of each parent were mapped to their respective pseudo-genome reference using STAR with default settings (Dobin *et al.*, 2013). We used DESeq2 (Love *et al.*, 2014) to extract fold-change difference between the parental pairs of each F1 as well as its associated p-value, accounting for variance between trays. Sequencing batch had not effect and was not included. We then correlated the fold-change difference between parents with the allelic fold-change obtained in the hybrid.

Functional enrichment of genes with ASE

GO enrichments were computed as described before (2.1.5), for each set of genes with region-specific ASE comparing against all expressed genes. To estimate a threshold below which most enrichments can be considered non-random, I computed 1000 GO enrichments with random sets of 2000 expressed genes. The 0.01%-quantile of the p-value distribution of the enrichment of each GO category was used to estimate a conservative p-value threshold below which an enrichment can be considered non-random. Finally, a dendogram based on molecular function was plotted as described before.

3 Results

3.1 Polygenic adaptation of *A. thaliana* in response to light

The majority of the findings presented in this chapter have been published in (Wieters *et al.*, 2021).

3.1.1 Significant phenotypic variation between treatments and regions

Ecological relevance of rosette growth variation

On the basis of the more than 15,000 rosette images I collected, I used rosette diameter as a proxy to describe rosette growth variation with three parameters; each refers to the ways in which growth can differ among genotypes: i) the time until the exponential growth phase is reached (t50), ii) the speed of growth during the linear growth phase (slope) and iii) the final size (FS) at which rosette diameter plateaus at the end of the rosette growth phase (Figure 10, Table 27). Of these parameters, FS displayed the highest broad-sense heritability in plants grown under both regimes: high light (HL, H^2= 0.636) and low light (LL, H^2= 0.794) (Table 7). FS in HL conditions correlated positively with plant biomass (r= 0.267, p= 4.6E-5) and seedling growth (r= 0.372, p= 9.1E-7) in the growth chamber. FS measured in HL also correlated positively with plant diameter measured under natural light in the field (r= 0.263, p= 0.0009).

Table 7: Estimated heritabilities and pseudo-heritability from EMMAX.

Rows contain the input sample size (N), heritability (H^2) and pseudo-heritability for each trait, treatment and population. The p-value of heritability is the genotype effect of the mixed linear model.

Trait	Treatment	Population	N	Heritability	P-value	Pseudo-heritability
Final size	HL	Europe	203	0.636	<2.2E-16	0.651
	HL	Spain	119	0.556	<2.2E-16	0.328
	HL	NE	84	0.595	1.64E-11	0.546
	LL	Europe	201	0.794	<2.2E-16	0.565
	LL	Spain	117	0.758	<2.2E-16	0.595
	LL	NE	84	0.583	1.02E-11	0.366
	GxE	Europe	200	NA	NA	0.506

	GxE	Spain	117	NA	NA	0.642
	GxE	NE	83	NA	NA	0.235
t50	HL	Europe	203	0.143	1.50E-10	0.390
	HL	Spain	119	0.121	7.10E-06	1.000
	HL	NE	84	0.092	0.02	0.250
	LL	Europe	201	0.141	9.47E-12	0.507
	LL	Spain	117	0.131	2.24E-06	0.615
	LL	NE	84	0.131	0	0.006
	GxE	Europe	200	NA	NA	0.062
	GxE	Spain	117	NA	NA	4.54E-05
	GxE	NE	83	NA	NA	0.128
Slope	HL	Europe	203	0.081	9.33E-08	0.395
	HL	Spain	119	0.074	0	0.250
	HL	NE	84	0.100	0	0.541
	LL	Europe	201	0.110	1.28E-09	0.236
	LL	Spain	117	0.155	7.36E-07	0.610
	LL	NE	84	0.200	4.10E-05	0.038
	GxE	Europe	200	NA	NA	0.479
	GxE	Spain	117	NA	NA	0.454
	GxE	NE	83	NA	NA	4.54E-05

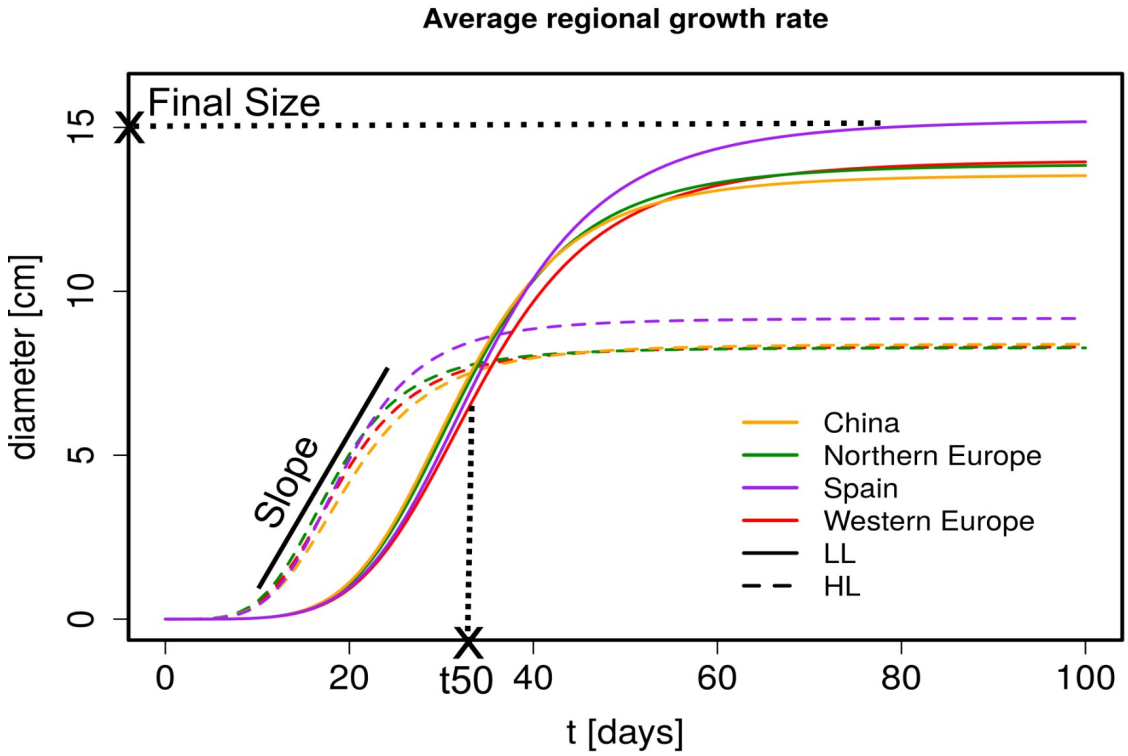

Figure 10: Regional growth rate estimates in HL and LL.

60

Estimated growth curves averaged over region (from drm function). The growth curves were estimated from diameter measurements at different time points. An illustration of the parameters that are estimated from these growth curves are included in the plot (Final Size is a diameter, t50 a time point and Slope the fold increase in the linear phase). HL (dashed line), LL (solid line), China (orange), Northern Europe (green), Spain (purple) and Western Europe (red).

Environmental plasticity has the strongest impact on plant growth variation

Light regimes revealed that plasticity has the strongest impact on rosette growth (Figure 10, MANOVA HL vs LL: F= 2275.37, df= 1, p<2.2E-16, Table 8). In plants grown under LL, the maximum growth rate was delayed and rosette growth plateaued at a larger size (Table 8, Figure 11).

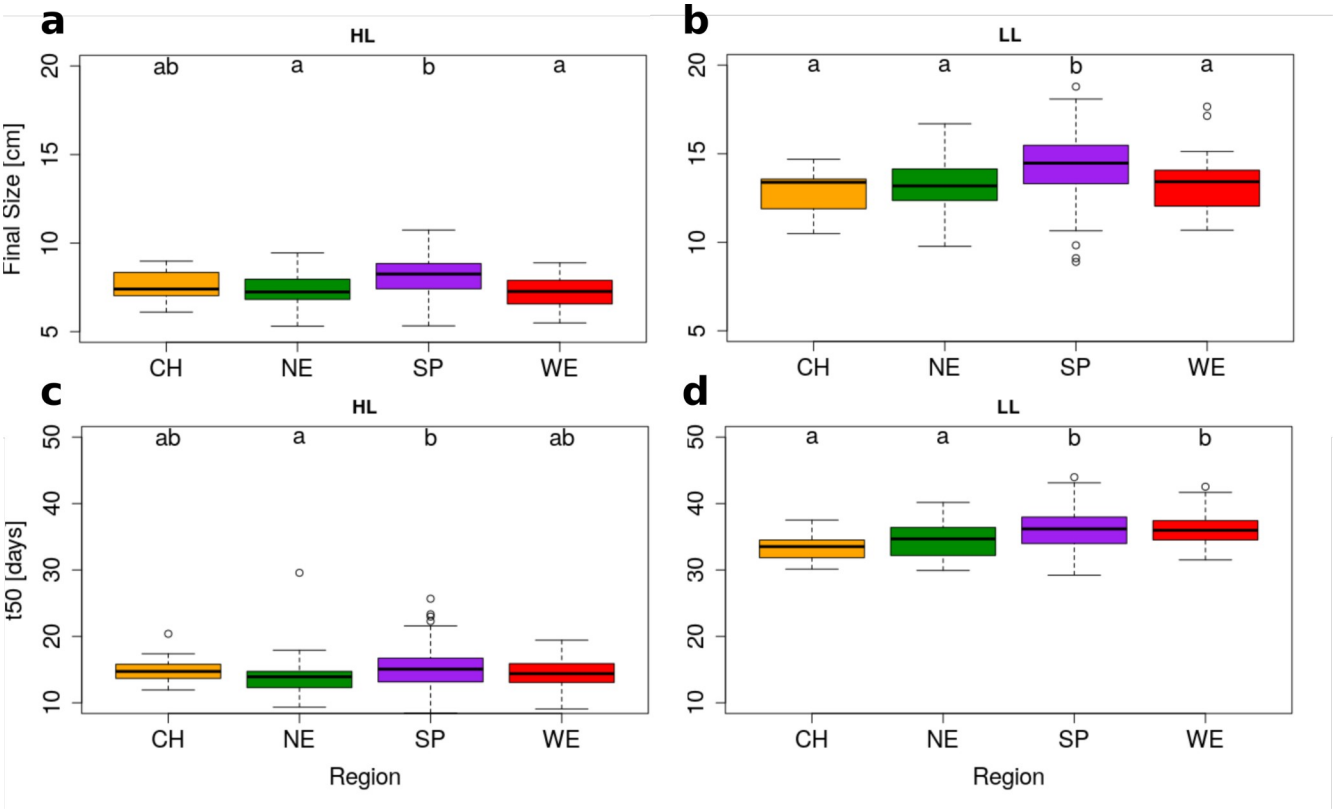

Figure 11: Significant regional differentiation of Final Size and t50 in HL and LL.

A. thaliana genotypes are grouped based on geographical origin. Box plots show regional variation in Final Size (upper row) and t50 (lower row) for HL (left) and LL (right). Groups that do not share a letter are significantly different according to Tukey's HSD (p<0.05). Region information: China (CH, n=20), Northern Europe (NE, n=58), Spain (SP, n=119) & Western Europe (WE, n=29).

Plants reached a larger diameter (and rosette area) by elongating their petiole and minimizing leaf blade overlap in LL, a reaction known as the shade avoidance response. This strong modification of leaf shape may explain the predominant impact of environmental variation I report here (Table 8). Nevertheless, I detected significant levels of genetic variation in growth

plasticity to light (F=2.0, df= 270, p<2.2E-16). I quantified growth plasticity as the individual deviation of the genotypic mean of each genotype in HL and LL from the average reaction of the population to the change in light regime (Figure 41).

Table 8: Multi- and uni-variate analyses of growth variation in response to light regime, genotype and their interaction.

The multivariate analysis was conducted on the estimates of FS, t50 and slope for all 270 genotypes in three replicates and accounting for block effects nested within light treatment.

	Multivariate analysis (MA-NOVA)			Final size		t50		Slope	
Response	df	F	p-value	F	p-value	F	p-value	F	p-value
Block	4	27.5	**< 2.2E-16**	30.15	**< 2.2E-16**	12.24	**9.8E-10**	30.50	**< 2.2E-16**
Light regime	1	7388.7	**< 2.2E-16**	15687.23	**< 2.2E-16**	9289.44	**< 2.2E-16**	34.01	**7.2E-9**
Genotype	279	3.6	**< 2.2E-16**	8.43	**< 2.2E-16**	2.51	**< 2.2E-16**	2.036	**< 2.2E-16**
Light*Genotype	270	2.0	**< 2.2E-16**	2.97	**< 2.2E-16**	1.59	**2.3E-07**	1.61	**4.4E-08**

Spanish genotypes show the most vigorous rosette growth

I found evidence for rosette growth variation across regions (MANOVA in Table 8, Figure 10 & Figure 11). Within Europe, Spanish genotypes reached the largest FS in both HL and LL plants (Table 8 & Table 29, MANOVA: F=16.37, df= 3, p= 5.35E-10). Although the growth slope did not differ significantly across regions, under HL conditions Spanish genotypes reached 50% of their FS (=t50) significantly later than the genotypes originating from Northern Europe (t50= 15.17 vs 13.79, respectively, GLHT z= 3.061, p= 0.011, Figure 11c). This effect was also observed for plants grown under LL conditions but I detected no regional difference in GxE (Figure 11d, Figure 12). Since Spain and Northern Europe did not differ in their average flowering time (Figure 36), the larger rosette size observed in Spain is not due to an extension of the duration of vegetative growth in this population.

Chinese genotypes show that growth rate variation is constrained in evolution

The growth rate of Chinese genotypes was comparable to that shown by most European genotypes (Table 29, Figure 11). Under LL conditions, Chinese genotypes had lower t50 and FS values only when compared to Spanish genotypes (Table 29, Figure 11). Under HL, genotypes from China did not differ significantly from those from any other region (Figure 11).

The analysis of Chinese genotypes indicates that the phenotypic evolution of rosette growth does not scale with the extent of genetic divergence (Fst between Europe and China is 0.057 on average, with a standard deviation of 0.147, and much greater than Fst between Spain and Northern Europe, KS test, D=0.39, p<2.2E-16).

The Chinese population was also the only one to show a difference in GxE (Figure 12). Compared to Spanish genotypes, Chinese genotypes displayed a GxE that was lower for t50 and higher for slope (t50: GLHT z= 2.748, p= 0.028; slope: GLHT z= -3.224, p= 0.006; Figure 12). When grown under the LL regime, these genotypes displayed a lower FS than genotypes from Spain. In contrast, within Europe, I observed no significant difference in the growth plasticity of plants in relation to light regime, despite the fact that Northern populations are exposed to lower average light intensity (Figure 3).

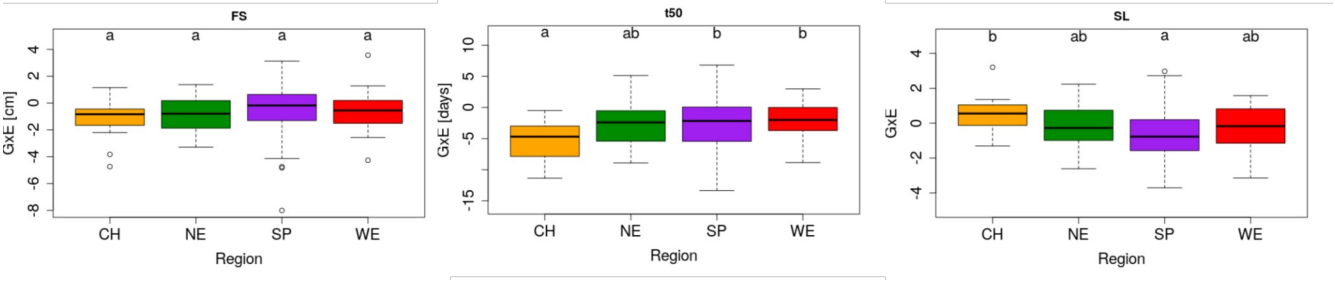

Figure 12: Regional differences for GxE for each trait.

GxE for FS (left), t50 (center) and Slope (SL, right). The phenotypic values are based on 217 genotypes of *Arabidopsis thaliana*. Groups that do not share a letter are significantly different according to Tukey's HSD (p<0.05). Region information: China (CH, n=14), Northern Europe (NE, n=58), Spain (SP, n=117) & Western Europe (WE, n=28).

3.1.2 Polygenic architecture of the genetic basis of growth

GWAS reveal only two SNPs significantly associated with rosette growth variation

I used GWAS to determine the genetic basis of variation in growth rate within Europe (Figure 37-39). The sample size (15) and strong population structure of Chinese genotypes precluded their inclusion in this analysis. Henceforth, I focused on the analysis of genetic variation within and among European populations. Overall, there were few significant genetic associations,

indicating that genetic variance for growth rate is generally polygenic. One SNP (chromosome 1, position 24783843) associated with t50 variations in LL plants (t50LL, effect size= -2.475, p= 2.6E-9, Figure 13, Table 9).

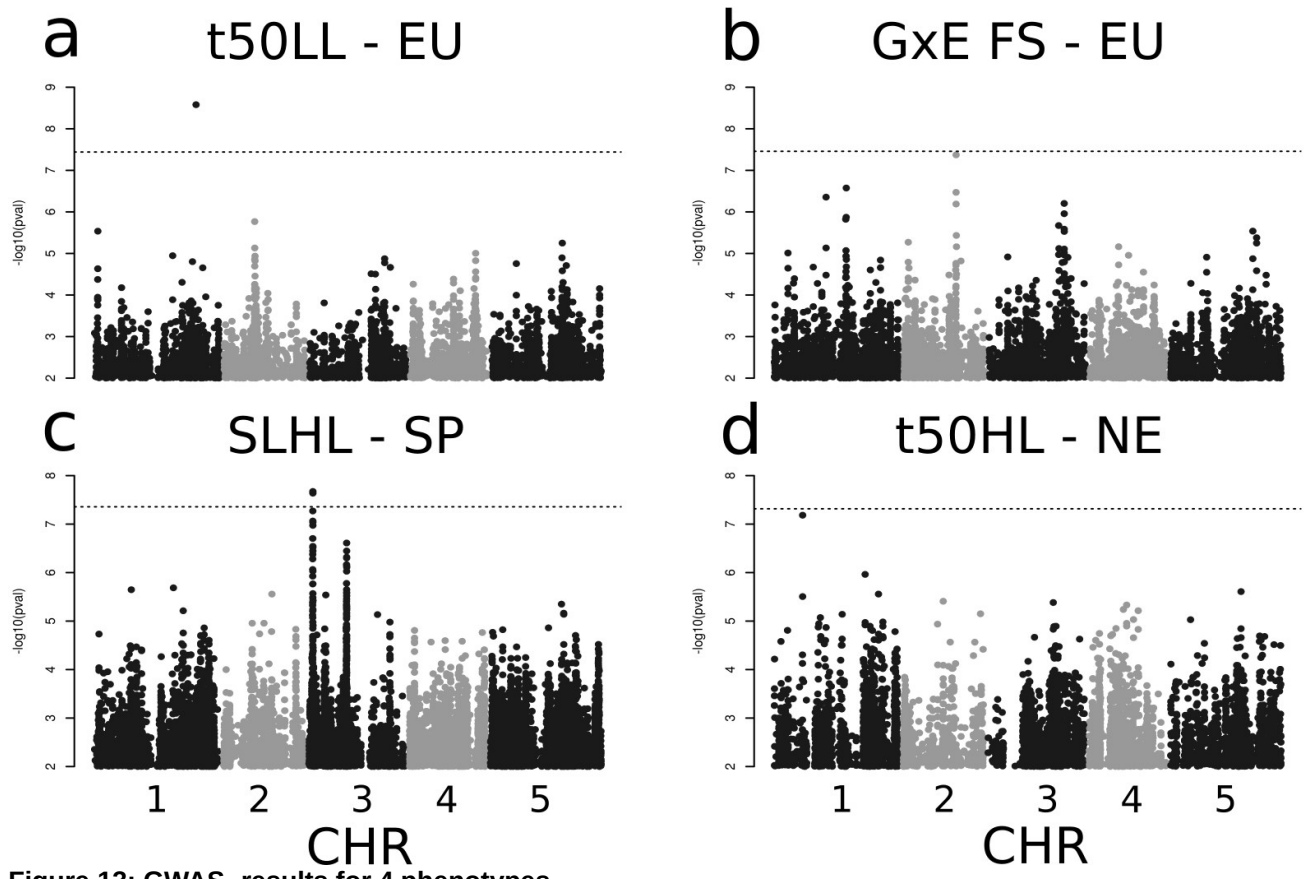

Figure 13: GWAS- results for 4 phenotypes.

Manhattan plots of GWAS of t50 in LL with all European genotypes (a), with a peak on chromosome 1, GxE of FS with all European genotypes (b) with a peak on chromosome 2, Slope in HL within Spain (c) with a peak on chromosome 3 and t50 in HL in Northern Europe (d) with a peak on chromosome 1. The dotted line shows the corresponding Bonferroni threshold adjusted for a p-value of 0.05.

Table 9: Associated SNPs for the different datasets, traits and environment.

For each associated SNP the chromosome, base, minor allele frequency (MAF), -log10(P) and effect size are given. The linkage disequilibrium (LD) for the focal SNP was estimated, with the number of SNPs and genes within the LD range. The p-value of two SNPs that exceeded the Bonferroni threshold are marked in bold, the others were just below threshold.

Dataset	Trait	Environment	Chromosome	Base Pair	MAF	-log10(P)	Effect size	LD range [kb]	#SNPs in LD	#genes in LD
Europe	FS	GXE	2	12818752	0.06	7.43	3.08	93	168	21
Europe	t50	LL	1	24783843	0.44	**8.58**	2.48	2	14	1
Europe	SL	HL	3	16408503	0.14	6.07	1.23	75	17	15
Spain	FS	GXE	1	12622218	0.08	7.66	3.1	73	8	17
Spain	FS	GXE	1	23431886	0.21	7.14	2.04	35	21	12
Spain	FS	GXE	2	12914087	0.08	6.44	2.99	70	12	23
Spain	t50	LL	2	9918415	0.44	6.04	2.52	20	28	4
Spain	SL	HL	3	951043	0.28	**7.67**	1.34	86	165	27
Spain	SL	HL	3	9165084	0.29	6.61	1.24	243	205	73
Northern Europe	FS	GXE	5	822188	0.47	6.84	1.36	40	66	12
Northern Europe	t50	HL	1	6909777	0.07	7.18	5.37	101	40	32
Northern Europe	SL	HL	2	15933315	0.17	6.83	1.59	96	1080	20
Northern Europe	SL	LL	3	5729894	0.13	6.28	1.05	192	60	53

A second SNP (chromosome 3, position 951043) was significantly associated with the slope of rosette diameter growth in HL plants within Spain (effect size= 1.229, p= 8.4E-7, Figure 13, Table 9) and was polymorphic only in the Spanish set of genotypes. This SNP was within a 1Mb DNA fragment showing strong local LD and enclosing 21 genes. Two additional SNPs were associated with GxE for FS and t50 in HL plants in Northern Europe, respectively, with p-values just below the Bonferroni threshold (Table 9). Yet, I found no SNP significantly associated with FS above the Bonferroni threshold, although FS was the most heritable trait (Table 7).

Polygenic scores and functional enrichments confirm the polygenic basis of growth variation

To confirm the polygenic basis of growth variation, I evaluated the biological relevance of marginally significant genetic associations. The associated sets were composed of 22 to 37 unlinked SNPs. I used their effect sizes to compute polygenic scores for each parameter

(Berg & Coop, 2014). First, I used 80% of the data to identify SNPs associating with rosette growth and test whether they are suited to correctly predict the phenotype of the remaining 20% of the data. This approach, however, did not yield significant predictions (rho= 0.07979094, p= 0.6189), which is not surprising because it usually does not perform well in structured populations (Berg *et al.*, 2019). A second approach to measure polygenic score accuracy was to use two of the three replicates to compute polygenic scores and test, whether they correlated significantly with the phenotype measured independently in the third replicate (Table 30A). The correlation was highest for FS measured in LL plants (Rho= 0.567, p= <2.2E-16). In fact, FS, the most heritable trait, could be predicted with the highest accuracy in plants grown under both light regimes (Table 30A). When I used random sets of SNPs as input, the computed polygenic scores were significantly correlated with the observed phenotype, indicating that population structure contributes to a significant but small fraction of the variance in polygenic scores. Nevertheless, with this third approach, I showed that polygenic scores computed on the effect sizes of SNPs associated at sub-significant level were markedly more correlated with the observed phenotype than those computed with random SNP sets (Table 30B).

A further question was, whether sub-significant associations could collectively reveal the specific molecular basis of each trait. I selected SNPs showing a sub-significant association (p<10E-4) and investigated functional enrichment among genes that mapped within 10kb of the SNP. To consolidate the confidence in the functional enrichment, I also pruned tandem duplicates from the annotated set, and determined a p-value threshold that was below the level of significance that can be obtained with GWAS on a permuted data set (see methods). Many traits showed functional enrichment within gene ontology (GO) categories, whose link to growth has been documented (Table 35). For example, genes associated with variation in FS, the most polygenic trait, were enriched among genes involved in the growth-related functions “cotyledon development”, “auxin polar transport” and “response to mechanical stimulus”(p= 0.0053 or lower). Additionally, several categories related to defense and stress reactions, such as “response to salt stress”, “response to chitin”, “regulation of defense response to fungus” and “negative regulation of defense response”, were enriched. Furthermore, I also

found that SNPs associated with FS plasticity to light are enriched among genes involved in the “shade avoidance response” (p= 0.0023), by which plants exposed to limited light conditions increase stem elongation (Filiault & Maloof, 2012; Ballaré & Pierik, 2017). Associated genomic regions included, for example, PHY RAPIDLY REGULATED 2 (PAR2, AT3G58850), a negative regulator of shade avoidance (Bou-Torrent *et al.*, 2008) or LONG HYPOCOTYL UNDER SHADE (BBX21, AT1G75540), a regulator of de-etiolation and shade avoidance (Holtan *et al.*, 2011).

As shown above, population structure impacts the results of GWAS and population structure outliers may drive this signal of association. Indeed, genes with elevated Fst reflecting population structure or even regional adaptation of (other) traits could create spurious associations with traits that have a distinct genetic basis but are also differentiated between regions. I thus verified that functional enrichment among genes with SNP associations were different from those observed among genes with elevated Fst. I determined enriched GO categories among genes in the vicinity of GWAS associated loci (p<10E-4) and among genes ranked by Fst between Spain and Northern Europe. I visualized overlaps in functional enrichment by clustering GO terms on the basis of the genes they shared (Figure 40). The enrichment based on Fst revealed three strongly enriched GO terms: “organ morphogenesis”, “circadian rhythm” and “virus-induced gene silencing” (p= 0.0009 or lower, Table 10).

Table 10: GO-enrichment of all genes ranked by their Fst or p-value of the closest SNP in a GWAS of the respective trait.

Shown are terms with an enrichment < 0.001. GO.ID and term give information on the enriched GO term. Nr_Genes is the number of genes in the respective term. The resultKS gives the Kolmogorov-Smirnov score for enrichment.

Trait	GO.ID	Term	Nr_Genes	resultKS
Fst	GO:0009887	animal organ morphogenesis	113	0.00069
	GO:0007623	circadian rhythm	171	0.00091
	GO:0009616	virus induced gene silencing	102	0.00091
FSHL	GO:0051567	histone H3-K9 methylation	183	0.00024
	GO:0006094	gluconeogenesis	164	0.00024
	GO:0032204	regulation of telomere maintenance	54	0.00025
	GO:0001676	long-chain fatty acid metabolic process	29	0.00027
	GO:0043247	telomere maintenance in response to DNA damage	52	0.00049

	GO:0016926	protein desumoylation	79	0.00052
	GO:0009651	response to salt stress	782	0.00066
	GO:0009630	gravitropism	154	0.00090
	GO:0035196	production of miRNAs involved in gene silencing	129	0.00093
	GO:0010565	regulation of cellular ketone metabolic process	44	0.00095
FSLL	GO:0007155	cell adhesion	92	0.00034
	GO:0044238	primary metabolic process	7924	0.00048
	GO:0009624	response to nematode	80	0.00067
	GO:0006012	galactose metabolic process	18	0.00073
	GO:0007062	sister chromatid cohesion	142	0.00089
GXEFS	GO:0010106	cellular response to iron ion starvation	116	0.00010
	GO:0006826	iron ion transport	120	0.00013
	GO:0010048	vernalization response	116	0.00024
	GO:0072523	purine-containing compound catabolic process	11	0.00026
	GO:0019747	regulation of isoprenoid metabolic process	11	0.00043
	GO:0006508	proteolysis	885	0.00046
	GO:0009616	virus induced gene silencing	102	0.00078
	GO:0009630	gravitropism	154	0.00086
GXESL	GO:0072523	purine-containing compound catabolic process	11	0.00030
	GO:0006468	protein phosphorylation	716	0.00048
	GO:0006096	glycolytic process	196	0.00078
GXET50	GO:0009793	embryo development ending in seed dormancy	576	0.00015
	GO:0009630	gravitropism	154	0.00022
	GO:0006468	protein phosphorylation	716	0.00024
	GO:0006857	oligopeptide transport	112	0.00026
	GO:0016926	protein desumoylation	79	0.00030
	GO:0000911	cytokinesis by cell plate formation	204	0.00040
	GO:0050665	hydrogen peroxide biosynthetic process	80	0.00057
	GO:0051567	histone H3-K9 methylation	183	0.00066
	GO:0009616	virus induced gene silencing	102	0.00066
	GO:0010143	cutin biosynthetic process	14	0.00094
SLHL	GO:0051225	spindle assembly	46	0.00033
	GO:0006468	protein phosphorylation	716	0.00040
SLLL	GO:0006468	protein phosphorylation	716	0.00021
	GO:0006306	DNA methylation	185	0.00022
	GO:0010050	vegetative phase change	70	0.00034
	GO:0009736	cytokinin-activated signaling pathway	83	0.00065
	GO:0009630	gravitropism	154	0.00069

	GO:0010090	trichome morphogenesis	152	0.00081
t50HL	GO:0009793	embryo development ending in seed dormancy	576	0.00034
	GO:0010112	regulation of systemic acquired resistance	12	0.00051
	GO:0048451	petal formation	72	0.00057
	GO:0048453	sepal formation	72	0.00057
	GO:0006346	methylation-dependent chromatin silencing	120	0.00093
	GO:0031048	chromatin silencing by small RNA	118	0.00093
	GO:0030048	actin filament-based movement	82	0.00098
t50LL	GO:0010638	positive regulation of organelle organization	151	0.00022
	GO:0000911	cytokinesis by cell plate formation	204	0.00027
	GO:0009630	gravitropism	154	0.00078
	GO:0045010	actin nucleation	103	0.00082
	GO:0006306	DNA methylation	185	0.00090
	GO:0006508	proteolysis	885	0.00095

Different regional patterns of directional allele frequency shift

Within the populations, I tried to identify patterns of directional selection, by looking at the symmetry of effect sizes at low and high frequencies within population. To illustrate this, I created “smile plots”, that show the effect sizes as a function of frequency for moderately associated SNPs. The “smile” pattern in these plots can be observed because effect sizes are smaller at intermediate frequencies, while they are larger at the extremes. Without directional, selection the sides at low and high frequencies are expected to be symmetric. Asymmetric patterns can be an indication for directional shifts towards larger or smaller phenotypes for a given trait. There are differences in symmetry between Spain (Figure 14) and Northern Europe (Figure 15).

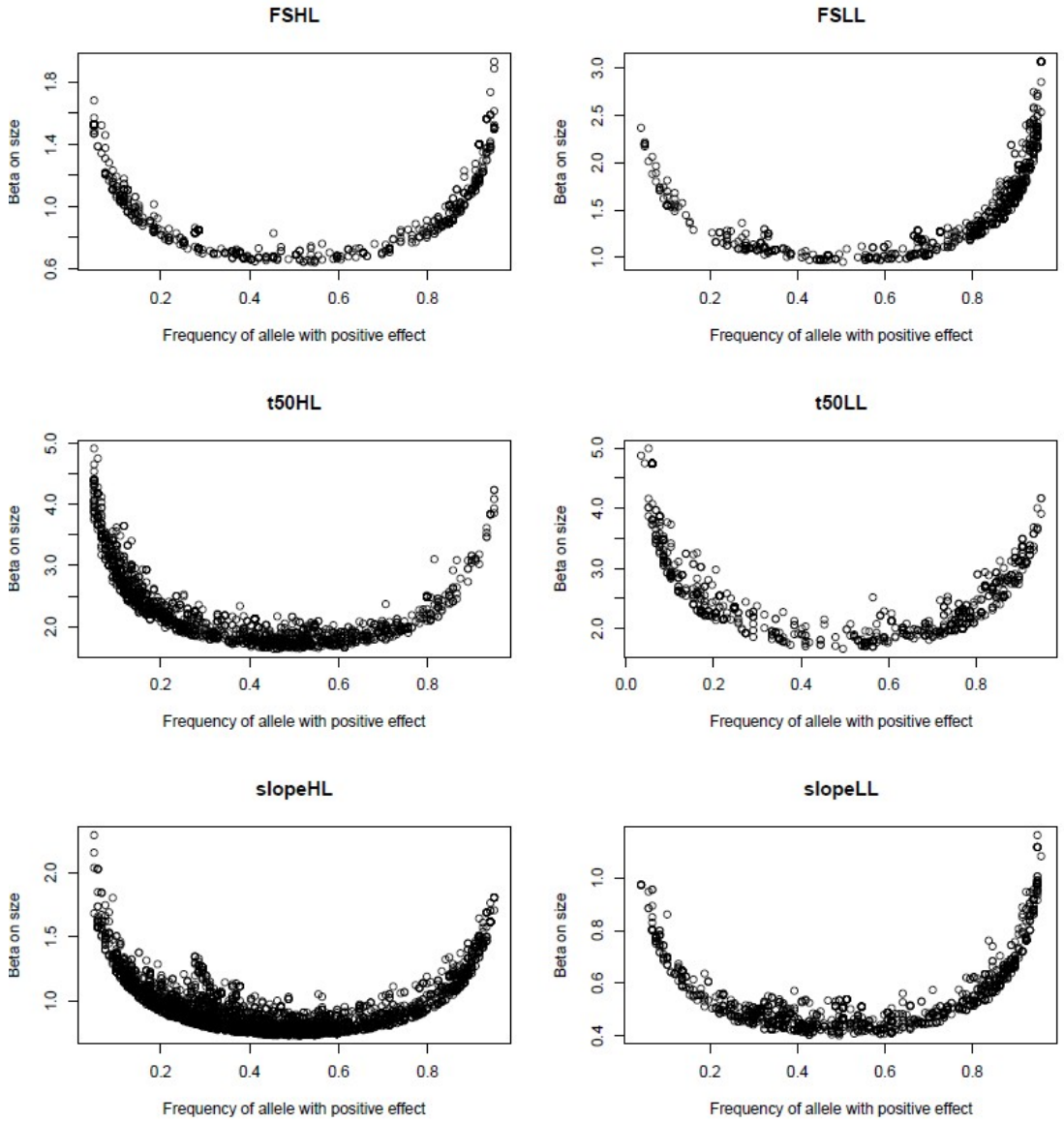

Figure 14: Smile plots within Spain.

Plots of the effect size of SNPs with MAF>0.05 and p<0.001 versus the frequency of the effect increasing allele for 115 individuals from Spain. Traits in HL are in the left and LL in the right column. FS in the first, t50 in the second and SL in the third row.

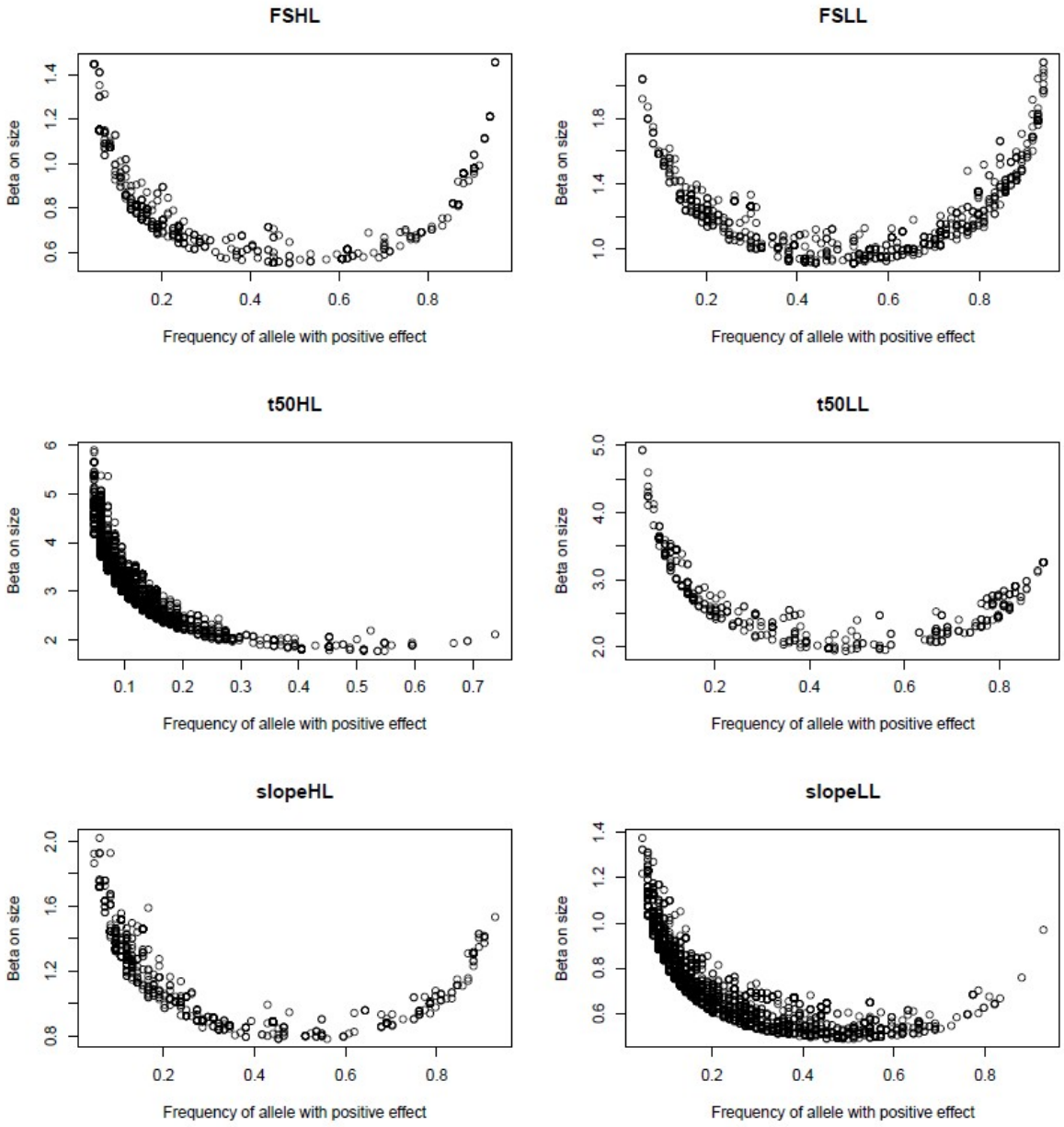

Figure 15: Smile plots within Northern Europe.

Plots of the effect size of SNPs with MAF>0.05 and p<0.001 versus the frequency of the effect increasing allele for 85 individuals from Northern Europe. Traits in HL are in the left and LL in the right column. FS in the first, t50 in the second and SL in the third row.

The smile plots for Spain are relatively symmetric, with SNPs on both sides of the frequency distribution, while the smile plots within Northern Europe show asymmetries towards low frequencies for t50 in HL and SL in LL.

Illustration of a population structure association

The light environments chosen for this experiment were of interest, because they in part reflect the natural variation in radiation between North and South Europe (Figure 3). So, I investigated, if the variation within the "home" environment of each region could give an interesting signal. A GWAS of these "matching home" phenotypes (HL for Spanish and LL for Northern European genotypes) can illustrate how loci with strong population structure can be detected with association studies (Figure 16).

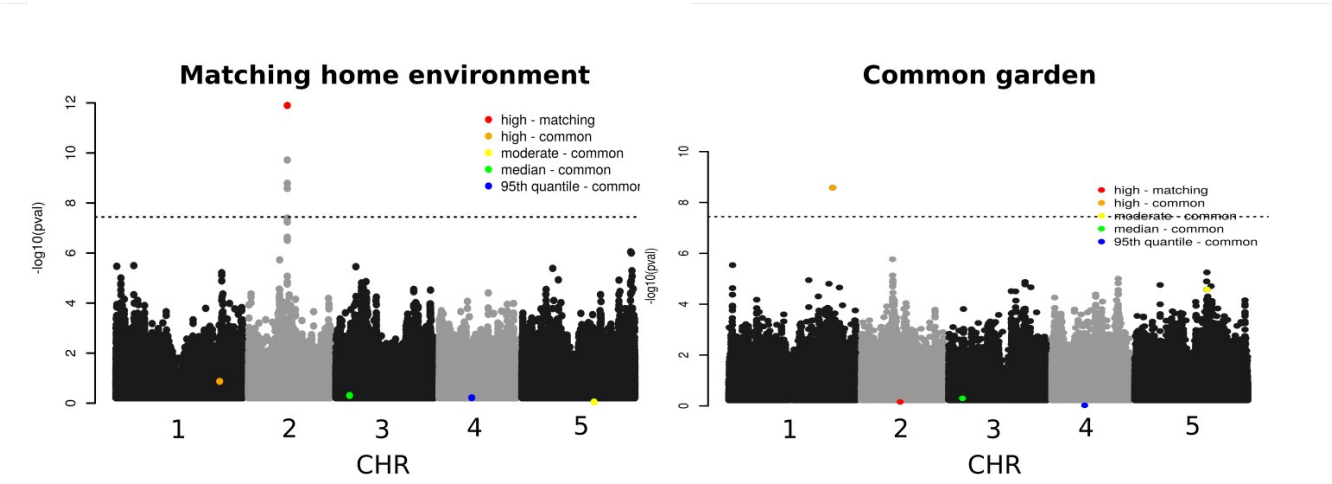

Figure 16: Manhattan plots of t50 in matching home environments or for t50 in a Common garden with LL.

On the left side Manhattan plot of a GWAS with 203 genotypes, where the phenotype of t50 in HL was assigned to 119 individuals from Spain and the phenotype of t50 in LL to 84 individuals from Northern Europe, mimicking their natural light environment. On the right side the GWAS in a common garden is plotted for comparison (see also Figure 13). Per chromosome a representative SNP was colored to compare association signal between the GWAS plots. The SNP colored in red is the peak for matching home environment, while the orange SNP is the peak for the common garden. The other colors represent SNPs with different strength of association in common garden, either above the moderate p-value threshold of 0.0001 (yellow), the median p-value (green) and the 95th-quantile of -log10(P) (blue). The dotted line represent the Bonferroni- corrected threshold.

The GWAS of the matching home environment unraveled a different architecture than the GWAS for the common garden in LL, where SNPs that were high and moderate in the common environment had a low association in the matching home environment. The GWAS with matching home environment had a peak around the SNP at base pair 9305610 on Chromosome 2 (MAF= 0.419, p= 1.26E-12) with 7 genes in proximity. One of them is RIBONUCLEOTIDE REDUCTASE 1 (RNR1, AT2G21790), which is involved in pollen DNA degradation (Tang *et al.*, 2012). Mutants in this gene show degraded pollen and a reduced germination rate in the offspring (Tang *et al.*, 2012). Another gene in proximity is ESSENTIAL MEIOTIC ENDONUCLEASE 1A (EME1A, A2G21800), for which mutants show defects in leaf development and chloroplast division (Garton *et al.*, 2007). Another interesting gene in that region is the not specifically characterized AT2G21820, which is described as a seed maturation protein, that was up-regulated under drought conditions (Zhang *et al.*, 2008).

Looking at the allele frequency of the SNP, the Col-0-allele was predominantly present in NE (80 of 84 individuals), while the alternative allele was almost exclusively present in SP (114 of 119). When combining this with the non-overlapping phenotypes of t50 in HL and LL (t50 in HL is smaller than any t50 in LL) this creates a strong association signal of this SNP. In the common garden measurement this signal is gone.

This was also observed for FS with values in HL for SP and values in LL for NE. For this, all SP individuals had a larger FS value than NE individuals, which resulted in a clear peak at the same SNP as for t50 (Chromosome 2, position 9305610), which falls on the SNP with an Fst of 0.785 between these populations (Figure 17).

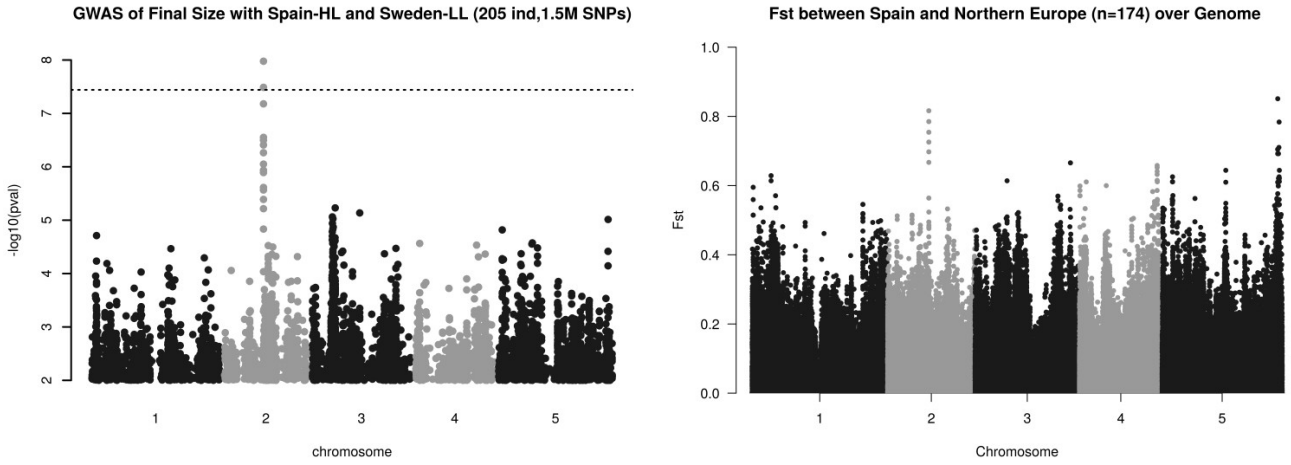

Figure 17: Manhattan plots of FS in matching home environments and Fst between SP and NE.

On the left side Manhattan plot of a GWAS with 203 genotypes, where the phenotype of FS in HL was assigned to 121 individuals from Spain and the phenotype of FS in LL to 84 individuals from Northern Europe, mimicking their natural light environment. The dotted line represent the Bonferroni- corrected threshold. The right side contains an Fst plot of 174 genotypes from unique locations in Spain and Northern Europe.

3.1.3 Signals of local adaptation of growth

No association between per-individual burden and growth

No significant difference was detected in total number of loss-of-function (LOF) mutations per genome in Northern Europe compared to Spain (GLHT: z= 0.634, p= 0.526, Figure 18). In addition, I detected no significant correlation between the number of LOF alleles per genome and the average FS in HL or LL conditions within Europe (r in HL= 0.079, p= 0.262, r in LL= 0.029, p= 0.684). Furthermore, I observed no significant difference in growth between Northern European and Chinese populations, despite their significantly higher burden of LOF alleles per genome (GLHT China versus Northern Europe: z= -20.259, p= <1E-4, Figure 19) ((Xu *et al.*, 2019).

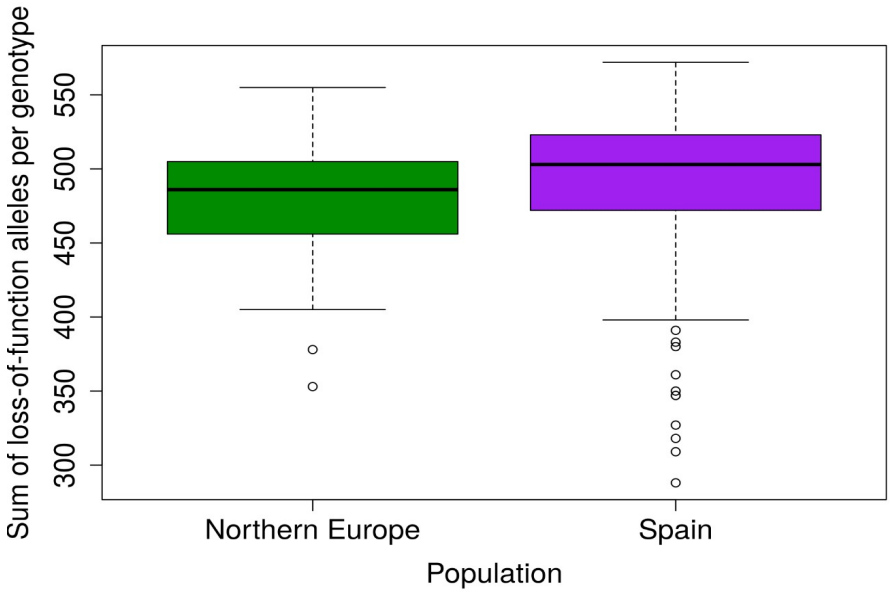

Figure 18: Loss-of-function alleles per population in Northern Europe and Spain.

Based on data from Monroe et al. (2018). The sum of LOF alleles per genotype for Northern Europe (green, n= 82) and Spain (purple, n= 118). The regions were not different from each other (GLHT: z= 0.634, p= 0.526, negative binomial distribution).

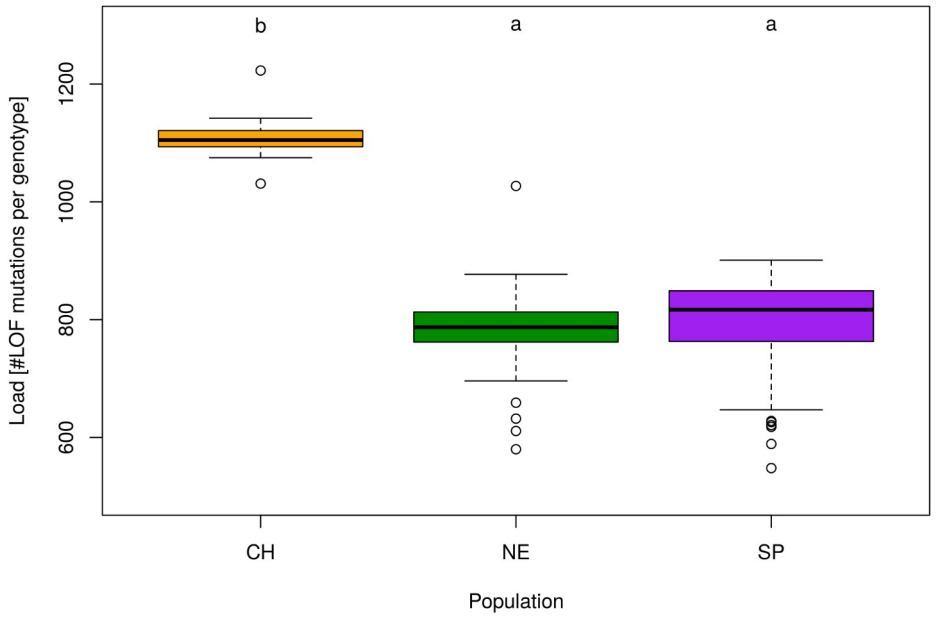

Figure 19: Loss-of-function alleles per population for China compared to Europe.

Based on data from Xu et al. (2019). Boxplot of the sum of LOF alleles per genotype for each region. Boxplots with different letters are significantly different according to Tukey's HSD ($p<0.05$). Region information: China (CH, orange, n= 19), Northern Europe (NE, green, n= 82) & Spain (SP, purple, n= 118).

A lower growth rate might also be associated with a small subset of LOF mutations. To test this hypothesis, I investigated genetic associations between LOF alleles and the three growth parameters. This analysis is similar to a GWAS, but utilizes information on approximately 2500 genes that have at least one LOF allele in any of the 1001 Genomes lines (1001 Genomes Consortium, 2016; Monroe *et al.*, 2018). I detected no association between LOF alleles and FS, yet there was a significant association of LOF variation at gene AT2G17750 with variation in both t50 in LL plants and t50 plasticity (Figure 20, effect size= -3.542, p= 7.49E-6, gene-Fst= 0.113, and effect size= -4.470, p= 4.99E-6 for t50 and t50 plasticity, respectively). AT2G17750 encodes the NEP-interacting protein (NIP1) active in chloroplasts, which was reported to mediate intra-plastidial trafficking of an RNA polymerase encoded in the nucleus (Azevedo *et al.*, 2008). NIP1 controls the transcription of the *rrn* operon in protoplasts or amyloplasts during seed germination and in chloroplasts during later developmental stages (Azevedo *et al.*, 2008). The LOF variant is present primarily in Northern Europe (MAF= 16 and 0.8% in Northern Europe and Spain, respectively), but is unlikely to be deleterious: it correlates with a decrease of t50, which is a faster entry in the exponential growth phase indicative of increased growth vigor (Figure 20).

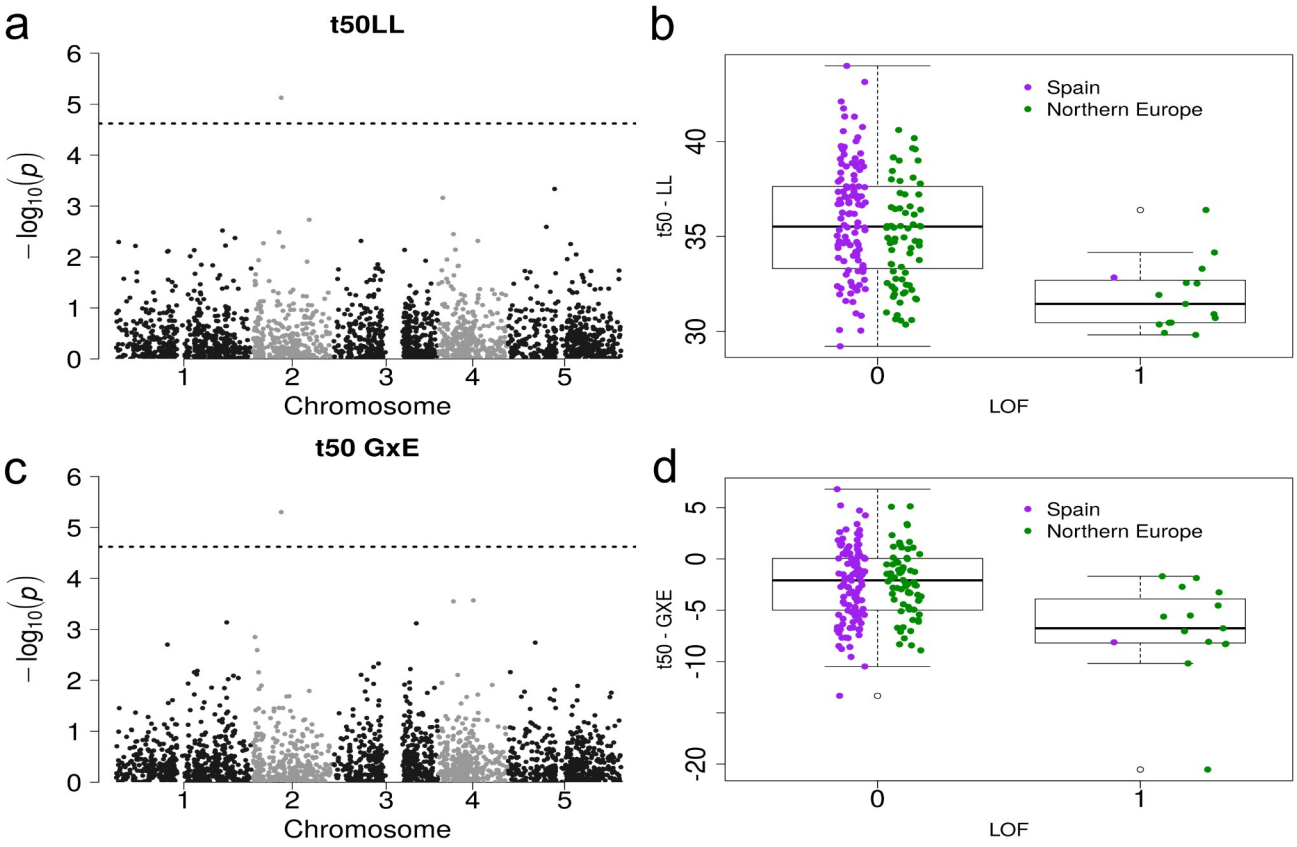

Figure 20: Loss-of-function association and phenotype of t50 in LL/GxE.

Manhattan plot of a GWAS with LOF alleles and t50LL (a) and t50GxE (c) as input phenotypes with the same association (AT2G17750) above the Bonferroni threshold (dashed line). Boxplot of the phenotype of t50LL (b) and t50GxE (d) versus the allele state at AT2G17750 (0 means functional, 1 is a LOF). The colors separate the populations into Spain (purple) and Northern Europe (green).

In an attempt to characterize the phenotype of this mutant in a common genetic background, we (Franziska Geuchen, a BSc. Student and me) investigated RNAi-silenced mutants of NIP1 and T-DNA mutants of the interacting polymerase RPOTmp (Geuchen, 2021).

T-DNA mutants of RPOTmp displayed a significantly smaller FS (Mutant vs WT, p= <2E-16) and larger t50 (Mutant vs WT, p-value= <2E-16) (Figure 21) (Geuchen, 2021).

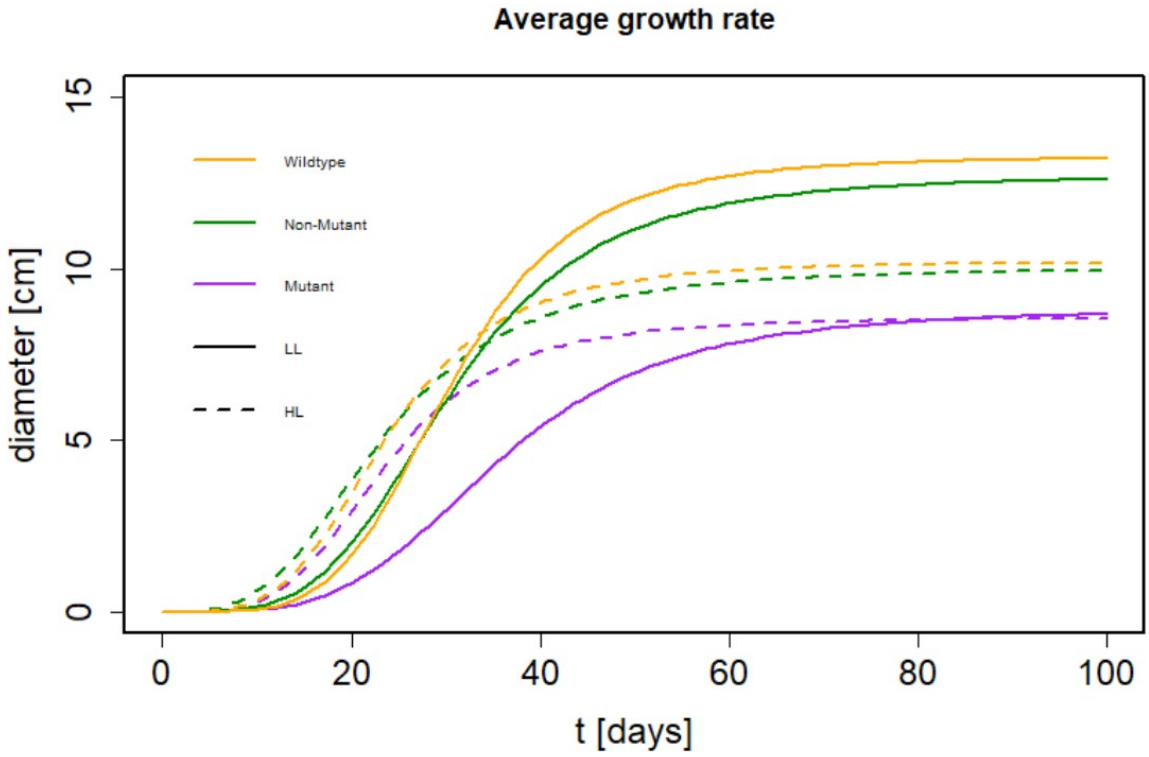

Figure 21: Growth rate estimates in HL and LL.

Estimated growth curves averaged over WT (orange), non-mutant (green) and mutant genotypes for RPOTmp. The growth curves were estimated from diameter measurements at different time points. Figure from Geuchen 2021.

RNAi-lines of NIP1 in Col-0 background had a small, but significant impact on growth until day 53 in HL and LL (RNAi line vs WT: F= 3.189, p= 0.0467). The growth curves could not be finished in time, so the impact on t50, where we discovered the association is not described here.

FS variation might reflect local adaptation at the regional scale

I used the 14 to 47 LD-pruned set of SNPs associating in GWAS at a sub-significant level (p<1E-4) to compute polygenic scores for each genotype and each trait, and used Qx, a summary statistic that quantifies their variance across locations of origin. A Qx value outside of neutral expectations inferred from the kinship variance in the population indicates excess differentiation of polygenic scores, as expected if individual populations evolved under

divergent selection (Berg & Coop, 2014). We observed that all traits displayed a strongly significant Qx (Table 11).

Table 11: Results from Polygenic adaptation test after Berg & Coop (2014).

The trait column contains the respective traits that were used as input and a random set of equal size which was used to predict FSHL (FS in HL conditions) in the last row. Qx is the test statistic for a signal of polygenic adaptation using all phenotypic data. Rho are the results from a spearman correlation of Z-scores predicted versus the input phenotypes. The regional Z-values for Northern Europe and Spain are the region specific effect on the trait. P-values from each test are in parentheses. The SNPs column contains the number of input SNPs for the estimation of polygenic adaptation (after pruning).

Phenotype	Qx (p)	Rho (p)	Northern Europe Z (p)	Spain Z (p)	SNPs
FSHL	**732 (<0.001)**	0.793 (<2.2E-16)	**-8.75 (<0.001)**	**6.88 (<0.001)**	27
FSLL	**908 (<0.001)**	0.781 (<2.2E-16)	**-4.72 (0.015)**	**4.74 (0.008)**	34
GXEFS	**1049 (<0.001)**	0.749 (<2.2E-16)	2.372 (0.092)	-0.373 (0.97)	46
t50HL	**1442 (<0.001)**	0.794 (<2.2E-16)	**-6.89 (<0.001)**	**7.69 (<0.001)**	47
t50LL	**826 (<0.001)**	0.854 (<2.2E-16)	**-5.36 (0.0013)**	**7.62 (0.0007)**	26
GXEt50	**394 (<0.001)**	0.614 (<2.2E-16)	1.04 (0.399)	-1.36 (0.233)	14
SLHL	**882 (<0.001)**	0.847 (<2.2E-16)	**-5.23 (<0.001)**	**4.64 (<0.001)**	28
SLLL	**1209 (<0.001)**	0.759 (<2.2E-16)	**4.49 (<0.001)**	**-6.18 (<0.001)**	35
GXESL	**463 (<0.001)**	0.644 (<2.2E-16)	**2.46 (0.0193)**	**-4.94 (<0.001)**	19
Random_FSHL_SNPs	206 (0.435)	0.391 (1.089E-08)	-3.02 (0.0567)	2.72 (0.0547)	27

Interestingly, FS measured in HL (FSHL) and t50 measured in LL (t50LL) displayed polygenic scores that differed significantly between regions (p= 0.0162 and 0.0309, respectively, Figure 41). Thus I further tested whether, at the phenotypic level, regional differentiation in growth rate departed from neutral expectations. First, I investigated whether variants associated with phenotypic variation in rosette diameter showed increased genetic differentiation. Compared to the Fst distribution of 10 000 random sets of SNPs, the 95th percentile of 1360 SNPs associating with all three parameters was always higher (p<10E-4).

Differentiation for FSHL plants was marginally more differentiated than predicted under neutral conditions (Qst= 0.325, p= 0.085, Figure 22). The other parameters did not depart from neutrality (Qst ranging from 0.029 to 0.27, min p= 0.11, Figure 22).

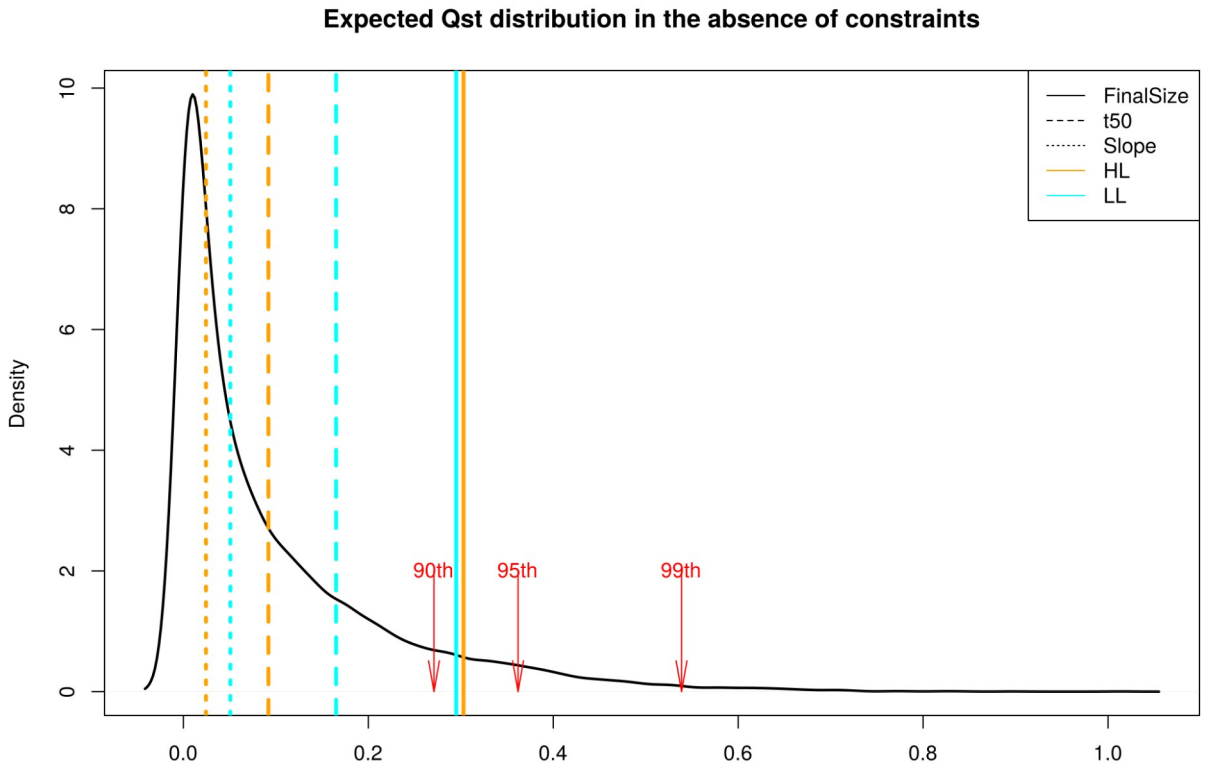

Figure 22: Qst for growth traits in HL and LL.

Expected distribution for quantitative trait differentiation between the Spanish and Northern European population. The expectation is based on a multivariate normal distribution assuming a neutral trait with polygenic basis. Vertical lines indicate observed Qst for the individual growth parameters, FS (Solid line), t50 (Dashed line), slope (Dot line), in HL (orange) and LL (cyan). The red arrows show the 90th, 95th and 99th percentiles of the distribution.

I used the Fst between Northern Europe and Spain as an estimate for nucleotide differentiation and compared it to the differentiation of these populations at the phenotypic level (Qst) (Kronholm *et al.*, 2012; Leinonen *et al.*, 2013; Dittberner *et al.*, 2018). For FS and t50, the Qst was significantly greater than genetic differentiation at 95% of single nucleotide (Table 12).

Table 12. FS and t50 quantitative differentiation (Qst) exceed differentiation given by single SNPs.

Qst for each trait measured in HL and LL plants. Linear mixed models were used to quantify the ratio of genetic variation between versus within Spain and Northern Europe (Qst). The 95th percentile of the distribution for single SNP Fst between these two regions was 0.205. Permutations confirmed that this test is conservative (see methods).

Trait	Qst	Percentile of Fst
FSHL	0.379	96.57
FSLL	0.282	95.80
t50HL	0.300	95.95
t50LL	0.189	94.79
SLHL	0.081	93.23
SLLL	0.010	91.62

Other climatic components like temperature could also have strong effects on growth differences between populations. Nevertheless, I detected only weak correlations between growth variation and temperature at the location of origin (Figure 23, Table 36).

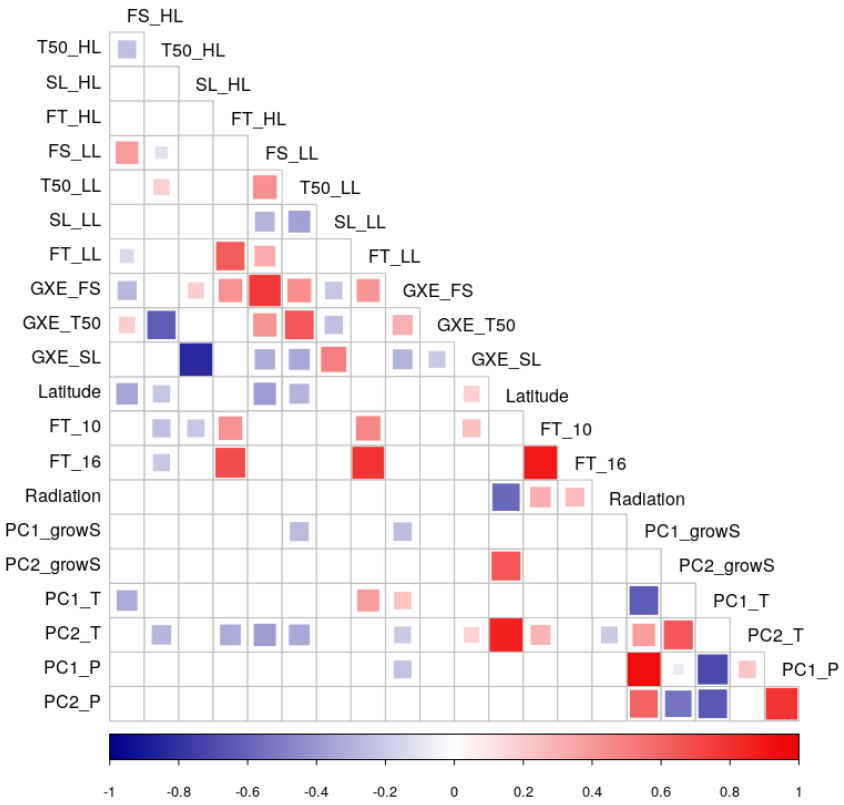

Figure 23: Correlation of phenotypic traits and climate.

Pearson correlations for each pair of traits/climatic variable. Colored boxes show significant correlations ($p<0.05$ after multiple testing correction (FDR) correction) and correction for populations structure (lmekin)) for 195 genotypes across experiments. The significance is illustrated by box size (larger box represents lower p-values) and the color shows the direction and strength of correlation. Abbreviations are: HL= high light, GxE= Genome x Environment interaction, LL= low light, SL = Slope, FT= Flowering time, FS= Final size, DiamFieldM2= Diameter in field conditions after 2 Months, Biomass21d= Biomass in controlled (HL) conditions after 21 days, Radiation in kJ/m²/day, PC1/2_growS= Principle component 1 and 2 of all climatic data in the estimated growing season (explaining 88.7 and 10.7% of the variance), PC1/2_T= Principle component 1 and 2 for climatic variables related to temperature (explaining 98.1 and 1.3% of the variance), PC1/2_P= Principle component 1 and 2 for climatic variables related to precipitation (explaining 89.8 and 8.22% of the variance).

3.2 Density-dependent growth under different environmental conditions

3.2.1 Significant effect of density on growth

We designed three separate experiments to measure variation in the growth response of *A. thaliana* genotypes to above- and below-ground competition. In total, more than 5900 plants were scored for 17 different phenotypes presented in this thesis (Table 27 & Table 28). I estimated the broad-sense heritability (H^2) for a selection of potential traits of focus in the field experiments (Table 13). The heritability for the experiment in the growth chamber could not be estimated, because it was conducted without replicates.

Generally, traits related to the life history had the highest heritability in both experiments (Table 13, bolting & germination, flowering days), with the exception of number of fruits in below-ground and the number of siliques and branches in above-ground competition. In below-ground competition the heritability for most traits was higher in HD conditions (e.g.: diameter in December with 0.535 in HD vs 0.408 in LD), but reduced for traits scored at the end of the growth season (diameter measurement in March, size difference between December and March, root length) (Table 13).

In above-ground competition most traits had a higher heritability in LD, especially at the end of the growth season (e.g.: FS with 0.215 in LD vs 0.106 in ID & 0.137 in HD). Some life history traits like flowering time displayed higher heritabilities in the competition treatments (e.g.: Flowering days with 0.936 in ID & 0.954 in HD vs 0.802 in LD).

Table 13: Broad-sense heritability (H^2) of Traits in the field experiments.

The first part is the first field experiment with below-ground competition, the second and third part the diameter and other measurements in the second field experiment with above-ground competition. Traits: 1) Germinated seeds per pot; Diameter in November- March; Leaf number (after 39 days); Root length (at the end of the experiment); Bolting time; largest measured diameter (DiameterMax); Difference in diameter between March and December (GrowthDecMar); Number of siliques of the genotypes that bolted (Fruits_bolted); Survival (1, if the plant was alive in March); 2) Diameter in October- April; 3) Height at flowering; Flowering time; Final height; Number of branches of the focal plant; Number of Siliques of the focal plant; Final Size; t50; Slope. HD= High density; ID= Intermediate density; LD= Low density

1)	Trait	Condition	N	H^2	2)	Trait	Condition	N	H^2	3)	Trait	Condition	N	H^2
	Germination	HD	348	0.812		DiameterOct	HD	254	0.034		Height_Flow	HD	234	0.363
		LD	348	0.645			ID	251	0.063			ID	227	0.485
	DiameterNov	HD	293	0.49			LD	299	0.058			LD	287	0.16
		LD	317	0.486		DiameterNov	HD	257	0.051		Flowering_Days	HD	234	0.954
	DiameterDec	HD	293	0.535			ID	253	0.036			ID	227	0.936
		LD	319	0.408			LD	301	0.038			LD	287	0.802
	DiameterJan	HD	280	0.396		DiameterDec	HD	255	0.105		Height_Final	HD	201	0.124
		LD	307	0.36			ID	253	0.108			ID	185	0.171
	DiameterFeb	HD	280	0.356			LD	301	0.129			LD	240	0.161
		LD	307	0.193		DiameterJan	HD	257	0.089		Branches_Focal	HD	200	4.67E-05
	DiameterMar	HD	279	0.184			ID	253	0.085			ID	185	0.086
		LD	307	0.225			LD	301	0.16			LD	240	0.283
	Leafnumber	HD	293	0.555		DiameterFeb	HD	257	0.105		Siliques_Focal	HD	199	0.006
		LD	314	0.335			ID	253	0.115			ID	185	0.017
	RootLength	HD	293	0.006			LD	301	0.18			LD	240	0.104
		LD	313	0.039		DiameterMar	HD	257	0.129		FS	HD	257	0.137
	Bolting	HD	279	0.976			ID	253	0.068			ID	253	0.106
		LD	309	0.978			LD	301	0.219			LD	298	0.215
	DiameterMax	HD	293	0.604		DiameterApr	HD	257	0.104		t50	HD	257	0.015
		LD	322	0.315			ID	253	0.06			ID	253	0.047
	GrowthDec-Mar	HD	279	0.243			LD	301	0.153			LD	298	0.116
		LD	306	0.478							SL	HD	257	0.011
	Fruits_bolted	HD	279	0.027								ID	253	0.013
		LD	309	1.56E-14								LD	298	0.102
	Survival	HD	348	0.658										
		LD	348	0.654										

The traits are highly correlated with each other and often describe similar phenotypes (Correlations in Table 31-34). I am interested in signals of adaptation for growth, especially at the end of the growth season, so I decided to focus on the diameter in December for below-

ground and FS and the Final Height for above-ground competition, which had the highest heritabilty (Table 13). For the Biomass measurements, I focus on the fresh biomass after 39 days, because it was the last time point with measurements in HD and LD conditions.

These traits are correlated among each other and to the traits observed in HL and LL conditions (Figure 24). Except for traits in the growth chamber all traits show a high correlation between treatments and experiments (Figure 24 A). Size traits (FS, height) are negatively correlated with flowering traits (Flowering & bolting) in the field. Interestingly, the sign of the correlation between FS and height in above-ground competition changed under density conditions.

Comparing the competition experiments to the experiments conducted under HL and LL conditions revealed a strong correlation between diameter measurements across all experimental conditions (Figure 24 B). Final height in LD in the field was not correlated with FS in the chamber, but negatively correlated to t50 under HL conditions ($r= -0.241$, $p= 0.00168$). The estimates of GxE were never correlated among experiments, with the exception of a weak negative correlation between GxE for final height between LD and HD and the biomass under HD conditions ($r= -0.166$, $p= 0.036$, Figure 24 B).

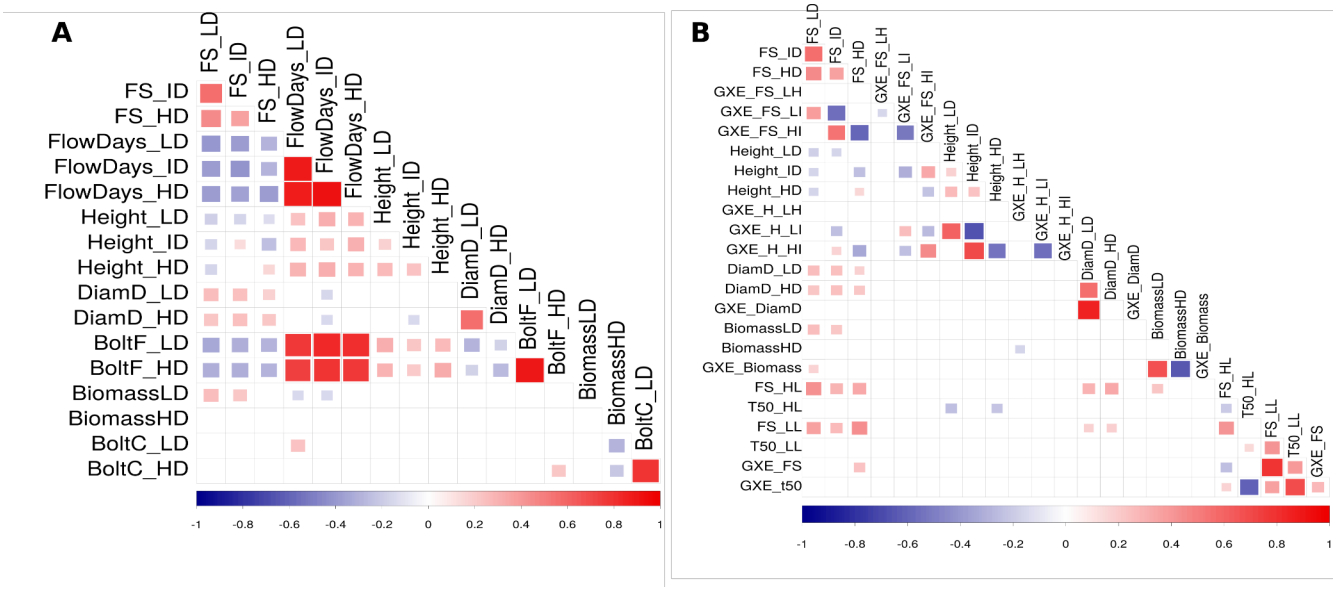

Figure 24: Correlation of phenotypic traits.

Pearson correlations for each pair of selected traits within density experiments (A) and between density and HL and LL experiments (B). Colored boxes show significant correlations ($p<0.05$ after multiple testing correction (FDR correction). The significance is illustrated by box size (larger box represents lower p-values) and the color shows the direction and strength of correlation. Abbreviations are: LD = Low density, ID= Intermediate density, HD= High density, FS= Final size, FlowDays= Flowering time in the above-ground competition field experiment, Height/H= Final plant height, DiamD= Diameter in December (below-ground competition Field experiment), BoltF= Bolting time in the 1st field experiment, Biomass= Biomass after 39 days, BoltC= Bolting time in the growth chamber.

The experiments with different density conditions revealed, that density has a strong impact on growth parameters (Table 14). In the experiments with 5 vs 100 plants per pot, density had by far the strongest impact on the growth parameters (p= <2E-16 for BM and diameter December). In above-ground competition the regional differences had a larger effect than the density treatment, but both were highly significant. For the rosette size parameters a significant correlation between density treatment and the region of origin could be observed, which was not the case for height.

Table 14: Analysis of growth variation after exposure to competition.

ANOVA results for the traits Biomass (BM), diameter in December in the below-ground competition field experiment (Diameter December), and FS and height in the above-ground field experiment (FS, height). Effects of competition, region/country of origin, their interaction and the block were tested. Significant results are marked in bold.

Response	df	Sum of Squares	F	P-value
BM				
Competition	1	10.274	2166.217	**< 2E-16**
Region	7	0.131	3.952	**0.000313**
Competition*Region	7	0.132	3.989	**0.000282**
Residuals	596	2.827		
Diameter December				
Block	1	14	2.963	0.085434
Competition	1	2626	554.806	**< 2E-16**
Region	7	662	19.992	**< 2E-16**
Competition*Region	7	124	3.73	**0.000527**
Residuals	1241	5874		
FS				
Block	3	1177773	290.341	**< 2E-16**
Competition	2	185543	686.115	**< 2E-16**
Country	5	6587851	9744.432	**< 2E-16**
Competition*Country	8	2754	2.546	**0.00923**
Residuals	2391	323293		
Height				
Block	3	72176	2.836	**0.0369**
Competition	2	3352467	197.591	**< 2E-16**
Country	5	120600608	2843.236	**< 2E-16**
Competition*Country	8	127607	1.88	0.0591
Residuals	1751	14854317		

Plants grown under higher density were smaller in all experiments (Figure 25). The larger sizes of Spanish plants in HL and LL could be confirmed in all other conditions. The biomass of plants from Spain was larger than for plants from North and South Sweden in LD, but this difference was no longer detectable under HD (Figure 25 A). In below-ground competition, genotypes from Spain had a larger diameter in December compared to genotypes from any other European region (except North Sweden), while under HD the Spanish genotypes were

only larger than genotypes from South Sweden (Figure 25 B). FS in above-ground competition was larger in Spain compared to the other regions under LD. When plants were exposed to competition, FS was larger compared to most European countries, but not different from China (Figure 25 C). The final height measurements show a clear latitudinal gradient in Europe, with a smaller final height in Spain compared to Sweden. This observation was less pronounced under competition, but Spanish genotypes still had smaller estimates than Swedish genotypes (Figure 25 D).

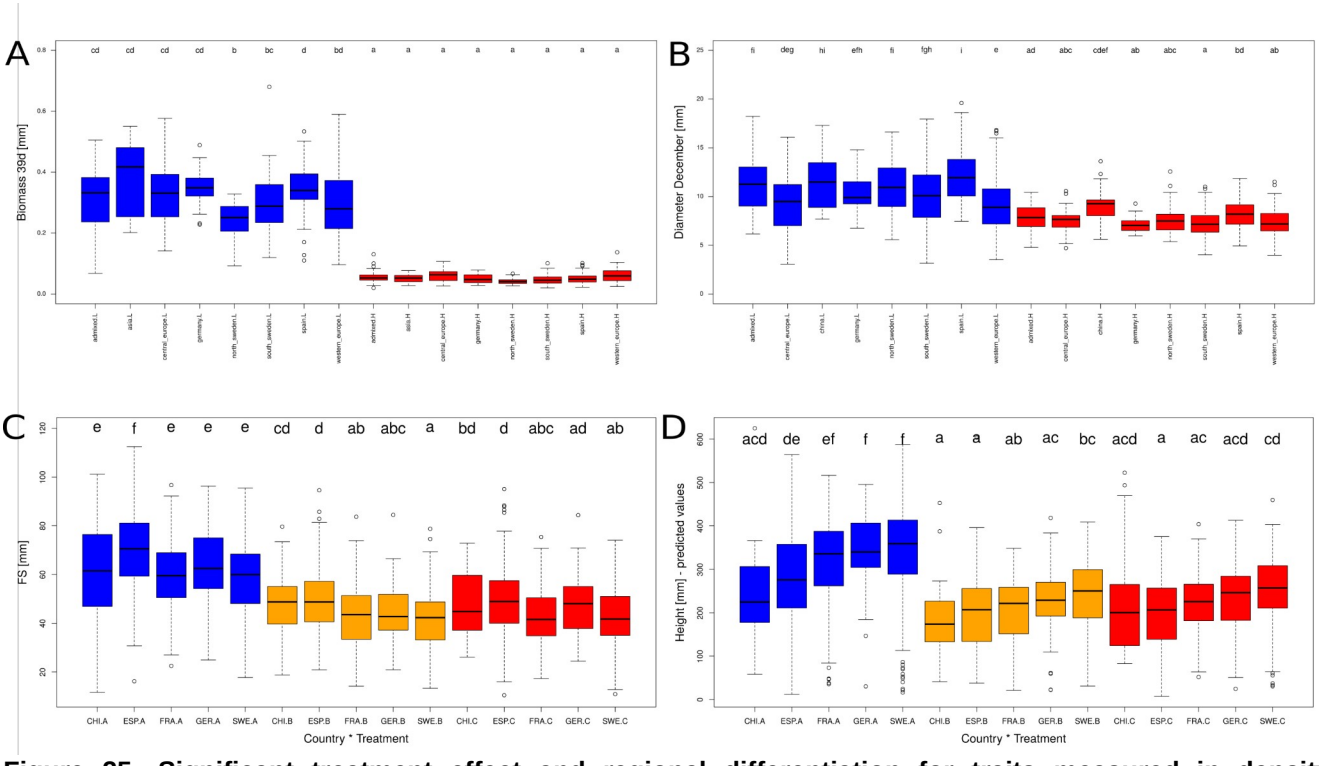

Figure 25: Significant treatment effect and regional differentiation for traits measured in density experiments.

A. thaliana genotypes are grouped based on the interaction between experimental condition and 1001 genomes group (A, B) or country of origin (C,D). Boxplots show the the treatment effect and regional variation of biomass in mg after 39 days (A, chamber), diameter in December in mm (B, below-ground competition field experiment), FS in mm (C, above-ground competition field experiment) and final plant height in mm (D, above-ground field experiment. Groups that do not share a letter are significantly different according to Tukey's HSD ($p<0.05$).

There was no regional differentiation between low and high density for FS in the field. For height a difference in GxE between moderate and high density was observed between Spain

and France (Figure 26A). Interestingly, for biomass after 39 days in controlled conditions (Figure 26B) and GxE for Diameter in below-ground competition (Figure 26C) the difference between Spain and Western Europe (plus Central Europe for diameter) was also the only significant regional distinction.

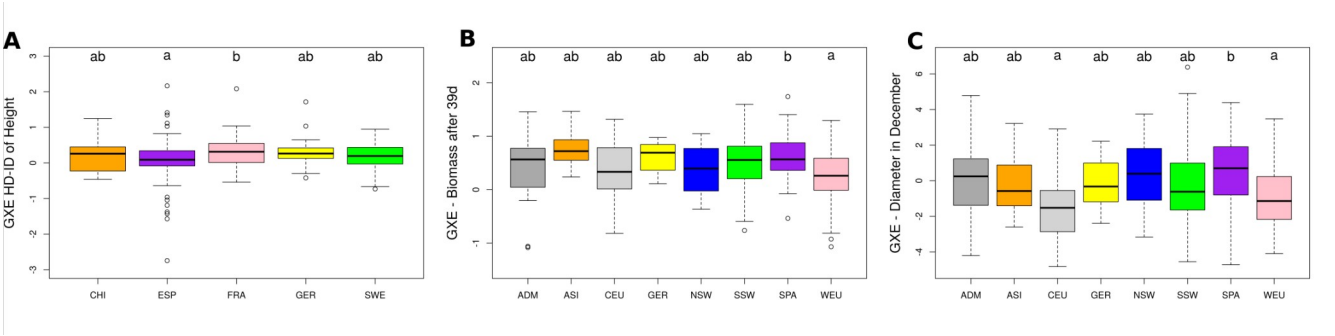

Figure 26: Regional differences for GxE to density conditions.

A) GxE HD to ID of Height in the above-ground competition field experiment. The phenotypic values are based on 284 genotypes of *A. thaliana* grown in high (HD) or intermediate density (ID). Region information: China (CHI, n= 16), Spain (ESP, n= 88), France (FRA, n= 46), Germany (GER, n= 22), South Sweden (SWE, n= 112). B) GxE of biomass after 39 days in the growth chamber. The phenotypic values are based on 283 genotypes of *A. thaliana* grown in low (LD) or high (HD) density. Region information: Admixed (ADM, n=25), Asia (ASI, n=5), Central Europe (CEU, n= 22), Germany (GER, n= 15), North Sweden (NSW, n= 20), South Sweden (SSW, n= 88), Spain (SPA, n= 57), Western Europe (WEU, n= 51). C) GxE of diameter in December in the below-ground competition field experiment. The phenotypic values are based on 315 genotypes of *A. thaliana* grown in low (LD) or high (HD) density. Region information: Admixed (ADM, n=29), Asia (ASI, n=10), Central Europe (CEU, n= 21), Germany (GER, n= 16), North Sweden (NSW, n= 21), South Sweden (SSW, n= 97), Spain (SPA, n= 62), Western Europe (WEU, n= 59). Groups that do not share a letter are significantly different according to Tukey's HSD ($p<0.05$).

3.2.2 Genetic basis of density related growth

Few significantly associated SNPs for density-related traits

I used GWAS to determine the genetic basis of variation in growth rate within Europe (Figure 27, Figure 42 - Figure 44). Overall, there were few significant genetic associations, indicating a polygenic basis of the growth in response to density. The only significant associations were discovered for final plant height (H) in low & intermediate density and the GxE between these two conditions (Figure 27).

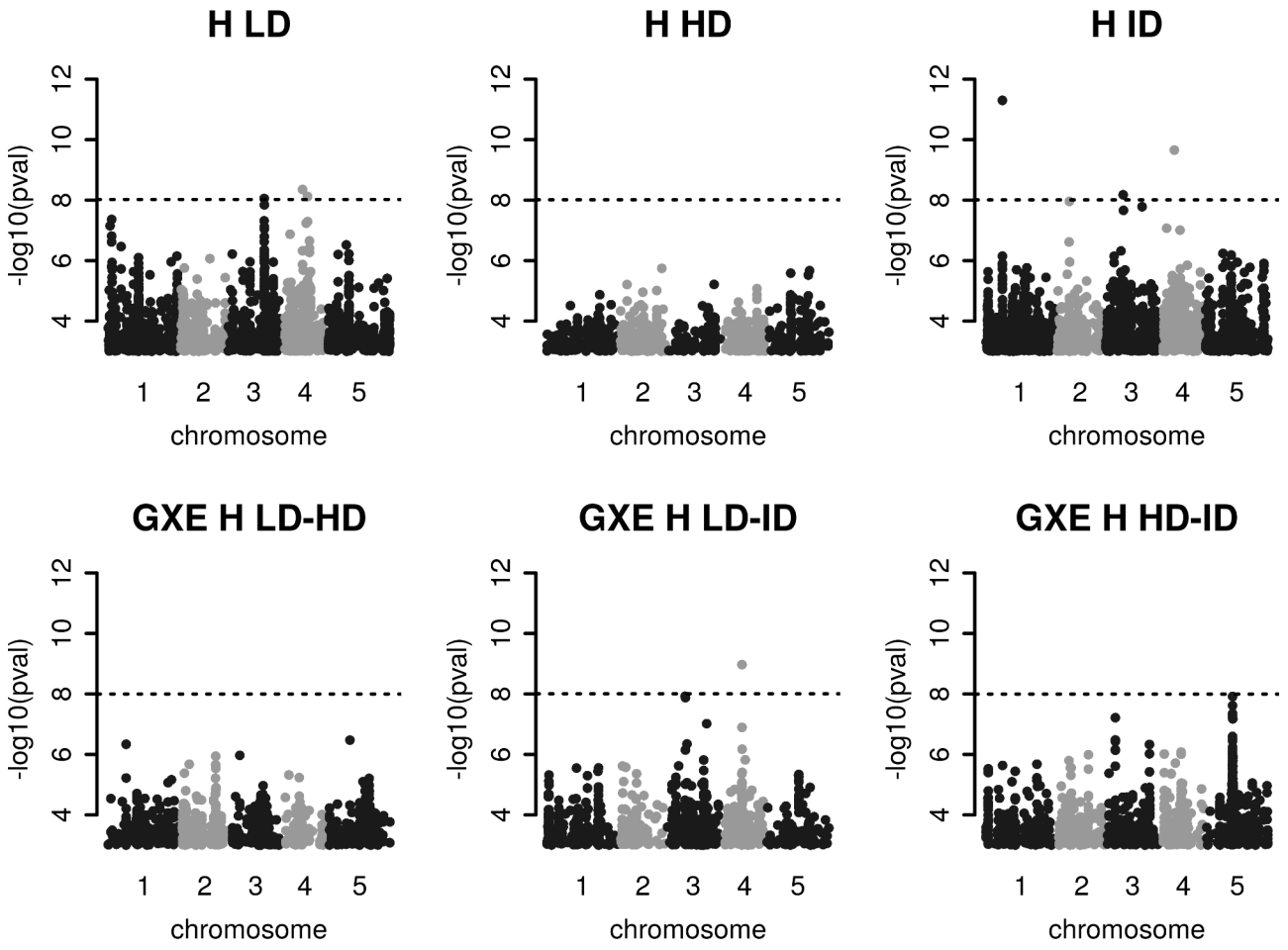

Figure 27: GWAS results for final plant height (H) in the above-ground competition field experiment.

Manhattan plots using at least 240 genotypes from Europe (France, Germany, Spain and Northern Europe) as input. The treatments are low density (LD, n= 301), high density (HD, n=273), intermediate density (ID, n= 274) and the GXE between low and high (LD-HD, n=259), low and intermediate (LD-ID, n=261) and high and intermediate (HD-ID, 240). The dotted line denotes the 5% Bonferroni-corrected threshold.

Interestingly, several SNPs on Chromosome 4 were significantly associated (Table 34). For H at LD, 2 SNPs on chromosome 4 were associated (base pair 8763510, effect size= 0.519, p= 4.45E-9 and base pair 10957505, effect size= 0.581, p= 7.59E-9), to a region containing 6 and 5 genes within 10kb down- and upstream of the SNP, respectively. The same region as for the first SNP was also significantly associated with GxE of LD-ID, but there were no obvious candidates in this region. The second SNP on Chromosome 4 (bp 10957505) was close to the gene BARELY ANY MERISTEM (BAM3, AT4G20270), encoding a receptor

kinase-like protein that is required for meristem function and male gametophyte development (DeYoung *et al.*, 2006). Another SNP on Chromosome 3 was significantly associated with H at LD (base pair 15524080, effect size= 0.618, p= 8.86E-9) with 6 genes in proximity, including ALDEHYDE OXIDASE 2 (AAO2, AT2G27150), which might be involved in the absiscic acid biosynthesis pathway and in plant defense and drought tolerance (Khan *et al.*, 2019).

For H under ID, I detected 3 peaks on different chromosomes. On Chromosome 1 (base pair 7067725, effect size= 0.833, p= 5.026E-12) 5 genes were in close proximity, including PROLYL-OLIGOPEPTIDASE ASSOCIATED WITH QUANTITATIVE RESISTANCE (POQR, AT1G20380), which is involved in the quantitative disease resistance against the mold fungus *Sclerotinia scleortiorum* (Badet *et al.*, 2017). For the peak on Chromosome 3 (base pair 7637722, effect size= 0.714, p= 6.656E-9), 6 genes were close, but they contained no obvious candidate. On Chromosome 4 (base pair 6325703, effect size= 0.777, p= 2.217E-10), 5 genes were adjacent, with SUCROSE PHOSPHATE SYNTHASE 4F (SPS4F, AT4G10120) among them, encoding an enzyme involved in sucrose synthsis in embryonic tissue which is also responsive to osmotic stress (Solís-Guzmán *et al.*, 2017).

Except for these SNPs, I mostly observed a more polygenic architecture with several moderately associated SNPs (-log10(p)<4) ranging from 19 to 170 after filtering. To investigate the molecular functions related to genes in linkage to these SNP, I conducted a GO-enrichment for these moderate associations.

Functional enrichment of growth, light, defense and other GO terms

The GO-enrichment analysis of moderately associated genes reveal an overall mixed signature, with many categories without an easily interpretable link to growth, but also several terms with functions linked to the phenotypes (Table 35). For FS, several GO terms related to defense were enriched: “defense response” (enriched for genes associated with FSID, FSGXELI & FSGXELH, p= 0.0029, 0.0082 & 0.0051, respectively), “regulation of response to stress” (FSID, p= 0.0089), “regulation of defense response to bacterium” (FSHD, p-value: 0.0082), “activation of innate immune response” and “defense response, incompatible interaction” (FSGXELH, p= 0.0083 & 0.0087). Some GO terms were related to the perception

of light (“tropism” for FSID and “blue light signaling pathway” & “cellular response to high light intensity” for FSHD, p= 0.0034 & 0.0082) and the regulation of growth (“negative regulation of flower development” & “regulation of root development” for FSHD, p= 0.0027 & 0.0034).

For H several GO terms were related to growth & nutrient uptake: “lignin biosynthetic process” (HLD, p= 0.0008), “floral meristem determinancy” (HLD, p= 0.0016), “sulfur compound catabolic process” & “sulfur compound transport” (HID, p= 0.0071 & 0.0075), “regulation of cell size” (HHD, p= 0.0046), “plant epidermis development” (HHD, p= 0.0051), “auxin homeostasis” (HHD, p= 0.0060) and “multidimensional cell growth” (HHD, p= 0.0063). For H, I could also observe several GO terms related to defense & stress: “defense response signaling pathway” (HLD, p= 0.0016), “respiratory burst involved in defense response” (HLD, p= 0.0082), “defense response” (HHD, HGXELH, p= 0.0089 & 0.0007), “innate immune response” (HGXELH, p= 0.0038) and “cold acclimation” (HGXEIH, p= 0.0044). Related to light, I observed an enrichment for “photosynthetic acclimation” (HID, p= 0.006) and directly related to the perception of density the “response to far red light” (HGXELI, p= 0.0003), which was also enriched for genes related to DGXE, along with “response to blue light” (p= 0.0016). Otherwise, I only observed few enrichments for diameter and biomass.

3.2.3 No strong signal of local adaptation in response to competition

To estimate signals of local adaptation for the growth traits measured with and without intra-specific competition, I used the population kinship matrix to parameterize a multivariate normal distribution and predict the amount of additive phenotypic divergence expected if the trait evolves neutrally (Koch, 2019b).

FS in LD was slightly more differentiated than predicted under neutral conditions, but the differentiation was not significant (Qst= 0.215, p= 0.0861, Figure 28). The other parameters did not depart from neutrality, but for FS, H and D the Qst was higher in LD conditions (Figure 28 & Figure 45). For biomass the Qst was marginally higher in HD (Qst 0.122 in LD and 0.140 in HD, Figure 46).

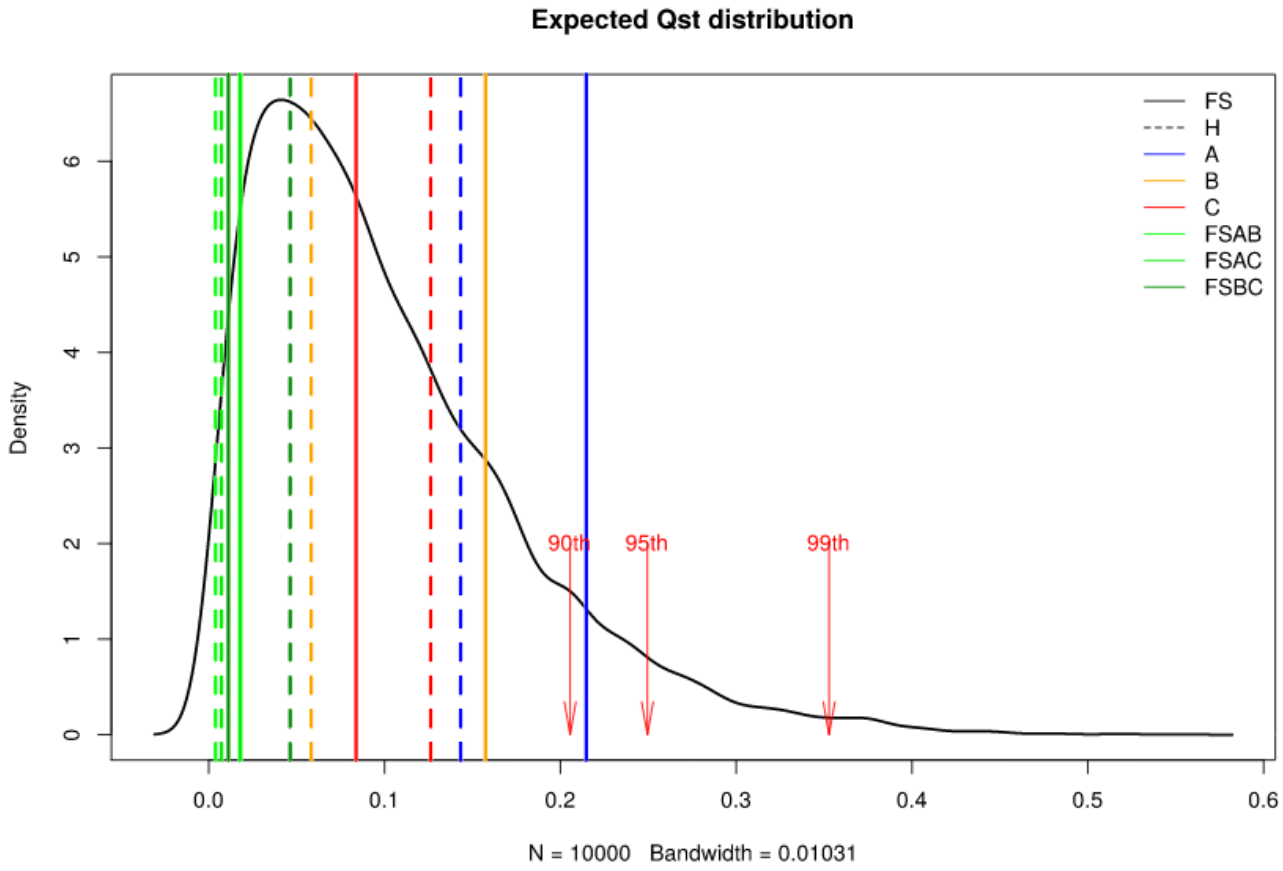

Figure 28: Estimated Qst distribution for FS and H.

Expected distribution for quantitative trait differentiation within Europe. The expectation is based on a multivariate normal distribution assuming a neutral trait with polygenic basis. Vertical lines indicate observed Qst for the individual growth parameters, FS (Solid line) & H (Dashed line) in LD (A, blue), HD (B, yellow), ID (C, red) and the GxE between these treatments (green). The red arrows show the 90th, 95th and 99th percentiles of the distribution.

3.2.4 Meta-analysis reveals functional GO enrichments

Up to this point, I generated a lot of gene sets based on GWAS and looked at their functional enrichment. Growth traits measured in different environments were the input data, so some overlap between the different GWAS sets was expected. To investigate potential overlaps between GWAS results I performed a meta-analysis of GWAS output tables with METAL (Willer *et al.*, 2010). The input files were grouped into several sets with the expectation of similar associated genes. In ALL, every GWAS result from the HLLL and the density

experiment was used as input. HLLL combined the results from the experiment with HL and LL conditions. The results from the density experiment were split into three sets, whether they were grown in LD (including HL and LL: NODENS), HD (HIDENS) or for the GxE between LD and HD conditions (GXEDENS). With METAL, the effect size estimates for each SNP are combined with the direction of the effect to compute a Z-score with a corresponding p-value (Willer *et al.*, 2010). SNPs with a strong effect that has the same direction across GWASs will get a higher Z-score. SNPs with moderately associated Z-scores across traits (-log10(p)<4) were tested for functional GO-enrichment.

Interestingly, for most of these gene sets terms directly related to growth were enriched (Table 15): “regulation of developmental growth” (enriched for ALL, HLLL, p= 0.0051 & 0.0037), “regulation of biological quality” (HLLL, p= 0.0058), “meristem maintenance” (HLLL, p= 0.0095) & “regulation of cell growth” (HIDENS, p= 0.0052). In NODENS and enrichment for genes involved in “photoprotection” was significantly enriched (p= 0.0035). Across the sets the function “stomatal lineage progression” was identified (enriched for HLLL, NODENS, HIDENS, GXEDENS, p= 0.0086, 0.0064, 0.0056 & 0.0071, respectively). As for the GO enrichments several terms related to defense/stress were identified, like “innate immune response-activating signal transduction” (HLLL, p= 0.0047), “defense response to fungus” (HIDENS, p= 0.0079) and “detection of external stimulus” (GXEDENS, p= 0.0094) were enriched.

Table 15: GO-enrichment of genes in LD (within 10kb) to SNPs with p<0.008 (based on permutation) in the meta-analysis of gene sets (METAL).

Shown are terms with an enrichment with p<0.001. The column Gene set contains information on the set of genes identified in GWAS, that was used as input. GO.ID and term give information on the enriched GO term. Annotated contains the number of all genes that are in the term, Significant is the number of genes that are associated in the input data set and Expected the number of genes that are expected to be enriched by chance. The resultFisher gives the Fisher score for enrichment. We only report GO terms with >5 genes in them. Gene sets are ALL (FSA, FSB, FSC, FSGXEAB, FSGXEAC, FSGXEBC, HA, HB, HC, HGXEAB, HGXEAC, HGXEBC, BL, BH, BGXE, DL, DH, DGXE), HLLL (FSHL, FSLL, FSGXE, t50HL, t50LL, t50GXE, SLHL, SLLL, SLGXE), NODEN (FSA, HA, FSHL, FSLL, BL, DL), HIDEN (FSB, FSC, HB, HC, BH, DH), GXEDEN (FSGXEAB, FSGXEAC, FSGXEBC, HGXEAB, HGXEAC, HGXEBC, BGXE, DGXE).

Gene set	GO ID	Term	Annotated	Significant	Expected	resultFisher
ALL	GO:0010106	cellular response to iron ion starvation	116	15	5.69	0.0006
	GO:0006826	iron ion transport	120	14	5.89	0.0023

	GO:1901659	glycosyl compound biosynthetic process	180	18	8.83	0.0033
	GO:0048638	regulation of developmental growth	277	24	13.59	0.0051
	GO:0046785	microtubule polymerization	70	9	3.43	0.0070
HLLL	GO:0140056	organelle localization by membrane tethering	24	6	1.48	0.0028
	GO:0048638	regulation of developmental growth	277	29	17.05	0.0037
	GO:0010204	Innate immune response-activating signal transduction	12	4	0.74	0.0047
	GO:0000162	tryptophan biosynthetic process	19	5	1.17	0.0049
	GO:0065008	regulation of biological quality	1616	124	99.46	0.0058
	GO:0010440	stomatal lineage progression	58	9	3.57	0.0086
	GO:0010073	meristem maintenance	284	28	17.48	0.0095
NODENS	GO:0042446	hormone biosynthetic process	747	65	43.84	0.0009
	GO:0010117	photoprotection	6	3	0.35	0.0035
	GO:0010440	stomatal lineage progression	58	9	3.4	0.0064
	GO:0043086	negative regulation of catalytic activity	59	9	3.46	0.0071
	GO:0070988	demethylation	8	3	0.47	0.0090
	GO:0051338	regulation of transferase activity	51	8	2.99	0.0092
HIDENS	GO:0045736	negative regulation of cyclin-dependant protein serine/threonine kinase activity	27	8	2.8	0.0048
	GO:0001558	regulation of cell growth	112	21	11.61	0.0052
	GO:0010675	regulation of cellular carbohydrate metabolic process	22	7	2.28	0.0053
	GO:0010440	stomatal lineage progression	58	13	6.01	0.0056
	GO:0009106	lipoate metabolic process	40	10	4.15	0.0065
	GO:0044786	cell cycle DNA replication	122	22	12.64	0.0069
	GO:0050832	defense response to fungus	350	51	36.27	0.0079
	GO:0015824	proline transport	74	15	7.67	0.0082
	GO:0006809	nitric oxide biosynthetic process	5	3	0.52	0.0095
GXEDEN	GO:0042133	neurotransmitter metabolic process	68	15	7.25	0.0047
	GO:0045736	negative regulation of cyclin-dependant protein serine/threonine kinase activity	27	8	2.88	0.0057
	GO:0010675	regulation of cellular carbohydrate metabolic process	22	7	2.35	0.0062
	GO:0010440	stomatal lineage progression	58	13	6.19	0.0071
	GO:0001558	regulation of cell growth	112	21	11.94	0.0072

	GO:0009106	lipoate metabolic process	40	10	4.27	0.0079
	GO:0009581	detection of external stimulus	41	10	4.37	0.0094
	GO:0044786	cell cycle DNA replication	122	22	13.01	0.0095

3.3 Differential gene expression of mutants in the light-signaling pathway

We observed several significant GO enrichments for genes detected with GWAS. Since the GO terms are not exactly tailored for the growth response we investigated here, we tried to identify genes that are important for the traits.

3.3.1 Transcriptomes reveal differential genetic basis between environments

100 samples meet the RNA mapping quality criteria. I did not include the *spa*-triple and *hfr1* mutants in further analyses, therefore I used the RNA data on 49 plants summarized in Table 16.

Table 16: RNA-seq sample sizes for light-signaling mutants.

Each value is the number of sequences that were used for further analyses for each Genotype x Environment combination. *Spa1234* are NA for the competition environments, because they were not grown in this condition. For each combination 4 replicates were grown.

Genotype	Environment				
	HL, single, day	HL, single, night	HL, competition, day	HL, competition, night	LL, single, night
	HLD	HLN	CD	CN	LLN
Col-0	1	4	2	3	3
cop1	0	3	3	3	4
phyb	1	4	4	1	3
spa1234	3	4	NA	NA	3

With these samples the next analysis steps were conducted. For HL conditions during the day the number of samples of sufficient quality was to low to run DESEQ2, so I focused on the other four environments. The lowest count of differentially expressed genes was observed in

HL conditions during the night with 161 genes, while HL with competition during the day revealed 4,551 associated genes. The overlap between the sets is shown in Figure 29.

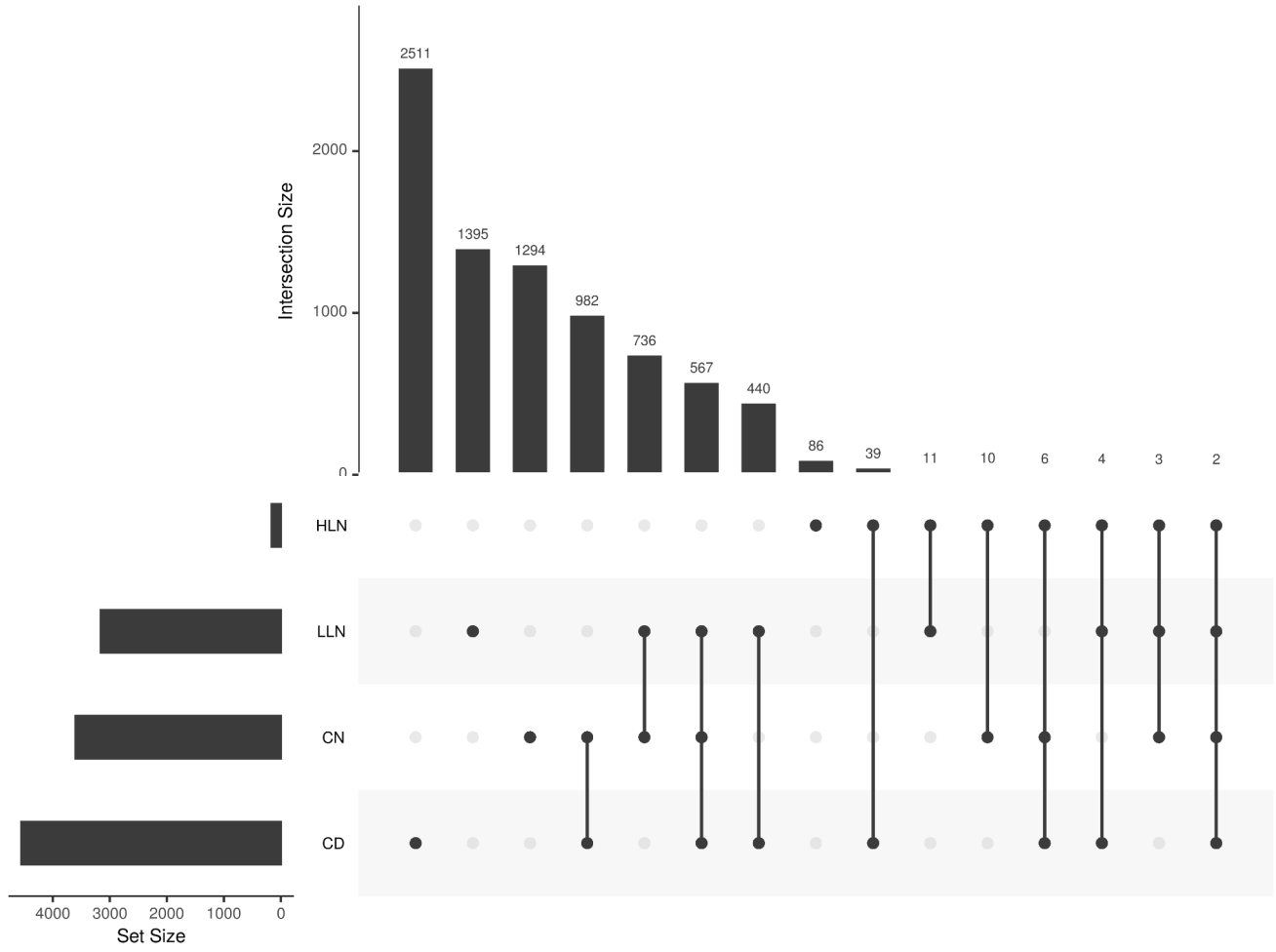

Figure 29: UpSet plot of the gene overlap between genes identified with RNA-seq.

Left: Barplot with gene number for each set. Right: Overlaps between terms. A single dot represents unique genes for the term, more dots connected with lines in a column represent overlaps for the sets with black dots. The bar plot on top shows the number of genes that are in each respective contrast. The overlaps are sorted by the highest number of genes.

For all categories a large proportion of genes is unique to the condition (single dots in Figure 29). Competition sampled during day and night has the highest overlap of genes, followed by other overlaps between the conditions that resemble limited light supply. Even though most

genes are specific to the different environments, I identified 2 genes that are shared across all conditions: RELATED TO AP2.4 (RAP2.4, AT1G22190) and CONSTANS-LIKE 9 (COL9, AT3G07650).

RAP2.4 is involved in the response to several abiotic stresses, but also in the defense against pathogens (Rae *et al.*, 2011; Sham *et al.*, 2019). COL9 is involved in the regulation of flowering time genes like CONSTANS and FT and its over-expression can delay flowering (Cheng & Wang, 2005). It was also reported to be involved in the light intensity-dependent root development (Kumari *et al.*, 2019).

Since most identified genes are private to each term, I tried to unravel their functional characterization by performing a GO enrichment of these genes.

3.3.2 GO terms can help defining functional characterizations of the new terms

All GO enrichments of the terms with a p-value below 0.008 are summarized in Table 37. Because of the high number of categories, I tried to re-organize the enrichment into four functional groups (Light, growth, stress/defense and plant hormones) and excluded genes that do not match any of these terms (Table 17).

Table 17: GO-enrichment of differentially expressed genes between mutants of light-signaling genes sorted into functional categories.

Shown is a selection of terms with an enrichment < 0.0008. GO.ID and term give information on the enriched GO term. Ann. states all genes that are in the term, Sign. is the number of genes that are associated in the input data set and Exp. the number of genes that are expected to be enriched by chance. The Fisher gives the Fisher score for enrichment. I only report GO terms with >5 genes in them. HLN :161 genes; CN: 3600 genes; CD: 4551 genes; LLN: 3158 genes

Set	GO.ID	Term	Ann.	Sign.	Exp.	Fisher
LIGHT		Terms related to light perception & response, photoperiod, photosystem, photoprotection.				
HLN	GO:0009644	response to high light intensity	197	9	1.71	5.4E-05
HLN	GO:0019684	photosynthesis, light reaction	306	12	2.65	0.00025
HLN	GO:0007623	circadian rhythm	163	7	1.41	0.00054
HLN	GO:0009769	photosynthesis, light harvesting in photosystem II	6	2	0.05	0.00109
CN	GO:0009853	photorespiration	157	68	31.65	3.2E-11
CN	GO:0007623	circadian rhythm	163	51	32.86	0.00049
CN	GO:0080167	response to karrikin	117	38	23.59	0.00113

CN	GO:0010017	red or far-red light signaling pathway	41	16	8.27	0.00422
CN	GO:0015996	chlorophyll catabolic process	56	20	11.29	0.00490
CD	GO:0009718	anthocyanin-containing compound biosynthesis	52	26	13.57	0.00019
CD	GO:0009658	chloroplast organization	234	80	61.06	0.00344
CD	GO:0009646	response to absence of light	33	16	8.61	0.00470
LLN	GO:0043481	anthocyanin accumulation in tissues in response to UV light	98	43	17.06	8.6E-10
LLN	GO:0010304	PSII associated light-harvesting complex II catabolic process	27	17	4.7	1.7E-07
LLN	GO:0015996	chlorophyll catabolic process	56	26	9.75	4.8E-07
LLN	GO:0010218	response to far red light	96	35	16.71	6.2E-06
LLN	GO:0010207	photosystem II assembly	169	52	29.42	1.4E-05
LLN	GO:0080167	response to karrikin	117	35	20.37	0.00059
LLN	GO:0010114	response to red light	99	30	17.24	0.00112
LLN	GO:0009637	response to blue light	121	35	21.07	0.00116
LLN	GO:0019684	photosynthesis, light reaction	306	90	53.28	0.00144
LLN	GO:0015979	photosynthesis	400	118	69.64	0.00171
LLN	GO:0071482	cellular response to light stimulus	73	23	12.71	0.00233
LLN	GO:0009646	response to absence of light	33	13	5.75	0.00234
LLN	GO:0009641	shade avoidance	17	8	2.96	0.00457
LLN	GO:0007623	circadian rhythm	163	41	28.38	0.00775
STRESS/ DEFENSE		Terms related to the response to stress, defense, resistance.				
HLN	GO:0042542	response to hydrogen peroxide	166	10	1.44	1.8E-06
HLN	GO:0010193	response to ozone	34	4	0.29	0.00020
HLN	GO:0009627	systemic acquired resistance	425	12	3.68	0.00032
HLN	GO:0009408	response to heat	258	10	2.24	0.00108
HLN	GO:0034976	response to endoplasmic reticulum stress	329	9	2.85	0.00226
HLN	GO:0010167	response to nitrate	112	5	0.97	0.00289
HLN	GO:0019430	removal of superoxide radicals	10	2	0.09	0.00320
CN	GO:0009651	response to salt stress	737	196	148.6	9.2E-06
CN	GO:0046686	response to cadmium ion	455	126	91.74	5.5E-05
CN	GO:0009269	response to desiccation	36	18	7.26	6.1E-05
CN	GO:0009744	response to sucrose	196	62	39.52	9.1E-05
CN	GO:0010583	response to cyclopentenone	128	41	25.81	0.00100
CN	GO:0010043	response to zinc ion	41	17	8.27	0.00149
CN	GO:0097237	cellular response to toxic substance	14	8	2.82	0.00252
CN	GO:0009750	response to fructose	138	42	27.82	0.00263
CN	GO:0006972	hyperosmotic response	237	65	47.78	0.00411

CN	GO:0006952	defense response	1420	324	286.31	0.00523
CN	GO:0009737	response to abscisic acid	562	138	113.31	0.00550
CD	GO:0010363	regulation of plant-type hypersensitive response	365	178	95.24	4.8E-21
CD	GO:0010200	response to chitin	399	187	104.11	1.2E-19
CD	GO:0031348	negative regulation of defense response	271	140	70.71	1.3E-19
CD	GO:0009627	systemic acquired resistance	425	220	110.89	5.0E-17
CD	GO:0050832	defense response to fungus	329	155	85.84	9.8E-17
CD	GO:0009862	systemic acquired resistance, salicylic acid mediated signaling pathway	237	118	61.84	3.3E-15
CD	GO:0043069	negative regulation of programmed cell death	163	88	42.53	2.7E-14
CD	GO:0002679	respiratory burst involved in defense response	117	67	30.53	8.3E-13
CD	GO:0034976	response to endoplasmic reticulum stress	329	156	85.84	3.4E-08
CD	GO:0002237	response to molecule of bacterial origin	93	48	24.27	1.3E-07
CD	GO:0042742	defense response to bacterium	384	150	100.19	1.5E-07
CD	GO:0009625	response to insect	43	26	11.22	2.0E-06
CD	GO:0009611	response to wounding	304	116	79.32	2.1E-06
CD	GO:0009595	detection of biotic stimulus	102	48	26.61	4.0E-06
CD	GO:0010583	response to cyclopentenone	128	55	33.4	2.4E-05
CD	GO:0010167	response to nitrate	112	49	29.22	3.7E-05
CD	GO:0010286	heat acclimation	79	36	20.61	0.00014
CD	GO:0009414	response to water deprivation	386	131	100.72	0.00032
CD	GO:0009814	defense response, incompatible interaction	515	258	134.37	0.00033
CD	GO:0052542	defense response by callose deposition	59	27	15.39	0.00085
CD	GO:0009617	response to bacterium	545	218	142.2	0.00091
CD	GO:0052033	pathogen-associated molecular pattern dependent induction by symbiont of host innate immune response	5	5	1.3	0.00121
CD	GO:0006914	autophagy	69	30	18	0.00127
CD	GO:0009651	response to salt stress	737	227	192.3	0.00186
CD	GO:0046686	response to cadmium ion	455	146	118.72	0.00218
CD	GO:0006972	hyperosmotic response	237	81	61.84	0.00329
CD	GO:0009620	response to fungus	464	204	121.07	0.00373
CD	GO:0006952	defense response	1420	583	370.51	0.00482
CD	GO:0009682	induced systemic resistance	18	10	4.7	0.00748
LLN	GO:0009862	systemic acquired resistance, salicylic acid mediated signaling pathway	237	72	41.26	5.7E-07
LLN	GO:0031348	negative regulation of defense response	271	79	47.18	1.0E-06
LLN	GO:0009617	response to bacterium	545	130	94.89	6.2E-05
LLN	GO:0009595	detection of biotic stimulus	102	31	17.76	0.00089
LLN	GO:0009746	response to hexose	161	44	28.03	0.00108
LLN	GO:0010363	regulation of plant-type hypersensitive response	365	86	63.55	0.00152
LLN	GO:0009409	response to cold	556	123	96.8	0.00216

LLN	GO:0009269	response to desiccation	36	13	6.27	0.00566
LLN	GO:0006833	water transport	134	35	23.33	0.00720
GROWTH		Terms related to growth, resource acquisition, life history				
HLN	GO:0015977	carbon fixation	13	2	0.11	0.00546
HLN	GO:0000103	sulfate assimilation	14	2	0.12	0.00634
CN	GO:0010075	regulation of meristem growth	154	61	31.05	2.1E-08
CN	GO:0008283	cell proliferation	245	77	49.4	1.8E-05
CN	GO:0009828	plant-type cell wall loosening	20	12	4.03	0.00011
CN	GO:0010089	xylem development	54	23	10.89	0.00014
CN	GO:0009825	multidimensional cell growth	97	30	19.56	0.00780
CD	GO:0008283	cell proliferation	245	104	63.93	1.6E-08
CD	GO:0009664	plant-type cell wall organization	205	95	53.49	1.4E-07
CD	GO:0009828	plant-type cell wall loosening	20	15	5.22	6.7E-06
CD	GO:0010075	regulation of meristem growth	154	64	40.18	2.0E-05
CD	GO:0042545	cell wall modification	160	72	41.75	6.2E-05
CD	GO:0048451	petal formation	59	28	15.39	0.00033
CD	GO:0048453	sepal formation	59	28	15.39	0.00033
CD	GO:0009612	response to mechanical stimulus	60	27	15.66	0.00117
CD	GO:0009957	epidermal cell fate specification	14	9	3.65	0.00296
CD	GO:0009909	regulation of flower development	319	104	83.23	0.00519
CD	GO:0009831	plant-type cell wall modification involvved in multidimensional cell growth	15	9	3.91	0.00569
CD	GO:0007568	aging	132	55	34.44	0.00650
LLN	GO:0019252	starch biosynthetic process	187	68	32.56	3.7E-10
LLN	GO:0009825	multidimensional cell growth	97	44	16.89	6.9E-08
LLN	GO:0009965	leaf morphogenesis	196	60	34.13	3.7E-06
LLN	GO:0008361	regulation of cell size	53	23	9.23	8.9E-06
LLN	GO:0048767	root hair elongation	161	48	28.03	7.0E-05
LLN	GO:0009932	cell tip growth	182	51	31.69	0.00024
LLN	GO:0009831	plant-type cell wall modification involved in multidimensional cell growth	15	9	2.61	0.00026
LLN	GO:0009828	plant-type cell wall loosening	20	10	3.48	0.00085
LLN	GO:0052325	cell wall pectin biosynthetic process	11	6	1.92	0.00575
PLANT HORMONES		Response and biosynthesis of plant hormones.				
HLN	GO:0009751	response to salicylic acid	434	12	3.76	0.00039

CN	GO:0009735	response to cytokinin	223	68	44.96	0.00015
CN	GO:0009753	response to jasmonic acid	438	118	88.31	0.00031
CN	GO:0009739	response to gibberellin	122	45	24.6	0.00037
CN	GO:0009695	jasmonic acid biosynthetic process	125	41	25.2	0.00059
CN	GO:0016126	sterol biosynthetic process	156	48	31.45	0.00106
CN	GO:0009813	flavonoid biosynthetic process	191	55	38.51	0.00260
CN	GO:0016132	brassinosteroid biosynthetic process	93	30	18.75	0.00398
CN	GO:0009723	response to ethylene	319	83	64.32	0.00621
CN	GO:0009755	hormone-mediated signaling pathway	670	161	135.09	0.00690
CN	GO:0071370	cellular response to gibberellin stimulus	58	20	11.69	0.00764
CD	GO:0009697	salicylic acid biosynthetic process	205	114	53.49	1.9E-19
CD	GO:0009867	jasmonic acid mediated signaling pathway	269	119	70.19	6.6E-11
CD	GO:0009723	response to ethylene	319	127	83.23	4.4E-08
CD	GO:0009963	positive regulation of flavonoid biosynthesis	101	46	26.35	1.8E-05
CD	GO:0009738	abscisic acid-activated signaling pathway	229	87	59.75	4.6E-05
CD	GO:0009863	salicylic acid mediated signaling pathway	334	161	87.15	5.1E-05
CD	GO:0009753	response to jasmonic acid	438	184	114.28	0.00018
CD	GO:0009751	response to salicylic acid	434	198	113.24	0.00744
CD	GO:0009693	ethylene biosynthetic process	108	40	28.18	0.00782
LLN	GO:0009739	response to gibberellin	122	40	21.24	2.6E-05
LLN	GO:0009926	auxin polar transport	86	34	14.97	3.5E-05
LLN	GO:0009867	jasmonic acid mediated signaling pathway	269	73	46.83	4.0E-05
LLN	GO:0009697	salicylic acid biosynthetic process	205	56	35.69	0.00025
LLN	GO:0019761	glucosinolate biosynthetic process	169	48	29.42	0.00025
LLN	GO:0009741	response to brassinosteroid	97	31	16.89	0.00034
LLN	GO:0016132	brassinosteroid biosynthetic process	93	28	16.19	0.00180
LLN	GO:0010817	regulation of hormone levels	822	213	143.12	0.00586
LLN	GO:0016126	sterol biosynthetic process	156	40	27.16	0.00602
LLN	GO:0010540	basipetal auxin transport	18	8	3.13	0.00698

All of the terms contain multiple functional enrichments related to light perception, light signaling, response to light, circadian clock or photoperiod. Terms related to plant growth and accumulation of resources are also highly represented.

Many GO terms were unique for single sets, but there were some terms that occur more than once. CN and LLN are both enriched for 12 terms associated to the functional categories in

Table 17, among them “circadian rhythm” (also enriched for HLN), “multidimensional cell growth” and “plant type cell wall loosening” (also enriched for LLN). CN and CD also have some overlapping signal, for 11 terms, among them “translation” & “defense response”.

HLN and LLN were enriched for the opposing “response to heat” and “response to cold”, which match the environment (higher temperature in HL). Figure 29 already illustrates, that there was some overlap of genes between terms, but there was a large proportion of genes unique to each term. HLN was enriched for “response to high light intensity” (p= 5.4E-5) and “photosynthesis, light reaction” (p= 0.00025). CN was enriched for “red or far-red light signaling pathway” (p= 0.00422), “regulation of meristem growth” (p= 2.1E-8) & “multidimensional cell growth” (p= 0.00780) and the response to jasmonic acid and gibberellin as well as hormones in general (“hromone-mediated signaling pathway”, p= 0.00690). For CD the “response to absence of light” (p= 0.00019), several terms related to defense, like “negative regulation of defense response” (p= 1.3E-19) or “respiratory burst involved in defense response” (p= 8.3E-13) were enriched. Furthermore, genes in this term were enriched for functions related to the cell wall, like “plant-type cell wall organization” (p= 1.4E-7) and several plant hormones, especially salicylic acid (e.g. “salicylic acid biosynthetic process”, p= 1.9E-19), jasmonic acid (e.g. “jasmonic acid mediated signaling pathway”, p= 6.6E-11) and ethylene (e.g. “response to ethylene”, p= 4.4E-8). The low light response (LN) was enriched for terms related to light frequency in “response to far red light” (p= 6.2E-6), “response to red light” (p= 0.00112), “response to blue light” (p= 0.00116) and also the “response to absence of light” (p= 0.00234) as well as “shade avoidance” (p= 0.00457). The GO terms included many different aspects of cell growth, including general terms (“multidimensional cell growth”, p= 6.9E-8 & “regulation of cell size”, p= 8.9E-6), tissue-specific growth (“leaf morphogenesis”, p= 3.7E-6 & “root hair elongation”, p= 7.0E-5) and cell wall functions (e.g. “plant-type cell wall modification involved in multidimensional cell growth”, p= 0.00026).

The terms displayed some specific signatures, so I checked for overlap of these terms with terms identified with GWAS using a hypergeometric test.

3.3.3 Overlap of gene expression categories with genes identified with GWAS

In summation, 11 terms were significantly overlapping between gene expression and GWAS (Table 18).

Table 18: Significant overlaps between defined gene sets from RNA-seq and genes identified using GWAS.

Level, describes the hierarchical level of the GWAS gene set, either as overlap between GWAS (Meta) or individual traits (Single). The name and size of the gene expression gene sets (RNA) are included as well as the name and size of the genes identified using GWAS. Overlap is the number of genes that are shared between the sets in each row, with the p-value from the hypergeometric test and the FDR-adjusted p-value.

Level	RNA Name	RNA Genes	GWAS Name	GWAS Genes	overlap	P-value	P-value adjusted
Meta	HLN	161	GxEDENS	1875	32	8.78E-05	0.011
Meta	HLN	161	HIDENS	1828	27	0.003	0.118
Meta	HLN	161	NODENS	1031	15	0.021	0.375
Meta	HLN	161	ALL	1071	15	0.028	0.428
Single	HLN	161	BM39LD	119	4	0.004	0.133
Single	CD	4551	HeightGxELH	290	93	0.003	0.118
Single	CD	4551	HeightID	654	189	0.009	0.238
Single	CD	4551	GxEt50	47	17	0.030	0.428
Single	CN	3600	GxEt50	47	14	0.033	0.428
Single	LLN	3158	FSHD	256	58	0.012	0.247
Single	LLN	3158	FSGxEHI	83	20	0.043	0.501

HLN was overlapping with 4 of 5 GWAS gene sets identified across traits. The overlap with GXEDENS was also the only overlap that was significant after correcting for multiple testing (adjusted p= 0.011). Overall, many overlaps were between the RNA-seq terms and GWAS of GxE. CD was significantly overlapping with Height and the GxE for Height (p= 0.003 and 0.009, respectively), while LLN was overlapping with FS in HD and the GxE (p= 0.012 and 0.043, respectively), both in above-ground competition. For GxE of t50 between HL and LL only 47 genes were in proximity to moderately associated markers, but these genes were significantly overlapping with genes differentially expressed in competition during the day and night (p= 0.030 and 0.033, respectively).

There were significant functional enrichments between light signaling expression and the GWAS for growth traits in different light conditions. In the last chapter I analyzed patterns of regional differentiation of allele-specific gene expression (ASE).

3.4 Regional divergence in allele-specific expression

To investigate the divergence of gene expression between parents (*trans*) and hybrids (*cis*), I analyzed 248 hybrid and 126 parental transcriptomes for 24 genotypes from Morocco, Sweden, Spain and China.

Parental genomes reveal strong *trans* effect, but also a significant *cis*-regulation

The parental transcriptomes were contrasted to identify *trans*-signatures of gene expression. To compare the contribution of *cis* and *trans* effects, ASE for genes in each hybrid was compared to the fold change in expression between the respective parents with a spearman rank correlation. For 44 out of the 45 comparisons the correlation between ASE in the hybrid (*cis*) and fold change in gene expression between the parents (*trans*) was significant (-log10(p) from 7.08 – 429.79, with median of 60.50). The correlation coefficients ranged between 0.08 and 0.58, with a median coefficient of 0.3 (Figure 30).

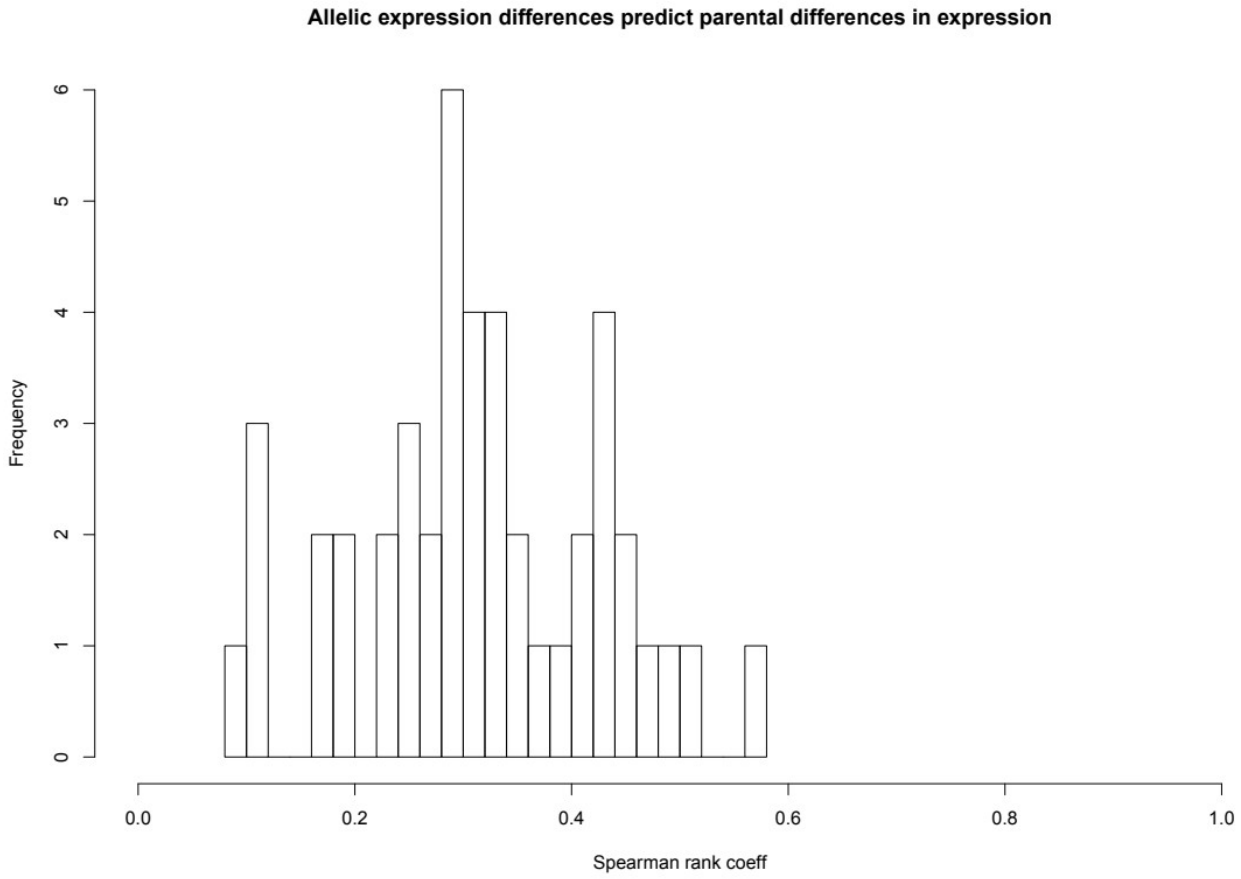

Figure 30: Histogram of spearman rank correlation coefficients between hybrids and parents.

To compute the pairwise correlations for 45 contrasts for each gene the differential expression between the parents was compared to the fold change of ASE in the cross.

When the correlation between *cis* and *trans* is high, a large proportion of the variance in gene expression is explained by *cis*. When a large proportion of the variance is not correlated, the *trans* effect is larger. For most cases the correlation was below 0.5, so there is a strong contribution of *cis*, but also a large *trans* component. To further explore the effect of *cis*-regulatory divergence, we investigated the regional divergence of *cis* variants.

Allele specific expression in hybrids between regions reveals *cis*-regulatory divergence

Cis-regulatory divergence in gene expression was estimated as the significant difference in the allele count in F1-hybrids of crosses between genotypes of different regional origin (Figure 31).

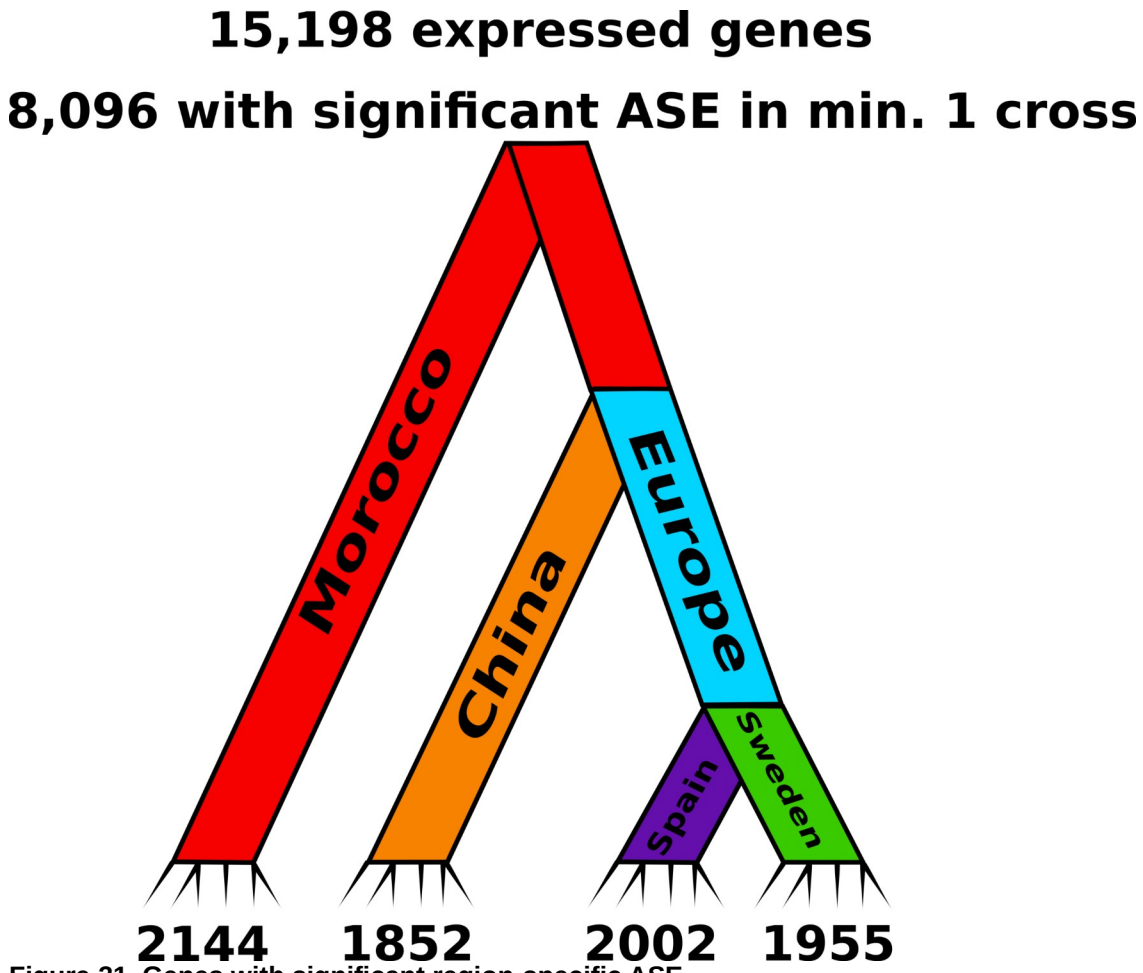

Figure 31. Genes with significant region-specific ASE.

The number of genes with a region-specific ASE signature is presented at the basal branches. Above the phylogeny are the number of total expressed genes and the number of genes with significant ASE.

Of the 15,198 expressed genes, 8,096 had a significant difference in ASE. Each region had the strongest contribution to approximately one quarter of these genes, with the strongest impact of Morocco (2144 genes).

The resulting genes were tested for functional enrichment. If the genes were evolving neutrally, there would be little to no functional enrichment, but the identified genes had clear signatures of functional enrichment. In order to assess a neutral expectation of functional enrichment, I computed a distribution of p-values based on enrichments of randomly selected genes. Based on random enrichment, 5% of the p-values were lower than 0.126, 1% lower than 0.031, and 0.01% lower than 0.0011. The enrichments of the genes with actual ASE signal identified some p-values that were even lower. To represent the divergence in functional enrichment, the GO terms were plotted in a dendrogram of functional classification (Figure 32).

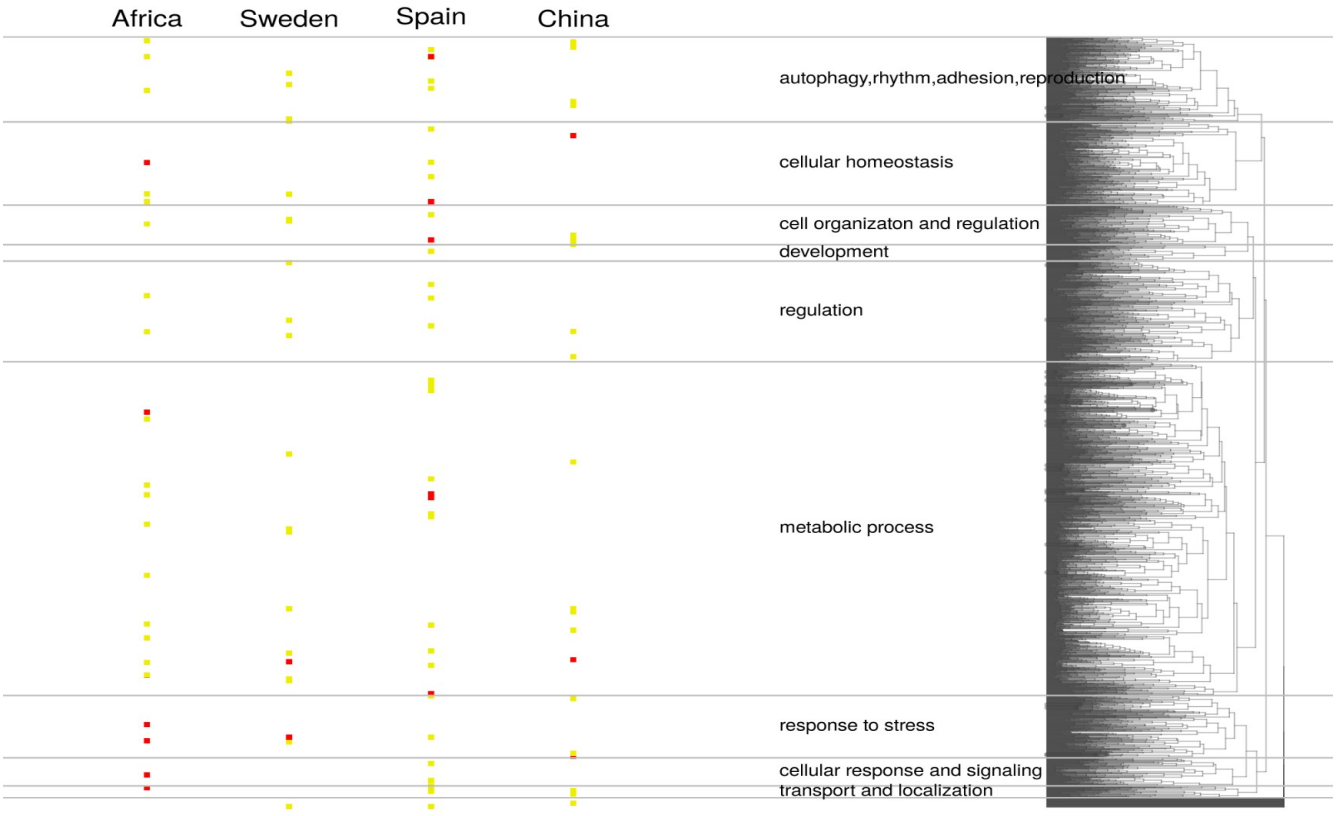

Figure 32: Functional enrichment dendrogram for GO enrichment of region-specific ASE genes.

The enrichment was based on gene sets that are specific to a region compared to all genes with ASE. The GO terms are arranged into 9 clusters of similar function on the right side of the plot. Depicted are only enrichments with a p-value < 0.01. Red dots represent enrichments with p-values < 0.001, yellow dots < 0.01.

Between regions the GO terms with the most significant enrichment were not overlapping and distributed across the functional categories (Figure 32).

The genes with ASE might display a signature of increased genetic differentiation. To investigate the signal of genetic differentiation I used the Fst for genes between Sweden and Spain. I compared the distribution of Fst values between ASE-genes to the distribution of all other genes (Figure 47).

In both regions, the genes with ASE signature displayed larger Fst values. In Sweden the median Fst of genes with ASE was larger than for the other genes (0.074 with ASE in Sweden vs 0.066 for other expressed genes) and the Kolmogorov-Smirnov test indicates a significant difference of the distribution (p= 8.64E-9). In Spain the median Fst of genes with ASE was also larger than for the other genes (0.072 with ASE in Spain vs 0.067 for other expressed genes) and the Kolmogorov-Smirnov test was significant (p= 0.00017).

Since the terms appear to be region-specific the next step was to investigate potential functional patterns associated to regions.

Functional enrichment of genes with ASE reveals region-specific patterns

To compare the signatures for genes with ASE to genes identified for differential gene expression in light-signaling mutants (Table 19) and to genes identified with GWAS (Table 20), I performed hypergeometric tests.

Table 19: Overlap between genes with region-specific ASE and genes with differential gene expression in mutants of the light-signaling pathway.

Information on the region for which the ASE of the genes was signficant and the number of genes is displayed in ASE-Region and ASE genes. For the gene sets identified with differential gene expression the name of the set and the number of genes are displayed in RNA Geneset and RNA genes. The number of overlapping genes and the p-value of the hypergeometric test are displayed in the last two columns. Only significant overlaps are shown. The test was performed on all genes that were expressed in the RNA-sequencing analysis of ASE (15,198 genes).

ASE-Region	ASE genes	RNA Geneset	RNA genes	Overlap	P-value
Morocco	2144	LLN	1711	497	0.003
Sweden	1955	CD	2225	572	0.021
Sweden	1955	HLN	76	25	0.030

Genes with ASE were significantly overlapping with genes identified in LLN (LL at Night, p= 0.003). Genes with Sweden-derived ASE were significantly overlapping with CD (competition during the day, p= 0.021) and HLN (HL at Night, p= 0.030).

Table 20: Overlap between genes with region-specific ASE and genes with association in GWAS.

Information on the region for which the ASE of the genes was signficant and the number of genes is displayed in ASE-Region and ASE genes. For the gene sets identified with GWAS the name of the set and the number of genes are displayed in GWAS Geneset and GWASgenes. The number of overlapping genes and the p-value of the hypergeometric test are displayed in the last two columns. Only significant overlaps are shown. The test was performed on all genes that were expressed in the RNA-sequencing analysis of ASE (15,198 genes).

ASE-Region	ASE genes	GWAS Geneset	GWAS genes	Overlap	P-value
China	1852	FSLL	64	23	0.006
Spain	2002	Height_HD	110	38	0.007
Spain	2002	Height_GXEAC	161	51	0.017
Sweden	1955	ALL	515	144	0.017
Spain	2002	HIDENS	880	239	0.036
Spain	2002	GXEDENS	898	243	0.040
Spain	2002	GxESL	49	17	0.041
Spain	2002	Height_ID	298	86	0.042
Spain	2002	NODENS	506	141	0.042
China	1852	Height_LD	396	104	0.046

The most significant overlap was between China-derived ASE genes and FSLL (p= 0.006). Spain-derived ASE genes were significantly overlapping with several GWAS signals, among them 3 out of 5 GWAS gene sets identified with meta analysis (HIDENS, p= 0.036; GXEDENS, p= 0.040; NODENS, p= 0.042). Sweden-derived ASE genes were significantly overlapping with genes identified across all traits with meta analysis (ALL, p= 0.017). Interestingly, GWAS genes associated with height in above-ground competition conditions were overlapping with ASE genes derived in China for LD (p= 0.046) and with Spain in HD and ID (p= 0.007 and 0.042, respectively).

At last, I checked for specific signatures of functional enrichment for region-specific ASE genes (Table 21). To estimate a threshold below which enrichments can be considered meaningful, I performed 1000 GO analyses with random sets of genes. The resulting distribution of p-values revealed, that the 0.01%-quantile was at a p-value of 0.0011, which I used to determine if a GO enrichment can be considered significant.

Table 21: GO-enrichment of genes with significant region-specific ASE.

Shown are terms with an enrichment < 0.0011. Region gives information on the region for which the genes with ASE were detected. GO.ID and term give information on the enriched GO term. Annotated states all genes that are in the term, Significant is the number of genes that are associated in the input data set and Expected the number of genes that are expected to be enriched by chance. The p-value gives the Fisher score for enrichment. I only report GO terms with >5 genes in them.

Region	Number	GO.ID	Term	Ann.	Sign.	Exp.	P-value
Morocco	1	GO:0019252	starch biosynthetic process	182	48	25.77	9.3E-06
Morocco	2	GO:0009825	multidimensional cell growth	97	27	13.73	0.00032
Morocco	3	GO:0019288	isopentenyl diphosphate biosynthetic process	225	51	31.85	0.00035
Morocco	4	GO:0009072	aromatic amino acid family metabolic process	216	49	30.58	0.00044
Morocco	5	GO:0016117	carotenoid biosynthetic process	99	27	14.02	0.00045
Morocco	6	GO:0006633	fatty acid biosynthetic process	130	33	18.4	0.00047
Morocco	7	GO:0009694	jasmonic acid metabolic process	133	33	18.83	0.00073
Morocco	8	GO:0009637	response to blue light	119	30	16.85	0.00094
China	1	GO:0010207	photosystem II assembly	150	35	18.3	0.00010
China	2	GO:0009902	chloroplast relocation	103	26	12.57	0.00020
China	3	GO:1901615	organic hydroxy compound metabolic process	605	102	73.81	0.00035
Spain	1	GO:0009611	response to wounding	269	57	35.66	0.00018
Spain	2	GO:0009612	response to mechanical stimulus	57	18	7.56	0.00027
Spain	3	GO:0000023	maltose metabolic process	148	35	19.62	0.00039
Spain	4	GO:0046209	nitric oxide metabolic process	7	5	0.93	0.00068
Spain	5	GO:0019252	starch biosynthetic process	182	40	24.13	0.00076
Spain	6	GO:0006766	vitamin metabolic process	88	23	11.67	0.00088
Sweden	1	GO:0009627	systemic acquired resistance	360	70	46.1	0.00019
Sweden	2	GO:0010205	photoinhibition	9	6	1.15	0.00026
Sweden	3	GO:0009753	response to jasmonic acid	382	70	48.92	0.00110

The GO enrichments revealed some functional signatures that seem to be region-specific. In Sweden, GO terms related to stress, specifically light stress, were enriched, like “photoinhibition” and “systemic acquired resistance”.

In HL conditions, the genotypes from Northern Europe displayed signs of stress, scored as number of leaves that turned red as a protection from strong irradiation (Figure 33).

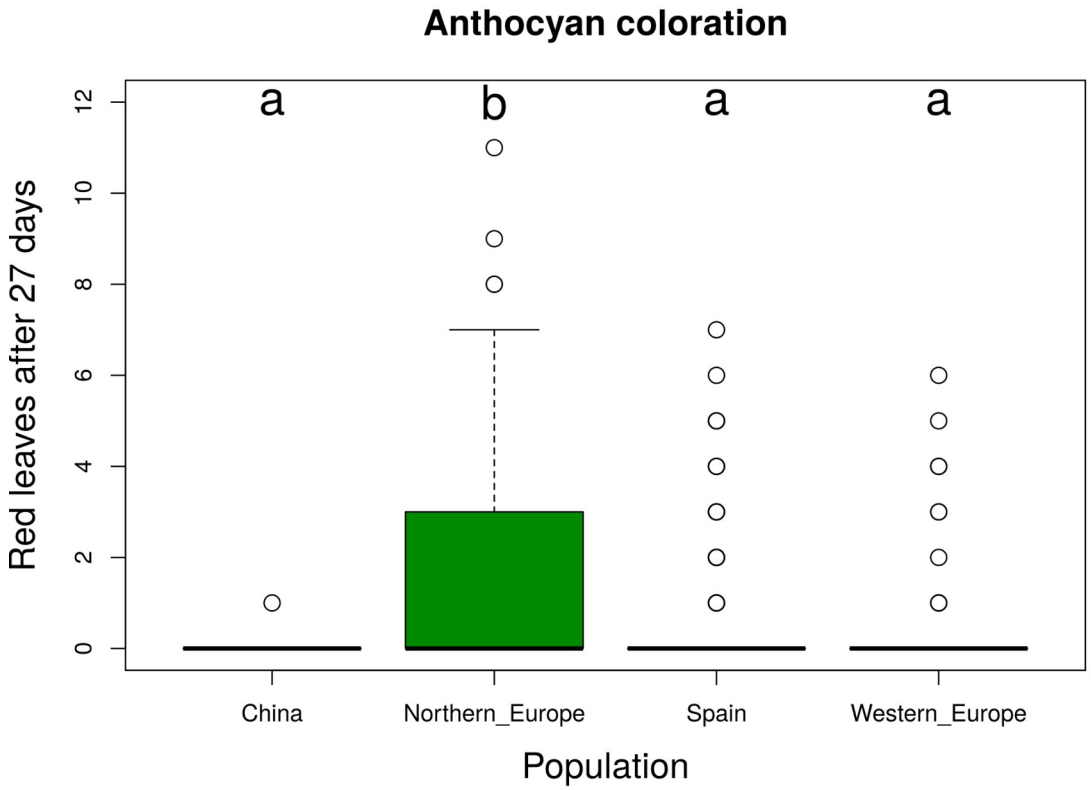

Figure 33: Red leaf coloration after 27 days in HL.

Number of leaves per genotype that are colored red after 27 days in HL are plotted per region. Groups that do not share a letter are significantly different according to Tukey's HSD ($p<0.05$).

The enrichment of genes with ASE in Spain were often characterized by the response to (biotic) stress, with the terms "response to wounding" and "response to mechanical stimulus". The functional enrichments for genes with ASE in China include the terms "photosystem II assembly" and "chloroplast relocation", which related to photosynthesis. In Morocco the signatures includes "starch biosynthetic process" with a very strong enrichment ($p= 9.3E-6$) and several other enrichments related to growth ("multidimensional cell growth"), light perception ("response to blue light") and other molecular functions.

Overall, the GO signature indicate region-specific signatures of molecular functions are underlying the variation in gene expression between *Arabidopsis thaliana* genotypes.

4 Discussion

4.1 Signatures of Local Adaptation of growth rate in *Arabidopsis thaliana*

Trait variation measured in controlled settings sometimes fails to reflect variation expressed in natural conditions (Külheim *et al.*, 2002; Brachi *et al.*, 2010). This is not the case for rosette growth variation in *A. thaliana*. I argue below that a significant part of the variation I characterized is ecologically relevant and can therefore inform about adaptation of complex traits in natural populations.

4.1.1 Growth rate is a plastic trait of ecological relevance

Environmental plasticity has the strongest impact on plant growth variation

Across all parameters measuring growth, I report a strong response to the different conditions. Plants reached a larger diameter (and rosette area) by elongating their petiole and minimizing leaf blade overlap in LL, a reaction known as the shade avoidance response. This strong modification of leaf shape may explain the predominant impact of variation between light environments. This observation was in agreement with the reduced relative growth rate reported in many plant species when light supply decreases, whereas the larger FS reflected the expected shade avoidance reaction (Brachi *et al.*, 2010).

The investigated competition conditions combine limited light supply with competition for other resources like space and nutrients. Under very strong competition (~100 plants/pot), the size decrease I document between conditions is very strong, yet even moderate competition of 5 plants lead to significant reductions in size. Interestingly, I observed the strongest effect of plant origin at moderate plant densities in the above-ground competition experiment (Table 14). A similar plastic response to both light and soil limitations across regions is indicated by GxE estimates of each trait, calculated as the residual of the response of HL/LD to LL/HD. Nevertheless, there are signals for regional differentiation and the interaction between

condition and region is significant for most traits (Table 8, Table 14). The genome-wide association signals for GxE traits also revealed several independent signals.

Overall, growth rate is plastic in the presented environments. As reported in many plant species, competition leads to a reduction in size and can induce earlier flowering to escape the competition (Cahill, 2003; Willis *et al.*, 2010; Mangla *et al.*, 2011; Skálová *et al.*, 2013; Ballaré & Pierik, 2017). This could suggest, that local adaptation mostly affected population establishment at low density, e.g. at the colonization of a habitat.

To understand, which traits and experimental conditions are most relevant I compared the heritabilites of traits among experiments.

Final rosette size is the most heritable trait among experimental conditions

Heritabilities describe the proportion of phenotypic variation that is explained by genetic diversity in the population under study. Heritabilities can thus vary either because the genotypic composition of the population is different or because of environmental variance (Falconer & Mackay Longman, 1996).

Heritabilities in both controlled conditions and in the field indicate, that the final size of the rosette is the most heritable component of plant growth, compared to other parameters of the growth dynamic (Table 7, Table 13).

This heritability was highest in controlled conditions, which is not surprising, since environmental variance is best controlled for in these conditions. In a growth chamber the variation of factors like temperature, precipitation and others can be controlled, which could partially explain a higher heritability of rosette diameter (Méndez-Vigo *et al.*, 2013). For flowering time, variation in the field is often lower than in controlled conditions, because the plants are exposed to environmental cues that induce flowering (Külheim *et al.*, 2002; Brachi *et al.*, 2010; Méndez-Vigo *et al.*, 2013). Interestingly, diameter measured in conditions of below-ground competition displayed a much higher heritability than the FS in above-ground competition.

In this experiment the survival of genotypes from China was strongly decreased by freezing, which is why I focused on the diameter in December (i.e. maximum rosette diameter), before a frost period in January. There also was a frost period in the above-ground competition experiment, but because of the earlier start of the experiment and sufficient nutrient availability the plants were larger in January. It appears that as a consequence Chinese genotypes could survive the cold temperatures better. Differences in survival to frost conditions have been observed within *Arabidopsis* genus before (Hannah *et al.*, 2006; Zhen & Ungerer, 2007; Davey *et al.*, 2009), with European populations of *A. lyrata* showing better frost resistance when they originated from Central Europe than Norway (Takou *et al.*, 2021).

Rosette growth rate is a complex trait of ecological relevance

The ecological relevance of growth rate variation of the rosette size is given by the strong correlations of the estimates of size across traits and experimental conditions (Figure 24). This study thus provides a strong indication that genetic variation measured across conditions is likely to be expressed in nature and directly relevant for plant performance. The FS of the rosette measured in controlled conditions is significantly correlated with hypocotyl length, biomass, rosette area and diameter measured in the field. Large plants are larger across experiments and traits that measure a biomass/size increase are correlated.

Plant growth is also influenced by life history, especially flowering time (Figure 24), as the start of flowering ends the vegetative growth phase in the annual plant *A. thaliana* (Andrés & Coupland, 2012). The significant negative correlation of FS to FT indicates, that plants that reach larger sizes flower earlier; size is thus not independent of the life history (Figure 24). Estimates of flowering time displayed much higher heritabilities in the different conditions (Table 13). But the expression of this phenotype is dependent on environmental cues and the flowering time under natural conditions may be highly different from controlled conditions, where only 30% of the genotypes flowered (Koornneef *et al.*, 2004; Andrés & Coupland, 2012).

Total biomass is the necessary resource for investing into the formation of branches to produce siliques and seeds after flowering. Plant growth should correlate with fitness as well

(Mitchell-Olds, 1996; Younginger *et al.*, 2017). Unfortunately, we did not obtain measurements of genetic variation for fitness. In the above-ground competition experiment, focal plants were collected and stored in bags to dry for later measurements, however, the siliques and branches often broke off during unpacking and could not be estimated precisely. To determine the adaptive relevance of variation in rosette size, population genetics methods were thus required.

4.1.2 Strong signatures of regional differentiation

Spanish genotypes show the most vigorous rosette growth

Across experimental conditions genotypes from Spain were significantly larger than genotypes from other regions, especially Northern Europe. Spanish plants always displayed larger rosette traits. A reduced rosette area in LL conditions compared to genotypes from South Europe (Italy) has been reported for Swedish genotypes before (Stewart *et al.*, 2017). Reciprocal transplant experiments between genotypes from North and South Europe revealed strong adaptive differentiation along this latitudinal cline (Agren & Schemske, 2012). Since Spain and Northern Europe do not differ in their average flowering time, the larger rosette size observed in Spain is not due to an extension of the duration of vegetative growth in this population.

GxE of biomass and diameter between density conditions revealed a significantly higher plasticity in Spain compared to Central and Western Europe, indicating a stronger growth decrease in response to increased plant density in Spain, while CE and WE were less responsive to the treatment. Together this could speak for a smaller amount of competition in the habitats of Spanish plants, because they grow slower and to larger sizes, while being affected by HD more strongly. Alternatively, the evolution of fast cycling early flowering genotypes in CE and WE may have led to a greater insensitivity of plant growth to plant-plant density, because early flowering individuals can escape before they are exposed to severe resource limitations. In Spain, flowering time has patterns of strong regional diversification and individuals from higher altitudes flower late (Picó *et al.*, 2008; Méndez-Vigo *et al.*, 2011, 2013; Exposito-Alonso *et al.*, 2018b).

Plant height could also point towards less competitive ability in genotypes from Spain. A larger height might be advantageous to overgrow competitors and extend the radius of seed dispersal (Morris *et al.*, 2013; Gruntman *et al.*, 2017). Plants from Spain had a smaller stem height, so they would be at disadvantage here, along with their late flowering. It is possible that the climatic conditions in Southern Europe create a situation with less competition.

The plant height is following a latitudinal cline within Europe with longer stems in the North. A correlation between stem growth and photoperiod has been reported, a response that is modulated by gibberellins that were also functionally enriched in response to competition in the RNAseq data (Xu *et al.*, 1997). Still, the ecological relevance of stem height is not known.

Chinese genotypes show that growth rate variation is constrained in evolution

Despite a long history of population isolation that was magnified by a strong bottleneck after the last glacial period (Durvasula *et al.*, 2017; Zou *et al.*, 2017), the growth rate of Chinese genotypes was comparable to that shown by most European genotypes.

When grown under the LL regime, these genotypes displayed a lower FS than genotypes from Spain. In contrast, within Europe, we observed no significant difference in the growth plasticity of plants in relation to light regime, despite the fact that Northern European populations are exposed to lower average light intensity. The analysis of Chinese genotypes indicates that the phenotypic evolution of rosette growth does not scale with the extent of genetic divergence. A parsimonious explanation to the fact that growth rate has not significantly changed despite extensive population divergence, is that the evolution of growth rate is likely to be constrained by stabilizing selection around a growth optimum (Mitchell-Olds, 1996).

4.2 Functional basis of genetic associations to growth rate

4.2.1 Polygenic signatures of adaptation

GWAS reveal few SNPs significantly associated with rosette growth variation

Despite clearly significant levels of heritability, only few traits displayed an association with a significance above the conservative Bonferroni threshold. For a complex trait like growth,

which integrates the expression of multiple levels of plant physiology, a polygenic architecture is expected (Pritchard *et al.*, 2010). Diverse genetic make-ups can result in such polygenic architecture: large effect size variants that are too rare to be detected, many variants with effect sizes too small to be individually significant, or the presence of multiple alleles at causal loci that will blur the genetic association signal (Korte & Farlow, 2013; Sasaki *et al.*, 2015). Local genetic variation in slope and t50, growth parameters which display moderate but significant genetic variance, appear to be controlled by low-frequency variants of comparatively larger effect, since some of them were associated above Bonferroni threshold. This genetic architecture resembles what has been reported in the species for flowering time (Shindo *et al.*, 2005; Méndez-Vigo *et al.*, 2013). In contrast to slope and t50, variation in FS appeared more polygenic since it has the highest heritability and no SNP association above Bonferroni confidence levels.

In response to intra-specific competition, I observed a similar polygenic architecture. Only the final plant height and its GxE had few significant associations. In proximity to the peaks of SNP association, genes were located, whose functions associated with biological processes that might be relevant for growth. Functional meristems are crucial for plant development and the association close to a gene required for meristem function could be directly linked to growth (Alonso-Blanco *et al.*, 2005; DeYoung *et al.*, 2006). The ALDEHYDE OXIDASE 2 association is linked to stress response and the biosynthesis of absiscic acid, which is involved in the regulation of growth (Himmelbach *et al.*, 1998; Khan *et al.*, 2019). Additional genes related to resistance and biosynthesis were also detected, which could be involved in the allocation of resources towards growth (Davila Olivas *et al.*, 2017; Züst & Agrawal, 2017; Solís-Guzmán *et al.*, 2017; Badet *et al.*, 2017).

Genes associated with loss-of-funcion variation are related to growth

While a large proportion of the SNPs found in the genome have no effect on protein function, variants that lead to a complete loss-of-function have recently been the focus of increased attention. Indeed, the availability of whole-genome sequences has revealed that most genes in the genome harbor loss-of-function mutations (LOF), at least at low frequency (Monroe *et al.*, 2018; Xu *et al.*, 2019).

The individual burden of LOF mutations is unrelated to rosette growth variation, but the LOF in a single gene was significantly correlated with t50 in LL. Genotypes with the LOF in NIP1 had shorter growth periods. RNAi-lines of this gene in the Col-0 background were significantly smaller and a mutation in the interacting RPOTmp strongly impacted the growth response. In this genetic background plants needed a longer time period to reach a smaller size. The response of t50 in mutants of RPOTmp is opposite to the correlation between the LOF of NIP1 and t50 in LL. Since NIP1 controls the intra-plastidial trafficking and the function of RPOTmp (Azevedo *et al.*, 2008), a negative regulation of RPOTmp might explain the phenotypes. RPOTmp seems to have important functions in plant growth as it transcribes the rrn operon from the PC promoter during germination (Courtois *et al.*, 2007). Without RPOTmp the rrn operon probably is not transcribed, at least in the early developmental stages, which would consequently lead to fewer ribosomes. In bacteria, the growth rate has been identified to correlate with the number of ribosomes that are synthesized (Ji *et al.*, 1994). So, if the number of ribosomes in plastids of *A. thaliana* decreases, a decreased rosette growth rate would not be surprising.

This case study of an individual gene illustrates, that it is possible to identify candidate genes for growth variation with association scans and verify their impact on growth variation. The interacting gene (RPOTmp) has a severe impact on growth, the RNAi-line of NIP1 did not deliver a clear result and needs to be investigated further. The individual confirmation of the phenotype is challenging as different aspects of the growth rate can be impacted and the occurrence of this LOF also seems to depend on the genetic background.

It is therefore possible to identify single genes with a large impact on the phenotype, but the growth traits mostly display a signature of moderately high associations of many SNPs below the Bonferroni threshold for multiple testing. How informative are these loci about the input traits?

Polygenic scores support the polygenic basis, but are sensitive to population structure

Traits with polygenic architecture are controlled by variation in many loci of low frequency and/or low effect sizes and dissecting their evolution is arguably a major challenge today in

evolutionary biology (Wellenreuther & Hansson, 2016; Csilléry *et al.*, 2018; Zan & Carlborg, 2019; Price *et al.*, 2020).

Polygenic scores predict the phenotype on the basis of the added effects of all associated SNPs (Berg & Coop, 2014; Barghi *et al.*, 2020). For all traits, the polygenic scores of moderately associated SNPs were highly correlated with the input phenotypes. This confirms that sub-significant genetic associations, despite their marginal significance, effectively recapitulate some of the traits' heritability.

But, random SNPs with outlier frequency are not always sufficiently corrected for with the kinship matrix and these may give rise to spurious associations. Indeed, in most cases, polygenic scores computed on the basis of completely random sets of SNPs were also significantly correlated with the input phenotypes, even though the strength of correlation was lower.

Studies of polygenic traits such as human height have shown that residual effects of population structure can give signals of genetic association (Pritchard & Di Rienzo, 2010; Sohail *et al.*, 2019). Similar effects were also encountered in studies of phenotypic variation in plant systems (Fustier *et al.*, 2019). They are expected whenever environmental variance co-varies with population structure, as is likely the case in human studies, but can also persist in common garden studies if populations are geographically differentiated in the genetic component of the trait.

To illustrate how problematic this can be, I performed the GWAS on a phenotypic dataset that assembled the phenotype measured under HL conditions for the Spanish genotypes with the phenotypes measured in LL conditions for the Northern European genotypes and assigned genotypes to their home environments in Spain and Northern Europe. In principle, these phenotypic measurements include environmental covariance, as for example in phenotypic measurements in humans or *in situ* in plant populations (Frachon *et al.*, 2018) (Figure 16 & 17). GWAS on this dataset revealed some very high peaks of associations, which all showed a particularly large Fst. These SNPs have no association with the phenotype, but are clearly population structure outliers that associate, despite controlling for population structure. This

analytical experiment illustrates how strong the signal of a population genetic outlier can be when the measurements are not taken within the same environment.

Population structure is a major confounding factor in the detection of trait associations

Different sub-populations of a species show different patterns of associations, so the results detected in GWAS strongly depend on the choice of populations (Berg *et al.*, 2019; Sohail *et al.*, 2019; Lopez-Arboleda *et al.*, 2021).

Genes close to SNPs associated with the different growth parameters, however, had clearly distinctive patterns of functional enrichment (Table 10). Even though population structure outliers may create some false-positive associations, the polygenic pattern of association that I observe at sub-significant level cannot be explained by the history of population divergence alone.

How can we explore new ways to detect whether complex traits are under selection

The choice of populations affects the outcome of association scans. In the analysis of growth traits in humans the outcome was highly dependent on the choice of populations (Berg *et al.*, 2019; Sohail *et al.*, 2019). In *A. thaliana* moderately associated SNPs ($p<10E-4$) for FT are rarely shared among sub-populations (Lopez-Arboleda *et al.*, 2021). So it may be worthwhile to investigate adaptations within a given sub-population. To identify signatures of adaptation that are less dependent on population structure, however, it is also necessary to think differently about the data.

New mutations that arise in the population are equally likely to increase or decrease the phenotype. At high or low frequencies, the effect sizes of these mutations should be comparable and a plot of allele frequency vs. effect size should be symmetric. In the presence of negative selection, alleles with large effect on the phenotype will generally be removed from the population, and the distribution of effect sizes will show the shape of a smile (Sunyaev *et al.*, in preparation). In my population, the smile plots show asymmetries (Figure 14 & Figure 15), suggesting, that there are different signals for adaptation of each trait. Indeed, asymmetries suggest that variants, which increase or decrease the phenotype are not

equally likely to be removed by drift (for a neutral trait) or by natural selection (when selection constrains the trait around an optimum).

In NE there are shifts towards low frequency for t50 in HL and SL in LL. This could mean that there is selection towards smaller values, with a depletion of new variants that increase the t50 or SL in these conditions. The Spanish genotypes are showing a more symmetric pattern, so this is not a bias in the mutations themselves. Asymmetry in a more recently migrated population (like NE) could point towards ongoing adaptation to the environment. I already observed a smaller t50 in NE, but an even shorter period could be advantageous in the short growth season for *A. thaliana* in Sweden (Debieu *et al.*, 2013). This approach appears to be promising, but it still has to be supported by a more thorough theoretical backbone. Indeed, other aspects, such as the so-called “winner’s curse”, i.e. the increased likelihood that low frequency variants are assigned a higher size effect, can shape the distribution of effects into a smile.

4.2.2 What can we learn about the functional basis of the associations?

The impact of insufficient population structure corrections on GWAS makes it impossible to compute the proportion of false positive among GWAS hits. This shortcoming is even more of a concern when considering marginally significant GWAS hits. A solution to this problem is to investigate the functional connection of associated genes to the observed phenotype. For this, I looked at the gene ontology (GO) of the genes in proximity to the identified markers. Functional enrichments among a random set of genes can happen by chance, but, after removing tandem duplicates, GO enrichment with p-values below 0.008 only occur with a probability of 1/1000. This means that GO enrichments with p-values <0.008 can be considered as biological significant enrichments. We were cautious in our analysis of GO enrichments, by removing tandem duplicates, only considering terms with a minimum of 5 annotated genes and choosing conservative thresholds that are very unlikely to occur by chance alone. So, the GO terms that we do detect are likely to be related to the trait.

GO enrichment show a diverse functional signature of moderately associated markers

Most traits showed at least one functional enrichment within gene ontology (GO) categories, whose link to growth has been documented (Table 35). For example, mechanical stimuli have been shown to strongly influence seedling growth, and I observed that FS, whose GWAS hits are enriched in genes involved in the response to these stimuli, correlated with hypocotyl length and biomass in 3-week-old plants (Braam & Davis, 1990). Genes associated with differences in the growth response to competition are related to the growth of a plant, via regulation of tissue development, cell size and growth (Table 35). Height at ID was enriched for terms related to sulfur compounds, which are important plant nutrients (Kopriva *et al.*, 2019).

The genes identified for plasticity were often enriched for genes involved in a typical plastic growth response: the response to light (shade avoidance for GxEFS, response to far red light for HGxELI and response to blue light for DGxELH, Table 35). It is particularly noteworthy, that these categories are enriched among variants associating with growth plasticity and not genetic variation in plant size. The enrichment of genes with high Fst in the GO category “circadian rhythm” may reflect the local adaptation to Northern variations in day length (De Montaigu *et al.*, 2015; Salmela & Weinig, 2019).

While there are several functional enrichments, the majority of enriched GO categories do not have an easily interpretable link to growth. Since I had measurements from diverse environments, I tried to combine the associations of the growth traits in a meta-analysis.

Combining measurements of growth across experiments via meta-analysis can improve the understanding of the functional basis

Meta-analysis across the different experimental conditions is a powerful tool to identify genetic associations that are robust to specific environmental conditions. For SNPs with associations robust to the experiment or growth parameter identified, I find an enrichment in several annotated molecular functions that are well known for affecting the regulation of growth for several sets of GWAS (Table 15).

Genes in the term cell/developmental growth are defined as processes that modulate “frequency, rate, extent or direction” of cell/developmental growth and can therefore be considered to be important genes for the size of the plants (TAIR). Other traits identified with the meta-analysis might also be interesting, like the “meristem maintenance” or “biosynthetic processes”. The term “stomatal lineage progression” was significantly enriched for 4 of the 5 meta-analysis gene sets (Table 15) and is defined as processes that culminate in the production of a stomatal complex (TAIR). The formation of stomata is important, as they are involved in the trade-off between growth and water conservation (Dittberner *et al.*, 2018). In *Sorghum bicolor* this term was enriched for genes, which were down-regulated in developing leaves, in line with other stress response terms, indicating a decreased stress-response, when these genes are down-regulated (Parvathaneni *et al.*, 2020).
Variation in stress-related functions is known to have an impact on plant growth in *A. thaliana* and the enrichment of defense traits could be due to trade-offs in the growth response (Todesco *et al.*, 2010; Züst & Agrawal, 2017). For trait-specific analyses of enrichments these terms were largely represented. Interestingly, in the meta-analysis I identify barely any other defense/stress-related GO terms.

The meta-analysis seems to be a good addition to the GO enrichment of individual traits, especially to identify more general patterns. The down-side is, that multiple phenotypic measurements have to be generated first. Altogether, functional enrichments among genes located in the vicinity of GWAS hits indicated that a biological signal is detectable among sub-significant genetic associations. I therefore conclude, that SNPs associating at marginal significance levels or with an association that is robust to the conditions in which growth was measured, are true positives in a proportion sufficient to produce a collective signal that can inform about the molecular mechanisms involved in growth change. The biological interpretation of the functions is still challenging with the currently available GO methodology.

GO enrichments are our best approach to understanding functional patterns, but are limited in several ways

The gene ontology is a valuable tool to highlight functions, especially if the number of associations for a trait is high. The GO database provides a comprehensive and widely used network on molecular function, biological role and cellular location and aims to provide a formal representation of the present knowledge on biological functions (Primmer *et al.*, 2013; Carbon *et al.*, 2019). The annotations are either based on experimental evidence, curated non-experimental evidence or (non-curated) computational evidence exploiting existing knowledge (Primmer *et al.*, 2013). Experimental evidence is considered the most reliable form of annotation evidence, but many genes are automatically annotated based on molecular properties which are improved over time (Primmer *et al.*, 2013; Zhao *et al.*, 2020).

This database integrates multiple levels of knowledge and is considered as the best standard currently available for the inference of molecular functions of genes (Zhao *et al.*, 2020). *A. thaliana* has the most comprehensive data, with the highest percentage of annotated genes among all species and a high share of experimental verification (du Plessis *et al.*, 2011; Primmer *et al.*, 2013). Still, the database suffers from several limitations.

Many genes have no annotated function yet, although the absence of an annotation does not mean the absence of a function (Primmer *et al.*, 2013). Additionally, annotated functions are not always correct, especially with computational inference (Primmer *et al.*, 2013; Carbon *et al.*, 2019). A specific problem for the characterization of genes in *A. thaliana* is that most experimental data is based on seedlings and not adult plants, especially in the case of light-signaling (Legris *et al.*, 2017; Poorter *et al.*, 2019). Terms that exactly describe what we investigate here do not necessarily exist (e.g. there are no terms for “rosette growth”, “growth rate”, “response to intra-specific competition” etc.).

Altogether, GO categories are multivariate classifications into functional entities that do not necessarily reflect how natural selection will optimize a complex trait. To this end, it is important to develop novel ways to determine the function of genes at the level of complex phenotypic traits such as plant growth in the presence of light limitation or plant growth in

conditions of high intra-specific competition. Therefore, in collaboration with Konstantin Kerner and Ute Höcker, we explored a novel approach for annotating ecological functions on the basis of gene expression modulation in different mutant backgrounds and environments.

4.2.3 Using environment-specific gene expression to improve the ecological interpretation of signals for functional enrichment

Environment-specific gene expression highlights specific functions

The creation of a customized database has the clear advantage, that it exactly delivers information on the genes that matches the environmental conditions the traits were characterized in. The newly defined terms can give an ad-hoc description of genes that are important for growth even if they have not been analyzed in other experiments.

Light signaling mutants are known to modify growth (de Wit *et al.*, 2016). Manipulating these genes in a single background and measuring the gene expression in different environments can then be used to identify genes whose expression associates with a modification of growth that is specific to these environments.

The mutants in genes controlling the light signaling response were chosen because they alter plant growth after exposure to different environments. Using these mutants, each contrasted to their common wild type, allows differentiating the genes that are under the control of the pathway. Plants were sampled at different time points, because in terms of growth the cell elongation predominantly takes place at night, while cell division occurs during the day (de Montaigu *et al.*, 2010). Furthermore, transcriptional variability is fluctuating throughout the day in *A. thaliana* and it is related to the environmental cues (Cortijo *et al.*, 2019). So examining expression difference at two time points provided complementary information.

We observed, that the majority of genes for all conditions is private to the environment (Figure 29). The number of genes identified between conditions is highly variable. In HLN conditions, which reflects growth in the absence of limiting factors, few genes showed expression changes. With a GO enrichment of the newly defined sets, I tried to link molecular functions with the environment in which they are associated with growth (Table 37). Growth modification in HLN associates with a change in expression of genes involved in the response to high light

intensity, photosynthesis as well as heat stress and the assimilation of carbon and sulfate. Altogether, these functions seem to contribute to plant growth in the absence of notable resource limitations.

The competition conditions CN (night) and CD (day) displayed similar GO term enrichments, associating with functions such as the response to light limitation, cell wall adjustments and hormonal response, especially via jasmonic acid and gibberellin (Navarro *et al.*, 2008; De Jong & Leyser, 2012). In CD, there are more terms related to a wide variety of stressors, such as e.g. “response to chitin”, “systemic acquired resistance” and “response to fungus”. This suggests that the perception of competition associates with the activation of stress responses. Growth in low light during the night (LLN), where light is limiting but not soil nutrients, has clear signatures of limited light, with enrichments for response to various light frequencies (blue light etc.), light limitation and shade. Furthermore, as in competition conditions, we detected the signature of biotic stress, which, in the absence of competitors, could indicate a trade-off in the growth response. Diverse growth response terms and the growth hormone auxin, which is associated with the shade avoidance response (de Wit *et al.*, 2016), were also enriched.

Altogether, we report that both similar and environment-specific differences in the functions associate with changes in plant growth in environment differing in the above- and/or below-ground limitations. The GO enrichments we detected among these genes provide a novel level of gene annotation, which I will henceforth call “ecological” annotation.

Ecological annotations are a novel way to describe gene functions

To test this novel annotation layer, I investigated whether it helped describe the functions highlighted by GWAS. Using gene expression divergence in light signaling mutants allowed me to aggregate genes based on their specific response to a change in growth phenotype. Overlaps of these gene sets to genes identified with GWAS would point to functions important for growth in this environment.

HLN associated genes are significantly enriched among genes that associate with growth in all environments ($p = 0.028$), confirming that this ecological annotation term describes some genes required for growth, regardless of resource limitations. I also found that these genes,

whose expression changes when growth differs between environments, were predominantly associated with SNPs associating with genetic variation in growth plasticity. Indeed, 5 of the 11 significant enrichments in ecological annotations are with genes located in the vicinity of GWAS hits for GxE (Table 18). Even though variation in these phenotypes is not independent from variation expressed in the other environments, the ecological annotations outlined above seem to capture signatures relevant for plant growth variation. Especially the meta-analysis of plasticity to plant density for all growth parameters revealed that 20% of the genes whose expression associated with growth in the absence of limitations (ecological annotation HLN) were located in the vicinity of a GWAS hit (p= 8.7E-05, p= 0.011 after FDR correction). I noted however that many enrichments had p-values that were no longer significant after FDR correction. This correction is very conservative, since the phenotypes tested here are correlated. Future investigations will have to determine whether a more appropriate statistical treatment can be identified.

In conclusion, the ecological annotation of the term HLN (plant growth in isolation and in exposure to elevated light levels) is enriched among genes associating with diverse growth parameters in many environments. We note, that the enrichments we detect show p-values in the realm of those identified for enrichment in GO categories. These enrichments, however, have the marked advantage that they have a phenotypic implication that can be clearly interpreted. Overall, I conclude that it is possible to create a customized database of genes associating with growth modifications in the presence of specific limiting environmental factors. Such database is informative because 1) it is based on well-studied mutants, 2) the candidate genes are based on actual difference in gene expression and 3) the gene expression changes were observed in the exact same environments in which phenotypic variation was quantified. We prioritized light signaling because of the known effect on plant growth response in my conditions in limiting light. In the future, one will have to examine whether the genes we identified as associating with growth also associate with growth in mutants whose growth is altered via other pathways, such as e.g. the genes altering chloroplast maturation, whose effect on t50 was discovered in this thesis.

4.3 Signatures of local adaptation

In the above, I showed that growth rate is clearly a polygenic trait whose elusive genetic basis can be partly resolved by GWAS and functional annotations based on the ecological conditions during growth. During the analyses I observed differential signatures of growth between regions. Here I will discuss whether there are signals of local adaptation among populations and which genes and functions underlie regional differences.

4.3.1 Size variation indicates local adaptation

FS variation might reflect local adaptation at the regional scale

Smaller rosettes are more compact in Northern latitudes, and populations adapted to cold temperatures often display increased compactness (Li *et al.*, 1998; Byars *et al.*, 2007; Jonas *et al.*, 2008; Luo *et al.*, 2015b). Freezing tolerance was indeed reported to be higher in Northern Europe (Horton *et al.*, 2016). As a hypothesis, the decreased FS and t50 observed for Northern European genotypes grown under both light regimes could be the result of polygenic adaptation to lower average temperatures.

The differentiation of polygenic scores between the individual populations of origin suggests that divergent selection may be acting locally. Local adaptation has indeed been reported at this scale in this species (Frachon *et al.*, 2018). This result should however be taken with caution, because, like the GWAS hits it is using, the Qx statistics is sensitive to population structure outliers. Clearly, population structure might underpin more of the GWAS signal detected for slope or t50, which are markedly less heritable than FS.

In fact, associated SNPs are collectively more likely to be differentiated than the rest of the genome. I nevertheless believe, that this pattern is not caused by the confounding effect of population structure, because the functional enrichments we find among the genes that locate close to these hits are mostly specific to the phenotypes. However, I cannot entirely exclude that a few spurious genetic associations could contribute to both higher Fst and over-dispersion of polygenic scores (Berg *et al.*, 2019; Fustier *et al.*, 2019; Sohail *et al.*, 2019). We also do not know how large our rate of false positive associations is, especially due to population structure.

Additional evidence based on approaches independent of GWAS is therefore required to support the adaptive significance of regional differences in growth rate in Europe. To this end, we used the population kinship matrix to parameterize a multivariate normal distribution and predict the amount of additive phenotypic divergence expected if the trait evolves entirely neutrally (Koch, 2019b). The Qst for FS in HL and LL was higher than for t50 and Slope but only marginally significant compared to the prediction under neutral conditions. In response to density, there was no significantly higher Qst than expected under neutral conditions.

Since the divergent Chinese population indicates that selection may constrain the divergence in growth rate variation, this test might be overly conservative. In addition, it predicts the divergence in additive genetic variance, but in the selfing species *A. thaliana*, the whole genetic variance, i.e. broad sense heritability, can contribute to adaptation.

The high Qst-values compared to the SNP Fst distribution (Table 12) suggest that selective forces have contributed to the regional adaptation of FS in Europe. Growth rate could be locally adapted to the conditions prevailing in each region, but the environmental factors contributing to adaptive divergence in plant growth remain to be determined in this species. Another way to interpret the size differences between populations could be an accumulation of deleterious mutations over time.

No association between per-individual burden and growth

In areas located at the edge of the distribution range of *A. thaliana*, populations may have accumulated an excess of deleterious mutations in the aftermath of their genetic isolation (Peischl *et al.*, 2013; 1001 Genomes Consortium, 2016). This could have resulted in a mutational load that would have decreased fitness components such as plant growth, because it influences the resources available for the production of progeny (Mitchell-Olds, 1996; Klopfstein *et al.*, 2006; Willi *et al.*, 2018). The lower FS observed in Northern Europe may result from maladaptive forces associated with the demographic history of the region.

This hypothesis could not be supported. The genomic burden, measured as total number of LOF mutations, was not different between genotypes from Spain and Northern Europe. This observation has been previously reported (Monroe *et al.*, 2018). Furthermore, the Chinese

displayed no significant difference in growth to Northern European populations, despite their significantly higher burden of LOF alleles per genome. Taken together, this result does not support the hypothesis that decreased FS in Northern Europe or China is controlled by deleterious variation. Minimal impact of genomic load on fitness has been documented in the close outcrossing relative *A. lyrata (Takou et al., 2021)*.

4.3.2 Are there different functional enrichments in gene expression variation between populations?

Significant impact of allele-specific expression indicates the polygenic basis of gene expression

The examination of allele-specific expression variation provides a view on the genetics of gene expression variation that is independent of the phenotype-based approach described above. To determine the phylogeographic history of *cis*-regulatory changes, we measured allele-specific expression (ASE) in F1 hybrids contrasting ASE in individuals from Spain and Sweden with genotypes from two outgroup population: China and Africa. In addition, we based the analysis on expression patterns quantified on plant leaves collected during the exponential growth phase in HL. This strategy allowed us to infer the likely evolutionary origin of *cis*-acting changes that modify expression during a crucial phase of the plant's growth. Altogether, we observed that about half of the expressed genes have a significant signature of ASE in at least one F1.

The comparison between parents and the hybrids revealed, that *cis*-regulatory variation explains a significant part of gene expression differences between parents (Figure 30). Clearly, however *trans* effects in gene expression also contribute to gene expression divergence. *Trans*-acting variation has even been shown to be the predominant source of expression variation in both animal and plant systems (Emerson *et al.*, 2010; Emerson & Li, 2010; Schaefke *et al.*, 2013; Albert & Kruglyak, 2015; Signor & Nuzhdin, 2018). Yet, ASE variation is typical for the polygenic basis of phenotypic variation: *cis*-acting changes are numerous variants and their effect on the phenotype is small, with probably infinitesimal consequences on fitness. If ASE variation is not exposed to natural selection, we expect ASE

to be randomly distributed in terms of function, since the allele-specific variation in the expression of each transcript evolves independently.

Region-specific patterns of functional enrichment of ASE genes can be detected

This is the first description of ASE derived in two European regions, using Africa (Morocco) and China as two outgroups. As expected given the long history of divergence from the African population, we detected the highest number of ASE in F1 comparing genotypes from Africa with the other regions. Yet, the number of ASE did not clearly scale with the history of colonization, indicating that the accumulation of ASE is not controlled by neutral processes alone.

Marked functional enrichments among region-specific ASE changes further indicate, that the accumulation of regulatory changes is not only driven by random processes. Indeed, enrichments that are significant at p-values below the threshold established by permutation differ between regions. The distribution of these mutations across the various functions that are expressed and display ASE variation is shaped by region-specific selection on specific functions.

Is ASE derived variation reflecting local adaptation in growth? We do observe a significant overlap between derived-ASE and genetic variants associating with plant growth (Table 17), as well as significant overlap with functions related to specific growth traits (Table 18).

Morocco-derived ASE genes were enriched among genes whose expression during the night (i.e. when cell elongation takes place) associates with a change in growth of plants developing under low light (LLN). Having verified that ASE associates both with genes whose expression was associated with growth in both mutant and GWAS analyses, the study of GO enrichment can provide a description of the molecular components that were recruited for local adaptation. Among genes with Morocco-derived ASE, we observed the strongest enrichment for “starch biosynthetic process” (p=9.3E-6, Table 21), which is associated with mobilization of energy reserves in the presence of abiotic stress (Thalmann & Santelia, 2017). The role of this functional category in plant growth modulation is further supported by the gene expression analysis of growth mutants. Indeed, “starch biosynthetic process” was also

one of the most strongly enriched functional categories among genes whose expression was modified in plants growing under low light (LLN, Table 37, p= 3.7E-10).

Patterns of functional enrichment among genes that evolved a *cis*-regulatory change in a specific regions provide a novel and complementary perspective on the molecular functions that contribute to the polygenic adaptation of plant growth. Our design allowed inferring functions that accumulated an excess of *cis*-regulatory change in Chinese genotypes. GO terms related to photosynthesis and pigments were strikingly enriched in this lineage (Table 21). This suggests, that the functioning of photosystems has been deeply remodeled in this lineage, which needs to be validated and further explored in future studies.

GO terms based on Spain-derived ASE genes contain functions, that were also identified among gene variants associating with plant growth traits, like “response to mechanical stimulus”, “response to karrikin” and stress responses in general. The Spain-derived ASE genes were also enriched for several terms related to (biotic) stress, which were also strongly enriched among genes whose expression associates with a growth change. Studying ASE gives a different view on functions associated with the polygenic basis of plant growth variation. For genotypes from Spain, we reported an increase in size phenotypes and the ASE signal for Spanish genotypes is strongly related to growth across environments and height phenotypes specifically (Table 20).

ASE derived in Sweden was enriched in genes whose expression associated with a reduction of plant size in competition (during the day) and those associating with a reduction of plant size due to high light (reduced elongation) (Table 19). The genes with ASE in Sweden included many genes related to light stress. This is intriguing, since the genotypes from Northern Europe displayed increased signs of anthocyan accumulation (red leaf coloration), which is a protection against high light intensity (Steyn *et al.*, 2002). This suggests, that Swedish plants might be more sensitive to the stress effect of high light exposure, compared to individuals originating from other regions. Sweden-derived ASE genes were significantly overlapping with genes identified across all traits in GWAS. So, there is a significant intersection between GWAS based on the genetic basis of growth phenotypes and ASE, which is based on gene expression variation during the exponential growth phase.

This result is noteworthy, since the independent signals gathered here point towards a shared genetic basis for two *a priori* independent traits, genetic variation in growth parameters and in gene expression. Hence, we can conclude that ASE variation contains information about the molecular basis of plant growth adaptation.

The findings on region-specific gene expression can be summarized in three points. First, the significant overlaps between ASE derived in the four regions and SNPs associating with phenotypic growth confirms that ASE contributes to the molecular basis of a complex phenotype like growth. Second, the fact that ASE is not randomly distributed in each region, but enriched in specific functions that differ between regions, provide a strong indication that these functions form some of the molecular components that sustained adaptive evolution in each region. Future studies will have to investigate specifically how the modification of genes involved in these functions is affecting the phenotype.

4.4 Synthesis and outlook

In this final section, I will summarize some of the aspects I have discussed in this thesis. The overall goal of this project was to test and validate novel approaches that provide a better understanding of the molecular components that form the basis for growth adaptation in *A. thaliana*. The results presented in this work highlight that while it is possible to identify meaningful signatures, these signatures are constrained by several factors.

The genetic basis of growth adaptation is complex and polygenic, which by definition makes identification of the single genetic variant that promotes adaptation difficult because the potential number of associated genes is infinitisemal and the effect sizes are low. Therefore, the polygenic basis of adaptation can only be unraveled through a collective analysis of modifications.

To understand the underlying molecular functions, I have used the existing Gene Ontology as a functional framework in which to study the underlying patterns. While this is the best framework we have available at the moment, it is incomplete and not designed to interpret signatures of selection. Yet, in the analyses I conducted here, there were enrichments in functions that were significantly stronger than expected by chance. Polygenic adaptation

recruits a myriad of variants with infinitesimal effects. My work demonstrates that this recruitment is not random, but it highlights some of the molecular functions that are predominantly remodeled. By combining information from a reductionist approach (using mutants), a quantitative genetic approach (using GWAS) and a genomic approach (identifying patterns of ASE evolution), I indeed identify molecular targets for polygenic selection on plant growth. The overlap between signatures of polygenic selection on *cis*-regulatory variation, the study of phenotypic variation via GWAS, and the experimental identification of regulatory changes associated with growth alterations collectively point to the predominant adaptive role of molecular functions related to light perception, hormones, defense/stress and growth regulation are involved in local adaptation.

While GWAS is now a standard tool in population genomics and ecology (Visscher *et al.*, 2017; Santure & Garant, 2018), this approach is not well suited for studying local adaptation. I illustrate this by showing that very strong peaks can occur when phenotypes differ between populations. Indeed, the discovery of genes associated with traits is affected by population structure. With the results we get from GWAS, the real rate of false positives cannot be determined. Mapping *cis*-regulatory variants and their origins throughout the genome allows us to look at genetic variation from a different perspective. It circumvents the problem of population structure because differences in gene expression are measured directly in a common genetic environment. The genes identified by this approach are numerous, and we expected them to be differentially enriched among locally adaptive functions and signaling pathways in the process of adaptation to different environments.

Overall, my work highlights the complex signatures of polygenic adaptation in *A. thaliana* overcoming the experimental limitations caused by a complex genetic architecture, confounding effects of population structure, and detection bias of genetic variants that are numerous but difficult to detect.

I hope, that this work can provide a valuable contribution to the understanding of the genetic basis of adaptation in *A. thaliana* and help improve analyses of this kind in the future.

Acknowledgements

I want to thank Prof. Dr. Juliette de Meaux for giving me the opportunity to work on this project and to grow my personal expertise under her supervision. Juliette helped me to dig deep into Evolution and develop the necessary scientific skills. I would like to thank Prof. Dr. Andreas Beyer and Dr. Sebastián Ramos-Onsins for advising me as part of my thesis committee and during my stay in Barcelona. I would like to thank my co-authors Dr. Margarita Takou, Dr. Kim Steige, Dr. Fei He, Dr. Sebastián Ramos-Onsins, Dr. Evan Koch and Prof. Dr. Shamil Sunyaev for helpful suggestions in shaping my work into a valuable scientific contribution. The members of the de Meaux lab have been a great help in the progress of the work, by offering advice, help and support. I would like to thank Dr. Gregor Schmitz, Dr. Hannes Dittberner, Dr. Maroua Bouzid Elkhesairi, Dr. Ulrike Goebel and Lea Hoerdemann, as well as the new members and students. The Bachelor students Lucas Aschenbrenner & Franziska Geuchen were of great help conducting experiments, as well as the students Gero Carus, Simon Mitreiter and Jennifer Escher and our student helpers. A big thank you goes to Kirsten Bell for her support during plant experiments and laboratory work.

Finally, I would like to thank my wife, family and friends for their support.

Bibliography

1001 Genomes Consortium T. **2016**. 1,135 Genomes Reveal the Global Pattern of Polymorphism in Arabidopsis thaliana. *Cell* **166**: 1–11.

Agren J, Schemske DW. **2012**. Reciprocal transplants demonstrate strong adapative differentiation of the model organism Arabidopsis thaliana in its native range. *New Phytologist* **194**: 1112–1122.

Albert FW, Kruglyak L. **2015**. The role of regulatory variation in complex traits and disease. *Nature Reviews Genetics* **16**: 197–212.

Alexa A, Rahnenfuhrer J. **2019**. topGO: Enrichment Analysis for Gene Ontology. R package version 2.36.0.

Alexa A, Rahnenführer J, Lengauer T. **2006**. Improved scoring of functional groups from gene expression data by decorrelating GO graph structure. *Bioinformatics* **22**: 1600–1607.

Alonso-Blanco C, Mendez-Vigo B, Koornneef M. **2005**. From phenotypic to molecular polymorphisms involved in naturally occurring variation of plant development. *International Journal of Developmental Biology* **49**: 717–732.

Alonso JM, Stepanova AN, Leisse TJ, Kim CJ, Chen H, Shinn P, Stevenson DK, Zimmerman J, Barajas P, Cheuk R, *et al.* 2003. Genome-wide insertional mutagenesis of Arabidopsis thaliana. *Science* **301**: 653–657.

Anders S, Pyl PT, Huber W. **2015**. HTSeq - A Python framework to work with high-throughput sequencing data. *Bioinformatics* **31**: 166–169.

Andrés F, Coupland G. **2012**. The genetic basis of flowering responses to seasonal cues. *Nature Reviews Genetics* **13**: 627–639.

Aschenbrenner L. **2017**. Evaluation of regional differences in the growth response of Arabidopsis thaliana. *Bachelor Thesis*.

Austen EJ, Rowe L, Stinchcombe JR, Forrest JRK. **2017**. Explaining the apparent paradox of persistent selection for early flowering. *New Phytologist* **215**: 929–934.

Azevedo J, Courtois F, Hakimi M-A, Demarsy E, Lagrange T, Lerbs-Mache S, Alcaraz J-P, Jaiswal P, Maréchal-Drouard L, Lerbs-Mache S. **2008**. Intraplastidial trafficking of a phage-type RNA polymerase is mediated by a thylakoid RING-H2 protein. *Proceedings of the National Academy of Sciences* **105**: 2–7.

Bac-Molenaar JA, Granier C, Keurentjes JJB, Vreugdenhil D. **2016**. Genome wide association mapping of time-dependent growth responses to moderate drought stress in Arabidopsis. *Plant, Cell & Environment* **39**: 88–102.

Bac-Molenaar JA, Vreugdenhil D, Granier C, Keurentjes JJB. **2015**. Genome-wide association mapping of growth dynamics detects time-specific and general quantitative trait loci. *Journal of Experimental Botany* **66**: 5567–5580.

Badet T, Voisin D, Mbengue M, Barascud M, Sucher J, Sadon P, Balagué C, Roby D, Raffaele S. **2017**. Parallel evolution of the POQR prolyl oligo peptidase gene conferring plant quantitative disease resistance. *PLoS Genetics* **13**: e1007143.

Ballaré CL. **2014**. Light Regulation of Plant Defense. *Annual Review of Plant Biology* **65**: 335–363.

Ballaré CL, Pierik R. **2017**. The shade-avoidance syndrome: Multiple signals and ecological consequences. *Plant Cell and Environment* **40**: 2530–2543.

Barghi N, Hermisson J, Schlötterer C. **2020**. Polygenic adaptation: a unifying framework to understand positive selection. *Nature Reviews Genetics*.

Baron E, Richirt J, Villoutreix R, Amsellem L, Roux F. **2015**. The genetics of intra- and interspecific competitive response and effect in a local population of an annual plant species. *Functional Ecology* **29**: 1361–1370.

Barrett RDH, Hoekstra HE. **2011**. Molecular spandrels: Tests of adaptation at the genetic level. *Nature Reviews Genetics* **12**: 767–780.

Barton NH, Keightley PD. **2002**. Understanding quantitative genetic variation. *Nature Reviews Genetics* **3**: 11–21.

Berg JJ, Coop G. **2014**. A Population Genetic Signal of Polygenic Adaptation. *PLoS Genetics* **10**: 1–25.

Berg JJ, Harpak A, Sinnott-Armstrong N, Joergensen AM, Mostafavi H, Field Y, Boyle EA, Zhang X, Racimo F, Pritchard JK, *et al.* 2019. Reduced signal for polygenic adaptation of height in UK Biobank. *eLife* **8**: 1–47.

Bolger AM, Lohse M, Usadel B. **2014**. Trimmomatic: A flexible trimmer for Illumina sequence data. *Bioinformatics* **30**: 2114–2120.

Bou-Torrent J, Roig-Villanova I, Galstyan A, Martínez-García JF. **2008**. PAR1 and PAR2 integrate shade and hormone transcriptional networks. *Plant Signaling and Behavior* **3**: 453–454.

Boyle EA, Li YI, Pritchard JK. **2017**. An Expanded View of Complex Traits: From Polygenic to Omnigenic. *Cell* **169**: 1177–1186.

Braam J, Davis RW. **1990**. Rain-, wind-, and touch-induced expression of calmodulin and calmodulin-related genes in Arabidopsis. *Cell* **60**: 357–364.

Brachi B, Faure N, Horton M, Flahauw E, Vazquez A, Nordborg M, Bergelson J, Cuguen J, Roux F. **2010**. Linkage and association mapping of Arabidopsis thaliana flowering time in nature. *PLoS Genetics* **6**: 1–17.

Browning BL. **2019**. Beagle 5.1. : 1–6.

Byars SG, Papst W, Hoffmann AA. **2007**. Local adaptation and cogradient selection in the alpine plant, Poa hiemata, along a narrow altitudinal gradient. *Evolution* **61**: 2925–2941.

Cahill JF. **2003**. Lack of relationship between below-ground competition and allocation to roots in 10 grassland species. *Journal of Ecology* **91**: 532–540.

Campitelli BE, Des Marais DL, Juenger TE. **2016**. Ecological interactions and the fitness effect of water-use efficiency: Competition and drought alter the impact of natural MPK12 alleles in Arabidopsis. *Ecology Letters* **19**: 424–434.

Carbon S, Douglass E, Dunn N, Good B, Harris NL, Lewis SE, Mungall CJ, Basu S, Chisholm RL, Dodson RJ, *et al.* 2019. The Gene Ontology Resource: 20 years and still GOing strong. *Nucleic Acids Research* **47**: 330–338.

Carus G. **2017**. Die genetische Basis der Wettbewerbsfähigkeit von Arabidopsis thaliana.

Casal JJ, Mazzella MA. **1998**. Conditional synergism between cryptochrome 1 and phytochrome B is shown by the analysis of phyA, phyB, and hy4 simple, double, and triple mutants in Arabidopsis. *Plant Physiology* **118**: 19–25.

Chen M, Chory J, Fankhauser C. **2004**. Light signal transduction in higher plants. *Annual Review Genetics* **38**: 87–117.

Cheng X-F, Wang Z-Y. **2005**. Overexpression of COL9, a CONSTANS-LIKE gene, delays flowering by reducing expression of CO and FT in Arabidopsis thaliana. *The Plant Journal* **43**: 758–768.

Chevin LM, Lande R. **2010**. When do adaptive plasticity and genetic evolution prevent extinction of a density-regulated population? *Evolution* **64**: 1143–1150.

Chiang GCK, Barua D, Dittmar E, Kramer EM, de Casas RR, Donohue K. **2013**. Pleiotropy in the wild: The dormancy gene dog1 exerts cascading control on life cycles. *Evolution* **67**: 883–893.

Clauss MJ, Koch MA. **2006**. Poorly known relatives of Arabidopsis thaliana. *Trends in Plant Science* **11**: 449–459.

Conway J, Gehlenborg N. **2019**. Package ‘ UpSetR ’.

Cortijo S, Aydin Z, Ahnert S, Locke JC. **2019**. Widespread inter-individual gene expression variability in Arabidopsis thaliana . *Molecular Systems Biology* **15**: e8591.

Courtois F, Merendino L, Demarsy E, Mache R, Lerbs-Mache S. **2007**. Phage-type RNA polymerase RPOTmp transcribes the rrn operon from the PC promoter at early developmental stages in Arabidopsis. *Plant Physiology* **145**: 712–721.

Csilléry K, Rodríguez-Verdugo A, Rellstab C, Guillaume F. **2018**. Detecting the genomic signal of polygenic adaptation and the role of epistasis in evolution. *Molecular ecology* **27**: 606–612.

Danecek P, Auton A, Abecasis G, Albers CA, Banks E, DePristo MA, Handsaker RE, Lunter G, Marth GT, Sherry ST, *et al.* 2011. The variant call format and VCFtools. *Bioinformatics* **27**: 2156–2158.

Davey MP, Ian Woodward F, Paul Quick W. **2009**. Intraspecfic variation in cold-temperature metabolic phenotypes of Arabidopsis lyrata ssp. petraea. *Metabolomics* **5**: 138–149.

Davila Olivas NH, Frago E, Thoen MPM, Kloth KJ, Becker FFM, van Loon JJA, Gort G, Keurentjes JJB, van Heerwaarden J, Dicke M. **2017**. Natural variation in life history strategy of Arabidopsis thaliana determines stress responses to drought and insects of different feeding guilds. *Molecular Ecology* **26**: 2959–2977.

Debieu M, Tang C, Stich B, Sikosek T, Effgen S, Josephs E, Schmitt J, Nordborg M, Koornneef M, de Meaux J. **2013**. Co-Variation between Seed Dormancy, Growth Rate and Flowering Time Changes with Latitude in Arabidopsis thaliana. *PLoS ONE* **8**: 1–12.

Deng XW, Matsui M, Wei N, Wagner D, Chu AM, Feldmann KA, Quail PH. **1992**. COP1, an Arabidopsis regulatory gene, encodes a protein with both a zinc-binding motif and a Gβ homologous domain. *Cell* **71**: 791–801.

DeYoung BJ, Bickle KL, Schrage KJ, Muskett P, Patel K, Clark SE. **2006**. The CLAVATA1-related BAM1, BAM2 and BAM3 receptor kinase-like proteins are required for meristem function in Arabidopsis. *The Plant Journal* **45**: 1–16.

Dittberner H, Korte A, Mettler-Altmann T, Weber APM, Monroe G, de Meaux J. **2018**. Natural variation in stomata size contributes to the local adaptation of water-use efficiency in Arabidopsis thaliana. *Molecular Ecology* **27**: 4052–4065.

Dobin A, Davis CA, Schlesinger F, Drenkow J, Zaleski C, Jha S, Batut P, Chaisson M, Gingeras TR. **2013**. STAR: ultrafast universal RNA-seq aligner. *Bioinformatics* **29**: 15–21.

Donohue K. **2002**. Germination timing influences natural selection on life-history characters in Arabidopsis thaliana. *Ecology* **83**: 1006–1016.

Donohue K, Polisetty CR, Wender NJ. **2005**. Genetic basis and consequences of niche construction: plasticity-induced genetic constraints on the evolution of seed dispersal in Arabidopsis thaliana. *The American naturalist* **165**: 537–550.

Durvasula A, Fulgione A, Gutaker RM, Alacakaptan SI, Flood PJ, Neto C, Tsuchimatsu T, Burbano HA, Picó FX, Alonso-Blanco C, *et al.* 2017. African genomes illuminate the early history and transition to selfing in Arabidopsis thaliana. *Proceedings of the National Academy of Sciences* **114**: 201616736.

Emerson JJ, Hsieh LC, Sung HM, Wang TY, Huang CJ, Lu HHS, Lu MYJ, Wu SH, Li WH. **2010**. Natural selection on cis and trans regulation in yeasts. *Genome Research* **20**: 826–836.

Emerson JJ, Li WH. **2010**. The genetic basis of evolutionary change in gene expression levels. *Philosophical Transactions of the Royal Society B: Biological Sciences* **365**: 2581–2590.

Escher J. **2018**. The genetic basis of intraspecific competition in Arabidopsis thaliana.

Exposito-Alonso M, Becker C, Schuenemann VJ, Reiter E, Setzer C, Slovak R, Brachi B, Hagmann J, Grimm DG, Chen J, *et al.* 2018a. The rate and potential relevance of new mutations in a colonizing plant lineage. *PLoS Genetics* **14**: 1–21.

Exposito-Alonso M, Brennan AC, Alonso-Blanco C, Picó FX. **2018b**. Spatio-temporal variation in fitness responses to contrasting environments in *Arabidopsis thaliana*. *Evolution*: 1570–1586.

Falconer DS, Mackay Longman TFC. **1996**. *Introduction to quantitative genetics (4th edn)*.

Fick SE, Hijmans RJ. **2017**. Worldclim 2: New 1-km spatial resolution climate surfaces for global land areas. International Journal of Climatology.

Filiault DL, Maloof JN. **2012**. A genome-wide association study identifies variants underlying the Arabidopsis thaliana shade avoidance response. *PLoS Genetics* **8**: 1–12.

Footitt S, Huang Z, Clay HA, Mead A, Finch-Savage WE. **2013**. Temperature, light and nitrate sensing coordinate Arabidopsis seed dormancy cycling, resulting in winter and summer annual phenotypes. *The Plant Journal* **74**: 1003–1015.

Fournier-Level a., Korte A, Cooper MD, Nordborg M, Schmitt J, Wilczek a. M. **2011**. A Map of Local Adaptation in Arabidopsis thaliana. *Science* **334**: 86–89.

Frachon L, Bartoli C, Carrère S, Bouchez O, Chaubet A, Gautier M, Roby D, Roux F. **2018**. A Genomic Map of Climate Adaptation in Arabidopsis thaliana at a Micro-Geographic Scale. *Frontiers in Plant Science* **9**: 1–15.

Fulgione A, Koornneef M, Roux F, Hermisson J, Hancock AM. **2018**. Madeiran Arabidopsis thaliana Reveals Ancient Long-Range Colonization and Clarifies Demography in Eurasia. *Molecular Biology and Evolution* **35**: 564–574.

Fustier MA, Martínez-Ainsworth NE, Aguirre-Liguori JA, Venon A, Corti H, Rousselet A, Dumas F, Dittberner H, Camarena MG, Grimanelli D, *et al.* 2019. *Common gardens in teosintes reveal the establishment of a syndrome of adaptation to altitude*.

Garton S, Knight H, Warren GJ, Knight MR, Thorlby GJ. **2007**. crinkled leaves 8 - A mutation in the large subunit of ribonucleotide reductase - leads to defects in leaf development and chloroplast division in Arabidopsis thaliana. *The Plant Journal* **50**: 118–127.

Van Gelderen K, Kang C, Pierik R. **2018**. Update on Light Signaling and Root Development Light Signaling, Root Development, and Plasticity. *Plant Physiology* **176**: 1049–1060.

Geuchen F. **2021**. The impact of RPOTmp on growth plasticity to light intensity in Arabidopsis thaliana.

Glander S, He F, Schmitz G, Witten A, Telschow A, de Meaux J. **2018**. Assortment of Flowering Time and Immunity Alleles in Natural Arabidopsis thaliana Populations Suggests Immunity and Vegetative Lifespan Strategies Coevolve. *Genome Biology and Evolution* **10**: 2278–2291.

González N, Inzé D. **2015**. Molecular systems governing leaf growth: From genes to networks. *Journal of Experimental Botany* **66**: 1045–1054.

Goudet J. **2005**. HIERFSTAT , a package for R to compute and test hierarchical F -statistics. *Molecular Ecology Notes* **5**: 184–186.

Gruntman M, Groß D, Májeková M, Tielbörger K. **2017**. Decision-making in plants under competition. *Nature Communications* **8**: 1–8.

Hancock AM, Brachi B, Faure N, Horton MW, Jarymowycz LB, Sperone FG, Toomajian C, Roux F, Bergelson J. **2011**. Adaptation to Climate Across the Arabidopsis thaliana Genome. *Science* **334**: 83–86.

Hanemian M, Vasseur F, Marchadier E, Gilbault E, Bresson J, Gy I, Violle C, Loudet O. **2019**. Transcriptional natural variation at FLM induces synergistic pleiotropy in Arabidopsis thaliana. *bioRxiv*: 658013.

Hannah MA, Wiese D, Freund S, Fiehn O, Heyer AG, Hincha DK. **2006**. Natural genetic variation of freezing tolerance in arabidopsis. *Plant Physiology* **142**: 98–112.

He F, Arce AL, Schmitz G, Koornneef M, Novikova P, Beyer A, De Meaux J. **2016**. The Footprint of Polygenic Adaptation on Stress-Responsive Cis-Regulatory Divergence in the Arabidopsis Genus. *Molecular Biology and Evolution* **33**: 2088–2101.

He F, Kang D, Ren Y, Qu L-J, Zhen Y, Gu H. **2007**. Genetic diversity of the natural populations of Arabidopsis thaliana in China. *Heredity* **99**: 423–431.

He H, De Souza Vidigal D, Basten Snoek L, Schnabel S, Nijveen H, Hilhorst H, Bentsink L. **2014**. Interaction between parental environment and genotype affects plant and seed performance in Arabidopsis. *Journal of Experimental Botany* **65**: 6603–6615.

van Heerwaarden J, van Zanten M, Kruijer W. **2015**. Genome-Wide Association Analysis of Adaptation Using Environmentally Predicted Traits. *PLoS Genetics* **11**: 1–23.

Hilson P, Allemeersch J, Altmann T, Aubourg S, Avon A, Beynon J, Bhalerao RP, Bitton F, Caboche M, Cannoot B, *et al.* 2004. Versatile gene-specific sequence tags for Arabidopsis functional genomics: Transcript profiling and reverse genetics applications. *Genome Research* **14**: 2176–2189.

Himmelbach A, Iten M, Grill E. **1998**. Signalling of abscisic acid to regulate plant growth. *The Royal Society* **353**.

Hoffmann MH. **2002**. Biogeography of Arabidopsis thaliana (L.) Heynh. (Brassicaceae). *Journal of Biogeography* **29**: 125–134.

Hoffmann M. **2005**. Evolution of the realized climatic niche in the genus Arabidopsis (Brassicaceae). *Evolution* **59**: 1425–1436.

Holtan HE, Bandong S, Marion CM, Adam L, Tiwari S, Shen Y, Maloof JN, Maszle DR, Ohto M aki, Preuss S, *et al.* 2011. Bbx32, an arabidopsis b-box protein, functions in light signaling by suppressing HY5-regulated gene expression and interacting with STH2/BBX21. *Plant Physiology* **156**: 2109–2123.

Hornitschek P, Kohnen M V., Lorrain S, Rougemont J, Ljung K, López-Vidriero I, Franco-Zorrilla JM, Solano R, Trevisan M, Pradervand S, *et al.* 2012. Phytochrome interacting factors 4 and 5 control seedling growth in changing light conditions by directly controlling auxin signaling. *The Plant Journal* **71**: 699–711.

Horton MW, Willems G, Sasaki E, Koornneef M, Nordborg M. **2016**. The genetic architecture of freezing tolerance varies across the range of Arabidopsis thaliana. *Plant Cell and Environment* **39**: 2570–2579.

Hothorn T, Bretz F, Westfall P, Heiberger RM, Schuetzenmeister A, Scheibe S. **2017**. Package ‘multcomp’ - Simultaneous Inference in General Parametric Models.

Hu J, Lei L, De Meaux J. **2017**. Temporal fitness fluctuations in experimental Arabidopsis thaliana populations. *PLoS ONE* **12**: 1–17.

Ji YE, Colston MJ, Cox RA. **1994**. The ribosomal RNA (rrn) operons of fast-growing mycobacteria: Primary and secondary structures and their relation to rrn operons of pathogenic slow-growers. *Microbiology* **140**: 2829–2840.

Jonas T, Rixen C, Sturm M, Stoeckli V. **2008**. How alpine plant growth is linked to snow cover and climate variability. *Journal of Geophysical Research: Biogeosciences* **113**: 1–10.

De Jong M, Leyser O. **2012**. Developmental Plasticity in plants. *Cold Spring Harbor Symposia on Quantitative Biology* **77**: 63–73.

Josephs EB, Berg JJ, Ross-Ibarra J, Coop G. **2019**. Detecting adaptive differentiation in structured populations with genomic data and common gardens. *Genetics* **211**: 989–1004.

Kang HMH, Sul JHJ, Service SK, Zaitlen NN a, Kong S-YY, Freimer NB, Sabatti C, Eskin E. **2010**. Variance component model to account for sample structure in genome-wide association studies. *Nature genetics* **42**: 348–354.

Kasulin L, Rowan BA, León RJC, Schuenemann VJ, Weigel D, Botto JF. **2017**. A single haplotype hyposensitive to light and requiring strong vernalization dominates *Arabidopsis thaliana* populations in Patagonia, Argentina. *Molecular Ecology* **26**: 3389–3404.

Kerdaffrec E, Filiault DL, Korte A, Sasaki E, Nizhynska V, Seren Ü, Nordborg M. **2016**. Multiple alleles at a single locus control seed dormancy in Swedish Arabidopsis. *eLife* **5**: 1–24.

Khan M, Imran QM, Shahid M, Mun BG, Lee SU, Khan MA, Hussain A, Lee IJ, Yun BW. **2019**. Nitric oxide- induced AtAO3 differentially regulates plant defense and drought tolerance in Arabidopsis thaliana. *BMC Plant Biology* **19**: 602.

Kleinboelting N, Huep G, Kloetgen A, Viehoever P, Weisshaar B. **2012**. GABI-Kat SimpleSearch: New features of the Arabidopsis thaliana T-DNA mutant database. *Nucleic Acids Research* **40**: 1211–1215.

Klopfstein S, Currat M, Excoffier L. **2006**. The Fate of Mutations Surfing on the Wave of a Range Expansion. *Molecular Biology and Evolution* **23**: 482–490.

Koch E. **2018**. The effects of demography and genetics on the neutral distribution of quantitative traits. *bioRxiv*: 1–30.

Koch MA. **2019a**. The plant model system Arabidopsis set in an evolutionary, systematic, and spatio-temporal context. *Journal of Experimental Botany* **70**: 55–67.

Koch EM. **2019b**. The effects of demography and genetics on the neutral distribution of quantitative traits. *Genetics* **211**: 1371–1394.

Koornneef M, Alonso-Blanco C, Vreugdenhil D. **2004**. Naturally occuring genetic variation in Arabidopsis thaliana. *Annual Review of Plant Biology* **55**: 141–172.

Kopriva S, Malagoli M, Takahashi H. **2019**. Sulfur nutrition: impacts on plant development, metabolism, and stress responses. *Journal of Experimental Botany* **70**: 4069–4073.

Körner C. **2015**. Paradigm shift in plant growth control. *Current Opinion in Plant Biology* **25**: 107–114.

Korte A, Farlow A. **2013**. The advantages and limitations of trait analysis with GWAS: a review. *Plant Methods* **9**: 29–38.

Kronholm I, Picó F, Alonso-Blanco C, Goudet J, de Meaux J. **2012**. Genetic basis of adaptation in Arabidopsis thaliana: Local adaptation at the seed dormancy QTL DOG1. *Evolution* **66**: 2287–2302.

Külheim C, Ågren J, Jansson S. **2002**. Rapid regulation of light harvesting and plant fitness in the field. *Science* **297**: 91–93.

Kumari S, Yadav S, Patra D, Singh S, Sarkar AK, Panigrahi KCS. **2019**. Uncovering the molecular signature underlying the light intensity-dependent root development in Arabidopsis thaliana. *BMC Genomics* **20**: 596.

Lasky JR, Des Marais DL, Lowry DB, Povolotskaya I, McKay JK, Richards JH, Keitt TH, Juenger TE. **2014**. Natural variation in abiotic stress responsive gene expression and local adaptation to climate in Arabidopsis thaliana. *Molecular Biology and Evolution* **31**: 2283–2296.

Laubinger S, Hoecker U. **2003**. The SPA1-like proteins SPA3 and SPA4 repress photomorphogenesis in the light. *The Plant Journal* **35**: 373–385.

Lee C-R, Svardal H, Farlow A, Exposito-Alonso M, Ding W, Novikova P, Alonso-Blanco C, Weigel D, Nordborg M. **2017**. On the post-glacial spread of human commensal Arabidopsis thaliana. *Nature Communications* **8**: 14458.

Legris M, Nieto C, Sellaro R, Prat S, Casal JJ. **2017**. Perception and signalling of light and temperature cues in plants. *Plant Journal* **90**: 683–697.

Leinonen T, McCairns RJS, O'Hara RB, Merilä J. **2013**. Q(ST)-F(ST) comparisons: evolutionary and ecological insights from genomic heterogeneity. *Nature reviews. Genetics* **14**: 179–90.

Li Y, Cheng R, Spokas KA, Palmer AA, Borevitz JO. **2014**. Genetic variation for life history sensitivity to seasonal warming in Arabidopsis thaliana. *Genetics* **196**: 569–577.

Li H, Durbin R. **2009**. Fast and accurate short read alignment with Burrows-Wheeler transform. *Bioinformatics* **25**: 1754–1760.

Li H, Handsaker B, Wysoker A, Fennell T, Ruan J, Homer N, Marth G, Abecasis G, Durbin R. **2009**. The Sequence Alignment/Map format and SAMtools. *Bioinformatics* **25**: 2078–2079.

Li B, Suzuki J-I, Hara T. **1998**. Latitudinal variation in plant size and relative growth rate in Arabidopsis thaliana. *Oecologia* **115**: 293–301.

Lopez-Arboleda WA, Reinert S, Nordborg M, Korte A. **2021**. Global genetic heterogeneity in adaptive traits. *bioRxiv*: 1–35.

Love MI, Huber W, Anders S. **2014**. Moderated estimation of fold change and dispersion for RNA-seq data with DESeq2. *Genome Biology* **15**: 550.

Luo Y, Dong X, Yu T, Shi X, Li Z, Yang W, Widmer A, Karrenberg S. **2015a**. A single nucleotide deletion in Gibberellin20-oxidase1 causes alpine dwarfism in Arabidopsis. *Plant Physiology* **168**: 930–937.

Luo Y, Widmer A, Karrenberg S. **2015b**. The roles of genetic drift and natural selection in quantitative trait divergence along an altitudinal gradient in Arabidopsis thaliana. *Heredity* **114**: 220–8.

Mangla S, Sheley RL, James JJ, Radosevich SR. **2011**. Intra and interspecific competition among invasive and native species during early stages of plant growth. *Plant Ecology* **212**: 531–542.

Manolio TA, Collins FS, Cox NJ, Goldstein DB, Hindorff LA, Hunter DJ, McCarthy MI, Ramos EM, Cardon LR, Chakravarti A, *et al.* 2009. Finding the missing heritability of complex diseases. *Nature* **461**: 747–753.

Marcer A, Vidigal DS, James PMA, Fortin M-J, Méndez-Vigo B, Hilhorst HWM, Bentsink L, Alonso-Blanco C, Picó FX. **2018**. Temperature fine-tunes Mediterranean Arabidopsis thaliana life-cycle phenology geographically. *Plant Biology* **20**: 148–156.

Masclaux F, Hammond RL, Meunier J, Gouhier-Darimont C, Keller L, Reymond P. **2010**. Competitive ability not kinship affects growth of Arabidopsis thaliana accessions. *New Phytologist* **185**: 322–331.

McKenna A, Hanna M, Banks E, Sivachenko A, Cibulskis K, Kernytsky A, Garimella K, Altshuler D, Gabriel S, Daly M, *et al.* 2010. The Genome Analysis Toolkit: A MapReduce framework for analyzing next-generation DNA sequencing data. *Genome Research* **20**: 1297–1303.

Mckown AD, Klápště J, Guy RD, Geraldes A, Porth I, Hannemann J, Friedmann M, Muchero W, Tuskan GA, Ehlting J, *et al.* 2014. Genome-wide association implicates numerous genes underlying ecological trait variation in natural populations of Populus trichocarpa. *New Phytologist* **203**: 535–553.

Méndez-Vigo B, Gomaa NH, Alonso-Blanco C, Xavier Picó F. **2013**. Among- and within-population variation in flowering time of Iberian Arabidopsis thaliana estimated in field and glasshouse conditions. *New Phytologist* **197**: 1332–1343.

Méndez-Vigo B, Picó FX, Ramiro M, Martinez-Zapater JM, Alonso-Blanco C. **2011**. Altitudinal and Climatic Adaptation Is Mediated by Flowering Traits and FRI, FLC, and PHYC Genes in Arabidopsis. *Plant Physiology* **157**: 1942–1955.

de Miguel M, Rodríguez-Quilón I, Heuertz M, Hurel A, Grivet D, Jaramillo-Correa JP, Vendramin GG, Plomion C, Majada J, Alía R, *et al.* 2020. Polygenic adaptation and negative selection across traits, years and environments in a long-lived plant species (Pinus pinaster Ait., Pinaceae). *bioRxiv*: 1–50.

Mitchell-Olds T. **1996**. Genetic constraints on life-history. *Evolution* **50**: 140–145.

Mitreiter S. **2017**. Density-dependent growth in Arabidopsis thaliana.

Mojica JP, Mullen J, Lovell JT, Monroe JG, Paul JR, Oakley CG, McKay JK. **2016**. Genetics of water use physiology in locally adapted Arabidopsis thaliana. *Plant Science* **251**: 12–22.

Monroe J, Powell T, Price N, Mullen J., Howard A, Evans K, Lovell J, McKay J. **2018**. Drought adaptation in Arabidopsis thaliana by extensive genetic loss-of- function. *eLife* **7**: 2–21.

De Montaigu A, Giakountis A, Rubin M, Tóth R, Cremer F, Sokolova V, Porri A, Reymond M, Weinig C, Coupland G. **2015**. Natural diversity in daily rhythms of gene expression contributes to phenotypic variation. *Proceedings of the National Academy of Sciences of the United States of America* **112**: 905–910.

de Montaigu A, Tóth R, Coupland G. **2010**. Plant development goes like clockwork. *Trends in Genetics* **26**: 296–306.

Montesinos-Navarro A, Wig J, Xavier Pico F, Tonsor SJ. **2011**. Arabidopsis thaliana populations show clinal variation in a climatic gradient associated with altitude. *New Phytologist* **189**: 282–294.

Morris GP, Ramu P, Deshpande SP, Hash CT, Shah T, Upadhyaya HD, Riera-Lizarazu O, Brown PJ, Acharya CB, Mitchell SE, *et al.* 2013. Population genomic and genome-wide association studies of agroclimatic traits in sorghum. *Proceedings of the National Academy of Sciences* **110**: 453–8.

Morrison GD, Linder CR. **2014**. Association mapping of germination traits in Arabidopsis thaliana under light and nutrient treatments: Searching for G×E effects. *G3: Genes, Genomes, Genetics* **4**: 1465–1478.

Muñoz-Parra E, Pelagio-Flores R, Raya-González J, Salmerón-Barrera G, Ruiz-Herrera LF, Valencia-Cantero E, López-Bucio J. **2017**. Plant-plant interactions influence developmental phase transitions, grain productivity and root system architecture in *Arabidopsis* via auxin and *PFT1/MED25* signalling. *Plant, Cell & Environment* **40**: 1887–1899.

Navarro L, Bari R, Achard P, Lisón P, Nemri A, Harberd NP, Jones JDG. **2008**. DELLAs Control Plant Immune Responses by Modulating the Balance of Jasmonic Acid and Salicylic Acid Signaling. *Current Biology* **18**: 650–655.

Novembre J, Barton NH. **2018**. Tread lightly interpreting polygenic tests of selection. *Genetics* **208**: 1351–1355.

Novikova PY, Hohmann N, Nizhynska V, Tsuchimatsu T, Ali J, Muir G, Guggisberg A, Paape T, Schmid K, Fedorenko OM, *et al.* 2016. Sequencing of the genus Arabidopsis identifies a complex history of nonbifurcating speciation and abundant trans-specific polymorphism. *Nature Genetics* **48**: 1077–1082.

Orr HA. **2002**. The population genetics of adaptation: the adaptation of DNA sequences. *Evolution; international journal of organic evolution* **56**: 1317–1330.

Osterlund MT, Hardtke CS, Ning W, Deng XW. **2000**. Targeted destabilization of HY5 during light-regulated development of Arabidopsis. *Nature* **405**: 462–466.

Paradis E, Claude J, Strimmer K. **2004**. APE: Analyses of phylogenetics and evolution in R language. *Bioinformatics* **20**: 289–290.

Parvathaneni RK, Kumar I, Braud M, Eveland AL. **2020**. Regulatory signatures of drought response in stress resilient Sorghum bicolor. *bioRxiv*: 1–24.

Peischl S, Dupanloup I, Kirkpatrick M, Excoffier L. **2013**. On the accumulation of deleterious mutations during range expansions. *Molecular Ecology* **22**: 5972–5982.

Pfeifer B, Wittelsburger U, Ramos-Onsins SE, Lercher MJ, Wittelsbürger U, Ramos-Onsins SE, Lercher MJ, Wittelsburger U, Ramos-Onsins SE, Lercher MJ. **2014**. PopGenome: An Efficient Swiss Army Knife for Population Genomic Analyses in R. *Molecular Biology and Evolution* **31**: 1929–1936.

Picó FX, Méndez-Vigo B, Martínez-Zapater JM, Alonso-Blanco C. **2008**. Natural genetic variation of Arabidopsis thaliana is geographically structured in the Iberian Peninsula. *Genetics* **180**: 1009–1021.

Pigliucci M. **2005**. Evolution of phenotypic plasticity: Where are we going now? *Trends in Ecology and Evolution* **20**: 481–486.

Pinheiro J, Bates D, DebRoy S, Sarkar D, Team RC. **2018**. nlme: linear and nonlinear mixed effects models.

du Plessis L, Skunca N, Dessimoz C. **2011**. The what, where, how and why of gene ontology--a primer for bioinformaticians. *Briefings in Bioinformatics* **12**: 723–735.

Poorter H, Niinemets Ü, Ntagkas N, Siebenkäs A, Mäenpää M, Matsubara S, Pons TL. **2019**. A meta-analysis of plant responses to light intensity for 70 traits ranging from molecules to whole plant performance. *New Phytologist* **223**: 1073–1105.

Poplin R, Ruano-Rubio V, DePristo MA, Fennell TJ, Carneiro MO, Van der Auwera GA, Kling DE, Gauthier LD, Levy-Moonshine A, Roazen D, *et al.* 2017. Scaling accurate genetic variant discovery to tens of thousands of samples. *bioRxiv*: 201178.

Postma FM, Ågren J. **2015**. Maternal environment affects the genetic basis of seed dormancy in *Arabidopsis thaliana*. *Molecular Ecology* **24**: 785–797.

Postma FM, Ågren J. **2016**. Early life stages contribute strongly to local adaptation in Arabidopsis thaliana. *Proceedings of the National Academy of Sciences of the United States of America* **113**: 201606303.

Price N, Lopez L, Platts AE, Lasky JR. **2020**. In the presence of population structure: From genomics to candidate genes underlying local adaptation. *Ecology and Evolution*: 1889–1904.

Primmer CR, Papakostas S, Leder EH, Davis MJ, Ragan MA. **2013**. Annotated genes and nonannotated genomes: Cross-species use of Gene Ontology in ecology and evolution research. *Molecular Ecology* **22**: 3216–3241.

Pritchard JK, Pickrell JK, Coop G. **2010**. The Genetics of Human Adaptation: Hard Sweeps, Soft Sweeps, and Polygenic Adaptation. *Current Biology* **20**: R208–R215.

Pritchard JK, Di Rienzo A. **2010**. Adaptation - not by sweeps alone. *Nature Reviews Genetics* **11**: 665–667.

Purcell S, Chang C. **2019**. PLINK 1.9.

R-Development-Core-Team. **2008**. R: A language and environment for statistical computing.

Rae L, Lao NT, Kavanagh TA. **2011**. Regulation of multiple aquaporin genes in Arabidopsis by a pair of recently duplicated DREB transcription factors. *Planta* **234**: 429–444.

Rasband W. **2012**. ImageJ. *U.S. National Institutes of Health*.

Ritz C, Baty F, Streibig JC, Gerhard D. **2015**. Dose-response analysis using R. *PLoS ONE* **10**: 1–13.

Rolauffs S, Fackendahl P, Sahm J, Fiene G, Hoecker U. **2012**. Arabidopsis COP1 and SPA genes are essential for plant elongation but not for acceleration of flowering time in response to a low red light to far-red light ratio. *Plant Physiology* **160**: 2015–2027.

Salmela MJ, Ewers BE, Weinig C. **2016**. Natural quantitative genetic variance in plant growth differs in response to ecologically relevant temperature heterogeneity. *Ecology and Evolution* **6**: 7574–7585.

Salmela MJ, Weinig C. **2019**. The fitness benefits of genetic variation in circadian clock regulation. *Current Opinion in Plant Biology* **49**: 86–93.

Santure AW, Garant D. **2018**. Wild GWAS—association mapping in natural populations. *Molecular Ecology Resources* **18**: 729–738.

Sasaki E, Zhang P, Atwell S, Meng D, Nordborg M. **2015**. " Missing " G x E Variation Controls Flowering Time in Arabidopsis thaliana. *PLoS Genetics*: 1–18.

Savolainen PA, Box PO, Carolina N, Carolina N, Oulu B, Box PO. **2013**. Genetic basis of local adaptation and flowering time variation in Arabidopsis lyrata. *Molecular Ecology* **22**: 709–723.

Schaefke B, Emerson JJ, Wang T-Y, Lu M-YJ, Hsieh L-C, Li W-H. **2013**. Inheritance of Gene Expression Level and Selective Constraints on Trans- and Cis-Regulatory Changes in Yeast. *Molecular Biology and Evolution* **30**: 2121–2133.

Sessions A, Burke E, Presting G, Aux G, McElver J, Patton D, Dietrich B, Ho P, Bacwaden J, Ko C, *et al.* 2002. A High-Throughput Arabidopsis Reverse Genetics System. *The Plant Cell* **14**: 2985–2994.

Sham A, Al-Ashram H, Whitley K, Iratni R, El-Tarabily KA, AbuQamar SF. **2019**. Metatranscriptomic Analysis of Multiple Environmental Stresses Identifies RAP2.4 Gene Associated with Arabidopsis Immunity to Botrytis cinerea. *Scientific Reports* **9**: 1–15.

Shi H, Kichaev G, Pasaniuc B. **2016**. Contrasting the Genetic Architecture of 30 Complex Traits from Summary Association Data. *American Journal of Human Genetics* **99**: 139–153.

Shindo C, Aranzana MJ, Lister C, Baxter C, Nicholls C, Nordborg M, Dean C. **2005**. Role of FRIGIDA and FLOWERING LOCUS C in determining variation in flowering time of Arabidopsis. *Plant Physiology* **138**: 1163–1173.

Signor SA, Nuzhdin S V. 2018. The Evolution of Gene Expression in cis and trans. *Trends in Genetics* **34**: 532–544.

Simons YB, Sella G. **2016**. The impact of recent population history on the deleterious mutation load in humans and close evolutionary relatives. *Current Opinion in Genetics and Development* **41**: 150–158.

Skálová H, Jarošík V, Dvořácková S, Pyšek P. **2013**. Effect of Intra-and Interspecific Competition on the Performance of Native and Invasive Species of Impatiens under Varying Levels of Shade and Moisture. *PLoS ONE* **8**: 1–9.

Smith H. **1982**. Light quality, photoperception and plant strategy. *Annual Reviews Plant Physiology* **33**: 481–518.

Sohail M, Maier RM, Ganna A, Bloemendal A, Martin AR, Turchin MC, Chiang CWK, Hirschhorn J, Daly MJ, Patterson N, *et al.* 2019. Polygenic adaptation on height is overestimated due to uncorrected stratification in genome-wide association studies. *eLife* **8**: 1–17.

Solís-Guzmán MG, Argüello-Astorga G, López-Bucio J, Ruiz-Herrera LF, López-Meza JE, Sánchez-Calderón L, Carreón-Abud Y, Martínez-Trujillo M. **2017**. Arabidopsis thaliana sucrose phosphate synthase (sps) genes are expressed differentially in organs and tissues, and their transcription is regulated by osmotic stress. *Gene Expression Patterns* **25–26**: 92–101.

Stetter MG, Thornton K, Ross-ibarra J. **2018**. Genetic architecture and selective sweeps after polygenic adaptation to distant trait optima. *PLoS Genetics*: 1–24.

Stewart JJ, Polutchko SK, Adams WW, Demmig-Adams B. **2017**. Acclimation of Swedish and Italian ecotypes of Arabidopsis thaliana to light intensity. *Photosynthesis Research* **134**: 215–229.

Steyn WJ, Wand SJE, Holcroft DM, Jacobs G. **2002**. Anthocyanins in vegetative tissues: A proposed unified function in photoprotection. *New Phytologist* **155**: 349–361.

Stock AJ, McGoey B V., Stinchcombe JR. **2015**. Water availability as an agent of selection in introduced populations of Arabidopsis Thaliana: Impacts on flowering time evolution. *PeerJ* **2015**: 1–16.

TAIR. The Arabidopsis Information Resource (TAIR).

Takou M, Hämälä T, Koch EM, Steige KA, Dittberner H, Yant L, Genete M, Sunyaev S, Castric V, Vekemans X, *et al.* 2021. Maintenance of Adaptive Dynamics and No Detectable Load in a Range-Edge Outcrossing Plant Population. *Molecular Biology and Evolution*.

Takou M, Wieters B, Kopriva S, Coupland G, Linstädter A. **2019**. Linking genes with ecological strategies in Arabidopsis thaliana. *Journal of Experimental Botany* **70**: 1141–1151.

Tang LY, Matsushima R, Sakamoto W. **2012**. Mutations defective in ribonucleotide reductase activity interfere with pollen plastid DNA degradation mediated by DPD1 exonuclease. *The Plant Journal* **70**: 637–649.

Thalmann M, Santelia D. **2017**. Starch as a determinant of plant fitness under abiotic stress. *New Phytologist* **214**: 943–951.

The Inkscape Team. **2007**. Inkscape.

Thornton KR, Jensen JD, Becquet C, Andolfatto P. **2007**. Progress and prospects in mapping recent selection in the genome. *Heredity* **98**: 340–348.

Todesco M, Balasubramanian S, Hu TT, Traw MB, Horton M, Epple P, Kuhns C, Sureshkumar S, Schwartz C, Lanz C, *et al.* 2010. Natural allelic variation underlying a major fitness trade-off in Arabidopsis thaliana. *Nature* **465**: 632–636.

Trabucco A, Zomer R. **2010**. Global soil water balance geospatial database. CGIAR Consortium for Spatial Information. *Published Online*.

Vasseur F, Exposito-Alonso M, Ayala-Garay OJ, Wang G, Enquist BJ, Vile D, Violle C, Weigel D. **2018**. Adaptive diversification of growth allometry in the plant Arabidopsis thaliana. *Proceedings of the National Academy of Sciences* **115**: 3416–3421.

Vetter MM, Kronholm I, He F, Häweker H, Reymond M, Bergelson J, Robatzek S, De Meaux J. **2012**. Flagellin perception varies quantitatively in arabidopsis thaliana and its relatives. *Molecular Biology and Evolution* **29**: 1655–1667.

Vidigal DS, Marques ACSS, J.Willems LA, Buijs G, Méndez-Vigo B, Hilhorst HM, Bentsink L, Picó FX, Alonso-Blanco C. **2016**. Altitudinal and climatic associations of seed dormancy and flowering traits evidence adaptation of annual life cycle timing in Arabidopsis thaliana. *Plant Cell and Environment* **39**: 1737–1748.

Visscher PM, Wray NR, Zhang Q, Sklar P, McCarthy MI, Brown MA, Yang J. **2017**. 10 Years of GWAS Discovery: Biology, Function, and Translation. *American Journal of Human Genetics* **101**: 5–22.

De Vylder J, Vandenbussche F, Hu Y, Philips W, Van Der Straeten D. **2012**. Rosette Tracker: an open source image analysis tool for automatic quantification of genotype effects.

Wei T, Simko V. **2017**. R package ‘corrplot’: Visualisation of a Correlation Matrix (Version 0.84).

Weigel D, Nordborg M. **2015**. Population Genomics for Understanding Adaptation in Wild Plant Species. *Annual review of genetics*: 1–24.

Wellenreuther M, Hansson B. **2016**. Detecting Polygenic Evolution: Problems, Pitfalls, and Promises. *Trends in Genetics* **32**: 155–164.

Whitlock MC, Guillaume F. **2009**. Testing for spatially divergent selection: Comparing QST to FST. *Genetics* **183**: 1055–1063.

Whittaker C, Dean C. **2017**. The *FLC* Locus: A Platform for Discoveries in Epigenetics and Adaptation. *Annual Review of Cell and Developmental Biology* **33**: 555–575.

Wieters B, Steige KA, He F, Koch EM, Ramos-Onsins SE, Gu H, Guo YL, Sunyaev S, de Meaux J. **2021**. Polygenic adaptation of rosette growth variation in Arabidopsis thaliana populations. *PLoS Genetics*: 1–27.

Wilczek AM, Roe JL, Knapp MC, Cooper MD, Lopez-Gallego C, Martin LJ, Muir CD, Sim S, Petipas R, Giakountis A, *et al.* 2009. Effects of Genetic Perturbation on Seasonal Life History Plasticity. *Science* **323**: 930–935.

Willer CJ, Li Y, Abecasis GR. **2010**. METAL: Fast and efficient meta-analysis of genomewide association scans. *Bioinformatics* **26**: 2190–2191.

Willi Y, Fracassetti M, Zoller S, Van Buskirk J. **2018**. Accumulation of Mutational Load at the Edges of a Species Range. *Molecular Biology and Evolution* **35**: 781–791.

Willis CG, Brock MT, Weinig C. **2010**. Genetic variation in tolerance of competition and neighbour suppression in Arabidopsis thaliana. *Journal of Evolutionary Biology* **23**: 1412–1424.

Wilson AJ, Pemberton JM, Pilkington JG, Clutton-Brock TH, Coltman DW, Kruuk LEB. **2007**. Quantitative genetics of growth and cryptic evolution of body size in an island population. *Evolutionary Ecology* **21**: 337–356.

de Wit M, Costa Galvão V, Fankhauser C. **2016**. Light-Mediated Hormonal Regulation of Plant Growth and Development. *Annual Review of Plant Biology* **67**: 513–537.

Wray NR, Ripke S, Mattheisen M, Trzaskowski M, Byrne EM, Abdellaoui A, Adams MJ, Agerbo E, Air TM, Andlauer TMF, *et al.* 2018. Genome-wide association analyses identify 44 risk variants and refine the genetic architecture of major depression. *Nature Genetics* **50**: 668–681.

Xu YL, Gage DA, Zeevaart JAD. **1997**. Gibberellins and stem growth in Arabidopsis thaliana: Effects of photoperiod on expression of the GA4 and GA5 loci. *Plant Physiology* **114**: 1471–1476.

Xu YC, Niu XM, Li XX, He W, Chen JF, Zou YP, Wu Q, Zhang YE, Busch W, Guoa YL. **2019**. Adaptation and phenotypic diversification in arabidopsis through loss-of-function mutations in protein-coding genes. *Plant Cell* **31**: 1012–1025.

Yang J, Benyamin B, Lund MS, Gordon S, Henders AK, Others. **2010**. Common {SNPs} explain a large proportion of the heritability for human height. *Nat Gen* **42**: 565–569.

Younginger BS, Sirová D, Cruzan MB, Ballhorn DJ. **2017**. Is Biomass a Reliable Estimate of Plant Fitness? *Applications in Plant Sciences* **5**: 1600094.

Yu G, Li F, Qin Y, Bo X, Wu Y, Wang S. **2010**. GOSemSim: An R package for measuring semantic similarity among GO terms and gene products. *Bioinformatics* **26**: 976–978.

Zan Y, Carlborg Ö. **2019**. A Polygenic Genetic Architecture of Flowering Time in the Worldwide Arabidopsis thaliana Population. *Molecular Biology and Evolution* **36**: 141–154.

Zhang Y, Xu W, Li Z, Xing WD, Wu W, Xue Y. **2008**. F-box protein DOR functions as a novel inhibitory factor for abscisic acid-induced stomatal closure under drought stress in Arabidopsis. *Plant Physiology* **148**: 2121–2133.

Zhao Y, Wang J, Chen J, Zhang X, Guo M, Yu G. **2020**. A Literature Review of Gene Function Prediction by Modeling Gene Ontology. *Frontiers in Genetics* **11**: 400.

Zhen Y, Ungerer MC. **2007**. Clinal variation in freezing tolerance among natural accessions of Arabidopsis thaliana. *New Phytologist* **0**: 071107070910003-???

Zou Y, Hou X, Wu Q, Chen J, Li Z, Han T, Niu X, Yang L, Xu Y, Zhang J, *et al.* 2017. Adaptation of Arabidopsis thaliana to the Yangtze River basin. *Genome Biology* **18**: 1–11.

Züst T, Agrawal AA. **2017**. Trade-Offs Between Plant Growth and Defense Against Insect Herbivory: An Emerging Mechanistic Synthesis. *Annual Review of Plant Biology* **68**: 513–534.

Supplementary Figures

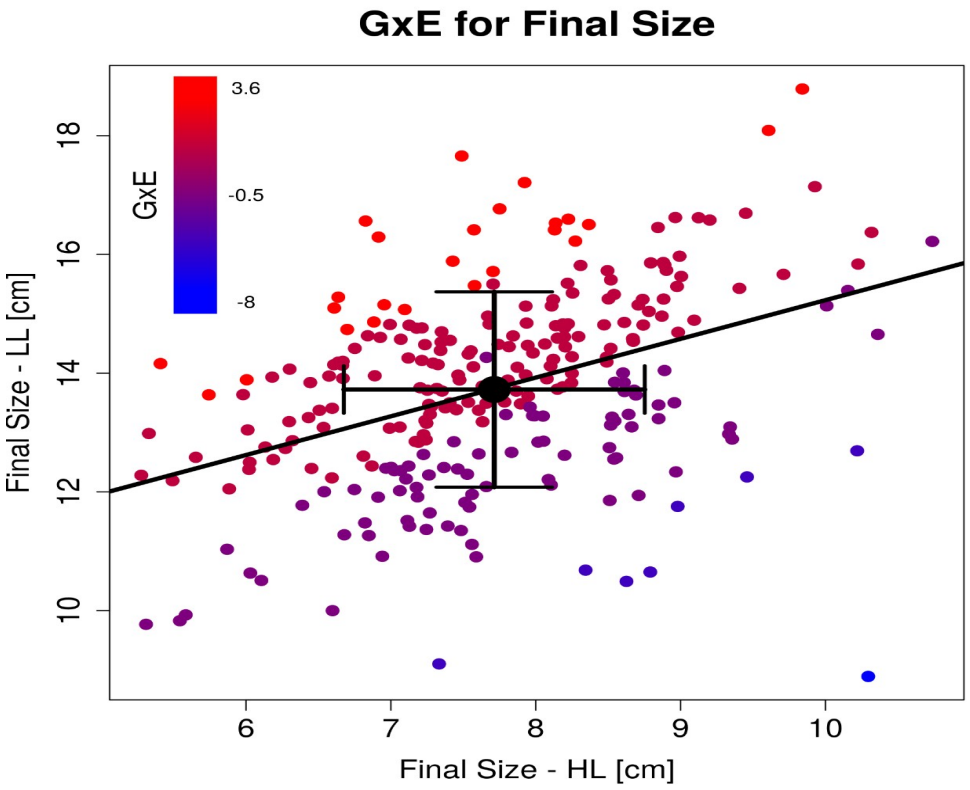

Figure 34: GxE for Final Size.

GxE was estimated based on a glm(Final Size ~ genotype * environment) and is indicated by the color. Each dot corresponds to a genotype with its phenotype in HL (x-axis) and LL (y-axis) (269 genotypes in total). The black dot shows the average over all genotypes with standard deviation. The line shows a linear model for Final Size in LL ~ Finals Size HL.

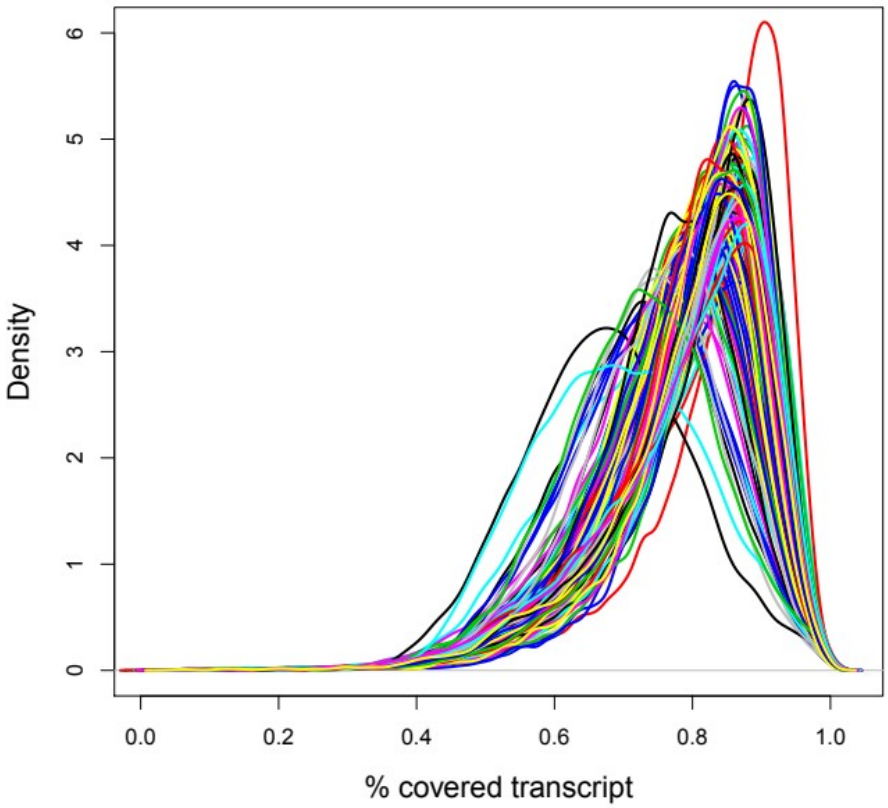

Figure 35: RNA transcript quality of hybrid transcriptomes.

Plotted is the density of average transcript coverage for each gene in each sample. Each colored line represent a single transcriptome. The transcript coverage per gene is estimated as the proportion of coverage per nucleotide in the gene, that is larger then the median nucleotide coverage in that gene.

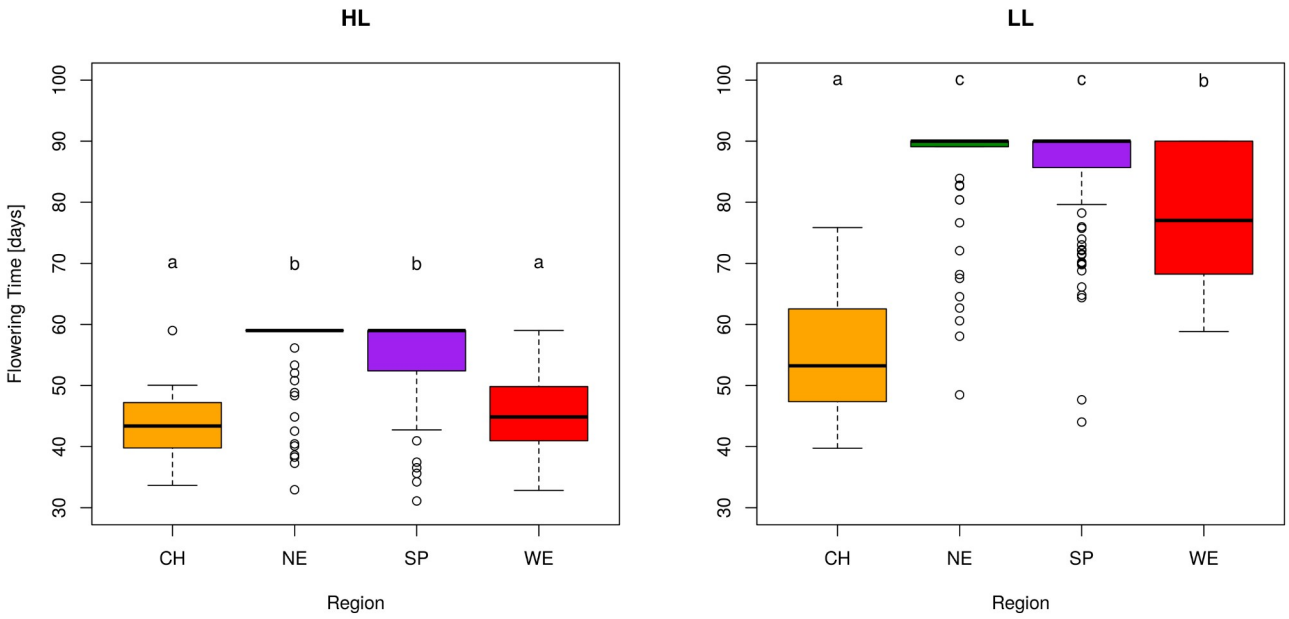

Figure 36: Flowering time in the experiment.

Flowering time of each genotype in HL (left) and LL conditions(right). Missing values were replaced with 59 (HL) or 90 (LL) days after sowing. Boxplots with different letters are significantly different according to Tukey's HSD (p-value < 0.05). Population information: China (CH, n=22), Northern Europe (NE, n=84), Spain (SP, n= 121) & Western Europe (WE, n= 53).

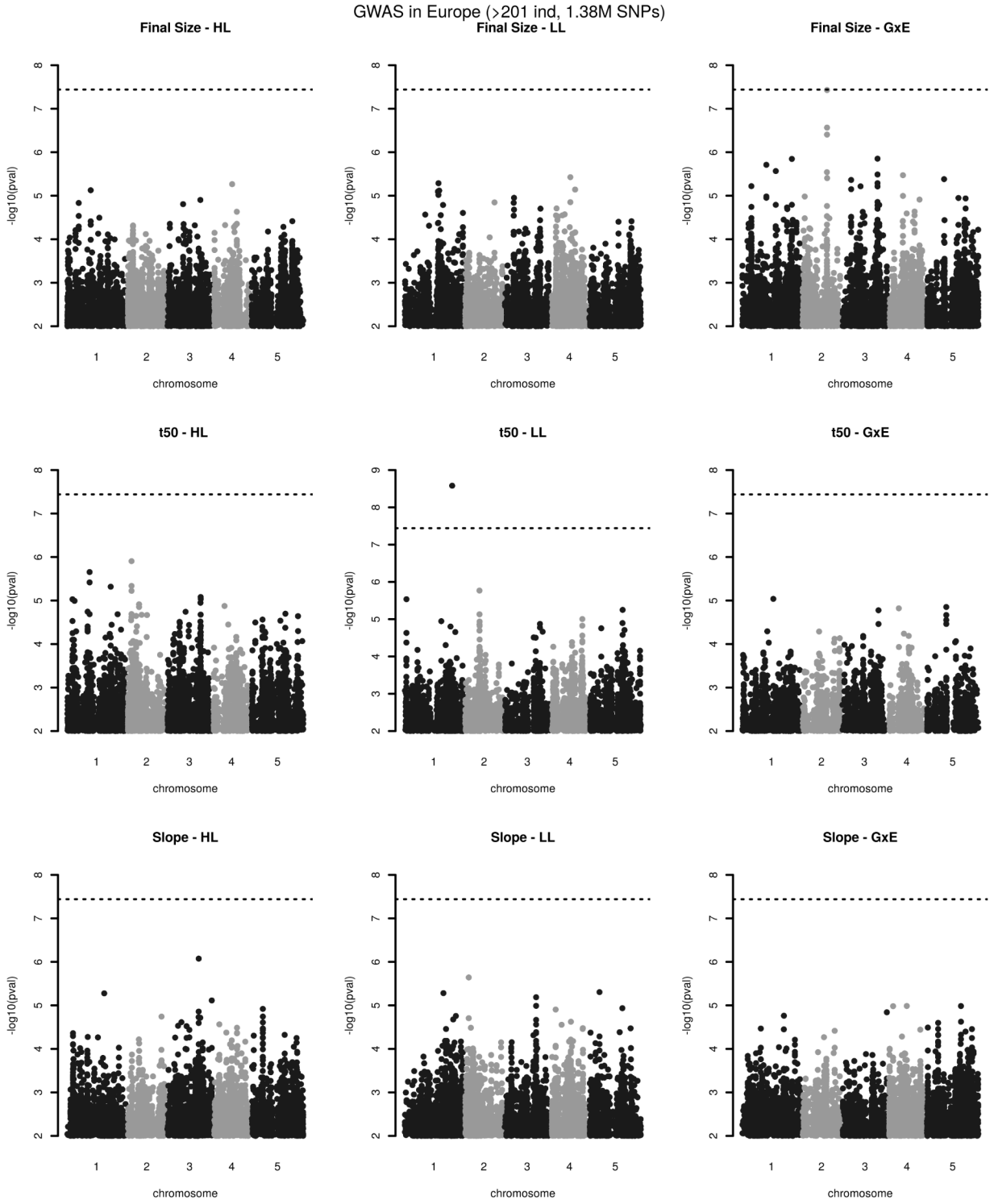

Figure 37: GWAS results for all phenotypes across Europe.

Manhattan plots using 201 (or more) genotypes from Europe (Spain and Northern Europe) as input. The traits are Final Size (upper row), t50 (2nd row) and Slope (lower row) in HL (left column), LL (middle column) and their GxE (right column). The dotted line denotes the 5% Bonferroni-corrected threshold.

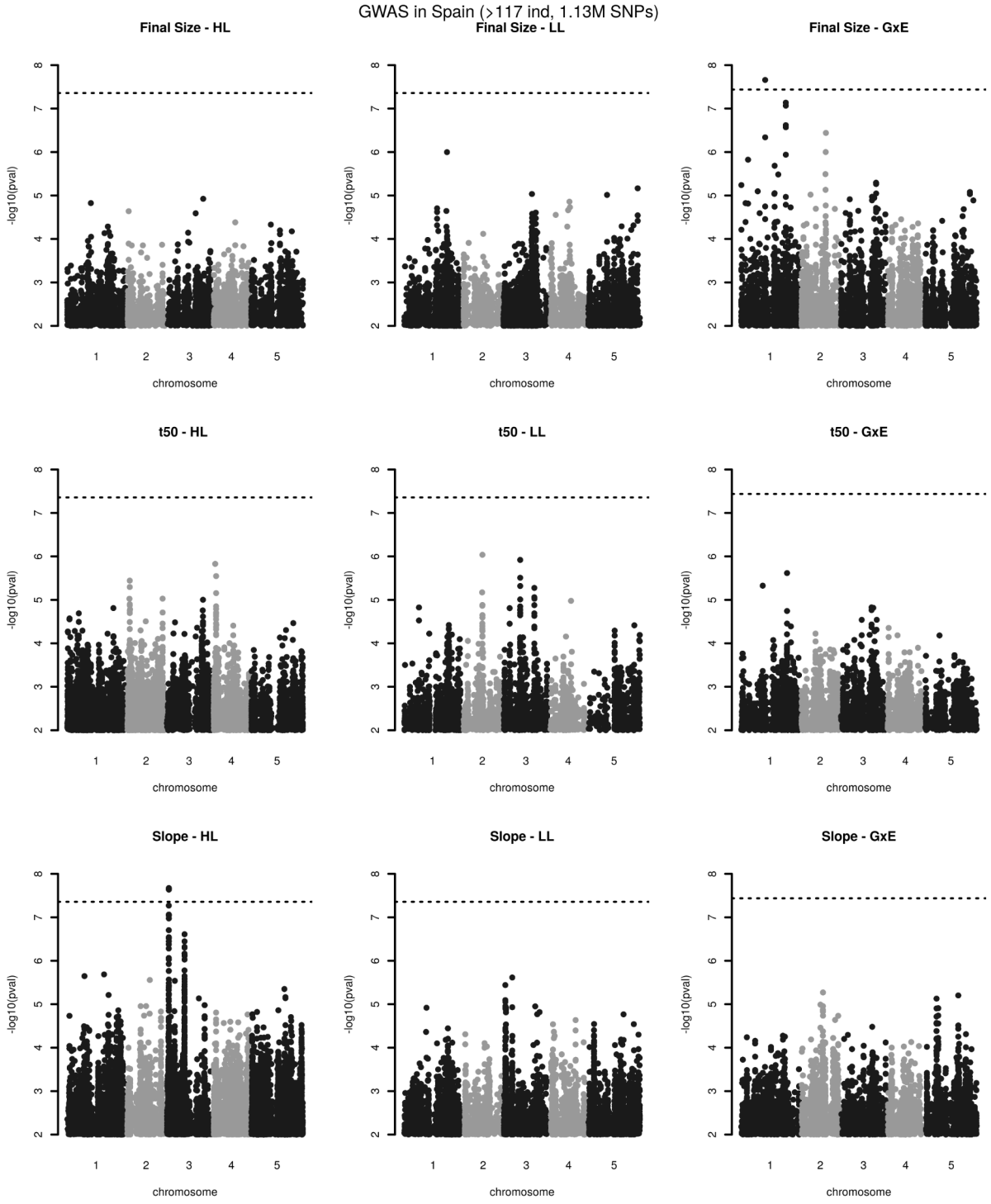

Figure 38: GWAS results for all phenotypes within Spain.

Manhattan plots using 117 (or more) genotypes from Spain as input. The traits are Final Size (upper row), t50 (2nd row) and Slope (lower row) in HL (left column), LL (middle column) and their GxE (right column). The dotted line denotes the 5% Bonferroni-corrected threshold.

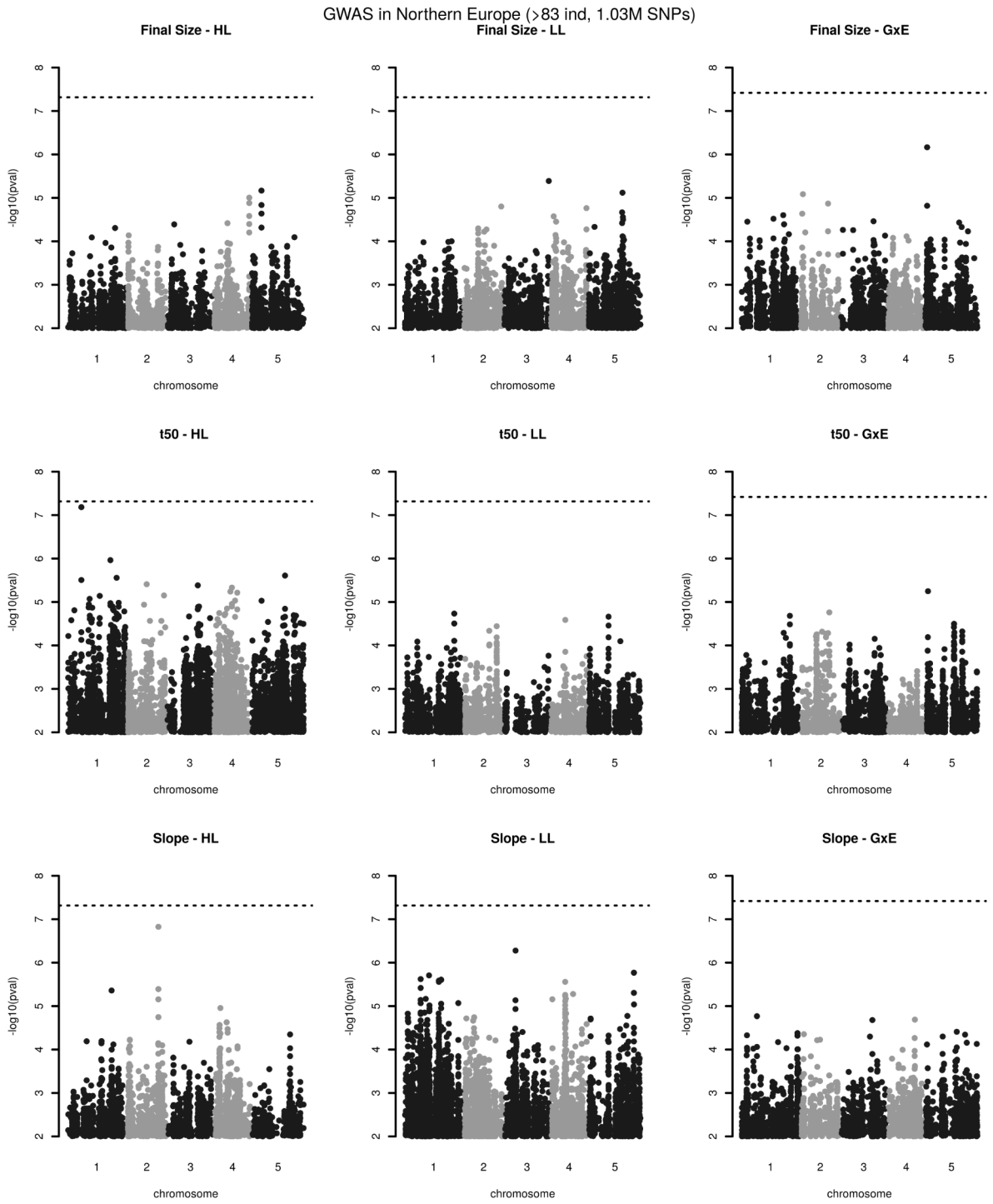

Figure 39: GWAS results for all phenotypes within Northern Europe.

Manhattan plots using 83 (or more) genotypes from Northern Europe as input. The traits are Final Size (upper row), t50 (2nd row) and Slope (lower row) in HL (left column), LL (middle column) and their GxE (right column). The dotted line denotes the 5% Bonferroni-corrected threshold.

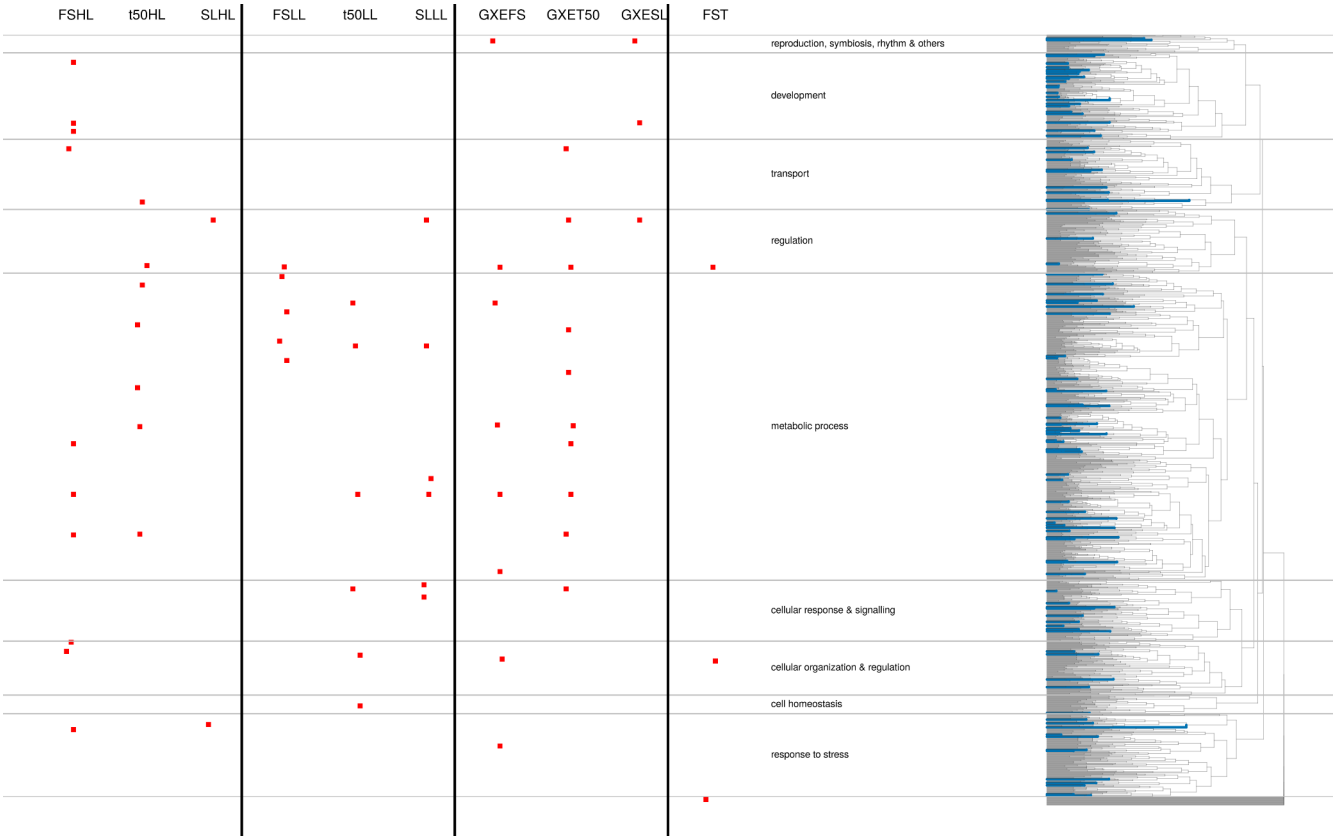

Figure 40: Functional enrichment dendrogram for GO enrichment.

The enrichment is either based on ranking genes by p-value of the nearest SNP in GWAS (columns 1-9) or Fst of the gene (column 10). The GO terms are arranged into 9 clusters of similar function on the right side of the plot. Depicted are only enrichments with a p-value < 0.001.

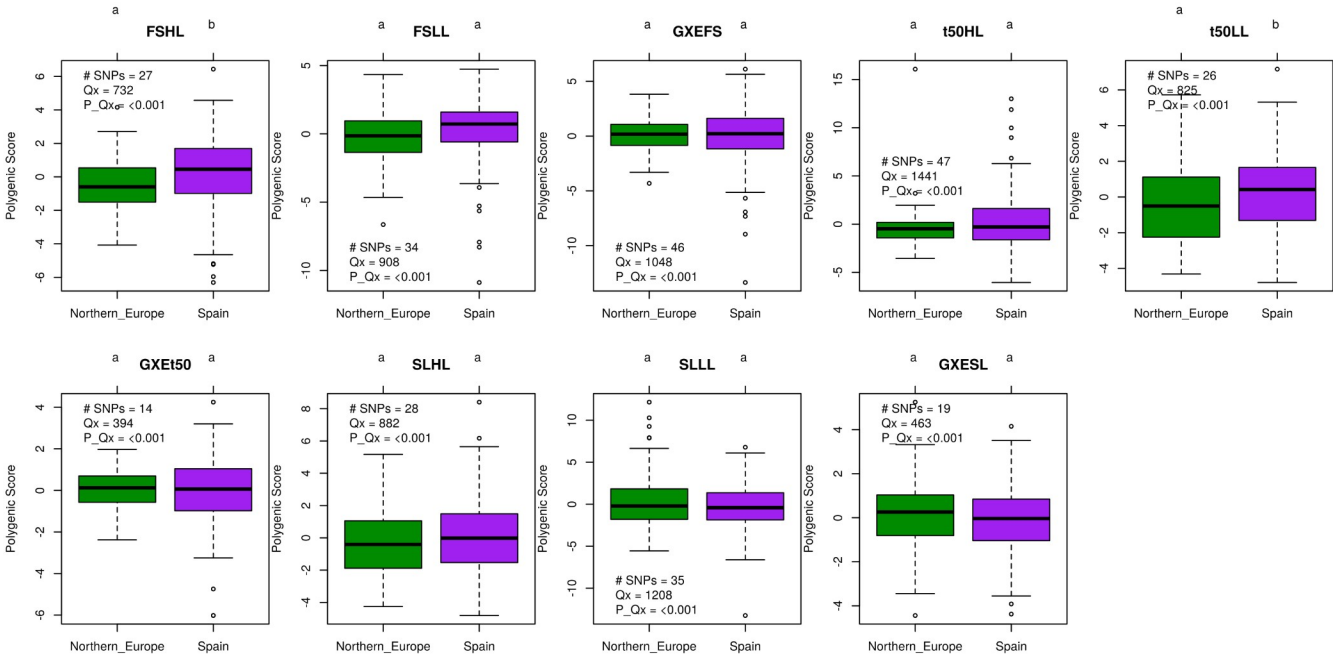

Figure 41: Polygenic Scores and regional differentiation for each trait.

Summary results from the analysis after Berg and Coop (2014). Each boxplot depicts the polygenic scores of a trait for genotypes from Northern Europe (green) & Spain (purple). Boxplots with different letters are significantly different according to Tukey's HSD ($p < 0.05$). Furthermore, the plot contain information about the number of SNPs used as input, the Qx score for excess variance in SNPs associated with the trait and the p-value of the Qx-analysis. Traits: FS= Final Size, t50, SL= Slope, HL= High Light treatment, LL= Low Light treatment.

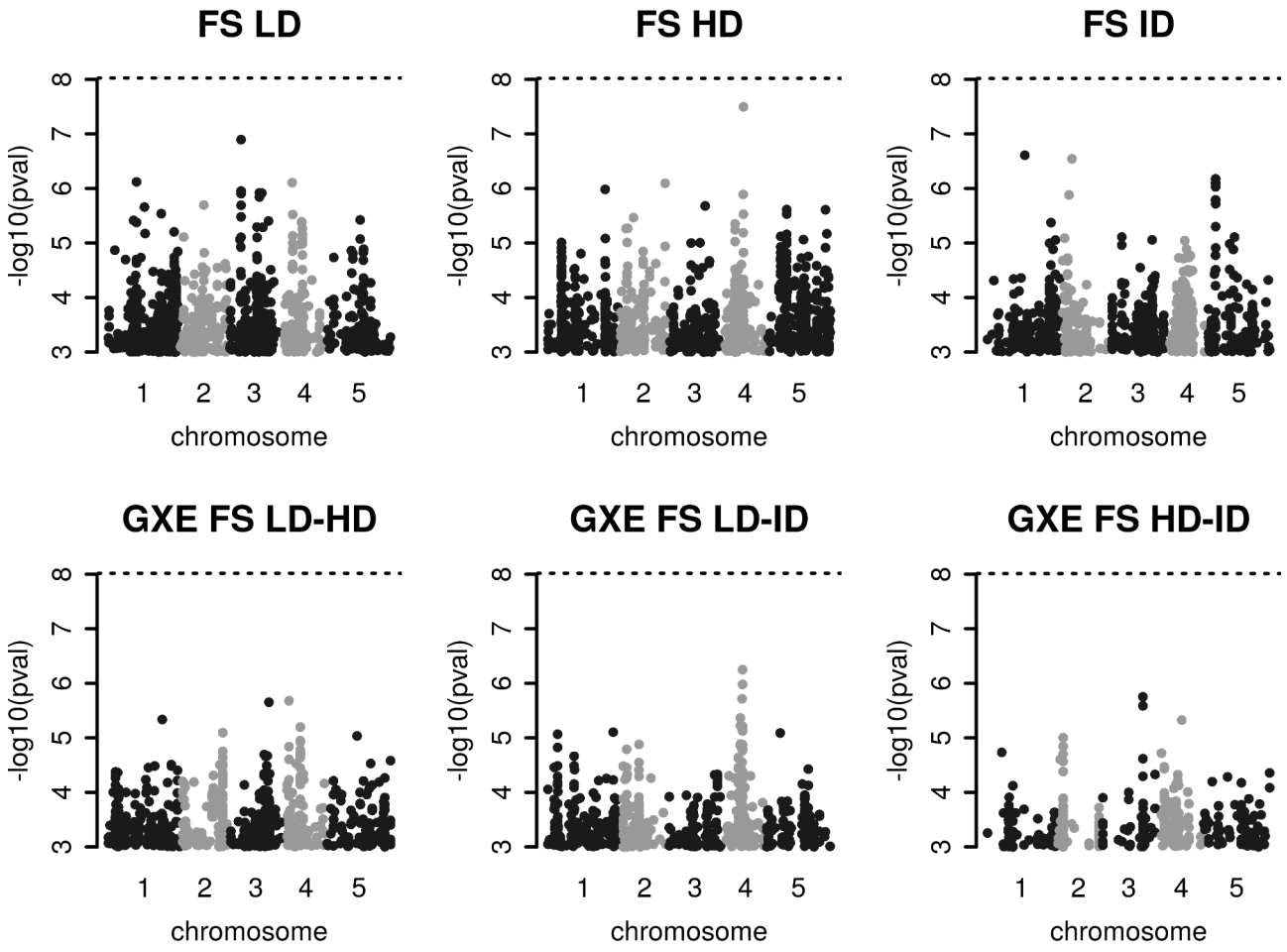

Figure 42: GWAS results for Final Size (FS) in the 2nd field experiment.

Manhattan plots using at least 282 genotypes from Europe (France, Germany, Spain and Northern Europe) as input. The treatments are low density (LD, n= 315), high density (HD, n=296), moderate density (ID, n= 297) and the GXE between LD and HD (n=295), LD and ID (n=295) and HD and ID (282). The dotted line denotes the 5% Bonferroni-corrected threshold.

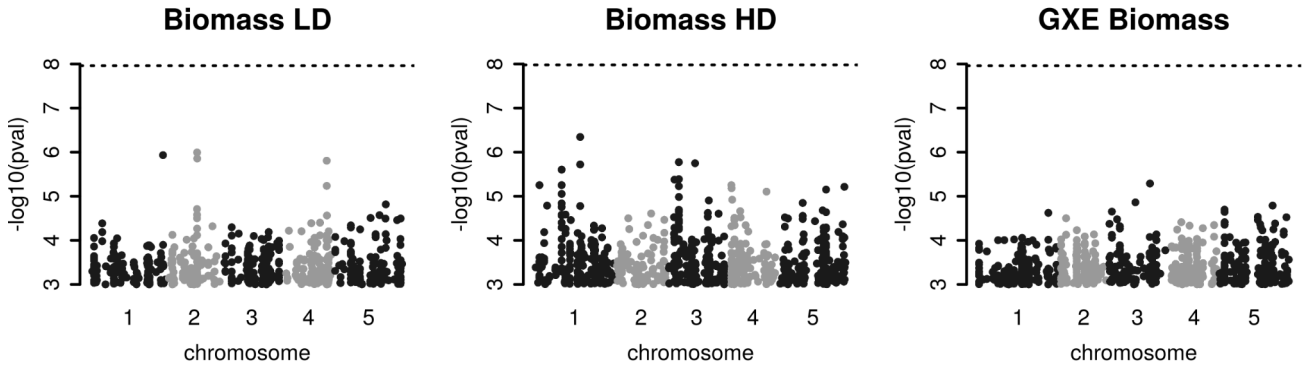

Figure 43: GWAS results for Biomass after 39 days (BM) in controlled conditions.

Manhattan plots using at least 235 genotypes from Europe (Central Europe, Germany, North & South Sweden, Spain, Western Europe) as input. The treatments are low density (LD, n= 236), high density (HD, n=268) and the GXE between HD and LD (n=235). The dotted line denotes the 5% Bonferroni-corrected threshold.

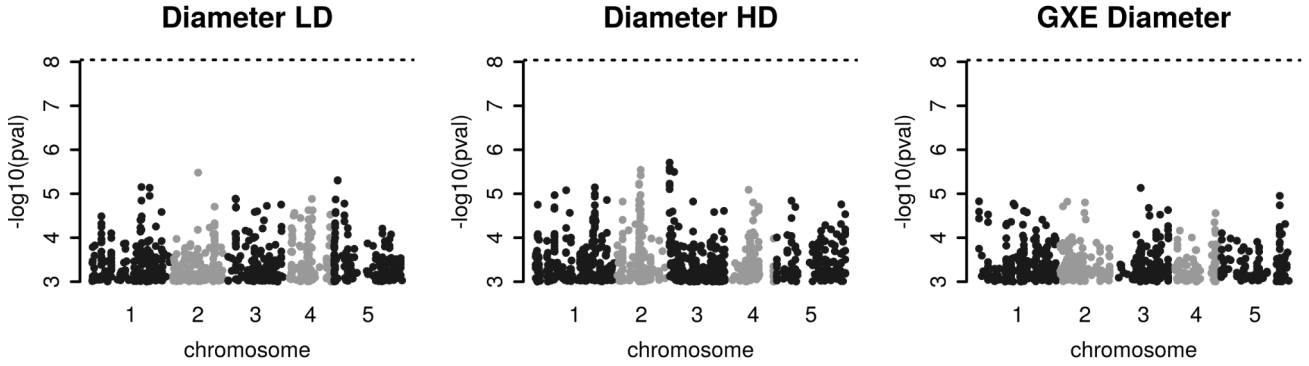

Figure 44: GWAS results for Diameter in December (Diameter) in the below-ground competition field experiment.

Manhattan plots using at least 313 genotypes from Europe (Central Europe, Germany, North & South Sweden, Spain, Western Europe) as input. The treatments are low density (LD, n= 331), high density (HD, n=315) and the GXE between HD and LD (n=313). The dotted line denotes the 5% Bonferroni-corrected threshold.

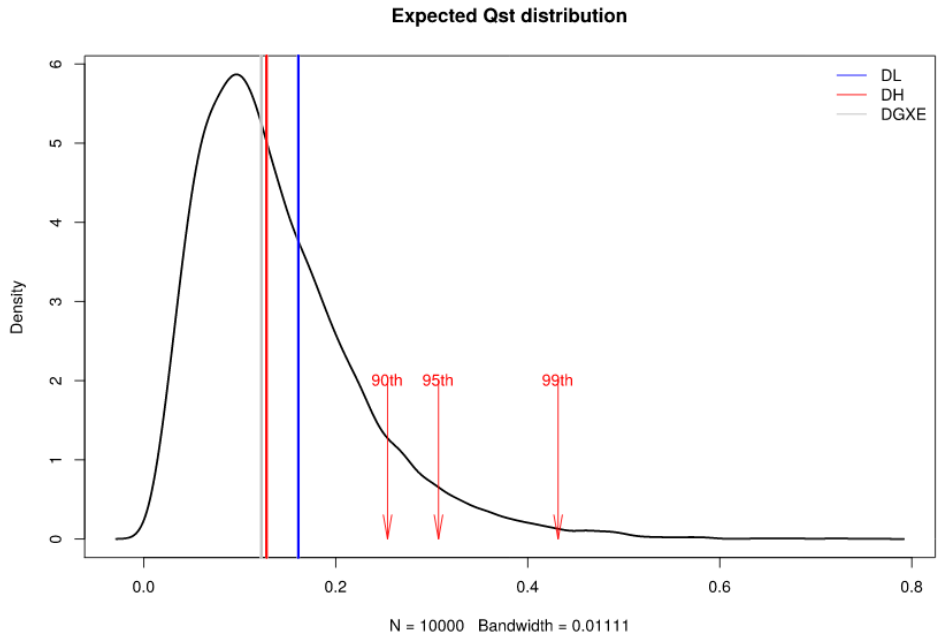

Figure 45: Estimated Qst distribution for Diameter.

Expected distribution for quantitative trait differentiation within Europe. The expectation is based on a multivariate normal distribution assuming a neutral trait with polygenic basis. Vertical lines indicate observed Qst for Diameter in the Field in December in LD (blue), HD (red) and the GxE between these treatments (grey). The red arrows show the 90th, 95th and 99th percentiles of the distribution.

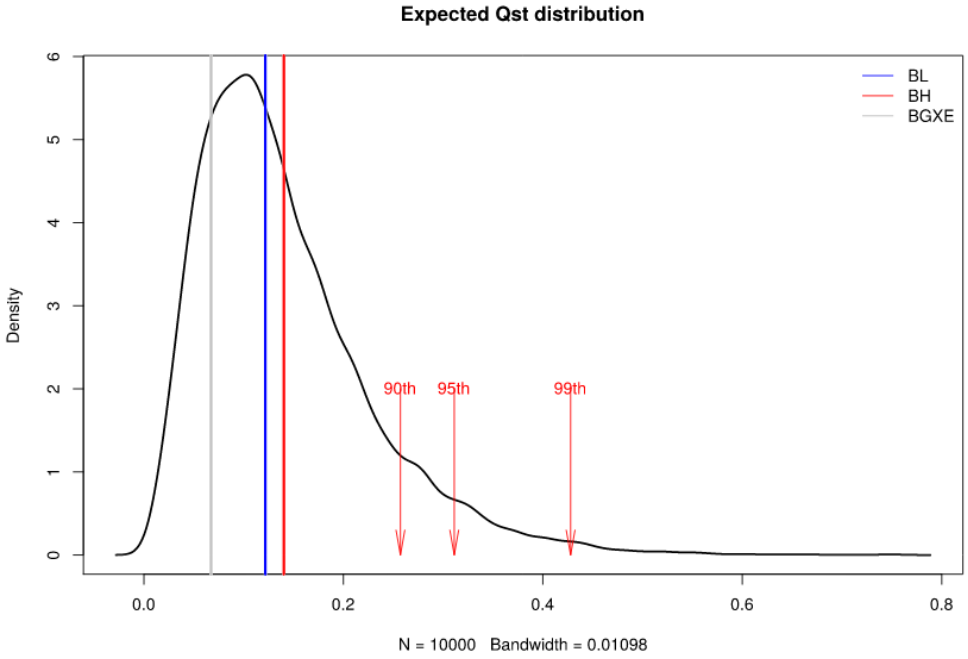

Figure 46: Estimated Qst-distribution for Biomass.

Expected distribution for quantitative trait differentiation within Europe. The expectation is based on a multivariate normal distribution assuming a neutral trait with polygenic basis. Vertical lines indicate observed Qst for Biomass in controlled conditions after 39 days in LD (blue), HD (red) and the GxE between these treatments (grey). The red arrows show the 90th , 95th and 99th percentiles of the distribution.

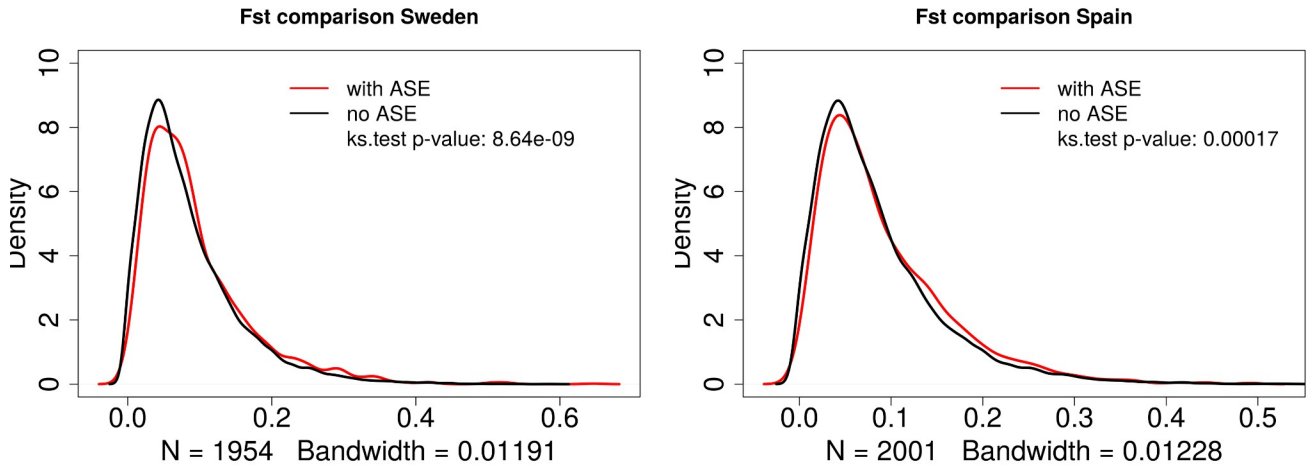

Figure 47: Fst distribution of genes with ASE in Sweden/Spain compared to genes without significant ASE.

Density of the Fst per gene is plotted for genes with derived ASE in Sweden (left) and Spain (right). The Fst of genes with ASE in the region (red) is compared to the Fst of other expressed genes (black). The distributions were compared with a Kolmogorov-Smirnov test. The number of genes with derived ASE is given as N below the plot, the number of other expressed genes was 15,198 – N.

Supplementary Tables

Table 22: Information on the genotypes used in this study.

The columns contain Genotype name and ID in 1001 Genomes, their country of origin, assigned region, group assigned via PCA in (1001 Genomes Consortium, 2016), info on the sampling location (latitude and longitude). The second part of the table gives information on the inclusion of genotypes in the different experiments, where a 1 marks that the genotype was successfully phenotyped in the respective experiment. The experiments where the analysis of growth rate in HL and LL, effect of HD and LD on Biomass in controlled conditions (DENS1_HD/LD), Diameter measurements in below-ground competition (DENS2_HD/LD) and growth measurement in above-ground competition (DENS3_LD/HD/ID).

Genotype	ID	Country	Region	Group	Latitude	Longitude	HL	LL	DENS1_HD	DENS1_LD	DENS2_HD	DENS2_LD	DENS3_LD	DENS3_HD	DENS3_ID
LDV-46	139	FRA	NA	western_europe	48.52	-4.07	0	0	1	1	1	1	1	1	1
Doubravnik7	410	CZE	NA	central_europe	49.42	16.35	0	0	1	1	1	1	0	0	0
Gr-1	430	AUT	NA	central_europe	47.00	15.50	0	0	1	1	1	1	0	0	0
Ale-Stenar-41-1	991	SWE	Northern Europe	south_sweden	55.38	14.05	1	1	0	0	0	0	0	0	0
Ale-Stenar-44-4	992	SWE	Northern Europe	south_sweden	55.38	14.05	1	1	0	0	0	0	0	0	0
Ale-Stenar-56-14	997	SWE	Northern Europe	south_sweden	55.38	14.05	1	1	1	1	1	1	1	1	1
Ale-Stenar-64-24	1002	SWE	Northern Europe	south_sweden	55.38	14.05	1	1	1	1	1	1	1	1	1
Brösarp-11-135	1061	SWE	Northern Europe	south_sweden	55.72	14.13	1	1	1	1	0	1	1	1	1
Brösarp-15-138	1062	SWE	Northern Europe	south_sweden	55.72	14.13	1	1	1	1	1	1	1	1	1
Brösarp-21-140	1063	SWE	Northern Europe	south_sweden	55.72	14.13	1	1	1	1	1	1	1	1	1
Brösarp-34-145	1066	SWE	Northern Europe	south_sweden	55.72	14.13	1	1	1	1	1	1	1	1	1
Tos-82-387	1254	SWE	NA	north_sweden	59.43	17.02	0	0	1	1	0	1	1	1	1
App1-12	5830	SWE	Northern Europe	south_sweden	56.33	15.97	1	1	1	1	0	1	1	0	1
App1-14	5831	SWE	Northern Europe	south_sweden	56.33	15.97	1	1	1	1	1	1	1	1	1
App1-16	5832	SWE	Northern Europe	south_sweden	56.33	15.97	1	1	1	1	1	1	1	0	1
Dra1-4	5865	SWE	NA	south_sweden	55.76	14.12	0	0	1	1	1	1	1	1	1
Dra2-1	5867	SWE	NA	south_sweden	55.76	14.12	0	0	1	0	1	1	1	1	1
DraIV 2-9	5907	CZE	NA	central_europe	49.41	16.28	0	0	1	1	1	1	0	0	0
Eden-1	6009	SWE	NA	north_sweden	62.88	18.18	0	0	1	1	1	1	1	1	1
Eden-6	6011	SWE	NA	north_sweden	62.88	18.18	0	0	1	1	1	1	1	1	1
Eden-7	6012	SWE	NA	north_sweden	62.88	18.18	0	0	1	1	1	1	1	1	1
Eds-1	6016	SWE	NA	north_sweden	62.90	18.40	0	0	1	1	1	1	1	1	1
Fjä1-2	6019	SWE	Northern Europe	south_sweden	56.06	14.29	1	1	1	1	1	1	1	1	1
Fjä1-5	6020	SWE	Northern Europe	south_sweden	56.06	14.29	1	1	1	1	1	1	1	1	0
Fjä2-4	6021	SWE	Northern Europe	south_sweden	56.06	14.29	1	1	1	1	1	1	1	1	1
Fly2-1	6023	SWE	Northern Europe	south_sweden	55.75	13.37	1	1	1	1	1	1	1	1	1
Fly2-2	6024	SWE	Northern Europe	south_sweden	55.75	13.37	1	1	1	1	1	1	1	1	1
Hov1-10	6035	SWE	Northern Europe	south_sweden	56.10	13.74	1	1	1	1	1	1	1	1	1
Hov3-2	6036	SWE	Northern Europe	south_sweden	56.10	13.74	1	1	1	1	1	1	1	1	1
Hov3-5	6038	SWE	Northern Europe	south_sweden	56.10	13.74	1	1	0	0	1	1	1	1	1
Hovdala-2	6039	SWE	Northern Europe	admixed	56.10	13.74	1	1	1	1	1	1	1	1	1
Kni-1	6040	SWE	Northern Europe	south_sweden	55.66	13.40	1	1	1	1	1	1	1	1	1
Lis-3	6041	SWE	Northern Europe	south_sweden	56.03	14.78	1	1	1	1	1	1	1	1	1

Nyl-7	6069	SWE	NA	north_sweden	62.95	18.28	0	0	1	1	1	1	1	1	0
Omn-5	6071	SWE	NA	north_sweden	62.93	18.34	0	0	1	1	1	1	1	1	1
Ömö1-7	6073	SWE	Northern Europe	south_sweden	56.15	15.82	1	1	1	0	1	1	1	1	1
Rev-2	6076	SWE	Northern Europe	south_sweden	55.69	13.45	1	1	1	1	1	1	1	1	1
Sparta-1	6085	SWE	Northern Europe	south_sweden	55.71	13.21	1	1	1	1	1	1	1	1	1
T1000	6090	SWE	NA	south_sweden	55.65	13.22	0	0	1	0	1	1	1	0	1
T1040	6094	SWE	Northern Europe	south_sweden	55.65	13.21	1	1	1	1	1	1	1	1	1
T1070	6097	SWE	NA	south_sweden	55.65	13.23	0	0	1	1	1	1	1	1	1
T1110	6100	SWE	NA	south_sweden	55.60	13.20	0	0	1	1	1	1	1	1	1
T1160	6104	SWE	NA	south_sweden	55.70	13.20	0	0	1	1	1	1	1	1	1
T450	6105	SWE	NA	south_sweden	55.80	13.12	0	0	1	1	1	1	1	1	1
T460	6106	SWE	Northern Europe	south_sweden	55.79	13.12	1	1	1	1	1	1	1	1	1
T470	6107	SWE	NA	south_sweden	55.79	13.12	0	0	1	1	1	1	1	1	1
T480	6108	SWE	NA	western_europe	55.80	13.12	0	0	1	1	1	1	1	1	1
T510	6109	SWE	Northern Europe	south_sweden	55.79	13.12	1	1	0	0	0	0	0	0	0
T530	6111	SWE	NA	south_sweden	55.80	13.12	0	0	1	1	1	1	1	1	1
T540	6112	SWE	Northern Europe	south_sweden	55.80	13.10	1	1	1	1	1	1	1	1	1
T570	6114	SWE	Northern Europe	south_sweden	55.81	13.13	1	1	1	1	1	1	1	1	1
T610	6118	SWE	NA	south_sweden	55.70	13.20	0	0	1	1	1	1	1	1	1
T670	6122	SWE	NA	south_sweden	55.84	13.31	0	0	1	1	1	1	1	1	1
T710	6125	SWE	NA	south_sweden	55.84	13.31	0	0	1	1	0	1	1	1	1
T720	6126	SWE	NA	south_sweden	55.84	13.30	0	0	1	1	1	1	1	1	1
T740	6128	SWE	NA	south_sweden	55.84	13.29	0	0	1	1	1	1	1	1	1
T780	6131	SWE	NA	south_sweden	55.84	13.32	0	0	1	1	1	1	1	1	1
T790	6132	SWE	NA	south_sweden	55.84	13.32	0	0	1	1	1	1	1	1	1
T800	6133	SWE	NA	south_sweden	55.84	13.29	0	0	1	1	1	1	1	1	1
T810	6134	SWE	NA	south_sweden	55.84	13.29	0	0	1	1	1	1	1	1	1
T840	6136	SWE	NA	south_sweden	55.93	13.55	0	0	1	1	1	1	1	1	1
T860	6138	SWE	NA	south_sweden	55.94	13.55	0	0	1	1	1	1	1	1	1
T880	6140	SWE	NA	south_sweden	55.94	13.55	0	0	1	0	1	1	1	1	1
T900	6142	SWE	Northern Europe	south_sweden	55.94	13.56	1	1	1	1	1	1	1	1	1
T930	6145	SWE	NA	south_sweden	55.95	13.55	0	0	1	1	1	1	1	1	1
T960	6148	SWE	NA	south_sweden	55.93	13.55	0	0	1	1	1	1	1	1	1
T980	6150	SWE	NA	south_sweden	55.93	13.53	0	0	1	1	1	1	1	1	1
T990	6151	SWE	NA	south_sweden	55.65	13.22	0	0	1	1	1	1	1	1	1
TAA 03	6153	SWE	NA	north_sweden	62.64	17.74	0	0	1	0	1	1	1	1	1
TAA 04	6154	SWE	NA	north_sweden	62.64	17.74	0	0	1	1	1	1	1	1	1
TAA 14	6163	SWE	NA	north_sweden	62.64	17.74	0	0	1	1	1	1	1	1	1
TBÖ 01	6184	SWE	NA	north_sweden	62.89	18.45	0	0	1	1	1	1	1	1	1
TDr-1	6188	SWE	Northern Europe	south_sweden	55.77	14.14	1	1	1	1	1	1	1	1	1
TDr-2	6189	SWE	Northern Europe	south_sweden	55.77	14.14	1	1	1	1	1	1	1	1	0
TDr-4	6191	SWE	Northern Europe	south_sweden	55.77	14.14	1	1	1	0	1	1	1	1	1
TDr-5	6192	SWE	NA	south_sweden	55.77	14.14	0	0	1	1	1	1	1	1	1
TDr-7	6193	SWE	NA	south_sweden	55.77	14.13	0	0	1	1	1	1	1	1	1
TDr-8	6194	SWE	NA	south_sweden	55.77	14.13	0	0	1	1	1	1	1	1	1
TDr-9	6195	SWE	NA	south_sweden	55.77	14.13	0	0	1	1	1	1	1	1	1
TDr-13	6198	SWE	NA	south_sweden	55.77	14.13	0	0	1	1	1	1	0	0	0
TDr-16	6201	SWE	Northern Europe	south_sweden	55.77	14.12	1	1	0	0	0	0	0	0	0

TDr-17	6202	SWE	NA	south_sweden	55.77	14.12	0	0	1	1	1	1	1	1	1
TDr-18	6203	SWE	NA	south_sweden	55.77	14.12	0	0	1	1	1	1	1	1	1
TEDEN 02	6209	SWE	NA	north_sweden	62.88	18.18	0	0	1	1	1	1	1	1	1
TFÄ 07	6217	SWE	NA	north_sweden	63.02	18.33	0	0	1	1	1	1	1	0	1
TOM 01	6235	SWE	NA	north_sweden	62.96	18.36	0	0	1	0	1	1	1	1	1
TOM 06	6240	SWE	NA	north_sweden	62.96	18.35	0	0	1	1	1	1	1	1	1
Tomegap-2	6242	SWE	Northern Europe	south_sweden	55.70	13.20	1	1	0	0	0	0	0	0	0
TV-10	6258	SWE	Northern Europe	south_sweden	55.58	14.33	1	1	0	0	0	0	0	0	0
TV-22	6268	SWE	NA	germany	55.58	14.33	0	0	1	1	1	1	1	1	1
TV-38	6284	SWE	Northern Europe	south_sweden	55.58	14.33	1	1	0	0	0	0	0	0	0
Udul 1-11	6296	CZE	NA	central_europe	49.28	16.63	0	0	1	1	1	1	0	0	0
Ull3-4	6413	SWE	Northern Europe	south_sweden	56.06	13.97	1	1	0	0	0	0	0	0	0
Zdrl 1-23	6424	CZE	NA	central_europe	49.39	16.25	0	0	1	1	1	1	0	0	0
Zdrl 2-21	6445	CZE	NA	central_europe	49.39	16.25	0	0	1	1	1	1	0	0	0
Bor-4	6903	CZE	NA	central_europe	49.40	16.23	0	0	1	1	1	1	0	0	0
Ei-2	6915	GER	NA	germany	50.30	6.30	0	0	1	1	1	1	1	1	1
LL-0	6933	ESP	Spain	spain	41.59	2.49	1	1	1	1	1	1	1	1	0
NFA-8	6944	UK	NA	western_europe	51.41	-0.64	0	0	1	1	1	1	0	0	0
Nok-3	6945	NED	NA	germany	52.24	4.45	0	0	1	1	1	1	0	0	0
Pu2-8	6957	CZE	NA	central_europe	49.42	16.36	0	0	1	1	1	1	0	0	0
Se-0	6961	ESP	Spain	spain	38.33	-3.53	1	1	1	1	1	1	1	1	1
Tamm-27	6969	FIN	NA	north_sweden	60.00	23.50	0	0	1	1	1	1	0	0	0
Ts-1	6970	ESP	Spain	spain	41.72	2.93	1	1	1	1	1	1	1	1	0
Ts-5	6971	ESP	Spain	spain	41.72	2.93	1	1	1	1	1	1	1	1	1
Ull2-5	6974	SWE	Northern Europe	south_sweden	56.06	13.97	1	1	1	1	1	1	1	1	0
Ws-2	6981	RUS	NA	admixed	52.30	30.00	0	0	1	1	1	1	0	0	0
Wt-5	6982	GER	NA	germany	52.30	9.30	0	0	1	1	1	1	1	1	1
Ak-1	6987	GER	Northern Europe	admixed	48.07	7.63	0	0	1	1	1	1	1	1	1
Alst-1	6989	UK	Western Europe	western_europe	54.80	-2.43	0	0	1	0	1	1	0	0	0
Baa-1	7002	NED	NA	germany	51.33	6.10	0	0	1	1	1	1	0	0	0
Bs-1	7003	SUI	NA	admixed	47.50	7.50	0	0	1	1	1	1	0	0	0
Benk-1	7008	NED	NA	germany	52.00	5.68	0	0	1	1	1	1	0	0	0
Bd-0	7013	GER	Northern Europe	south_sweden	52.46	13.29	1	1	1	0	1	1	1	1	0
Bur-0	7058	ESP	Spain	admixed	40.43	-4.75	0	0	1	1	1	1	0	0	0
Ca-0	7062	GER	NA	germany	50.30	8.27	0	0	1	1	1	1	1	1	1
En-2	7119	GER	NA	germany	50.00	8.50	0	0	1	1	1	1	1	1	1
Fr-2	7133	GER	NA	germany	50.11	8.68	0	0	1	1	1	1	1	1	1
Gie-0	7147	GER	Western Europe	admixed	50.58	8.68	1	1	1	1	1	1	1	1	1
Gr-5	7158	AUT	NA	central_europe	47.00	15.50	0	0	1	1	1	1	0	0	0
Hau-0	7164	DEN	Northern Europe	south_sweden	55.68	12.57	1	1	1	1	1	1	0	0	0
Hh-0	7169	GER	Northern Europe	admixed	54.42	9.89	1	1	1	1	1	1	1	1	1
Hh-0	7169	GER	Northern Europe	admixed	54.42	9.89	1	1	1	1	1	1	1	1	1
Jm-0	7177	CZE	NA	central_europe	49.00	15.00	0	0	1	1	1	1	0	0	0
Kyoto	7207	JPN	NA	central_europe	35.01	135.75	0	0	1	1	1	1	0	0	0
Mnz-0	7244	GER	NA	germany	50.00	8.27	0	0	1	1	1	1	1	1	1
Mh-0	7255	POL	NA	germany	50.95	20.50	0	0	1	0	1	1	0	0	0
Np-0	7268	GER	Northern Europe	admixed	52.70	10.98	1	1	1	1	1	1	1	1	1
Ob-0	7276	GER	NA	germany	50.20	8.58	0	0	1	1	1	1	1	1	1

Oy-0	7288	NOR	Northern Europe	admixed	60.39	6.19	1	1	1	1	1	1	0	0	0
Pt-0	7305	GER	Northern Europe	admixed	53.48	10.61	1	1	1	1	1	1	1	1	1
Sf-1	7327	ESP	Spain	spain	41.78	3.03	1	1	1	1	1	1	1	1	1
Sf-2	7328	ESP	Spain	spain	41.78	3.03	1	1	1	1	1	1	1	1	1
Sp-0	7343	GER	Northern Europe	south_sweden	52.53	13.18	1	1	1	1	1	1	1	0	1
Sten-0	7346	GER	Northern Europe	south_sweden	52.61	11.86	1	1	1	1	1	1	1	1	1
Sten-0	7346	GER	Northern Europe	south_sweden	52.61	11.86	1	1	1	1	1	1	1	1	1
Ting-1	7354	SWE	Northern Europe	south_sweden	56.50	14.90	1	1	1	1	1	1	1	1	1
Utrecht	7382	NED	NA	admixed	52.09	5.11	0	0	1	1	1	1	0	0	0
Van-0	7383	CAN	NA	western_europe	49.27	-123.21	0	0	1	1	1	1	0	0	0
Gy-0	8214	FRA	NA	western_europe	49.00	2.00	0	0	1	1	1	1	1	1	1
Lis-2	8222	SWE	Northern Europe	south_sweden	56.03	14.78	1	1	1	1	1	1	1	1	1
THÖ 03	8227	SWE	NA	north_sweden	62.80	17.91	0	0	1	1	1	1	1	1	1
Brö1-6	8231	SWE	Northern Europe	south_sweden	56.30	16.00	1	1	1	1	1	1	1	1	1
Gul1-2	8234	SWE	Northern Europe	south_sweden	56.46	15.81	1	1	1	1	1	1	1	1	1
Kävlinge-1	8237	SWE	Northern Europe	south_sweden	55.80	13.10	1	1	1	1	1	1	1	1	1
Kulturen-1	8240	SWE	Northern Europe	south_sweden	55.71	13.20	1	1	1	1	1	1	1	1	1
Liarum	8241	SWE	Northern Europe	south_sweden	55.95	13.82	1	1	1	1	1	1	1	1	1
Lillö-1	8242	SWE	Northern Europe	south_sweden	56.15	15.79	1	1	1	0	1	1	1	1	1
San-2	8247	SWE	NA	south_sweden	56.07	13.74	0	0	1	1	1	1	1	1	1
Vimmerby	8249	SWE	Northern Europe	south_sweden	57.70	15.80	1	1	1	1	1	1	1	1	1
Bå1-2	8256	SWE	Northern Europe	admixed	56.40	12.90	1	1	1	1	1	1	1	1	1
Bå5-1	8259	SWE	Northern Europe	south_sweden	56.40	12.90	1	1	1	1	1	1	1	1	1
Bla-1	8264	ESP	Spain	spain	41.68	2.80	1	1	1	1	1	1	1	1	1
Dra3-1	8283	SWE	Northern Europe	south_sweden	55.76	14.12	0	0	0	0	0	0	0	0	0
Hov4-1	8306	SWE	Northern Europe	south_sweden	56.10	13.74	1	1	1	1	1	1	1	1	1
Hovdala-6	8307	SWE	Northern Europe	south_sweden	56.10	13.74	1	1	1	1	1	1	1	1	1
Lis-1	8326	SWE	Northern Europe	south_sweden	56.03	14.78	1	1	1	1	1	1	1	1	1
Lund	8335	SWE	Northern Europe	south_sweden	55.71	13.20	1	1	1	1	1	1	1	1	1
Mir-0	8337	ITA	NA	western_europe	44.00	12.37	0	0	0	0	0	0	0	0	0
Ost-0	8351	SWE	NA	north_sweden	60.25	18.37	0	0	1	1	1	1	1	1	1
Rev-1	8369	SWE	Northern Europe	south_sweden	55.69	13.45	1	1	1	1	1	1	1	0	1
Sanna-2	8376	SWE	NA	north_sweden	62.69	18.00	0	0	1	1	1	1	1	1	1
Sr:5	8386	SWE	NA	central_europe	58.90	11.20	0	0	1	1	1	1	1	1	1
St-0	8387	SWE	NA	germany	59.00	18.00	0	0	1	1	1	1	0	0	0
Kelsterbach-4	8420	GER	NA	germany	50.07	8.53	0	0	1	1	1	1	1	1	1
Fjä1-1	8422	SWE	Northern Europe	south_sweden	56.06	14.29	1	1	1	0	1	1	1	1	1
Ull1-1	8426	SWE	Northern Europe	south_sweden	56.06	13.97	1	1	1	1	1	1	1	1	1
Vinslöv	9057	SWE	Northern Europe	south_sweden	56.10	13.92	1	1	1	1	1	1	1	1	1
Böt 1	9339	SWE	Northern Europe	south_sweden	57.71	15.07	1	1	1	1	1	1	1	1	1
EdJ 2	9363	SWE	NA	north_sweden	62.91	18.40	0	0	1	1	1	1	1	1	1
EkS 2	9369	SWE	Northern Europe	south_sweden	57.68	15.00	1	1	1	1	1	1	1	1	1
FlyA 3	9380	SWE	Northern Europe	south_sweden	55.75	13.37	1	1	1	1	1	1	1	1	1
Grön 12	9386	SWE	NA	north_sweden	62.81	18.19	0	0	1	1	1	1	1	1	1
Grön 14	9388	SWE	NA	north_sweden	62.81	18.19	0	0	1	1	1	1	1	1	1
Hal-1	9395	SWE	NA	south_sweden	57.51	15.01	0	0	1	1	1	1	1	1	1
Hamm-1	9399	SWE	Northern Europe	south_sweden	55.42	13.99	1	1	1	0	1	1	1	1	1
HolA-1-1	9404	SWE	Northern Europe	south_sweden	55.75	13.40	1	1	1	1	1	1	1	1	1

HolA-1-2	9405	SWE	Northern Europe	south_sweden	55.75	13.40	1	1	1	0	1	1	1	1	1
HolA-2-2	9407	SWE	Northern Europe	south_sweden	55.75	13.40	1	1	1	1	1	1	1	1	1
Kal-1	9408	SWE	Northern Europe	south_sweden	56.05	13.95	1	1	1	0	1	1	1	1	1
Kia-1	9409	SWE	Northern Europe	south_sweden	56.06	14.30	1	1	1	1	1	1	1	1	1
Lan-1	9421	SWE	Northern Europe	south_sweden	55.97	14.40	1	1	1	1	1	1	1	1	1
Puk-1	9436	SWE	Northern Europe	south_sweden	56.16	14.68	1	1	1	1	1	1	1	1	0
Puk-2	9437	SWE	Northern Europe	south_sweden	56.16	14.68	1	1	0	0	0	0	0	0	0
Ste-2	9453	SWE	Northern Europe	south_sweden	57.80	18.52	1	1	1	1	1	1	1	1	1
Ste-3	9454	SWE	Northern Europe	south_sweden	57.80	18.52	1	1	1	1	1	1	1	1	1
Tur-4	9470	SWE	Northern Europe	south_sweden	57.65	14.80	1	1	1	0	1	1	1	1	1
Yst-1	9481	SWE	Northern Europe	south_sweden	55.42	13.85	1	1	0	0	0	0	0	0	0
IP-Alo-0	9506	POR	Spain	admixed	40.11	-7.47	1	0	1	1	1	1	0	0	0
IP-All-0	9517	ESP	Spain	western_europe	42.19	-7.80	1	1	1	1	1	1	1	1	1
IP-Ang-0	9519	ESP	NA	spain	41.94	2.64	0	0	1	0	1	1	1	1	1
IP-Ara-4	9520	ESP	Spain	spain	41.70	-3.68	1	1	0	0	0	0	0	0	0
IP-Bar-1	9521	ESP	Spain	spain	41.43	2.13	1	1	1	1	1	1	1	1	1
IP-Ber-0	9524	ESP	Spain	spain	42.52	-0.56	1	1	1	1	1	1	1	1	1
IP-Bis-0	9525	ESP	Spain	spain	42.49	0.54	1	1	1	1	1	1	1	1	1
IP-Cab-3	9526	ESP	Spain	spain	41.54	2.39	1	1	1	1	1	1	1	1	1
IP-Cad-0	9527	ESP	Spain	spain	40.37	-5.74	1	1	0	0	0	0	0	0	0
IP-Cal-0	9528	ESP	Spain	spain	40.94	-1.37	1	1	1	0	1	1	1	1	1
IP-Cdc-3	9531	ESP	Spain	spain	41.21	-4.54	1	1	1	1	1	1	1	1	1
IP-Cdo-0	9532	ESP	Spain	spain	42.23	-4.64	1	1	1	1	1	1	1	1	1
IP-Cmo-3	9534	ESP	Spain	spain	40.05	-4.65	1	1	0	0	0	0	0	0	0
IP-Coc-1	9535	ESP	Spain	spain	42.31	3.19	1	1	1	0	1	1	1	1	0
IP-Deh-1	9539	ESP	Spain	spain	40.29	-6.67	1	1	1	1	1	1	1	1	1
IP-Elb-0	9540	ESP	Spain	spain	41.81	2.34	1	1	1	1	1	1	1	1	1
IP-Hor-0	9547	ESP	Spain	spain	41.67	2.62	1	1	1	1	1	1	1	1	1
IP-Hoy-0	9548	ESP	Spain	spain	40.40	-5.00	1	1	0	0	0	0	0	0	0
IP-Jim-1	9551	ESP	Spain	admixed	42.28	-5.92	1	1	1	1	1	1	1	1	1
IP-Lab-7	9552	ESP	Spain	spain	40.87	-4.50	1	1	0	0	0	0	0	0	0
IP-Ldd-0	9553	ESP	Spain	spain	41.58	-4.71	1	1	0	0	0	0	0	0	0
IP-Men-2	9556	ESP	Spain	spain	39.66	-4.34	1	1	1	1	1	1	1	1	1
IP-Moa-0	9557	ESP	Spain	spain	42.46	0.70	1	1	1	1	1	1	1	1	1
IP-Moc-11	9558	ESP	Spain	admixed	41.57	-5.64	1	1	1	0	1	1	1	1	1
IP-Mun-0	9561	ESP	Spain	admixed	40.71	-5.04	1	1	1	1	1	1	1	1	1
IP-Mur-0	9562	ESP	Spain	spain	41.67	2.00	1	1	1	1	1	1	1	1	1
IP-Nog-17	9564	ESP	Spain	spain	40.45	-1.60	1	1	1	1	1	1	1	0	1
IP-Orb-10	9565	ESP	Spain	admixed	42.97	-1.23	1	1	1	1	1	1	1	1	1
IP-Pal-0	9567	ESP	Spain	spain	42.34	1.30	1	1	1	1	1	1	1	1	1
IP-Pan-0	9568	ESP	Spain	spain	42.76	-0.23	1	1	1	1	1	1	1	1	1
IP-Pds-1	9569	ESP	Spain	western_europe	42.87	-6.45	1	1	1	1	1	1	1	1	1
IP-Rds-0	9573	ESP	Spain	spain	41.86	2.99	1	1	1	1	1	1	1	1	1
IP-Ria-0	9577	ESP	Spain	spain	42.34	2.17	1	1	1	1	1	1	1	1	1
IP-Sac-0	9578	ESP	Spain	western_europe	42.13	-6.70	1	1	1	1	1	1	1	1	1
IP-Scm-0	9580	ESP	Spain	spain	38.68	-3.57	1	1	1	1	1	1	1	1	1
IP-Sdv-3	9581	ESP	Spain	spain	42.84	-5.12	1	1	0	0	0	0	0	0	0
IP-Ses-0	9582	ESP	Spain	spain	41.48	-1.63	1	1	0	0	0	0	0	0	0

IP-Stp-0	9584	ESP	Spain	spain	41.19	-3.58	1	1	1	1	1	1	1	1	1
IP-Svi-0	9585	ESP	Spain	western_europe	43.40	-7.39	1	1	1	1	1	1	1	0	1
IP-Tam-0	9586	ESP	Spain	spain	41.03	-3.27	1	1	1	0	1	1	1	0	1
IP-Tdc-0	9587	ESP	Spain	spain	41.50	-1.88	1	1	1	1	1	1	1	1	1
IP-Tol-7	9588	ESP	Spain	spain	42.11	0.60	1	1	0	0	0	0	0	0	0
IP-Tor-1	9589	ESP	Spain	spain	41.60	-2.83	1	1	1	1	1	1	1	1	1
IP-Vad-0	9591	ESP	Spain	admixed	42.86	-3.59	1	1	1	1	1	1	1	1	1
IP-Vae-2	9592	ESP	Spain	admixed	42.10	-5.44	1	1	1	1	1	1	0	0	0
IP-Vaz-0	9593	ESP	Spain	spain	42.26	-2.99	1	1	1	1	0	1	1	0	1
IP-Vdm-0	9594	ESP	Spain	spain	42.04	1.01	1	1	1	0	1	1	1	1	1
IP-Vdt-0	9595	ESP	Spain	admixed	40.89	-5.50	1	1	1	1	1	1	1	1	1
IP-Ver-5	9596	ESP	Spain	admixed	41.95	-7.45	1	1	1	0	1	1	1	1	1
IP-Vig-1	9597	ESP	Spain	spain	42.31	-2.53	1	1	1	1	1	1	1	1	1
IP-Vin-0	9599	ESP	Spain	western_europe	42.80	-5.77	1	1	0	0	0	1	1	1	1
IP-Voz-0	9601	ESP	Spain	spain	41.85	-1.88	1	1	1	1	0	1	1	1	1
IP-Vpa-1	9602	ESP	Spain	spain	40.50	-3.96	1	1	1	0	1	1	1	1	1
Toc-1	9739	ROU	NA	central_europe	46.01	22.33	0	0	1	1	1	1	0	0	0
Staro-2	9756	SRB	NA	central_europe	44.30	21.08	0	0	1	1	0	1	0	0	0
Fell3-7	9776	GER	NA	central_europe	48.43	8.79	0	0	1	1	1	1	1	1	1
Bach-7	9778	GER	NA	central_europe	48.41	8.84	0	0	1	1	1	1	1	1	1
Erg2-6	9784	GER	NA	central_europe	48.50	8.80	0	0	1	1	1	1	1	0	1
Wank-2	9795	GER	NA	central_europe	48.50	9.11	0	0	1	1	1	1	1	1	1
Obe1-15	9804	GER	NA	central_europe	48.45	8.87	0	0	1	1	1	1	1	1	1
Schl-7	9807	GER	NA	central_europe	48.60	9.22	0	0	1	1	1	1	1	1	1
Amu-0	9819	ESP	Spain	spain	42.35	-3.03	1	1	0	0	0	0	0	0	0
Are-0	9820	ESP	Spain	spain	41.00	-4.71	1	1	1	1	1	1	1	1	1
Aru-0	9821	ESP	Spain	spain	41.81	2.49	1	1	1	1	1	1	1	1	1
Aul-0	9822	ESP	Spain	spain	40.52	-4.02	1	1	1	1	1	1	1	1	1
Bes-5	9824	ESP	Spain	admixed	42.91	-4.91	1	1	0	0	0	0	0	0	0
Boa-0	9825	ESP	Spain	spain	40.40	-3.88	1	1	1	1	1	1	1	1	1
Bor-0	9826	ESP	Spain	western_europe	42.49	-6.71	1	1	1	0	1	1	1	1	1
Cha-0	9833	ESP	Spain	spain	40.38	-4.21	1	1	1	0	0	0	1	1	1
IP-Cha-0	9833	ESP	NA	spain	40.38	-4.21	1	1	1	0	0	0	1	1	1
Cho-0	9834	ESP	Spain	spain	40.51	-3.90	1	1	0	0	1	1	1	1	1
Cir-0	9835	ESP	Spain	admixed	40.61	-6.57	1	1	1	1	1	1	1	1	1
Cod-0	9836	ESP	Spain	spain	41.25	-1.32	1	1	1	0	1	1	1	1	1
Cot-0	9838	ESP	Spain	admixed	41.83	-5.38	1	1	1	1	1	1	1	1	1
Coy-0	9839	ESP	Spain	admixed	40.44	-4.27	1	1	0	0	0	0	0	0	0
Dar-0	9840	ESP	Spain	spain	41.13	-1.43	1	1	0	0	0	0	1	1	1
Ees-0	9841	ESP	Spain	spain	40.59	-4.15	1	1	1	1	0	1	1	1	1
Elp-0	9843	ESP	Spain	spain	40.53	-3.92	1	1	1	1	1	1	1	1	1
Esn-2	9844	ESP	Spain	spain	42.27	0.19	1	1	1	0	0	1	1	1	1
Evs-0	9845	ESP	Spain	spain	40.48	-3.96	1	1	1	0	1	1	1	1	1
Ezc-2	9846	ESP	Spain	spain	42.31	-3.02	1	1	1	1	1	1	1	1	1
Gud-3	9849	ESP	Spain	spain	40.65	-4.11	1	1	0	0	0	0	0	0	0
Hec-0	9850	ESP	Spain	spain	42.86	-0.70	1	1	0	0	0	0	0	0	0
Hue-3	9851	ESP	Spain	western_europe	42.96	-6.10	1	1	1	0	1	1	1	1	1
Ini-0	9852	ESP	Spain	spain	40.46	-3.75	1	1	1	1	1	1	1	1	1

Lam-0	9855	ESP	Spain	spain	40.57	-3.89	1	1	0	0	0	1	1	1	1
Lch-0	9856	ESP	Spain	spain	40.51	-4.00	1	1	1	1	1	1	1	1	1
Leg-0	9857	ESP	Spain	spain	40.33	-3.80	1	1	0	0	1	1	1	1	1
Loz-0	9858	ESP	Spain	admixed	40.98	-3.80	1	1	0	0	1	1	1	1	1
Lro-0	9859	ESP	Spain	spain	40.50	-3.88	1	1	1	1	0	0	1	1	1
Lum-0	9860	ESP	Spain	spain	42.24	-2.62	1	1	1	1	1	1	1	1	1
Mac-0	9861	ESP	Spain	spain	40.72	-3.21	1	1	1	1	1	1	1	1	1
Mat-0	9864	ESP	Spain	spain	41.76	2.69	1	1	1	1	1	1	1	1	1
Mie-1	9867	ESP	Spain	spain	40.94	-3.22	1	1	1	1	1	1	1	1	1
Moe-0	9868	ESP	Spain	spain	41.78	2.37	1	1	1	1	0	1	1	1	1
Moz-0	9870	ESP	Spain	spain	41.91	0.17	1	1	0	0	0	0	0	0	0
Oja-0	9874	ESP	Spain	spain	42.34	-3.00	1	1	1	0	1	1	1	1	1
Pad-0	9876	ESP	Spain	spain	41.34	0.99	1	1	0	0	0	0	1	1	1
Pdl-0	9877	ESP	Spain	spain	43.02	-5.60	1	1	0	0	0	0	0	0	0
Pee-0	9878	ESP	Spain	spain	40.78	-3.62	1	1	1	1	1	1	1	1	0
Pie-0	9881	ESP	Spain	admixed	40.46	-5.32	1	1	1	1	1	1	1	1	1
Piq-0	9883	ESP	Spain	spain	42.10	-2.56	1	1	1	1	1	1	1	1	1
Pru-0	9886	ESP	Spain	spain	42.38	1.73	1	1	1	1	1	1	1	1	1
Pva-1	9888	ESP	Spain	spain	40.93	-3.31	1	1	1	1	0	1	1	1	1
Rib-1	9890	ESP	Spain	admixed	43.16	-5.07	1	1	1	1	1	1	1	1	1
Sal-0	9891	ESP	Spain	spain	41.93	2.92	1	1	0	0	0	0	0	0	0
Sam-0	9892	ESP	Spain	admixed	42.68	-6.96	1	1	1	0	1	1	1	1	1
Sfb-6	9895	ESP	Spain	spain	41.78	2.57	1	1	1	1	1	1	1	1	1
Smt-1	9897	ESP	Spain	admixed	40.95	-5.63	1	1	1	1	1	1	1	1	1
Som-0	9898	ESP	Spain	spain	41.14	-3.58	1	1	0	0	0	0	0	0	0
Tau-0	9899	ESP	Spain	spain	42.54	0.84	1	1	1	1	1	1	1	1	1
Urd-1	9901	ESP	Spain	spain	42.27	-2.98	1	1	0	0	0	0	0	0	0
Usa-0	9902	ESP	Spain	spain	40.71	-3.24	1	1	1	1	1	1	1	1	1
Val-0	9903	ESP	Spain	spain	42.31	-3.10	1	1	0	0	0	0	0	0	0
Vas-0	9904	ESP	Spain	spain	40.95	-3.31	1	1	1	1	1	1	1	1	1
Mah-6	9906	ESP	Spain	admixed	40.00	4.25	1	1	1	1	1	1	1	1	1
ARR-17	9927	FRA	Western Europe	western_europe	44.05	3.69	1	1	1	1	1	1	0	0	0
MOU2-25	9931	FRA	Western Europe	western_europe	43.98	4.31	1	1	0	0	0	0	0	0	0
WAV-8	9938	FRA	Western Europe	western_europe	50.65	2.99	1	1	1	1	1	1	1	0	1
Agu-1	9942	ESP	Spain	spain	41.32	-1.34	1	1	1	1	1	1	1	1	1
Pra-6	9948	ESP	Spain	spain	41.05	-3.54	1	1	1	1	1	1	1	1	1
Qui-0	9949	ESP	Spain	western_europe	42.69	-6.93	1	1	1	1	1	1	1	1	1
Vie-0	9950	ESP	Spain	spain	42.63	0.76	1	1	1	1	1	1	1	1	1
Copac-1	10005	ROU	NA	central_europe	46.11	21.95	0	0	1	1	1	1	0	0	0
Petro-1	10017	SRB	NA	central_europe	44.34	21.46	0	0	1	1	1	1	0	0	0
Arb0	18513	MAR	NA	africa	31.42	-7.53	0	0	0	0	0	0	1	0	0
Zin9	18515	MAR	NA	africa	35.45	-5.43	0	0	0	0	0	0	1	0	0
IFr0	22002	MAR	NA	africa	33.55	-5.17	0	0	0	0	0	0	1	0	0
Taz0	22005	MAR	NA	africa	34.09	-4.10	0	0	0	0	0	0	1	0	0
Bab0	22008	MAR	NA	africa	35.04	-5.02	0	0	0	0	0	0	1	0	0
Elh2	35616	MAR	NA	africa	31.47	-7.41	0	0	0	0	0	0	1	0	0
Militärring A2	100048	GER	NA	germany	50.90	6.98	0	0	1	1	1	1	0	0	0
Militärring B1	100049	GER	NA	germany	50.89	6.97	0	0	1	1	1	1	0	0	0

Bernhardstr. 110	100050	GER	NA	germany	50.91	6.97	0	0	0	0	0	1	0	0	0
MilitärringA2	100051	GER	NA	germany	50.90	6.98	0	0	0	0	0	0	1	1	1
MilitärringB1	100052	GER	NA	germany	50.89	6.97	0	0	0	0	0	0	1	1	1
Bernhardstr.110	100053	GER	NA	germany	50.91	6.97	0	0	0	0	0	0	1	1	1
Mol-2	115927	FRA	Western Europe	western_europe	46.92	4.10	1	1	1	0	1	1	1	1	1
All1-2	115930	FRA	Western Europe	western_europe	45.26	1.48	1	1	0	0	1	1	1	1	1
All1-4	115932	FRA	Western Europe	western_europe	45.26	1.48	1	1	1	1	1	1	1	1	1
All1-5	115934	FRA	Western Europe	western_europe	45.26	1.48	1	1	1	1	0	0	1	1	1
All1-8	115936	FRA	Western Europe	western_europe	45.26	1.48	1	1	1	1	1	1	1	1	0
All2-1	115938	FRA	Western Europe	western_europe	45.26	1.48	1	1	1	1	1	1	1	1	1
All2-4	115940	FRA	Western Europe	western_europe	45.26	1.48	1	1	1	1	1	1	1	1	1
All2-5	115942	FRA	Western Europe	western_europe	45.26	1.48	1	1	1	1	1	1	1	1	1
Cam-10	115944	FRA	Western Europe	western_europe	48.28	-4.60	1	1	1	1	1	1	1	1	1
Cam-11	115946	FRA	Western Europe	western_europe	48.28	-4.60	1	1	1	1	1	1	1	1	1
Cam-2	115948	FRA	Western Europe	western_europe	48.28	-4.60	1	1	1	1	1	1	1	1	1
Cam-6	115950	FRA	Western Europe	western_europe	48.28	-4.60	1	1	1	1	1	1	1	1	1
Cam-8	115952	FRA	Western Europe	western_europe	48.28	-4.60	1	1	1	1	1	1	1	1	1
Cla-3	115954	FRA	Western Europe	western_europe	48.80	2.26	1	1	1	0	1	1	1	1	1
Cla-5	115956	FRA	Western Europe	western_europe	48.80	2.26	1	1	1	0	1	1	0	0	0
Cla-6	115958	FRA	Western Europe	western_europe	48.80	2.26	1	1	1	1	1	1	1	1	1
Cur-10	115960	FRA	Western Europe	western_europe	45.00	1.74	1	1	1	1	1	1	1	1	1
Cur-2	115962	FRA	Western Europe	western_europe	45.00	1.74	1	1	0	0	1	1	1	1	1
Cur-5	115964	FRA	Western Europe	western_europe	45.00	1.74	1	1	1	1	1	1	1	1	1
Fet-6	115968	FRA	Western Europe	western_europe	47.20	4.17	1	1	1	0	1	1	1	1	0
All2-6	115970	FRA	Western Europe	western_europe	45.26	1.48	1	1	1	1	1	1	1	1	1
Lac-2	115972	FRA	Western Europe	western_europe	47.70	6.82	1	1	1	0	1	1	1	1	1
Lac-7	115974	FRA	Western Europe	western_europe	47.70	6.82	1	1	1	1	1	1	1	1	1
Ldv-1	115976	FRA	Western Europe	western_europe	48.51	-4.07	1	1	1	1	1	1	1	1	1
Ldv-11	115978	FRA	Western Europe	western_europe	48.51	-4.07	1	1	1	1	1	1	1	1	1
Ldv-2	115980	FRA	Western Europe	western_europe	48.51	-4.07	1	1	1	1	1	1	1	1	1
Ldv-3	115982	FRA	Western Europe	western_europe	48.51	-4.07	1	1	1	1	1	1	1	1	1
Mib-11	115986	FRA	Western Europe	western_europe	47.33	5.32	1	1	1	1	1	1	1	1	1
Mib-18	115988	FRA	Western Europe	western_europe	47.33	5.32	1	1	1	1	1	1	1	1	1
Mib-3	115990	FRA	Western Europe	western_europe	47.33	5.32	1	1	1	1	0	1	1	1	1
Mib-9	115992	FRA	Western Europe	western_europe	47.33	5.32	1	1	1	1	1	1	1	1	1
Mog-1	115994	FRA	Western Europe	western_europe	48.67	-4.06	1	1	1	1	1	0	1	1	1
Mog-11	115996	FRA	Western Europe	western_europe	48.67	-4.06	1	1	1	1	1	1	1	1	1
Mol-12	116000	FRA	Western Europe	western_europe	46.92	4.10	1	1	0	0	1	1	1	1	1
Mol-4	116002	FRA	Western Europe	western_europe	46.92	4.10	1	1	1	1	1	1	1	1	1
Par-10	116004	FRA	Western Europe	western_europe	46.65	0.25	1	1	1	1	1	1	1	1	1
Par-13	116006	FRA	Western Europe	western_europe	46.65	0.25	1	1	1	1	1	1	1	1	1
Par-3	116008	FRA	Western Europe	western_europe	46.65	0.25	1	1	1	1	1	1	1	1	1
Par-4	116010	FRA	Western Europe	western_europe	46.65	0.25	1	1	1	1	1	1	1	1	1
Pyl-1	116012	FRA	Western Europe	western_europe	44.65	-1.17	0	1	1	1	0	1	1	1	1
Pyl-3	116014	FRA	Western Europe	western_europe	44.65	-1.17	1	1	1	1	1	1	1	1	1
Pyl-4	116016	FRA	Western Europe	western_europe	44.65	-1.17	1	1	1	1	1	1	1	1	1
Vou-1	116020	FRA	Western Europe	western_europe	46.65	0.17	1	1	1	0	1	1	1	1	1
Vou-10	116022	FRA	Western Europe	western_europe	46.65	0.17	1	1	1	1	1	1	1	1	1

Vou-6	116024	FRA	Western Europe	western_europe	46.65	0.17	1	1	1	1	1	1	1	1	1
Vou-9	116026	FRA	Western Europe	western_europe	46.65	0.17	1	1	1	1	1	1	1	1	1
Zdy-62	2000000	CHI	China	asia	NA	NA	0	0	0	0	0	0	1	1	1
Aqs-11	2189710	CHI	China	asia	30.75	117.97	0	1	0	0	0	0	1	1	1
Ayx-42	2189718	CHI	China	asia	30.43	116.15	0	0	1	1	1	1	1	1	1
Jjgs-30	2204161	CHI	China	asia	26.76	114.31	1	1	1	1	1	1	1	1	1
Jjj-32	2204162	CHI	China	asia	29.60	115.92	1	1	1	0	1	1	1	1	1
Zkh-29	2204168	CHI	China	asia	29.11	118.38	0	1	0	0	0	0	1	1	1
Zla-62	2204170	CHI	China	asia	30.05	119.92	1	1	0	0	0	0	1	1	1
Hwc-61	2204174	CHI	China	asia	30.53	114.47	1	1	0	0	0	1	1	0	1
Cbb-60	2204175	CHI	China	asia	29.79	106.48	0	0	1	1	1	1	0	0	1
Gwx-11	2204177	CHI	China	asia	32.73	105.12	1	1	1	0	1	1	1	1	1
Smx-34	2204179	CHI	China	asia	33.16	106.75	0	1	0	0	1	1	1	1	1
Hnzjj-75	2204239	CHI	China	asia	29.41	110.44	0	0	0	0	0	0	1	1	1
Hyl-40	2204313	CHI	China	asia	28.52	110.72	1	1	1	1	1	1	1	1	1
Ygs-39	2204316	CHI	China	asia	NA	NA	1	1	1	1	1	1	1	1	1
HNxy-46	2204317	CHI	China	asia	28.52	110.72	0	0	1	0	1	1	1	1	1
Xem	2204324	CHI	China	asia	NA	NA	1	1	1	0	1	1	1	1	1
Ahthx-23	6414606	CHI	China	asia	30.45	117.29	0	1	0	0	0	0	1	1	1
Hha-21	6414609	CHI	China	asia	31.17	107.13	1	1	1	0	0	0	1	1	0
JSnj-8	6414610	CHI	China	asia	32.05	118.84	0	1	0	1	0	0	1	1	1

Table 23: Genotypes that were sequenced for this study.

Information on the genotype names, country of origin, ID used in this study and (if applicable) ID in the 1001 Genomes data set.

Genotype name	Country	ID	ID1001Genomes
Militärring A2	Germany	100048	NA
Militärring B1	Germany	100049	NA
Bernhardstr. 110	Germany	100050	NA
MilitärringA2	Germany	100051	NA
MilitärringB1	Germany	100052	NA
Bernhardstr.110	Germany	100053	NA
Mol-2	France	115927	NA
All1-2	France	115930	1
All1-4	France	115932	3
All1-5	France	115934	4
All1-8	France	115936	7
All2-1	France	115938	9
All2-4	France	115940	12
All2-5	France	115942	13
Cam-10	France	115944	17
Cam-11	France	115946	18
Cam-2	France	115948	NA
Cam-6	France	115950	64

Cam-8	France	115952	NA
Cla-3	France	115954	NA
Cla-5	France	115956	NA
Cla-6	France	115958	NA
Cur-10	France	115960	79
Cur-2	France	115962	80
Cur-5	France	115964	83
Fet-6	France	115968	NA
All2-6	France	115970	NA
Lac-2	France	115972	93
Lac-7	France	115974	98
Ldv-1	France	115976	99
Ldv-11	France	115978	101
Ldv-2	France	115980	110
Ldv-3	France	115982	121
Mib-11	France	115986	163
Mib-18	France	115988	NA
Mib-3	France	115990	180
Mib-9	France	115992	228
Mog-1	France	115994	NA
Mog-11	France	115996	236
Mol-12	France	116000	237
Mol-4	France	116002	NA
Par-10	France	116004	257
Par-13	France	116006	NA
Par-3	France	116008	258
Par-4	France	116010	259
Pyl-1	France	116012	NA
Pyl-3	France	116014	NA
Pyl-4	France	116016	NA
Vou-1	France	116020	390
Vou-10	France	116022	391
Vou-6	France	116024	395
Vou-9	France	116026	398

Table 24: Climatic information on the genotypes in HL and LL.

Information on the country of origin, assigned region, Genotype name and ID in 1001 Genomes. Climatic parameters are: Radiation [kJ m^{-2} day^{-1}] in the growing season, The first 2 PCs for PCA on data based on growing season, Temperature variables from bioclim data and precipitation variables from bioclim data.

Genotype	ID	Country	Region	Radiation_GS	Radiation	PC1_growS	PC2_growS	PC1_T	PC2_T	PC1_P	PC2_P
Ahthx-23	6414606	China	China	15323.727	15323.727	76.637	-10.831	252.659	-2.721	934.429	-283.015
Aqs-11	2189710	China	China	15474.273	15474.273	63.727	-3.774	268.271	-2.563	736.026	-242.715

Ayx	2189718	China	China	14992.727	14992.727	81.620	-4.205	230.459	0.127	960.713	-304.008
Cbb	2204175	China	China	12056.667	12056.667	37.293	0.734	111.269	-1.608	504.260	-327.447
Ctl-62	NA	China	China	11824.750	11824.750	35.966	2.640	105.582	-2.603	494.650	-346.619
Gwx-11	2204177	China	China	13477.300	13477.300	4.270	-15.280	91.504	2.529	78.061	-318.699
Hha-21	6414609	China	China	12360.750	12360.750	38.758	-2.381	141.825	-1.910	545.391	-338.739
Hnxy-46	2204317	China	China	13778.818	13778.818	66.975	-6.223	185.049	-0.479	800.696	-244.871
Hnzjj-75	2204239	China	China	14068.100	14068.100	81.812	-5.745	139.844	4.140	850.784	-313.032
Hwc-61	2204174	China	China	13811.273	13811.273	54.694	-5.223	265.829	-2.742	661.351	-256.200
Hyl-40	2204313	China	China	13778.818	13778.818	66.975	-6.223	185.049	-0.479	800.696	-244.871
Jjgs-30	2204161	China	China	14217.833	14217.833	70.771	-10.426	148.125	-3.642	950.156	-149.257
Jjj-32	2204162	China	China	14900.909	14900.909	73.789	-1.470	258.083	-2.906	858.349	-199.737
Jnf-27	NA	China	China	14642.917	14642.917	80.870	-22.560	145.284	-4.881	1192.446	-203.141
JSnj-8	6414610	China	China	16826.000	16826.000	43.484	-8.257	292.829	1.727	410.676	-266.484
Scg-68	NA	China	China	14908.000	14908.000	28.517	-17.121	208.611	2.375	219.663	-289.600
Scg-77	NA	China	China	14908.000	14908.000	28.517	-17.121	208.611	2.375	219.663	-289.600
Smx-34	2204179	China	China	14525.100	14525.100	18.250	-6.144	196.374	1.541	155.970	-291.163
Xyl	NA	China	China	NA	NA	NA	NA	NA	NA	NA	NA
Zkh-29	2204168	China	China	15098.273	15098.273	85.303	-17.213	224.770	-3.164	1102.130	-194.506
Zla-62	2204170	China	China	15044.545	15044.545	63.136	-1.017	240.896	-2.694	721.969	-173.334
Bd-0	7013	Germany	Northern Europe	14551.286	14551.286	-11.967	4.367	49.602	9.739	-204.120	-45.256
Gie-0	7147	Germany	Western Europe	13572.375	NA	NA	NA	NA	NA	NA	NA
Hh-0	7169	Germany	Northern Europe	13907.857	13907.857	14.739	10.280	-39.102	12.129	103.910	-10.681
Np-0	7268	Germany	Northern Europe	14176.000	14176.000	-8.372	6.028	18.234	9.340	-170.235	-42.455
Pt-0	7305	Germany	Northern Europe	14054.143	14054.143	0.514	7.023	-2.214	10.398	-58.056	-26.062
Sp-0	7343	Germany	Northern Europe	14457.714	14457.714	-12.935	3.744	48.865	9.493	-214.288	-46.271
Ste-0	7346	Germany	Northern Europe	14350.143	14350.143	-12.326	2.130	34.984	8.215	-216.094	-59.505
Oy-0	7288	Norway	Northern Europe	13201.167	13201.167	100.627	-13.860	-58.713	11.696	1564.201	307.087
Agu-1	9942	Spain	Spain	17192.100	17192.100	-31.128	-5.895	-17.055	0.684	-353.218	-41.105
Amu-0	9819	Spain	Spain	16603.889	16603.889	-17.102	2.461	-72.739	-4.195	-217.772	25.290
Are-0	9820	Spain	Spain	17418.857	17418.857	-39.068	-9.639	6.053	-9.215	-421.726	-7.605
Aru-0	9821	Spain	Spain	15551.000	15551.000	14.112	12.119	-76.143	1.433	59.281	-3.744
Aul-0	9822	Spain	Spain	15278.889	15278.889	-34.318	-5.711	57.894	-12.797	-408.872	-0.293
Bes-5	9824	Spain	Spain	19105.000	19105.000	1.066	3.822	-111.289	4.628	148.023	110.903
Bla-1	8264	Spain	Spain	14713.500	14713.500	-1.187	6.119	-95.544	-13.965	-66.392	4.917
Boa-0	9825	Spain	Spain	15348.111	15348.111	-34.110	-6.334	54.425	-14.449	-408.134	6.896
Bor-0	9826	Spain	Spain	14971.818	14971.818	17.369	-10.632	-74.703	-6.948	311.156	179.289
Bur-0	9829	Spain	Spain	17859.286	NA	NA	NA	NA	NA	NA	NA
Cha-0	9833	Spain	Spain	15373.667	15373.667	-39.084	-8.864	64.370	-13.894	-444.830	-8.670
Cho-0	9834	Spain	Spain	15282.444	15282.444	-34.253	-5.628	55.266	-13.679	-409.895	5.049
Cir-0	9835	Spain	Spain	15784.636	15784.636	16.309	-11.301	-47.708	-11.647	232.324	216.835
Cod-0	9836	Spain	Spain	17208.000	17208.000	-30.929	-7.014	-9.601	1.202	-347.563	-42.694
Cot-0	9838	Spain	Spain	15623.750	15623.750	-27.050	-14.397	-15.970	-8.566	-260.310	47.014
Coy-0	9839	Spain	Spain	16489.000	16489.000	-35.384	-6.970	49.756	-10.415	-412.484	-4.231
Dar-0	9840	Spain	Spain	17207.200	17207.200	-35.615	-10.220	18.577	-0.718	-377.621	-56.029

Ees-0	9841	Spain	Spain	17953.143	17953.143	-19.915	-15.128	22.031	-4.010	-200.866	43.735
Elp-0	9843	Spain	Spain	15280.222	15280.222	-35.788	-5.706	51.626	-14.285	-428.288	1.225
Esn-2	9844	Spain	Spain	15795.455	15795.455	-13.642	-4.137	13.993	-11.025	-157.153	4.996
Evs-0	9845	Spain	Spain	15301.667	NA	NA	NA	NA	NA	NA	NA
Ezc-2	9846	Spain	Spain	16679.444	16679.444	-19.795	-0.511	-74.025	-4.031	-229.847	24.790
Glo-1	9848	Spain	Spain	15710.778	15710.778	-13.585	-14.897	-67.396	-9.973	-146.672	100.330
Gud-3	9849	Spain	Spain	17951.286	17951.286	-30.218	-8.160	10.744	-7.065	-361.693	2.774
Hec-0	9850	Spain	Spain	18722.333	18722.333	28.343	7.805	-100.867	4.174	371.664	98.109
Hue-3	9851	Spain	Spain	18652.500	18652.500	15.897	-6.903	-150.384	4.211	523.998	188.703
Ini-0	9852	Spain	Spain	15313.444	15313.444	-34.407	-6.178	53.752	-14.030	-393.521	13.425
IP-All-0	9517	Spain	Spain	13816.500	13816.500	74.449	-27.588	-176.231	-8.389	1067.080	377.442
IP-Alo-0	9506	Spain	Spain	16387.583	16387.583	32.330	-4.888	-113.758	-8.696	425.198	266.963
IP-Ara-4	9520	Spain	Spain	16717.444	16717.444	-38.028	-4.018	6.679	-9.571	-433.258	-6.213
IP-Bar-1	9521	Spain	Spain	14940.333	14940.333	-5.564	5.490	-81.228	-3.924	-106.609	-29.006
IP-Ber-0	9524	Spain	Spain	17239.667	17239.667	5.812	11.574	-61.225	-1.869	-5.250	48.618
IP-Bis-0	9525	Spain	Spain	19644.333	19644.333	29.765	10.432	-64.248	0.711	256.134	51.236
IP-Cab-3	9526	Spain	Spain	14755.000	14755.000	-3.235	9.718	-104.776	-14.079	-106.233	-12.363
IP-Cad-0	9527	Spain	Spain	19742.000	19742.000	2.877	-22.319	-37.990	1.017	312.264	210.995
IP-Cal-0	9528	Spain	Spain	18075.000	18075.000	-28.625	-7.184	11.902	0.497	-343.068	-65.860
IP-Cdc-3	9531	Spain	Spain	17259.714	17259.714	-38.010	-8.265	2.254	-9.975	-413.257	-2.853
IP-Cdo-0	9532	Spain	Spain	16563.556	16563.556	-30.620	-5.884	-11.445	-8.037	-344.308	19.159
IP-Cmo-3	9534	Spain	Spain	15025.714	15025.714	-41.570	-11.102	39.952	-16.901	-480.498	-2.158
IP-Coc-1	9535	Spain	Spain	14662.583	14662.583	-14.759	2.976	-88.237	-11.190	-208.826	10.323
IP-Deh-1	9539	Spain	Spain	16268.000	16268.000	15.602	-4.768	-97.392	-6.134	220.625	204.051
IP-Elb-0	9540	Spain	Spain	17868.250	17868.250	24.375	7.816	-65.193	7.107	164.944	22.586
IP-Hom-4	9546	Spain	Spain	18065.556	18065.556	-22.021	-5.743	10.634	-8.498	-252.453	-13.674
IP-Hor-0	9547	Spain	Spain	14750.750	14750.750	12.981	14.227	-66.602	-10.559	51.088	6.684
IP-Hoy-0	9548	Spain	Spain	19451.250	19451.250	-22.469	-13.277	-11.455	-2.117	-129.766	72.619
IP-Jim-1	9551	Spain	Spain	16620.000	16620.000	-13.785	-11.804	-8.704	-8.576	-32.555	94.472
IP-Lab-7	9552	Spain	Spain	18756.833	18756.833	-35.249	-9.154	12.604	-7.737	-394.145	-12.095
IP-Ldd-0	9553	Spain	Spain	15660.250	15660.250	-34.616	-10.312	0.805	-9.688	-376.237	5.864
IP-Men-2	9556	Spain	Spain	14298.125	14298.125	-30.017	-11.746	87.511	-15.459	-378.459	16.253
IP-Moa-0	9557	Spain	Spain	17678.750	17678.750	35.276	6.324	-65.185	9.531	295.594	43.420
IP-Moc-11	9558	Spain	Spain	14084.714	14084.714	-17.447	-22.041	-24.433	-9.822	-164.559	76.808
IP-Mun-0	9561	Spain	Spain	19006.500	19006.500	-30.036	-8.859	21.987	-6.642	-322.326	15.482
IP-Mur-0	9562	Spain	Spain	15928.818	15928.818	7.808	15.073	-8.076	0.297	-23.403	-36.308
IP-Nog-17	9564	Spain	Spain	18810.625	18810.625	-17.566	-7.963	-0.816	-4.529	-210.846	-0.260
IP-Orb-10	9565	Spain	Spain	15999.444	15999.444	25.020	5.394	-89.050	-1.877	288.719	107.364
IP-Pal-0	9567	Spain	Spain	17945.125	17945.125	31.461	14.099	-59.490	9.594	184.399	14.157
IP-Pan-0	9568	Spain	Spain	20773.500	20773.500	35.882	10.864	-146.716	14.612	645.571	118.881
IP-Pds-1	9569	Spain	Spain	16431.778	16431.778	21.664	-7.364	-113.052	0.242	425.726	170.974
IP-Rds-0	9573	Spain	Spain	14635.583	14635.583	1.070	12.471	-59.888	-11.766	-79.472	-3.302
IP-Ria-0	9577	Spain	Spain	19193.500	19193.500	35.359	1.580	-87.572	3.925	364.770	57.524
IP-Sac-0	9578	Spain	Spain	17987.125	17987.125	12.202	-10.489	-76.859	1.927	390.114	198.336

IP-Scm-0	9580	Spain	Spain	14560.625	NA	NA	NA	NA	NA	NA	NA
IP-Sdv-3	9581	Spain	Spain	17245.625	17245.625	-2.966	-3.450	-71.992	0.414	31.973	86.351
IP-Ses-0	9582	Spain	Spain	17869.778	17869.778	-30.886	-10.483	-0.860	1.901	-328.607	-18.714
IP-Stp-0	9584	Spain	Spain	18454.750	18454.750	-25.000	-11.689	-7.644	-3.912	-231.567	35.789
IP-Svi-0	9585	Spain	Spain	12523.500	12523.500	50.034	-8.098	-226.239	-4.789	637.282	222.831
IP-Tam-0	9586	Spain	Spain	18162.625	18162.625	-34.046	-5.843	7.755	-6.898	-380.892	3.385
IP-Tdc-0	9587	Spain	Spain	17776.889	17776.889	-32.332	-10.860	8.124	-8.782	-351.632	-21.662
IP-Tol-7	9588	Spain	Spain	17825.889	17825.889	2.483	0.991	21.091	3.066	-32.193	-2.797
IP-Tor-1	9589	Spain	Spain	17563.667	17563.667	-34.054	-6.967	-11.485	-8.033	-366.132	5.578
IP-Vad-0	9591	Spain	Spain	15233.600	15233.600	5.297	10.196	-81.642	-5.144	14.485	66.284
IP-Vae-2	9592	Spain	Spain	15335.000	15335.000	-24.079	-11.165	-17.549	-8.875	-245.534	46.029
IP-Vaz-0	9593	Spain	Spain	19108.500	19108.500	-2.775	4.686	-74.677	3.271	10.244	71.984
IP-Vdm-0	9594	Spain	Spain	17700.778	17700.778	13.257	12.277	-9.425	4.829	3.951	-12.890
IP-Vdt-0	9595	Spain	Spain	17660.286	17660.286	-34.861	-10.547	-12.857	-9.274	-374.733	13.952
IP-Ver-5	9596	Spain	Spain	14293.167	14293.167	90.924	-41.945	-112.494	-12.980	1383.454	470.189
IP-Vig-1	9597	Spain	Spain	15861.600	15861.600	-26.717	-5.841	-56.990	-7.354	-283.792	7.074
IP-Vin-0	9599	Spain	Spain	18854.714	18854.714	1.348	-7.554	-64.832	0.465	204.321	120.303
IP-Voz-0	9601	Spain	Spain	17296.000	17296.000	-26.130	-5.447	-25.348	-7.480	-295.393	-6.101
IP-Vpa-1	9602	Spain	Spain	15260.778	15260.778	-35.825	-7.185	53.946	-14.739	-433.015	0.501
Lam-0	9855	Spain	Spain	15239.889	15239.889	-33.707	-5.282	51.063	-13.039	-405.296	4.314
Lch-0	9856	Spain	Spain	15278.889	15278.889	-34.576	-6.202	58.837	-13.706	-417.186	0.746
Leg-0	9857	Spain	Spain	15337.556	15337.556	-32.526	-6.662	59.512	-14.266	-388.945	11.847
LL-0	6933	Spain	Spain	14808.250	14808.250	8.099	8.716	-65.362	-10.434	30.210	-4.755
Loz-0	9858	Spain	Spain	20577.833	20577.833	-9.555	-11.129	-9.563	1.870	148.124	124.671
Lro-0	9859	Spain	Spain	15282.444	15282.444	-34.047	-5.235	54.671	-14.036	-409.274	5.839
Lum-0	9860	Spain	Spain	16848.667	16848.667	-21.031	-2.607	-63.612	-4.482	-235.147	19.399
Mac-0	9861	Spain	Spain	15841.125	15841.125	-36.432	-6.849	59.086	-12.688	-410.792	4.937
Mah-6	9906	Spain	Spain	15567.417	15567.417	-16.790	2.646	-112.625	-15.745	-231.661	20.788
Mat-0	9864	Spain	Spain	14663.083	14663.083	5.417	7.442	-40.574	-14.347	0.761	10.849
Mie-1	9867	Spain	Spain	18245.125	18245.125	-36.442	-6.149	11.085	-7.852	-405.408	0.035
Moe-0	9868	Spain	Spain	17287.222	17287.222	19.769	8.043	-67.217	4.510	114.270	-0.971
MOU2-25	9931	Spain	Spain	14267.667	NA	NA	NA	NA	NA	NA	NA
Moz-0	9870	Spain	Spain	14612.727	14612.727	-33.119	-12.304	37.757	-3.774	-342.943	-19.071
Oja-0	9874	Spain	Spain	16603.889	16603.889	-18.908	-0.976	-70.136	-4.807	-227.783	24.476
Pad-0	9876	Spain	Spain	17316.200	17316.200	-4.646	10.338	6.495	-9.115	-145.745	-1.189
Pdl-0	9877	Spain	Spain	18465.000	18465.000	15.441	-2.710	-138.597	6.482	427.421	159.299
Pee-0	9878	Spain	Spain	16714.250	16714.250	-32.693	-4.864	60.432	-11.180	-393.425	2.238
Pie-0	9881	Spain	Spain	19289.000	19289.000	-25.236	-7.235	-21.179	-6.497	-247.326	53.550
Piq-0	9883	Spain	Spain	17524.250	17524.250	-9.173	-0.766	-61.045	-0.091	-123.598	39.731
Pra-6	9948	Spain	Spain	18031.556	18031.556	-29.133	-8.288	4.609	-5.166	-296.971	20.574
Prd-0	9885	Spain	Spain	17865.889	17865.889	-28.463	-7.263	-6.792	-5.462	-295.858	20.109
Pru-0	9886	Spain	Spain	19860.000	19860.000	30.953	4.231	-73.937	3.310	283.652	50.521
Pva-1	9888	Spain	Spain	16481.125	16481.125	-34.448	-5.488	40.665	-9.790	-415.630	-3.575
Qui-0	9949	Spain	Spain	15623.200	15623.200	28.539	-9.695	-124.663	-3.360	538.336	214.352

Rib-1	9890	Spain	Spain	15746.222	15746.222	7.077	2.996	-143.700	0.721	105.517	89.906
Sal-0	9891	Spain	Spain	14548.333	14548.333	2.083	12.771	-53.707	-12.078	-70.880	-4.315
Sam-0	9892	Spain	Spain	16369.333	16369.333	28.293	-10.100	-129.679	-2.062	582.209	223.359
Se-0	6961	Spain	Spain	16131.889	16131.889	-31.219	-7.329	68.838	-17.593	-380.389	38.790
Sf-1	7327	Spain	Spain	14648.917	14648.917	-10.139	3.763	-97.063	-13.736	-155.227	-12.804
Sf-2	7328	Spain	Spain	14648.917	NA	NA	NA	NA	NA	NA	NA
Sfb-6	9895	Spain	Spain	14638.500	14638.500	11.412	9.954	-40.658	-12.448	57.086	5.469
Smt-1	9897	Spain	Spain	16086.000	16086.000	-26.601	-14.634	-0.663	-9.400	-254.478	49.806
Som-0	9898	Spain	Spain	20526.000	20526.000	-13.291	-11.426	-1.921	1.925	74.315	106.334
Tau-0	9899	Spain	Spain	19486.667	NA	NA	NA	NA	NA	NA	NA
Ts-1	6970	Spain	Spain	19486.667	19486.667	41.525	5.477	-104.756	7.187	449.505	72.879
Ts-5	6971	Spain	Spain	14677.917	14677.917	-5.057	2.893	-111.606	-12.966	-91.048	-2.160
Urd-1	9901	Spain	Spain	19108.500	NA	NA	NA	NA	NA	NA	NA
Usa-0	9902	Spain	Spain	15841.125	NA	NA	NA	NA	NA	NA	NA
Val-0	9903	Spain	Spain	17217.250	17217.250	-8.051	4.545	-71.722	-0.677	-134.194	43.121
Vas-0	9904	Spain	Spain	16481.125	NA	NA	NA	NA	NA	NA	NA
Vie-0	9950	Spain	Spain	19077.000	19077.000	45.383	7.961	-133.653	11.852	615.264	101.753
Ale-Stenar-41-1	991	Sweden	Northern Europe	14894.714	14894.714	-5.100	15.183	-1.345	8.939	-140.029	-3.076
Ale-Stenar-44-4	992	Sweden	Northern Europe	14894.714	14894.714	-5.100	15.183	-1.345	8.939	-140.029	-3.076
Ale-Stenar-56-14	997	Sweden	Northern Europe	14894.714	14894.714	-5.100	15.183	-1.345	8.939	-140.029	-3.076
Ale-Stenar-64-24	1002	Sweden	Northern Europe	14894.714	14894.714	-5.100	15.183	-1.345	8.939	-140.029	-3.076
App1-12	5830	Sweden	Northern Europe	14999.500	14999.500	-8.448	7.489	0.926	12.144	-183.784	-15.785
App1-14	5831	Sweden	Northern Europe	14999.500	14999.500	-8.448	7.489	0.926	12.144	-183.784	-15.785
App1-16	5832	Sweden	Northern Europe	14999.500	14999.500	-8.448	7.489	0.926	12.144	-183.784	-15.785
Bå1-2	8256	Sweden	Northern Europe	14472.500	14472.500	26.497	8.222	-12.451	13.746	202.091	6.393
Bå5-1	8259	Sweden	Northern Europe	14472.500	14472.500	26.497	8.222	-12.451	13.746	202.091	6.393
Böt 1	9339	Sweden	Northern Europe	14448.000	14448.000	5.393	4.936	46.640	18.209	-80.440	-45.754
Brö1-6	8231	Sweden	Northern Europe	14909.286	14909.286	-9.264	11.865	2.997	11.854	-190.818	-16.709
Brösarp-11-135	1061	Sweden	Northern Europe	14646.714	14646.714	-0.415	13.372	-9.538	14.299	-97.426	-8.890
Brösarp-15-138	1062	Sweden	Northern Europe	14646.714	14646.714	-0.415	13.372	-9.538	14.299	-97.426	-8.890
Brösarp-21-140	1063	Sweden	Northern Europe	14646.714	14646.714	-0.415	13.372	-9.538	14.299	-97.426	-8.890
Brösarp-34-145	1066	Sweden	Northern Europe	14646.714	14646.714	-0.415	13.372	-9.538	14.299	-97.426	-8.890
Dra3-1	8283	Sweden	Northern Europe	14604.571	14604.571	2.564	12.616	-6.947	14.790	-45.557	-1.921
EkS2	9369	Sweden	Northern Europe	14409.167	14409.167	2.930	3.770	76.633	17.078	-104.455	-47.493
Fjä1-1	8422	Sweden	Northern Europe	14565.429	14565.429	-5.119	14.516	4.877	13.191	-196.083	-40.542
Fjä1-2	6019	Sweden	Northern Europe	14565.429	14565.429	-5.119	14.516	4.877	13.191	-196.083	-40.542
Fjä1-5	6020	Sweden	Northern Europe	14565.429	14565.429	-5.119	14.516	4.877	13.191	-196.083	-40.542
Fjä2-4	6021	Sweden	Northern Europe	14565.429	14565.429	-5.119	14.516	4.877	13.191	-196.083	-40.542
Fly2-1	6023	Sweden	Northern Europe	14466.429	14466.429	2.457	12.936	-2.185	13.578	-70.834	-13.787
Fly2-2	6024	Sweden	Northern Europe	14466.429	14466.429	2.457	12.936	-2.185	13.578	-70.834	-13.787
FlyA 3	9380	Sweden	Northern Europe	14510.714	14510.714	0.625	13.730	2.053	13.462	-101.010	-18.325
Gul1-2	8234	Sweden	Northern Europe	14798.833	14798.833	-4.308	6.419	15.353	15.160	-132.611	-11.573
Ham-1	9399	Sweden	Northern Europe	14777.571	14777.571	-4.027	14.459	-0.593	13.952	-129.418	-6.542
Hau-0	7164	Sweden	Northern Europe	12841.250	12841.250	-1.778	13.311	-8.258	13.385	-150.546	-26.406

HolA-1-1	9404	Sweden	Northern Europe	14496.143	14496.143	1.002	13.530	0.668	13.206	-97.285	-19.011
HolA-1-2	9405	Sweden	Northern Europe	14496.143	14496.143	1.002	13.530	0.668	13.206	-97.285	-19.011
HolA-2-2	9407	Sweden	Northern Europe	14496.143	14496.143	1.002	13.530	0.668	13.206	-97.285	-19.011
Hov1-10	6035	Sweden	Northern Europe	14442.429	14442.429	6.454	12.285	13.675	12.222	16.586	10.056
Hov3-2	6036	Sweden	Northern Europe	14442.429	14442.429	6.454	12.285	13.675	12.222	16.586	10.056
Hov3-5	6038	Sweden	Northern Europe	14442.429	14442.429	6.454	12.285	13.675	12.222	16.586	10.056
Hov4-1	8306	Sweden	Northern Europe	14442.429	14442.429	6.454	12.285	13.675	12.222	16.586	10.056
Hovdala-2	6039	Sweden	Northern Europe	14442.429	14442.429	6.454	12.285	13.675	12.222	16.586	10.056
Hovdala-6	8307	Sweden	Northern Europe	14442.429	14442.429	6.454	12.285	13.675	12.222	16.586	10.056
Kal-1	9408	Sweden	Northern Europe	14489.000	14489.000	3.280	13.314	-0.763	14.391	-56.341	-10.893
Kävlinge-1	8237	Sweden	Northern Europe	14564.714	NA	NA	NA	NA	NA	NA	NA
Kia-1	9409	Sweden	Northern Europe	14589.143	14589.143	-6.502	15.564	3.757	13.329	-221.010	-43.854
Kni-1	6040	Sweden	Northern Europe	14510.000	14510.000	2.979	13.640	-3.226	14.147	-67.932	-15.305
Kulturen-1	8240	Sweden	Northern Europe	14552.571	NA	NA	NA	NA	NA	NA	NA
Lan-1	9421	Sweden	Northern Europe	14725.000	14725.000	-10.185	16.549	-1.095	13.460	-273.059	-46.463
Liarum	8241	Sweden	Northern Europe	14466.143	14466.143	8.039	12.285	10.996	13.343	38.834	14.532
Lillö-1	8242	Sweden	Northern Europe	15021.857	15021.857	-13.036	14.484	4.180	12.990	-244.382	-18.206
Lis-1	8326	Sweden	Northern Europe	14867.143	14867.143	-7.794	14.990	-24.173	15.635	-210.963	-30.408
Lis-2	8222	Sweden	Northern Europe	14867.143	14867.143	-7.794	14.990	-24.173	15.635	-210.963	-30.408
Lis-3	6041	Sweden	Northern Europe	14867.143	14867.143	-7.794	14.990	-24.173	15.635	-210.963	-30.408
Lund	8335	Sweden	Northern Europe	14535.857	14535.857	-1.059	15.437	12.910	14.287	-128.279	-19.845
Ömö1-7	6073	Sweden	Northern Europe	15046.714	15046.714	-12.713	14.799	-2.127	13.432	-240.861	-18.046
Puk-1	9436	Sweden	Northern Europe	14671.571	14671.571	-4.771	12.758	7.881	14.067	-164.461	-29.786
Puk-2	9437	Sweden	Northern Europe	14671.571	14671.571	-4.771	12.758	7.881	14.067	-164.461	-29.786
Rev-1	8369	Sweden	Northern Europe	14528.714	14528.714	1.000	13.537	-0.239	13.436	-97.032	-19.708
Rev-2	6076	Sweden	Northern Europe	14528.714	14528.714	1.000	13.537	-0.239	13.436	-97.032	-19.708
Sparta-1	6085	Sweden	Northern Europe	14516.000	14516.000	0.519	14.771	6.502	14.351	-98.200	-13.878
Ste-2	9453	Sweden	Northern Europe	15713.000	15713.000	-10.948	9.601	15.545	11.780	-209.368	-27.484
Ste-3	9454	Sweden	Northern Europe	15713.000	15713.000	-10.948	9.601	15.545	11.780	-209.368	-27.484
T1040	6094	Sweden	Northern Europe	14567.429	14567.429	-4.751	15.746	19.375	13.765	-186.574	-29.398
T460	6106	Sweden	Northern Europe	14564.714	14564.714	-0.951	14.738	4.530	14.158	-131.623	-25.900
T510	6109	Sweden	Northern Europe	14564.714	14564.714	-0.951	14.738	4.530	14.158	-131.623	-25.900
T540	6112	Sweden	Northern Europe	14564.714	14564.714	-0.951	14.738	4.530	14.158	-131.623	-25.900
T570	6114	Sweden	Northern Europe	14564.714	14564.714	-0.951	14.738	4.530	14.158	-131.623	-25.900
T900	6142	Sweden	Northern Europe	14445.714	14445.714	7.281	12.017	3.262	12.081	25.200	9.299
TDr-1	6188	Sweden	Northern Europe	14627.429	14627.429	0.294	13.807	-10.961	14.204	-90.880	-9.064
TDr-16	6201	Sweden	Northern Europe	14627.429	14627.429	0.294	13.807	-10.961	14.204	-90.880	-9.064
TDr-2	6189	Sweden	Northern Europe	14627.429	14627.429	0.294	13.807	-10.961	14.204	-90.880	-9.064
TDr-4	6191	Sweden	Northern Europe	14627.429	14627.429	0.294	13.807	-10.961	14.204	-90.880	-9.064
Ting-1	7354	Sweden	Northern Europe	14627.000	14627.000	2.821	5.326	30.471	15.354	-76.559	-30.508
Tomegap-2	6242	Sweden	Northern Europe	14552.571	14552.571	-3.289	15.474	16.971	13.934	-164.977	-25.882
Tur-4	9470	Sweden	Northern Europe	14471.167	14471.167	5.830	4.331	46.449	18.256	-63.964	-37.198
TV-10	6258	Sweden	Northern Europe	14786.714	14786.714	-5.730	15.516	-18.156	14.578	-174.366	-17.043
TV-38	6284	Sweden	Northern Europe	14786.714	14786.714	-5.730	15.516	-18.156	14.578	-174.366	-17.043

Ull1-1	8426	Sweden	Northern Europe	14517.857	14517.857	1.796	12.318	1.922	13.876	-78.860	-17.450
Ull2-5	6974	Sweden	Northern Europe	14517.857	14517.857	1.796	12.318	1.922	13.876	-78.860	-17.450
Ull3-4	6413	Sweden	Northern Europe	14517.857	14517.857	1.796	12.318	1.922	13.876	-78.860	-17.450
Vimmerby	8249	Sweden	Northern Europe	14631.000	14631.000	0.631	3.626	74.766	14.875	-146.572	-75.623
Vinslöv	9057	Sweden	Northern Europe	14452.571	14452.571	1.553	12.757	12.947	13.672	-81.623	-17.329
Yst-1	9481	Sweden	Northern Europe	14744.714	14744.714	-3.200	14.185	1.584	14.252	-133.541	-14.443

Table 25: Loadings of the climate PCAs for climatic variables.

The input variables for the respective PCA are in the column Climatic_variable and the loading for PC1 and PC2 are in the following columns. The PCAs were performed with data within the projected growing season (PCA_growing_season, 185 unique locations), for bioclimatic variables related to temperature (PCA_temperature, 180 unique locations) and bioclimatic variables related to precipitation (PCA_precipitation, 180 unique locations).

PCA	Climatic_variable	Loading_PC1	Loading_PC2
PCA_growing_season	Nr_Growing months	0.01600499	-0.049452905
PCA_growing_season	T_GS	0.02623586	-0.02651129
PCA_growing_season	SWC_GS	0.464594418	0.883839925
PCA_growing_season	Water vapor_GS	0.004470745	0.002279636
PCA_growing_season	Wind_GS	-0.001360704	0.044602003
PCA_growing_season	Rain_GS	0.884977801	-0.462259682
PCA_temperature	Bioclim1_T_Annual	0.0167630604	-0.24782427
PCA_temperature	Bioclim2_Diurnal_Range	0.0017027645	-0.143442019
PCA_temperature	Bioclim3_Isothermality	-0.0296229006	-0.360223399
PCA_temperature	Bioclim4_T_Seasonality	0.9968579789	0.002052454
PCA_temperature	Bioclim5_MaxT_Wrmst_Month	0.0306226315	-0.332748229
PCA_temperature	Bioclim_MinT_Cldst_Month	0.0006124082	-0.185584425
PCA_temperature	Bioclim7_T_Ann_Range	0.0300102233	-0.147163804
PCA_temperature	Bioclim8_T_Wettest_Qtr	0.043713079	-0.083137066
PCA_temperature	Bioclim9_T_Driest_Qtr	-0.0248263603	-0.698202444
PCA_temperature	Bioclim10_T_Wrmst_Qtr	0.0272742483	-0.251687118
PCA_temperature	Bioclim11_T_Cldst_Qtr	0.0017186824	-0.252343876
PCA_precipitation	Bioclim12_Ann_Precip	0.86052732	0.13508777
PCA_precipitation	Bioclim13_P_Wettest_Month	0.14165015	-0.08258757
PCA_precipitation	Bioclim14_P_Driest_Month	0.02023758	0.02227374
PCA_precipitation	Bioclim15_P_Seasonality	0.01438276	-0.03826312
PCA_precipitation	Bioclim16_P_Wettest_Qtr	0.37470765	-0.14494559
PCA_precipitation	Bioclim17_P_Driest_Qtr	0.07450232	0.08643361
PCA_precipitation	Bioclim18_P_Wrmst_Qtr	0.2538205	-0.68250367
PCA_precipitation	Bioclim19_P_Cldst_Qtr	0.16861279	0.69186643

Table 26: Sample information on the sequenced individuals for *cis*-regulatory divergence.

Sequence_CCG is the sequence number assigned by the CCG, Cross_ID is the numeric code for each individual plant, Cross_nr the number for the individual Cross, consisting of Parents 1 and 2. Direction is 1 if Parent1 was the maternal plant and 2 if Parent2 was the maternal plant. Replicate is the replicate number of the individual cross. Hybrid is 1 if the plant was a hybrid and 0 if the plant was a parent. Experiment shows whether the plant was grown in the 1st or 2nd run of the experiment.

Sequence_CCG	Cross_ID	Cross_nr	Cross	Parent1	Parent2	Direction	Replicate	Hybrid	Experiment
112934	30101	1	C1xM1	M1	C1	2	3	1	1
112936	30202	2	M1xC2	M1	C2	1	3	1	1
112938	30404	4	M1xS2	M1	S2	1	3	1	1
112940	30505	5	M1xE1	M1	E1	1	3	1	1
112942	30606	6	M1xE2	M1	E2	1	3	1	1
112944	30909	9	C1xE1	C1	E1	1	3	1	1
112946	31212	12	C3xM2	M2	C3	2	3	1	1
112948	31414	14	M2xS3	M2	S3	1	3	1	1
112950	31515	15	M2xE2	M2	E2	1	3	1	1
112952	31717	17	C2xS2	C2	S2	1	3	1	1
112954	32020	20	C2xE3	C2	E3	1	3	1	1
112956	32526	26	M3xE4	M3	E4	1	3	1	1
112958	32728	28	C3xS4	C3	S4	1	3	1	1
112960	32829	29	C3xE3	C3	E3	1	3	1	1
112962	32930	30	C3xE4	C3	E4	1	3	1	1
112964	33132	32	M4xC5	M4	C5	1	3	1	1
112966	33233	33	M4xS4	M4	S4	1	3	1	1
112968	33435	35	M4xE4	M4	E4	1	3	1	1
112970	33536	36	M4xE5	M4	E5	1	3	1	1
112972	33738	38	C4xS5	C4	S5	1	3	1	1
112974	33839	39	C4xE4	C4	E4	1	3	1	1
112976	33940	40	C4xE5	C4	E5	1	3	1	1
112978	34041	41	M5xC5	M5	C5	1	3	1	1
112980	34142	42	M5xC6	M5	C6	1	3	1	1
112982	34243	43	M5xS5	M5	S5	1	3	1	1
112984	34344	44	M5xS6	M5	S6	1	3	1	1
112986	34445	45	M5xE5	M5	E5	1	3	1	1
115199	10202	2	M1xC2	M1	C2	1	1	1	1
115201	10505	5	M1xE1	M1	E1	1	1	1	1
115203	11616	16	M2xE3	M2	E3	1	1	1	1
115205	11818	18	C2xS3	C2	S3	1	1	1	1
115207	12324	24	M3xS4	M3	S4	1	1	1	1

115209	12526	26	M3xE4	M3	E4	1	1	1	1
115211	12627	27	C3xS3	C3	S3	1	1	1	1
115213	12728	28	C3xS4	C3	S4	1	1	1	1
115215	13031	31	M4xC4	M4	C4	1	1	1	1
115217	13435	35	M4xE4	M4	E4	1	1	1	1
115219	13637	37	S4xC4	C4	S4	2	1	1	1
115221	13738	38	C4xS5	C4	S5	1	1	1	1
115223	14142	42	M5xC6	M5	C6	1	1	1	1
115225	14243	43	M5xS5	M5	S5	1	1	1	1
115227	14344	44	M5xS6	M5	S6	1	1	1	1
115229	14445	45	M5xE5	M5	E5	1	1	1	1
115231	14546	46	M5xE6	M5	E6	1	1	1	1
115233	14647	47	C5xS5	C5	S5	1	1	1	1
115235	15758	58	C6xS1	C6	S1	1	1	1	1
115237	16671	71	E5xE2	E5	E2	1	1	1	1
115239	17382	82	S6xE1	S6	E1	1	1	1	1
115241	17602	2	M2	M2	NA	NA	1	0	1
115243	18006	6	M6	M6	NA	NA	1	0	1
115245	18107	7	C1	C1	NA	NA	1	0	1
115247	18309	9	C3	C3	NA	NA	1	0	1
115249	18410	10	C4	C4	NA	NA	1	0	1
115251	18511	11	C5	C5	NA	NA	1	0	1
115253	19117	17	S5	S5	NA	NA	1	0	1
115255	19218	18	S6	S6	NA	NA	1	0	1
115257	19622	22	E4	E4	NA	NA	1	0	1
115259	19723	23	E5	E5	NA	NA	1	0	1
115261	19824	24	E6	E6	NA	NA	1	0	1
115263	23233	33	M4xS4	M4	S4	1	2	1	1
115265	24647	47	C5xS5	C5	S5	1	2	1	1
115267	26773	73	E4xE5	E4	E5	1	2	1	1
115269	29622	22	E4	E4	NA	NA	2	0	1
115271	34849	49	C5xE5	C5	E5	1	3	1	1
115273	35253	53	M6xS6	M6	S6	1	3	1	1
115275	35556	56	M6xE1	M6	E1	1	3	1	1
115277	35859	59	C6xE6	C6	E6	1	3	1	1
115279	35960	60	C6xE1	C6	E1	1	3	1	1
115281	36061	61	S1xS4	S1	S4	1	3	1	1
115283	36671	71	E5xE2	E5	E2	1	3	1	1
115285	36773	73	E4xE5	E4	E5	1	3	1	1
115287	36877	77	S5xS4	S4	S5	2	3	1	1
115289	37180	80	S4xE3	S4	E3	1	3	1	1
115291	37382	82	S6xE1	S6	E1	1	3	1	1
115293	37501	1	M1	M1	NA	NA	3	0	1
116054	37703	3	M3	M3	NA	NA	3	0	1

116056	37804	4	M4	M4	NA	NA	3	0	1
116058	37905	5	M5	M5	NA	NA	3	0	1
116060	38006	6	M6	M6	NA	NA	3	0	1
116062	38107	7	C1	C1	NA	NA	3	0	1
116064	38208	8	C2	C2	NA	NA	3	0	1
116066	38309	9	C3	C3	NA	NA	3	0	1
116068	38410	10	C4	C4	NA	NA	3	0	1
116070	38511	11	C5	C5	NA	NA	3	0	1
116072	38713	13	S1	S1	NA	NA	3	0	1
116074	38915	15	S3	S3	NA	NA	3	0	1
116076	39016	16	S4	S4	NA	NA	3	0	1
116078	39117	17	S5	S5	NA	NA	3	0	1
116080	39218	18	S6	S6	NA	NA	3	0	1
116082	39319	19	E1	E1	NA	NA	3	0	1
116084	39420	20	E2	E2	NA	NA	3	0	1
116086	39521	21	E3	E3	NA	NA	3	0	1
116088	39622	22	E4	E4	NA	NA	3	0	1
116090	39723	23	E5	E5	NA	NA	3	0	1
116092	39824	24	E6	E6	NA	NA	3	0	1
116094	50101	1	C1xM1	M1	C1	2	5	1	1
116096	50909	9	C1xE1	C1	E1	1	5	1	1
116098	51111	11	C2xM2	M2	C2	2	5	1	1
116100	53132	32	C5xM4	M4	C5	2	5	1	1
116102	53940	40	C4xE5	C4	E5	1	5	1	1
116104	57501	1	M1	M1	NA	NA	5	0	1
116106	57804	4	M4	M4	NA	NA	5	0	1
116108	57905	5	M5	M5	NA	NA	5	0	1
116110	58107	7	C1	C1	NA	NA	5	0	1
116112	58208	8	C2	C2	NA	NA	5	0	1
116114	58511	11	C5	C5	NA	NA	5	0	1
116116	58713	13	S1	S1	NA	NA	5	0	1
116118	59622	22	E4	E4	NA	NA	5	0	1
120505	60306	3	M1xC2	M1	C2	2	6	1	2
120511	60411	4	S1xM1	M1	S1	1	6	1	2
120477	61043	10	M1xS2	M1	S2	1	6	1	2
120509	61875	18	M1xE1	M1	E1	1	6	1	2
120489	61980	19	M1xE1	M1	E1	2	6	1	2
120515	602379	2	C2xS3	C2	S3	2	6	1	2
120507	604388	4	C2xE2	C2	E2	1	6	1	2
120513	608405	8	M3xC3	M3	C3	1	6	1	2
120521	611416	11	M3xC4	M3	C4	2	6	1	2
120479	612419	12	M3xC4	M3	C4	2	6	1	2
120481	613424	13	M3xC4	M3	C4	2	6	1	2
120483	615434	15	M3xS3	M3	S3	2	6	1	2

120485	618447	18	M3xE3	M3	E3	1	6	1	2
120487	619451	19	M3xE4	M3	E4	2	6	1	2
120519	622464	22	C3xE3	C3	E3	1	6	1	2
120491	624471	24	C3xE4	C3	E4	1	6	1	2
120501	630131	30	M4xC4	M4	C4	1	6	1	2
120493	637165	37	M4xC5	M4	C5	1	6	1	2
120503	640178	40	M4xS4	M4	S4	1	6	1	2
120495	642187	42	M4xS5	M4	S5	1	6	1	2
120497	645199	45	M4xS5	M4	S5	1	6	1	2
120499	653243	53	M4xE5	M4	E5	2	6	1	2
120523	658274	58	S4xC4	C4	S4	2	6	1	2
120517	660285	60	C4xS5	C4	S5	1	6	1	2
120565	60202	2	M1xC2	M1	C2	1	6	1	2
120525	60725	7	M1xS2	M1	S2	1	6	1	2
120535	61151	11	M1xS2	M1	S2	2	6	1	2
120533	62088	20	C1xS1	C1	S1	1	6	1	2
120571	62293	22	C1xS1	C1	S1	2	6	1	2
120541	603384	3	C2xE2	C2	E2	1	6	1	2
120549	605392	5	C2xE2	C2	E2	2	6	1	2
120553	606397	6	C2xE3	C2	E3	1	6	1	2
120555	607401	7	C2xE3	C2	E3	1	6	1	2
120543	610413	10	M3xC3	M3	C3	1	6	1	2
120527	614429	14	M3xC4	M3	C4	2	6	1	2
120561	616439	16	M3xS3	M3	S3	2	6	1	2
120531	617443	17	M3xS3	M3	S3	2	6	1	2
120529	633145	33	M4xC4	M4	C4	1	6	1	2
120539	635156	35	M4xC4	M4	C4	2	6	1	2
120551	638172	38	M4xC5	M4	C5	2	6	1	2
120537	639176	39	M4xC5	M4	C5	2	6	1	2
120569	641182	41	M4xS4	M4	S4	1	6	1	2
120557	643191	43	M4xS5	M4	S5	1	6	1	2
120567	648214	48	M4xE4	M4	E4	1	6	1	2
120563	650227	50	M4xE4	M4	E4	2	6	1	2
120559	657268	57	S4xC4	C4	S4	2	6	1	2
120545	671328	71	C4xS5	C4	S5	1	6	1	2
120547	681354	81	C4xE4	C4	E4	1	6	1	2
122347	60516	5	S1xM1	M1	S1	1	6	1	2
122349	61456	14	M1xS2	M1	S2	2	6	1	2
122320	61770	17	M1xE1	M1	E1	1	6	1	2
122334	90414	4	M2xS3	M2	S3	2	9	1	2
122391	90835	8	M2xE2	M2	E2	2	9	1	2
122383	91878	18	C2xS3	C2	S3	1	9	1	2
122387	92296	22	C2xS3	C2	S3	2	9	1	2
122310	620455	20	C3xS4	C3	S4	2	6	1	2

122345	621459	21	C3xS4	C3	S4	2	6	1	2
122318	623467	23	C3xE3	C3	E3	1	6	1	2
122308	629126	29	C3xE4	C3	E4	2	6	1	2
122314	646203	46	M4xS5	M4	S5	1	6	1	2
122316	647209	47	M4xE4	M4	E4	1	6	1	2
122312	680349	80	C4xS5	C4	S5	2	6	1	2
122389	913427	13	S3xS5	S3	S5	2	9	1	2
122340	928125	28	M3	M3	NA	NA	9	0	2
122338	932144	32	M4	M4	NA	NA	9	0	2
122385	938175	38	M5	M5	NA	NA	9	0	2
122336	941185	41	M5	M5	NA	NA	9	0	2
122381	947212	47	M6	M6	NA	NA	9	0	2
122342	950230	50	C2	C2	NA	NA	9	0	2
122328	110730	7	C6	C6	NA	NA	11	0	2
122326	111048	10	S1	S1	NA	NA	11	0	2
122355	112298	22	S1	S1	NA	NA	11	0	2
122371	120838	8	S1	S1	NA	NA	12	0	2
122379	1049223	49	S5	S5	NA	NA	10	0	2
122324	1123106	23	E1	E1	NA	NA	11	0	2
122332	1134154	34	E1	E1	NA	NA	11	0	2
122365	1137170	37	E2	E2	NA	NA	11	0	2
122373	1149224	49	E2	E2	NA	NA	11	0	2
122322	1150232	50	E2	E2	NA	NA	11	0	2
122357	1155260	55	E3	E3	NA	NA	11	0	2
122330	1157273	57	E3	E3	NA	NA	11	0	2
122377	1159284	59	E4	E4	NA	NA	11	0	2
122375	1161294	61	E4	E4	NA	NA	11	0	2
122361	1223107	23	E5	E5	NA	NA	12	0	2
122369	1234155	34	E5	E5	NA	NA	12	0	2
122351	1255261	55	E5	E5	NA	NA	12	0	2
122359	1281360	81	E5	E5	NA	NA	12	0	2
122367	1363303	63	E6	E6	NA	NA	13	0	2
122353	1365311	65	E6	E6	NA	NA	13	0	2
122363	1381361	81	E6	E6	NA	NA	13	0	2
123648	71152	11	C1xS2	C1	S2	2	7	1	2
123634	71666	16	C1xE2	C1	E2	2	7	1	2
123608	71771	17	C1xE2	C1	E2	2	7	1	2
123638	71876	18	M2xC2	M2	C2	1	7	1	2
123576	90205	2	M2xS3	M2	S3	2	9	1	2
123093	90519	5	M2xS3	M2	S3	2	9	1	2
123111	90942	9	M2xE3	M2	E3	1	9	1	2
123662	91459	14	C2xS2	C2	S2	1	9	1	2
123115	91668	16	C2xS2	C2	S2	1	9	1	2
123580	92191	20	C2xS3	C2	S3	1	9	1	2

123654	702380	2	C4xE4	C4	E4	1	7	1	2
123650	707402	7	M5xC5	M5	C5	1	7	1	2
123612	708406	8	M5xC5	M5	C5	1	7	1	2
123628	709410	9	M5xC5	M5	C5	2	7	1	2
123610	710414	10	M5xC5	M5	C5	2	7	1	2
123644	712420	12	M5xC6	M5	C6	1	7	1	2
123614	716440	16	M5xS5	M5	S5	1	7	1	2
123642	719452	19	M5xE5	M5	E5	1	7	1	2
123624	723468	23	C5xS5	C5	S5	1	7	1	2
123632	729127	29	C5xS6	C5	S6	1	7	1	2
123636	731137	31	C5xS6	C5	S6	1	7	1	2
123640	732142	32	C5xS6	C5	S6	1	7	1	2
123652	735157	35	C5xE5	C5	E5	1	7	1	2
123618	738173	38	C5xE5	C5	E5	2	7	1	2
123616	741183	41	C5xE6	C5	E6	1	7	1	2
123620	742188	42	C5xE6	C5	E6	1	7	1	2
123630	743192	43	M6xS6	M6	S6	1	7	1	2
123626	745200	45	M6xS6	M6	S6	1	7	1	2
123646	747210	47	M6xS6	M6	S6	2	7	1	2
123622	781355	81	C6xS1	C6	S1	1	7	1	2
123107	904391	4	S5xS2	S5	S2	2	9	1	2
123079	905395	5	S4xS3	S4	S3	1	9	1	2
123113	906400	6	E5xE2	E5	E2	1	9	1	2
123091	908408	8	E5xE2	E5	E2	1	9	1	2
123101	912422	12	S4xE3	S4	E3	1	9	1	2
123089	915437	15	S3xS5	S3	S5	2	9	1	2
123109	917446	17	S3xS5	S3	S5	2	9	1	2
123103	920458	20	M2	M2	NA	NA	9	0	2
123105	921462	21	M2	M2	NA	NA	9	0	2
123660	923470	23	M2	M2	NA	NA	9	0	2
123083	924474	24	M2	M2	NA	NA	9	0	2
123658	930134	30	M3	M3	NA	NA	9	0	2
123081	931139	31	M4	M4	NA	NA	9	0	2
123097	935159	35	M5	M5	NA	NA	9	0	2
123099	942190	42	M6	M6	NA	NA	9	0	2
123656	943194	43	M6	M6	NA	NA	9	0	2
123095	948217	48	C1	C1	NA	NA	9	0	2
123087	949222	49	C1	C1	NA	NA	9	0	2
123085	953246	53	C2	C2	NA	NA	9	0	2
123578	957271	57	C2	C2	NA	NA	9	0	2
123582	100415	4	C3	C3	NA	NA	10	0	2
123600	101047	10	C4	C4	NA	NA	10	0	2
123598	101155	11	C5	C5	NA	NA	10	0	2
123594	101460	14	C5	C5	NA	NA	10	0	2

123590	101984	19	C6	C6	NA	NA	10	0	2
123584	1005396	5	S2	S2	NA	NA	10	0	2
123588	1015438	15	S3	S3	NA	NA	10	0	2
123596	1023105	23	S3	S3	NA	NA	10	0	2
123592	1031140	31	S3	S3	NA	NA	10	0	2
123602	1036164	36	S4	S4	NA	NA	10	0	2
123606	1041186	41	S4	S4	NA	NA	10	0	2
123117	1047213	47	S5	S5	NA	NA	10	0	2
123586	1057272	57	S6	S6	NA	NA	10	0	2
123604	1081358	81	E1	E1	NA	NA	10	0	2
123145	91154	11	M2xE3	M2	E3	1	9	1	2
123141	918450	18	S3xS5	S3	S5	2	9	1	2
123143	919454	19	S3xS5	S3	S5	2	9	1	2
123149	934152	34	M4	M4	NA	NA	9	0	2
123147	940181	40	M5	M5	NA	NA	9	0	2
123139	958277	58	C2	C2	NA	NA	9	0	2
123121	100729	7	C4	C4	NA	NA	10	0	2
123137	101879	18	C6	C6	NA	NA	10	0	2
123135	102192	20	C6	C6	NA	NA	10	0	2
123123	1002383	2	S1	S1	NA	NA	10	0	2
123125	1012423	12	S2	S2	NA	NA	10	0	2
123119	1013428	13	S3	S3	NA	NA	10	0	2
123127	1048218	48	S5	S5	NA	NA	10	0	2
123131	1055259	55	S6	S6	NA	NA	10	0	2
123133	1056267	56	S6	S6	NA	NA	10	0	2
123129	1058278	58	S6	S6	NA	NA	10	0	2
125306	70307	3	C1xS1	C1	S1	2	7	1	2
125346	70517	5	C1xS2	C1	S2	1	7	1	2
125362	70833	8	C1xS2	C1	S2	2	7	1	2
125370	71457	14	C1xE1	C1	E1	1	7	1	2
125310	71562	15	C1xE2	C1	E2	1	7	1	2
125336	71981	19	M2xC2	M2	C2	1	7	1	2
125322	72294	22	M2xC2	M2	C2	2	7	1	2
125388	80413	4	M2xC2	M2	C2	2	8	1	2
125396	82090	20	M2xS3	M2	S3	2	8	1	2
125352	704389	4	C4xE5	C4	E5	1	7	1	2
125342	705393	5	C4xE5	C4	E5	1	7	1	2
125358	706398	6	C4xE5	C4	E5	2	7	1	2
125326	711417	11	M5xC6	M5	C6	1	7	1	2
125348	713425	13	M5xC6	M5	C6	2	7	1	2
125314	714430	14	M5xC6	M5	C6	2	7	1	2
125308	715435	15	M5xS5	M5	S5	1	7	1	2
125366	717444	17	M5xS5	M5	S5	2	7	1	2
125320	718448	18	M5xS6	M5	S6	2	7	1	2

125324	720456	20	M5xE5	M5	E5	1	7	1	2
125356	722465	22	M5xE6	M5	E6	1	7	1	2
125350	724472	24	C5xS5	C5	S5	1	7	1	2
125360	725110	25	C5xS5	C5	S5	2	7	1	2
125312	728123	28	C5xS5	C5	S5	2	7	1	2
125330	733146	33	C5xE5	C5	E5	1	7	1	2
125340	734150	34	C5xE5	C5	E5	1	7	1	2
125332	739177	39	C5xE6	C5	E6	1	7	1	2
125318	740179	40	C5xE6	C5	E6	1	7	1	2
125354	749220	49	M6xE6	M6	E6	2	7	1	2
125328	750228	50	M6xE6	M6	E6	2	7	1	2
125304	753244	53	M6xE6	M6	E6	2	7	1	2
125344	756264	56	M6xE1	M6	E1	1	7	1	2
125368	757269	57	M6xE1	M6	E1	2	7	1	2
125334	758275	58	C6xS6	C6	S6	1	7	1	2
125338	759280	59	C6xS6	C6	S6	1	7	1	2
125316	761290	61	C6xS6	C6	S6	2	7	1	2
125372	766313	66	C6xS6	C6	S6	2	7	1	2
125374	771329	71	C6xS6	C6	S6	2	7	1	2
125380	802381	2	C6xS1	C6	S1	1	8	1	2
125386	803386	3	C6xS1	C6	S1	2	8	1	2
125378	808407	8	C6xS1	C6	S1	2	8	1	2
125376	818449	18	C6xE6	C6	E6	1	8	1	2
125394	823469	23	C6xE6	C6	E6	2	8	1	2
125364	826119	26	C6xE1	C6	E1	1	8	1	2
125382	832143	32	C6xE1	C6	E1	1	8	1	2
125398	842189	42	S1xS4	S1	S4	1	8	1	2
125390	844197	44	S1xS4	S1	S4	2	8	1	2
125384	860287	60	S1xS4	S1	S4	2	8	1	2
125392	861291	61	S3xS6	S3	S6	2	8	1	2
122377	1159284	59	E4	E4	NA	NA	11	0	2
126615	838174	38	C4xS5	C4	S5	2	8	1	2
126617	815436	15	S3	S3	NA	NA	8	0	2
126619	831138	31	M4xC4	M4	C4	1	8	1	2
126621	881356	81	S3xS5	S3	S5	2	8	1	2
126623	80834	8	C1xS2	C1	S2	1	8	1	2
126625	811418	11	C5	C5	NA	NA	8	0	2
126627	841184	41	M5xC5	M5	C5	1	8	1	2
126629	813426	13	S1	S1	NA	NA	8	0	2
126631	822466	22	E4	E4	NA	NA	8	0	2
126633	81667	16	M2xE3	M2	E3	1	8	1	2
126635	81045	10	C1xE2	C1	E2	2	8	1	2
126637	828124	28	C3xS4	C3	S4	2	8	1	2
126639	809411	9	C3	C3	NA	NA	8	0	2

126641	804390	4	M4	M4	NA	NA	8	0	2
126643	814431	14	S2	S2	NA	NA	8	0	2
126645	80518	5	M1xE1	M1	E1	2	8	1	2
126647	830133	30	C3xE4	C3	E4	1	8	1	2
126649	863298	63	S3xS6	S3	S6	1	8	1	2
126651	850229	50	C5xE6	C5	E6	1	8	1	2
126653	858276	58	C6xS1	C6	S1	2	8	1	2
126655	819453	19	E1	E1	NA	NA	8	0	2
126657	835158	35	M4xE4	M4	E4	2	8	1	2
126659	859281	59	C6xE6	C6	E6	1	8	1	2
126567	81772	17	C2xS2	C2	S2	1	8	1	2
126569	810415	10	C4	C4	NA	NA	8	0	2
126571	837167	37	S4xC4	C4	S4	2	8	1	2
126573	81153	11	M2xC2	M2	C2	1	8	1	2
126575	812421	12	C6	C6	NA	NA	8	0	2
126577	807403	7	C1	C1	NA	NA	8	0	2
126579	856265	56	M6xE1	M6	E1	1	8	1	2
126581	846205	46	M5xE6	M5	E6	1	8	1	2
126583	836162	36	M4xE5	M4	E5	1	8	1	2
126585	857270	57	C6xS6	C6	S6	1	8	1	2
126587	816441	16	S4	S4	NA	NA	8	0	2
126589	81458	14	M2xS3	M2	S3	2	8	1	2
126591	849221	49	C5xE5	C5	E5	1	8	1	2
126593	824473	24	E6	E6	NA	NA	8	0	2
126595	817445	17	S5	S5	NA	NA	8	0	2
126597	834151	34	M4xS5	M4	S5	1	8	1	2
126599	81982	19	C2xE2	C2	E2	1	8	1	2
126601	847211	47	C5xS5	C5	S5	1	8	1	2
126603	821461	21	E3	E3	NA	NA	8	0	2
126605	81877	18	C2xS3	C2	S3	2	8	1	2
126607	82295	22	M3xC4	M3	C4	2	8	1	2
126609	805394	5	M5	M5	NA	NA	8	0	2
126611	806399	6	M6	M6	NA	NA	8	0	2
126613	820457	20	E2	E2	NA	NA	8	0	2

Table 27: Genotypic mean of each genotype in controlled conditions.

Each row shows the genotypic mean of each accession. The phenotypes are FS (Final size), t50, SL (Slope), FT (Flowering time) in HL and LL conditions and the GXE. BM (Biomass) and BC (Bolting in controlled conditions) in HD and LD, and the GxE.

Genotype	ID	Country	FS HL	FS LL	GXE FS	T50 HL	T50 LL	GXE T50	SL HL	GXE SL	FT HL	FT LL	BM HD	BM LD	GXE BM	BC HD	BC LD	GXE BC
LDV-46	139	FRA	NA	NA	NA	NA	NA	NA	NA	NA	NA	NA	0.07	0.29	NA	NA	NA	NA

Doubravnik7	410	CZE	NA	NA	NA	NA	NA	NA	NA	NA	NA	NA	0.07	0.39	0.33	NA	NA	NA
Gr-1	430	AUT	NA	NA	NA	NA	NA	NA	NA	NA	NA	NA	0.04	0.17	0.06	NA	NA	NA
Ale-Stenar-41-1	991	SWE	8.67	14.54	-0.74	10.53	34.52	0.47	5.72	-1.64	NA	NA	NA	NA	NA	NA	NA	NA
Ale-Stenar-44-4	992	SWE	7.20	13.75	-0.05	11.84	33.55	-1.80	4.85	-0.37	NA	NA	NA	NA	NA	NA	NA	NA
Ale-Stenar-56-14	997	SWE	6.64	15.28	2.04	15.57	32.43	-6.66	4.06	0.46	NA	81.00	0.05	0.41	0.83	6.00	21.00	NA
Ale-Stenar-64-24	1002	SWE	7.66	14.27	-1.16	13.78	37.29	-0.57	3.76	0.90	NA	NA	0.07	0.42	0.48	NA	27.00	NA
Brösarp-11-135	1061	SWE	7.13	11.42	-2.31	15.56	35.42	-3.65	4.91	-0.25	NA	NA	0.04	0.19	0.12	16.00	9.00	-1.83
Brösarp-15-138	1062	SWE	5.87	11.03	-1.44	16.50	31.69	-8.32	3.75	0.77	NA	88.50	0.06	0.24	0.12	19.00	NA	NA
Brösarp-21-140	1063	SWE	7.25	13.16	-0.69	14.00	30.46	-7.04	6.97	-2.56	52.50	80.33	0.05	0.68	1.18	13.00	NA	NA
Brösarp-34-145	1066	SWE	7.94	14.84	0.30	11.10	34.72	0.11	4.86	-1.05	NA	NA	0.10	0.42	0.09	NA	23.00	NA
Tos-82-387	1254	SWE	NA	NA	NA	NA	NA	NA	NA	NA	NA	NA	0.06	0.24	0.00	12.00	15.00	-1.03
App1-12	5830	SWE	6.01	13.04	0.43	12.80	33.76	-2.56	4.01	0.15	NA	90.00	0.07	0.41	0.41	NA	5.00	NA
App1-14	5831	SWE	7.12	14.25	0.53	11.15	32.06	-2.60	4.09	-0.20	NA	NA	0.04	0.33	0.83	NA	NA	NA
App1-16	5832	SWE	6.67	13.91	0.64	18.12	31.45	-10.18	4.69	-0.22	49.00	NA	0.06	0.14	-0.39	12.00	6.00	-1.95
Dra1-4	5865	SWE	NA	NA	NA	NA	NA	NA	NA	NA	NA	NA	0.07	0.22	-0.11	9.00	14.00	-0.81
Dra2-1	5867	SWE	NA	NA	NA	NA	NA	NA	NA	NA	NA	NA	0.07	NA	NA	NA	21.00	NA
DraIV 2-9	5907	CZE	NA	NA	NA	NA	NA	NA	NA	NA	NA	NA	0.03	0.26	0.95	NA	NA	NA
Eden-1	6009	SWE	NA	NA	NA	NA	NA	NA	NA	NA	NA	NA	0.05	0.26	0.37	15.00	12.00	-1.48
Eden-6	6011	SWE	NA	NA	NA	NA	NA	NA	NA	NA	NA	NA	0.04	0.09	-0.37	NA	20.00	NA
Eden-7	6012	SWE	NA	NA	NA	NA	NA	NA	NA	NA	NA	NA	0.04	0.28	0.65	NA	15.00	NA
Eds-1	6016	SWE	NA	NA	NA	NA	NA	NA	NA	NA	NA	NA	0.04	0.24	0.37	NA	16.00	NA
Fjä1-2	6019	SWE	6.99	13.07	-0.52	12.24	39.16	3.40	5.27	-0.44	NA	NA	0.05	0.35	0.59	NA	20.00	NA
Fjä1-5	6020	SWE	6.70	14.74	1.43	12.00	40.60	5.09	3.79	-0.06	NA	NA	0.05	0.33	0.64	NA	15.00	NA
Fjä2-4	6021	SWE	8.25	14.00	-0.86	13.28	35.54	-1.25	6.91	-2.34	NA	NA	0.06	0.26	0.10	15.00	15.00	-1.25
Fly2-1	6023	SWE	6.30	13.18	0.28	13.46	38.09	1.12	4.78	-0.32	NA	NA	0.07	0.23	-0.17	NA	13.00	NA
Fly2-2	6024	SWE	6.03	10.63	-2.00	14.59	34.11	-3.99	3.89	-0.18	NA	63.00	0.06	0.27	0.13	NA	14.00	NA
Hov1-10	6035	SWE	6.27	12.73	-0.15	17.71	38.00	-3.21	5.85	-2.61	NA	NA	0.03	0.25	0.86	3.00	28.00	0.98
Hov3-2	6036	SWE	7.61	12.64	-1.57	12.20	32.23	-3.49	5.71	-0.73	NA	NA	0.03	0.27	0.81	12.00	8.00	-1.66
Hov3-5	6038	SWE	7.46	13.97	-0.10	13.99	33.54	-3.96	4.77	-0.08	NA	NA	NA	NA	NA	NA	NA	NA
Hovdala-2	6039	SWE	6.39	11.77	-1.22	10.46	30.58	-3.39	3.99	0.36	47.67	77.00	0.03	0.24	0.58	NA	NA	NA
Kni-1	6040	SWE	6.82	11.48	-1.95	12.33	34.16	-1.69	3.90	-0.93	NA	NA	0.05	0.20	-0.03	10.00	12.00	-1.07
Lis-3	6041	SWE	6.67	14.13	0.86	14.52	38.99	0.97	2.51	1.45	48.00	84.00	0.04	0.27	0.48	1.00	NA	NA
Nyl-7	6069	SWE	NA	NA	NA	NA	NA	NA	NA	NA	NA	NA	0.04	0.28	0.67	NA	25.00	NA
Omn-5	6071	SWE	NA	NA	NA	NA	NA	NA	NA	NA	NA	NA	0.03	0.24	0.76	NA	18.00	NA
Ömö1-7	6073	SWE	6.51	13.37	0.26	14.68	29.93	-8.27	5.94	-1.44	NA	NA	0.04	NA	NA	NA	15.00	NA
Rev-2	6076	SWE	7.24	12.88	-0.97	13.03	35.47	-1.07	6.41	-1.86	NA	NA	0.05	0.30	0.52	NA	12.00	NA
Sparta-1	6085	SWE	7.00	12.41	-1.19	12.29	31.73	-4.07	3.94	0.18	NA	NA	0.03	0.27	0.71	NA	26.00	NA
T1000	6090	SWE	NA	NA	NA	NA	NA	NA	NA	NA	NA	NA	0.03	NA	NA	NA	18.00	NA
T1040	6094	SWE	7.47	13.88	-0.19	12.50	33.30	-2.71	7.29	-2.49	NA	NA	0.05	0.28	0.37	NA	27.00	NA
T1070	6097	SWE	NA	NA	NA	NA	NA	NA	NA	NA	NA	NA	0.06	0.24	-0.03	NA	17.00	NA
T1110	6100	SWE	NA	NA	NA	NA	NA	NA	NA	NA	NA	NA	0.05	0.38	0.60	NA	NA	NA
T1160	6104	SWE	NA	NA	NA	NA	NA	NA	NA	NA	NA	NA	0.04	0.18	0.21	NA	11.00	NA
T450	6105	SWE	NA	NA	NA	NA	NA	NA	NA	NA	NA	NA	0.03	0.24	0.78	NA	NA	NA
T460	6106	SWE	8.11	15.13	0.42	12.74	37.92	1.67	3.92	0.06	NA	NA	0.04	0.17	0.20	NA	15.00	NA
T470	6107	SWE	NA	NA	NA	NA	NA	NA	NA	NA	NA	NA	0.04	0.45	1.13	NA	NA	NA
T480	6108	SWE	NA	NA	NA	NA	NA	NA	NA	NA	NA	NA	0.08	0.50	0.47	7.00	8.00	-1.12
T510	6109	SWE	7.67	14.96	0.68	11.67	34.65	-0.53	4.18	-0.30	NA	NA	NA	NA	NA	NA	NA	NA

T530	6111	SWE	NA	NA	NA	NA	NA	NA	NA	NA	NA	NA	0.05	0.30	0.48	NA	NA	NA
T540	6112	SWE	8.20	12.62	-2.19	15.07	32.46	-6.12	5.18	0.50	NA	NA	0.03	0.22	0.63	14.00	NA	NA
T570	6114	SWE	6.93	14.60	1.07	13.18	35.56	-1.13	6.31	-2.19	NA	NA	0.03	0.28	0.91	NA	12.00	NA
T610	6118	SWE	NA	NA	NA	NA	NA	NA	NA	NA	NA	NA	0.03	0.24	0.76	NA	12.00	NA
T670	6122	SWE	NA	NA	NA	NA	NA	NA	NA	NA	NA	NA	0.07	0.33	0.17	NA	14.00	NA
T710	6125	SWE	NA	NA	NA	NA	NA	NA	NA	NA	NA	NA	0.04	0.29	0.60	NA	17.00	NA
T720	6126	SWE	NA	NA	NA	NA	NA	NA	NA	NA	NA	NA	0.03	0.41	1.23	NA	19.00	NA
T740	6128	SWE	NA	NA	NA	NA	NA	NA	NA	NA	NA	NA	0.07	0.35	0.29	NA	31.00	NA
T780	6131	SWE	NA	NA	NA	NA	NA	NA	NA	NA	NA	NA	0.06	0.37	0.45	NA	NA	NA
T790	6132	SWE	NA	NA	NA	NA	NA	NA	NA	NA	NA	NA	0.04	0.29	0.72	11.00	15.00	-0.94
T800	6133	SWE	NA	NA	NA	NA	NA	NA	NA	NA	NA	NA	0.03	0.23	0.64	NA	13.00	NA
T810	6134	SWE	NA	NA	NA	NA	NA	NA	NA	NA	NA	NA	0.04	0.37	0.94	NA	20.00	NA
T840	6136	SWE	NA	NA	NA	NA	NA	NA	NA	NA	NA	NA	0.04	0.35	0.77	12.00	13.00	-1.17
T860	6138	SWE	NA	NA	NA	NA	NA	NA	NA	NA	NA	NA	0.04	0.18	0.24	NA	11.00	NA
T880	6140	SWE	NA	NA	NA	NA	NA	NA	NA	NA	NA	NA	0.04	NA	NA	NA	13.00	NA
T900	6142	SWE	7.18	12.08	-1.71	14.90	35.45	-2.96	3.23	0.29	NA	NA	0.04	0.26	0.51	9.00	15.00	-0.74
T930	6145	SWE	NA	NA	NA	NA	NA	NA	NA	NA	NA	NA	0.03	0.20	0.54	NA	27.00	NA
T960	6148	SWE	NA	NA	NA	NA	NA	NA	NA	NA	NA	NA	0.02	0.23	0.93	NA	14.00	NA
T980	6150	SWE	NA	NA	NA	NA	NA	NA	NA	NA	NA	NA	0.03	0.12	-0.04	NA	13.00	NA
T990	6151	SWE	NA	NA	NA	NA	NA	NA	NA	NA	NA	NA	0.02	0.30	1.35	NA	18.00	NA
TAA 03	6153	SWE	NA	NA	NA	NA	NA	NA	NA	NA	NA	NA	0.04	NA	NA	NA	24.00	NA
TAA 04	6154	SWE	NA	NA	NA	NA	NA	NA	NA	NA	NA	NA	0.04	0.33	0.83	NA	NA	NA
TAA 14	6163	SWE	NA	NA	NA	NA	NA	NA	NA	NA	NA	NA	0.05	0.18	-0.03	NA	29.00	NA
TBÖ 01	6184	SWE	NA	NA	NA	NA	NA	NA	NA	NA	NA	NA	0.05	0.24	0.18	8.00	23.00	-0.20
TDr-1	6188	SWE	7.84	14.63	0.18	14.62	32.19	-5.94	5.51	-0.64	41.33	61.33	0.06	0.43	0.57	NA	NA	NA
TDr-2	6189	SWE	7.06	13.09	-0.58	9.94	30.64	-2.80	4.13	0.75	45.00	73.00	0.05	0.37	0.67	NA	NA	NA
TDr-4	6191	SWE	7.11	11.52	-2.20	14.17	32.74	-4.94	6.98	-0.66	50.00	84.00	0.05	NA	NA	NA	NA	NA
TDr-5	6192	SWE	NA	NA	NA	NA	NA	NA	NA	NA	NA	NA	0.03	0.37	1.10	NA	NA	NA
TDr-7	6193	SWE	NA	NA	NA	NA	NA	NA	NA	NA	NA	NA	0.05	0.21	0.05	NA	NA	NA
TDr-8	6194	SWE	NA	NA	NA	NA	NA	NA	NA	NA	NA	NA	0.05	0.39	0.82	NA	6.00	NA
TDr-9	6195	SWE	NA	NA	NA	NA	NA	NA	NA	NA	NA	NA	0.02	0.38	1.60	NA	NA	NA
TDr-13	6198	SWE	NA	NA	NA	NA	NA	NA	NA	NA	NA	NA	0.03	0.24	0.87	22.00	3.00	-3.25
TDr-16	6201	SWE	8.11	12.11	-2.60	10.84	31.52	-2.84	4.29	1.23	NA	NA	NA	NA	NA	NA	NA	NA
TDr-17	6202	SWE	NA	NA	NA	NA	NA	NA	NA	NA	NA	NA	0.04	0.31	0.60	NA	14.00	NA
TDr-18	6203	SWE	NA	NA	NA	NA	NA	NA	NA	NA	NA	NA	0.04	0.29	0.76	NA	16.00	NA
TEDEN 02	6209	SWE	NA	NA	NA	NA	NA	NA	NA	NA	NA	NA	0.03	0.28	0.81	NA	14.00	NA
TFÄ 07	6217	SWE	NA	NA	NA	NA	NA	NA	NA	NA	NA	NA	0.04	0.14	-0.18	10.00	15.00	-0.85
TOM 01	6235	SWE	NA	NA	NA	NA	NA	NA	NA	NA	NA	NA	0.03	NA	NA	14.00	12.00	-1.41
TOM 06	6240	SWE	NA	NA	NA	NA	NA	NA	NA	NA	NA	NA	0.03	0.10	-0.01	16.00	12.00	-1.54
Tomegap-2	6242	SWE	9.36	12.89	-3.07	14.39	31.95	-5.95	6.60	-2.56	NA	NA	NA	NA	NA	NA	NA	NA
TV-10	6258	SWE	7.25	11.37	-2.48	15.06	33.16	-5.41	4.09	0.29	NA	NA	NA	NA	NA	NA	NA	NA
TV-22	6268	SWE	NA	NA	NA	NA	NA	NA	NA	NA	NA	NA	0.07	0.32	0.20	NA	26.00	NA
TV-38	6284	SWE	8.02	12.84	-1.78	16.23	32.00	-7.74	5.46	-0.89	NA	NA	NA	NA	NA	NA	NA	NA
UduI 1-11	6296	CZE	NA	NA	NA	NA	NA	NA	NA	NA	NA	NA	0.06	0.39	0.47	NA	NA	NA
Ull3-4	6413	SWE	8.10	14.12	-0.59	13.36	34.39	-2.48	3.31	1.02	NA	NA	NA	NA	NA	NA	NA	NA
Zdrl 1-23	6424	CZE	NA	NA	NA	NA	NA	NA	NA	NA	NA	NA	0.07	0.29	0.15	NA	NA	NA
Zdrl 2-21	6445	CZE	NA	NA	NA	NA	NA	NA	NA	NA	NA	NA	0.07	0.27	0.01	NA	NA	NA
Bor-4	6903	CZE	NA	NA	NA	NA	NA	NA	NA	NA	NA	NA	0.08	0.51	0.47	NA	NA	NA

Ei-2	6915	GER	NA	NA	NA	NA	NA	NA	NA	NA	NA	NA	0.03	0.23	0.74	NA	NA	NA
LL-0	6933	ESP	5.88	12.05	-0.44	21.18	39.57	-5.12	5.64	-0.86	52.33	73.00	0.05	0.32	0.57	NA	NA	NA
NFA-8	6944	UK	NA	NA	NA	NA	NA	NA	NA	NA	NA	NA	0.09	0.40	0.16	NA	NA	NA
Nok-3	6945	NED	NA	NA	NA	NA	NA	NA	NA	NA	NA	NA	0.03	0.23	0.59	NA	NA	NA
Pu2-8	6957	CZE	NA	NA	NA	NA	NA	NA	NA	NA	NA	NA	0.04	0.38	0.95	21.00	NA	NA
Se-0	6961	ESP	8.99	15.97	0.37	12.29	37.11	1.31	5.03	-1.41	53.00	72.00	0.05	0.30	0.46	NA	NA	NA
Tamm-27	6969	FIN	NA	NA	NA	NA	NA	NA	NA	NA	NA	NA	0.04	0.32	0.80	3.00	12.00	0.13
Ts-1	6970	ESP	7.10	15.07	1.37	22.30	39.08	-6.73	5.52	-1.33	49.00	66.00	0.05	0.50	1.04	NA	NA	NA
Ts-5	6971	ESP	7.68	14.83	0.54	18.34	38.69	-3.17	7.06	-2.54	NA	83.00	0.06	0.13	-0.54	NA	NA	NA
Ull2-5	6974	SWE	7.83	12.67	-1.77	15.75	37.21	-2.05	6.02	-1.69	NA	NA	0.07	0.34	0.27	15.00	15.00	-1.25
Ws-2	6981	RUS	NA	NA	NA	NA	NA	NA	NA	NA	NA	NA	0.09	0.33	-0.04	NA	NA	NA
Wt-5	6982	GER	NA	NA	NA	NA	NA	NA	NA	NA	NA	NA	0.04	0.37	0.90	NA	NA	NA
Ak-1	6987	GER	NA	NA	NA	NA	NA	NA	NA	NA	NA	NA	0.06	0.23	0.05	NA	NA	NA
Alst-1	6989	UK	NA	NA	NA	NA	NA	NA	NA	NA	NA	NA	0.08	NA	NA	NA	NA	NA
Baa-1	7002	NED	NA	NA	NA	NA	NA	NA	NA	NA	NA	NA	0.06	0.36	0.41	NA	NA	NA
Bs-1	7003	SUI	NA	NA	NA	NA	NA	NA	NA	NA	NA	NA	0.07	0.51	0.59	NA	NA	NA
Benk-1	7008	NED	NA	NA	NA	NA	NA	NA	NA	NA	NA	NA	0.03	0.35	0.98	NA	12.00	NA
Bd-0	7013	GER	7.78	13.51	-0.88	15.02	39.64	1.11	5.62	-2.01	37.67	65.67	0.05	NA	NA	NA	NA	NA
Bur-0	7058	ESP	NA	NA	NA	NA	NA	NA	NA	NA	NA	NA	0.05	0.33	0.49	3.00	7.00	-0.41
Ca-0	7062	GER	NA	NA	NA	NA	NA	NA	NA	NA	NA	NA	0.08	0.33	0.11	NA	NA	NA
En-2	7119	GER	NA	NA	NA	NA	NA	NA	NA	NA	NA	NA	0.05	0.45	0.90	NA	NA	NA
Fr-2	7133	GER	NA	NA	NA	NA	NA	NA	NA	NA	NA	NA	0.05	0.39	0.77	NA	NA	NA
Gie-0	7147	GER	7.79	13.30	-1.10	12.05	36.45	0.89	4.44	-0.30	45.67	70.67	0.13	0.43	-0.14	NA	NA	NA
Gr-5	7158	AUT	NA	NA	NA	NA	NA	NA	NA	NA	NA	NA	0.05	0.24	0.31	NA	NA	NA
Hau-0	7164	DEN	7.53	12.30	-1.84	16.51	34.93	-5.10	2.78	1.94	NA	83.67	0.04	0.43	1.07	22.00	2.00	-3.65
Hh-0	7169	GER	8.54	12.55	-2.59	16.00	30.60	-8.91	4.26	1.17	NA	NA	0.07	0.46	0.59	5.00	12.00	-0.38
Hh-0	7169	GER	8.54	12.55	-2.59	16.00	30.60	-8.91	4.26	1.17	NA	NA	0.07	0.46	0.59	5.00	12.00	-0.38
Jm-0	7177	CZE	NA	NA	NA	NA	NA	NA	NA	NA	NA	NA	0.09	0.15	-0.82	NA	NA	NA
Kyoto	7207	JPN	NA	NA	NA	NA	NA	NA	NA	NA	NA	NA	0.07	0.25	-0.07	NA	NA	NA
Mnz-0	7244	GER	NA	NA	NA	NA	NA	NA	NA	NA	NA	NA	0.04	0.26	0.65	NA	NA	NA
Mh-0	7255	POL	NA	NA	NA	NA	NA	NA	NA	NA	NA	NA	0.04	NA	NA	NA	NA	NA
Np-0	7268	GER	8.20	14.76	-0.04	11.99	35.64	0.13	6.68	-0.77	39.33	58.67	0.10	0.13	-1.06	NA	NA	NA
Ob-0	7276	GER	NA	NA	NA	NA	NA	NA	NA	NA	NA	NA	0.08	0.34	0.12	NA	NA	NA
Oy-0	7288	NOR	7.07	12.36	-1.31	12.61	34.72	-1.40	3.75	1.02	49.33	81.00	0.05	0.07	-1.08	NA	NA	NA
Pt-0	7305	GER	8.20	14.44	-0.37	12.46	30.45	-5.51	4.83	0.34	40.00	69.00	0.05	0.36	0.58	NA	NA	NA
Sf-1	7327	ESP	10.32	16.37	-0.55	16.38	41.31	1.42	6.62	-2.42	53.00	73.33	0.06	0.32	0.29	NA	NA	NA
Sf-2	7328	ESP	9.12	16.62	0.89	11.12	34.55	-0.09	5.46	-2.68	49.00	68.67	0.05	0.50	0.91	NA	NA	NA
Sp-0	7343	GER	7.59	10.91	-3.29	13.55	32.52	-4.54	4.59	2.22	43.33	68.33	0.05	0.35	0.58	NA	NA	NA
Sten-0	7346	GER	6.44	13.84	0.79	10.50	31.82	-2.19	6.32	-1.92	52.00	78.33	0.05	0.21	0.15	NA	NA	NA
Sten-0	7346	GER	6.44	13.84	0.79	10.50	31.82	-2.19	6.32	-1.92	52.00	78.33	0.05	0.21	0.15	NA	NA	NA
Ting-1	7354	SWE	7.07	14.57	0.90	11.61	34.89	-0.24	5.43	-1.72	NA	NA	0.03	0.31	0.95	NA	18.00	NA
Utrecht	7382	NED	NA	NA	NA	NA	NA	NA	NA	NA	NA	NA	0.07	0.21	-0.20	NA	NA	NA
Van-0	7383	CAN	NA	NA	NA	NA	NA	NA	NA	NA	NA	NA	0.05	0.19	0.03	NA	NA	NA
Gy-0	8214	FRA	NA	NA	NA	NA	NA	NA	NA	NA	NA	NA	0.04	0.26	0.56	NA	NA	NA
Lis-2	8222	SWE	7.51	11.82	-2.30	11.66	31.92	-3.25	2.87	0.72	NA	NA	0.04	0.28	0.53	NA	14.00	NA
THÖ 03	8227	SWE	NA	NA	NA	NA	NA	NA	NA	NA	NA	NA	0.04	0.29	0.78	NA	19.00	NA
Brö1-6	8231	SWE	6.75	14.42	1.06	11.66	36.58	1.41	4.46	-0.32	NA	NA	0.05	0.35	0.65	7.00	12.00	-0.71
Gul1-2	8234	SWE	6.61	14.14	0.93	14.38	36.44	-1.45	5.52	-0.72	NA	NA	0.05	0.41	0.81	16.00	15.00	-1.32

Kävlinge-1	8237	SWE	7.21	14.76	0.94	14.74	36.39	-1.86	3.75	1.00	NA	NA	0.03	0.23	0.57	5.00	12.00	-0.38
Kulturen-1	8240	SWE	6.81	12.60	-0.81	14.14	36.41	-1.24	5.05	-0.66	NA	NA	0.07	0.33	0.23	10.00	14.00	-0.92
Liarum	8241	SWE	7.57	14.11	-0.07	9.80	38.45	5.14	4.97	-0.99	56.00	NA	0.05	0.15	-0.16	19.00	NA	NA
Lillö-1	8242	SWE	7.74	14.48	0.14	13.88	39.00	1.60	4.89	-1.46	NA	NA	0.08	NA	NA	NA	19.00	NA
San-2	8247	SWE	NA	NA	NA	NA	NA	NA	NA	NA	NA	NA	0.05	0.27	0.28	15.00	11.00	-1.56
Vimmerby	8249	SWE	5.31	9.77	-2.15	12.34	32.55	-3.31	3.59	1.28	NA	NA	0.03	0.17	0.48	16.00	10.00	-1.72
Bå1-2	8256	SWE	7.99	13.28	-1.31	12.06	34.76	-0.81	4.90	-0.71	38.67	63.67	0.06	0.26	0.15	NA	NA	NA
Bå5-1	8259	SWE	6.64	14.18	0.94	13.99	33.09	-4.41	3.66	1.07	51.50	87.00	0.05	0.38	0.76	NA	NA	NA
Bla-1	8264	ESP	8.61	14.85	-0.36	13.16	34.19	-2.48	7.92	-2.62	56.00	74.67	0.05	0.21	0.05	NA	NA	NA
Dra3-1	8283	SWE	NA	NA	NA	NA	NA	NA	NA	NA	NA	NA	NA	NA	NA	NA	NA	NA
Hov4-1	8306	SWE	6.97	12.40	-1.17	14.28	37.78	-0.01	3.00	0.35	NA	NA	0.06	0.12	-0.59	NA	41.00	NA
Hovdala-6	8307	SWE	7.98	14.34	-0.25	11.91	32.77	-2.66	4.20	-0.17	55.00	74.33	0.04	0.35	0.74	19.00	NA	NA
Lis-1	8326	SWE	7.90	13.48	-1.02	10.42	33.40	-0.53	5.28	-0.91	53.33	84.00	0.04	0.41	0.95	NA	NA	NA
Lund	8335	SWE	6.03	12.50	-0.13	14.88	39.59	1.20	4.27	0.06	NA	NA	0.04	0.23	0.33	14.00	13.00	-1.33
Mir-0	8337	ITA	NA	NA	NA	NA	NA	NA	NA	NA	NA	NA	NA	NA	NA	NA	NA	NA
Ost-0	8351	SWE	NA	NA	NA	NA	NA	NA	NA	NA	NA	NA	0.07	0.24	-0.05	NA	12.00	NA
Rev-1	8369	SWE	5.58	9.93	-2.26	29.58	32.55	-20.54	3.92	0.79	NA	NA	0.03	0.29	1.08	8.00	9.00	-1.13
Sanna-2	8376	SWE	NA	NA	NA	NA	NA	NA	NA	NA	NA	NA	0.03	0.33	1.05	9.00	13.00	-0.89
Sr:5	8386	SWE	NA	NA	NA	NA	NA	NA	NA	NA	NA	NA	0.05	0.14	-0.32	NA	NA	NA
St-0	8387	SWE	NA	NA	NA	NA	NA	NA	NA	NA	NA	NA	0.06	0.34	0.32	NA	NA	NA
Kelsterbach-4	8420	GER	NA	NA	NA	NA	NA	NA	NA	NA	NA	NA	0.04	0.37	0.79	NA	NA	NA
Fjä1-1	8422	SWE	7.63	13.18	-1.06	12.48	30.37	-5.62	4.12	0.03	NA	NA	0.05	NA	NA	NA	NA	NA
Ull1-1	8426	SWE	9.45	16.69	0.64	14.27	35.55	-2.23	3.49	0.74	33.33	49.67	0.08	0.26	-0.14	NA	NA	NA
Vinslöv	9057	SWE	7.18	11.92	-1.87	14.37	30.86	-7.02	4.77	-1.35	51.00	81.67	0.07	0.29	0.10	NA	NA	NA
Böt 1	9339	SWE	8.05	12.85	-1.81	13.85	35.53	-1.84	3.27	0.35	NA	NA	0.08	0.37	0.19	14.00	20.00	-0.90
EdJ 2	9363	SWE	NA	NA	NA	NA	NA	NA	NA	NA	NA	NA	0.04	0.31	0.64	NA	24.00	NA
EkS 2	9369	SWE	6.19	12.54	-0.25	14.09	34.28	-3.31	3.53	0.65	NA	NA	0.04	0.19	0.31	14.00	9.00	-1.69
FlyA 3	9380	SWE	6.94	10.92	-2.63	17.93	34.73	-6.71	3.00	1.14	NA	NA	0.02	0.12	0.39	9.00	16.00	-0.68
Grön 12	9386	SWE	NA	NA	NA	NA	NA	NA	NA	NA	NA	NA	0.05	0.28	0.42	NA	20.00	NA
Grön 14	9388	SWE	NA	NA	NA	NA	NA	NA	NA	NA	NA	NA	0.04	0.14	-0.19	NA	22.00	NA
Hal-1	9395	SWE	NA	NA	NA	NA	NA	NA	NA	NA	NA	NA	0.06	0.31	0.25	15.00	14.00	-1.32
Hamm-1	9399	SWE	8.08	13.91	-0.78	14.66	37.21	-0.96	4.12	1.61	NA	NA	0.04	NA	NA	NA	17.00	NA
HolA-1-1	9404	SWE	7.27	13.31	-0.57	15.28	30.71	-8.08	6.25	-1.08	NA	NA	0.07	0.28	0.07	16.00	17.00	-1.19
HolA-1-2	9405	SWE	6.85	11.26	-2.19	15.22	36.48	-2.25	5.32	-1.23	NA	NA	0.05	NA	NA	12.00	16.00	-0.97
HolA-2-2	9407	SWE	8.20	14.61	-0.19	14.61	29.82	-8.30	3.98	0.11	NA	NA	0.04	0.39	0.87	8.00	12.00	-0.85
Kal-1	9408	SWE	7.24	13.20	-0.64	9.34	36.15	3.30	4.21	-0.69	NA	NA	0.06	NA	NA	NA	28.00	NA
Kia-1	9409	SWE	6.60	10.00	-3.20	14.16	30.91	-6.76	3.56	0.55	NA	NA	0.04	0.28	0.50	10.00	23.00	-0.42
Lan-1	9421	SWE	6.02	12.38	-0.25	14.34	40.17	2.32	6.50	-2.30	NA	NA	0.06	0.39	0.60	8.00	23.00	-0.20
Puk-1	9436	SWE	7.96	13.43	-1.14	17.28	32.37	-8.42	3.52	1.60	NA	NA	0.08	0.14	-0.76	NA	16.00	NA
Puk-2	9437	SWE	8.85	13.46	-1.99	17.66	36.24	-4.93	2.98	1.18	NA	NA	NA	NA	NA	NA	NA	NA
Ste-2	9453	SWE	8.51	11.86	-3.26	12.16	31.00	-4.67	3.65	2.24	NA	NA	0.04	0.35	0.85	NA	20.00	NA
Ste-3	9454	SWE	8.47	14.81	-0.26	12.82	34.95	-1.38	4.23	0.04	NA	NA	0.03	0.35	1.14	NA	15.00	NA
Tur-4	9470	SWE	8.19	13.77	-1.02	13.95	30.36	-7.10	3.19	1.63	NA	NA	0.07	NA	NA	NA	17.00	NA
Yst-1	9481	SWE	6.88	14.86	1.37	13.39	36.54	-0.37	2.83	0.47	NA	NA	NA	NA	NA	NA	NA	NA
IP-Alo-0	9506	POR	8.33	NA	NA	18.38	NA	NA	3.71	NA	52.67	NA	0.03	0.38	1.24	NA	NA	NA
IP-All-0	9517	ESP	8.97	12.34	-3.24	17.68	33.49	-7.71	2.71	-0.89	34.67	48.33	0.04	0.43	1.09	NA	NA	NA
IP-Ang-0	9519	ESP	NA	NA	NA	NA	NA	NA	NA	NA	NA	NA	0.03	NA	NA	13.00	NA	NA
IP-Ara-4	9520	ESP	8.14	16.53	1.79	13.37	42.10	5.22	3.93	-0.48	NA	NA	NA	NA	NA	NA	NA	NA

IP-Bar-1	9521	ESP	10.01	15.13	-1.48	12.87	37.38	0.99	4.58	-0.13	NA	NA	0.05	0.35	0.54	21.00	3.00	-3.20
IP-Ber-0	9524	ESP	9.41	15.43	-0.58	12.11	38.50	2.88	4.90	-0.93	NA	NA	0.06	0.34	0.32	6.00	11.00	-0.65
IP-Bis-0	9525	ESP	8.56	12.57	-2.59	13.40	30.07	-6.84	4.05	1.49	NA	NA	0.05	0.31	0.54	NA	8.00	NA
IP-Cab-3	9526	ESP	9.34	13.09	-2.85	17.40	33.70	-7.21	4.48	-0.39	52.00	72.00	0.04	0.34	0.78	NA	NA	NA
IP-Cad-0	9527	ESP	8.51	12.75	-2.37	16.75	38.68	-1.58	5.28	-0.59	NA	NA	NA	NA	NA	NA	NA	NA
IP-Cal-0	9528	ESP	7.48	11.35	-2.74	15.70	39.72	0.51	6.51	-2.14	NA	NA	0.09	NA	NA	8.00	7.00	-1.39
IP-Cdc-3	9531	ESP	8.54	15.33	0.18	13.49	35.19	-1.81	4.73	-0.18	NA	NA	0.04	0.37	0.93	NA	12.00	NA
IP-Cdo-0	9532	ESP	8.22	16.59	1.76	15.07	36.99	-1.60	3.93	0.07	NA	NA	0.04	0.29	0.54	NA	NA	NA
IP-Cmo-3	9534	ESP	7.43	15.89	1.85	15.70	39.75	0.54	6.31	-2.91	52.50	69.00	NA	NA	NA	NA	NA	NA
IP-Coc-1	9535	ESP	8.22	15.51	0.69	13.38	35.47	-1.42	6.37	-1.86	NA	NA	0.09	NA	NA	8.00	18.00	-0.44
IP-Deh-1	9539	ESP	7.35	13.70	-0.26	16.99	35.04	-5.47	7.21	-3.31	54.67	NA	0.04	0.50	1.29	13.00	2.00	-3.12
IP-Elb-0	9540	ESP	8.88	15.86	0.38	17.78	35.34	-5.95	4.43	-1.52	NA	NA	0.05	0.44	0.85	NA	12.00	NA
IP-Hor-0	9547	ESP	7.32	14.14	0.21	11.98	34.32	-1.17	4.75	-0.05	NA	84.00	0.05	0.34	0.63	19.00	3.00	-3.10
IP-Hoy-0	9548	ESP	8.60	14.00	-1.20	14.91	38.82	0.40	3.92	-0.45	NA	81.00	NA	NA	NA	NA	NA	NA
IP-Jim-1	9551	ESP	6.61	15.10	1.88	12.13	34.98	-0.66	4.24	-0.35	NA	NA	0.04	0.45	1.16	NA	24.00	NA
IP-Lab-7	9552	ESP	7.18	14.76	0.97	20.11	33.14	-10.48	3.49	0.95	NA	NA	NA	NA	NA	NA	NA	NA
IP-Ldd-0	9553	ESP	6.43	13.25	0.21	15.24	34.64	-4.11	4.87	0.03	NA	NA	NA	NA	NA	NA	NA	NA
IP-Men-2	9556	ESP	5.33	12.98	1.05	23.34	38.36	-8.49	6.56	-3.70	52.00	90.00	0.02	0.11	0.23	19.00	2.00	-3.50
IP-Moa-0	9557	ESP	7.56	11.96	-2.21	13.93	32.00	-5.44	2.98	2.73	NA	NA	0.05	0.36	0.59	8.00	20.00	-0.34
IP-Moc-11	9558	ESP	7.21	14.21	0.39	16.54	36.71	-3.35	5.78	-1.03	NA	NA	0.05	NA	NA	5.00	8.00	-0.78
IP-Mun-0	9561	ESP	8.66	13.10	-2.17	13.62	32.44	-4.69	3.37	0.59	NA	NA	0.08	0.11	-1.06	NA	21.00	NA
IP-Mur-0	9562	ESP	7.26	12.28	-1.58	11.53	32.29	-2.75	4.29	0.18	NA	NA	0.05	0.33	0.46	9.00	12.00	-0.97
IP-Nog-17	9564	ESP	7.43	12.85	-1.19	15.50	32.15	-6.86	2.72	1.97	NA	NA	0.08	0.33	0.12	NA	19.00	NA
IP-Orb-10	9565	ESP	10.22	12.69	-4.13	14.05	32.38	-5.18	4.52	-1.11	NA	NA	0.05	0.24	0.14	13.00	11.00	-1.42
IP-Pal-0	9567	ESP	9.33	12.97	-2.96	12.54	33.31	-2.75	3.63	0.65	NA	NA	0.06	0.23	-0.08	NA	20.00	NA
IP-Pan-0	9568	ESP	10.36	14.65	-2.31	9.63	33.17	0.03	4.32	-0.17	NA	NA	0.04	0.53	1.23	10.00	18.00	-0.66
IP-Pds-1	9569	ESP	8.85	13.23	-2.22	13.49	31.55	-5.45	5.50	-0.94	NA	NA	0.05	0.24	0.25	NA	13.00	NA
IP-Rds-0	9573	ESP	7.32	13.74	-0.18	19.08	34.01	-8.58	5.58	-0.29	52.00	79.00	0.05	0.39	0.63	13.00	NA	NA
IP-Ria-0	9577	ESP	9.93	17.14	0.61	15.52	31.60	-7.43	5.51	-1.44	NA	NA	0.07	0.46	0.50	NA	23.00	NA
IP-Sac-0	9578	ESP	7.61	13.37	-0.84	14.38	36.68	-1.21	3.89	0.65	45.00	67.50	0.03	0.27	0.78	NA	NA	NA
IP-Scm-0	9580	ESP	8.12	15.24	0.51	16.69	34.16	-6.04	3.32	0.99	52.00	82.67	0.05	0.30	0.40	18.00	NA	NA
IP-Sdv-3	9581	ESP	8.79	10.65	-4.75	13.01	33.29	-3.23	7.73	-3.71	NA	NA	NA	NA	NA	NA	NA	NA
IP-Ses-0	9582	ESP	8.61	13.84	-1.37	11.35	36.17	1.32	5.54	-1.16	56.00	NA	NA	NA	NA	NA	NA	NA
IP-Stp-0	9584	ESP	8.96	16.62	1.05	15.29	36.63	-2.17	5.51	-1.01	NA	NA	0.08	0.37	0.25	NA	18.00	NA
IP-Svi-0	9585	ESP	10.29	8.89	-8.01	17.49	32.23	-8.78	3.40	-0.21	31.00	45.00	0.07	0.39	0.37	NA	NA	NA
IP-Tam-0	9586	ESP	8.49	14.19	-0.91	11.63	37.13	1.99	5.39	-0.81	NA	NA	0.03	NA	NA	8.00	18.00	-0.44
IP-Tdc-0	9587	ESP	8.19	14.83	0.04	15.87	37.89	-1.49	3.25	1.04	NA	NA	0.04	0.17	0.16	15.00	NA	NA
IP-Tol-7	9588	ESP	7.35	14.52	0.57	16.02	35.51	-4.02	3.80	0.20	NA	NA	NA	NA	NA	NA	NA	NA
IP-Tor-1	9589	ESP	9.20	16.58	0.77	8.46	36.22	4.25	4.84	-1.11	NA	NA	0.05	0.28	0.43	16.00	18.00	-1.13
IP-Vad-0	9591	ESP	9.09	14.89	-0.81	16.71	34.07	-6.15	6.01	-1.76	50.50	70.67	0.06	0.39	0.55	NA	20.00	NA
IP-Vae-2	9592	ESP	7.93	13.97	-0.57	14.90	32.99	-5.42	5.93	-0.80	NA	NA	0.04	0.34	0.81	4.00	NA	NA
IP-Vaz-0	9593	ESP	7.75	16.77	2.41	12.56	34.70	-1.36	7.06	-2.40	NA	NA	0.06	0.31	0.30	NA	27.00	NA
IP-Vdm-0	9594	ESP	7.71	15.71	1.40	12.32	35.33	-0.50	6.88	-3.50	NA	NA	0.04	NA	NA	NA	NA	NA
IP-Vdt-0	9595	ESP	8.74	15.24	-0.10	16.19	36.82	-2.89	3.36	0.20	NA	NA	0.05	0.30	0.57	7.00	11.00	-0.80
IP-Ver-5	9596	ESP	8.25	14.28	-0.58	13.14	34.54	-2.11	5.51	-1.30	41.50	77.00	0.05	NA	NA	NA	NA	NA
IP-Vig-1	9597	ESP	8.50	15.25	0.14	11.93	34.71	-0.73	4.57	-0.99	37.67	84.00	0.05	0.33	0.52	NA	NA	NA
IP-Vin-0	9599	ESP	7.87	14.10	-0.38	16.68	37.64	-2.55	5.29	-0.19	NA	NA	NA	NA	NA	NA	NA	NA
IP-Voz-0	9601	ESP	7.82	14.45	0.03	19.05	35.60	-6.96	3.93	0.07	NA	NA	0.03	0.31	0.88	8.00	NA	NA

IP-Vpa-1	9602	ESP	8.84	16.45	1.00	16.92	36.75	-3.68	5.03	-1.32	NA	NA	0.04	NA	NA	4.00	NA	NA
Toc-1	9739	ROU	NA	NA	NA	NA	NA	NA	NA	NA	NA	NA	0.04	0.37	0.79	22.00	NA	NA
Staro-2	9756	SRB	NA	NA	NA	NA	NA	NA	NA	NA	NA	NA	0.09	0.32	-0.11	9.00	14.00	-0.81
Fell3-7	9776	GER	NA	NA	NA	NA	NA	NA	NA	NA	NA	NA	0.09	0.37	0.07	NA	NA	NA
Bach-7	9778	GER	NA	NA	NA	NA	NA	NA	NA	NA	NA	NA	0.04	0.30	0.69	NA	NA	NA
Erg2-6	9784	GER	NA	NA	NA	NA	NA	NA	NA	NA	NA	NA	0.11	0.19	-0.77	NA	NA	NA
Wank-2	9795	GER	NA	NA	NA	NA	NA	NA	NA	NA	NA	NA	0.06	0.34	0.34	NA	NA	NA
Obe1-15	9804	GER	NA	NA	NA	NA	NA	NA	NA	NA	NA	NA	0.06	0.46	0.66	NA	NA	NA
Schl-7	9807	GER	NA	NA	NA	NA	NA	NA	NA	NA	NA	NA	0.03	0.39	1.32	NA	NA	NA
Amu-0	9819	ESP	8.78	15.04	-0.35	16.51	37.97	-2.05	3.74	1.22	NA	NA	NA	NA	NA	NA	NA	NA
Are-0	9820	ESP	9.46	12.25	-3.81	18.38	41.73	-0.16	3.38	1.78	44.00	NA	0.02	0.34	1.34	NA	NA	NA
Aru-0	9821	ESP	8.88	15.25	-0.24	16.93	36.70	-3.75	8.24	-3.47	NA	NA	0.04	0.35	0.73	18.00	NA	NA
Aul-0	9822	ESP	6.67	14.20	0.93	16.12	36.79	-2.84	5.44	-1.47	NA	90.00	0.04	0.31	0.71	2.00	NA	NA
Bes-5	9824	ESP	7.53	13.51	-0.63	12.55	34.57	-1.49	4.32	0.20	NA	NA	NA	NA	NA	NA	NA	NA
Boa-0	9825	ESP	8.96	13.50	-2.06	19.05	37.36	-5.20	5.49	-0.67	53.67	85.50	0.05	0.27	0.41	13.00	2.00	-3.12
Bor-0	9826	ESP	9.71	15.66	-0.65	14.85	32.61	-5.75	6.59	-1.62	47.67	84.00	0.04	NA	NA	13.00	16.00	-1.05
Cha-0	9833	ESP	8.25	15.35	0.49	15.07	39.31	0.73	7.19	-3.17	NA	84.00	0.10	NA	NA	18.00	5.00	-2.53
IP-Cha-0	9833	ESP	8.25	15.35	0.49	15.07	39.31	0.73	7.19	-3.17	NA	84.00	0.10	NA	NA	18.00	5.00	-2.53
Cho-0	9834	ESP	9.61	18.09	1.88	15.37	40.76	1.87	2.11	0.77	NA	NA	NA	NA	NA	NA	NA	NA
Cir-0	9835	ESP	8.13	16.41	1.68	16.01	37.63	-1.89	3.80	-0.87	55.00	85.00	0.05	0.23	0.18	NA	NA	NA
Cod-0	9836	ESP	7.41	14.55	0.54	16.55	37.35	-2.71	5.27	-1.46	NA	NA	0.06	NA	NA	2.00	NA	NA
Cot-0	9838	ESP	8.64	13.31	-1.94	15.11	32.27	-6.35	5.79	-1.81	47.00	65.33	0.02	0.33	1.46	NA	NA	NA
Coy-0	9839	ESP	8.67	14.58	-0.69	14.02	37.59	0.06	3.99	1.17	NA	NA	NA	NA	NA	NA	NA	NA
Dar-0	9840	ESP	7.33	9.10	-4.84	13.90	33.22	-4.19	3.82	0.93	NA	NA	NA	NA	NA	NA	NA	NA
Ees-0	9841	ESP	10.74	16.22	-1.12	13.99	37.63	0.13	3.39	0.06	NA	NA	0.07	0.36	0.35	17.00	NA	NA
Elp-0	9843	ESP	8.98	15.46	-0.12	17.01	40.54	0.02	4.05	-1.16	52.00	81.50	0.03	0.39	1.08	13.00	4.00	-2.43
Esn-2	9844	ESP	8.55	13.85	-1.31	15.58	33.98	-5.11	5.20	-0.13	NA	NA	0.08	NA	NA	20.00	4.00	-2.86
Evs-0	9845	ESP	9.84	18.79	2.34	13.30	40.22	3.41	5.49	-2.12	NA	84.00	0.08	NA	NA	18.00	2.00	-3.45
Ezc-2	9846	ESP	10.15	15.39	-1.37	13.46	30.05	-6.92	3.63	1.66	NA	NA	0.05	0.33	0.57	6.00	12.00	-0.56
Gud-3	9849	ESP	6.54	13.09	-0.05	12.35	36.18	0.32	4.13	0.43	NA	NA	NA	NA	NA	NA	NA	NA
Hec-0	9850	ESP	8.22	14.83	0.00	14.00	37.56	0.05	4.62	-0.48	NA	NA	NA	NA	NA	NA	NA	NA
Hue-3	9851	ESP	8.09	12.21	-2.49	11.42	37.23	2.31	3.15	1.16	NA	NA	0.04	NA	NA	NA	14.00	NA
Ini-0	9852	ESP	8.54	13.19	-1.95	17.01	33.87	-6.65	5.19	-1.08	53.00	85.50	0.03	0.26	0.70	18.00	5.00	-2.53
Lam-0	9855	ESP	5.98	13.64	1.05	17.57	34.39	-6.69	5.71	-1.84	50.50	90.00	NA	NA	NA	NA	10.00	NA
Lch-0	9856	ESP	7.95	13.61	-0.94	15.89	38.92	-0.48	5.74	-2.57	50.50	87.00	0.05	0.27	0.39	NA	NA	NA
Leg-0	9857	ESP	8.50	15.73	0.63	15.05	37.06	-1.50	4.00	0.62	57.50	NA	NA	NA	NA	NA	NA	NA
Loz-0	9858	ESP	7.98	13.28	-1.30	14.23	32.72	-5.03	4.38	0.31	NA	NA	NA	NA	NA	NA	NA	NA
Lro-0	9859	ESP	5.54	9.83	-2.32	17.45	32.84	-8.13	2.25	2.97	52.00	NA	0.03	0.26	0.79	22.00	2.00	-3.65
Lum-0	9860	ESP	8.87	14.96	-0.52	10.43	31.95	-1.99	5.80	-0.21	53.00	NA	0.04	0.46	0.99	22.00	7.00	-2.40
Mac-0	9861	ESP	8.27	16.22	1.35	16.12	35.94	-3.69	3.64	-0.48	NA	NA	0.03	0.36	1.23	3.00	12.00	0.13
Mat-0	9864	ESP	7.24	14.48	0.64	15.02	40.01	1.47	5.75	-2.61	49.50	77.00	0.04	0.35	0.77	NA	NA	NA
Mie-1	9867	ESP	8.31	15.81	0.90	10.55	35.48	1.42	5.02	-1.62	NA	NA	0.03	0.47	1.40	8.00	11.00	-0.93
Moe-0	9868	ESP	7.63	13.78	-0.46	15.14	32.39	-6.26	6.28	-0.77	54.00	87.00	0.02	0.49	1.74	18.00	NA	NA
Moz-0	9870	ESP	7.29	14.17	0.27	15.30	41.30	2.49	3.32	1.24	NA	NA	NA	NA	NA	NA	NA	NA
Oja-0	9874	ESP	8.52	13.13	-2.00	19.88	37.56	-5.83	6.48	-1.57	37.33	70.00	0.05	NA	NA	NA	NA	NA
Pad-0	9876	ESP	6.83	16.56	3.13	25.68	39.64	-9.55	5.62	-1.78	NA	NA	NA	NA	NA	NA	NA	NA
Pdl-0	9877	ESP	8.49	14.27	-0.83	16.61	39.11	-1.01	5.28	-0.99	NA	NA	NA	NA	NA	NA	NA	NA
Pee-0	9878	ESP	8.25	13.84	-1.01	15.01	34.15	-4.37	4.61	0.14	NA	NA	0.05	0.22	0.08	20.00	7.00	-2.30

Pie-0	9881	ESP	8.90	15.73	0.23	11.51	35.73	0.71	4.95	-1.16	NA	NA	0.04	0.38	0.80	22.00	5.00	-2.73
Piq-0	9883	ESP	10.22	15.84	-0.99	13.12	36.25	-0.37	6.07	-2.45	35.67	73.33	0.05	0.44	0.80	NA	NA	NA
Pru-0	9886	ESP	8.53	13.26	-1.87	15.79	33.74	-5.56	5.60	-1.76	50.50	70.67	0.06	0.35	0.36	NA	NA	NA
Pva-1	9888	ESP	8.30	14.62	-0.28	16.95	38.68	-1.78	4.44	-0.71	NA	NA	0.03	0.32	0.97	17.00	NA	NA
Rib-1	9890	ESP	8.61	13.69	-1.53	10.58	29.22	-4.87	4.00	1.00	NA	NA	0.05	0.46	0.96	10.00	14.00	-0.92
Sal-0	9891	ESP	9.00	15.63	0.02	17.72	36.73	-4.50	3.73	0.86	NA	90.00	NA	NA	NA	NA	NA	NA
Sam-0	9892	ESP	5.41	14.16	2.15	22.99	38.82	-7.68	5.71	-2.21	NA	NA	0.05	NA	NA	5.00	3.00	-1.76
Sfb-6	9895	ESP	8.37	16.50	1.53	12.81	43.13	6.81	7.17	-3.04	NA	NA	0.05	0.50	0.94	20.00	3.00	-3.15
Smt-1	9897	ESP	8.79	15.86	0.46	13.17	37.12	0.44	3.73	0.07	NA	NA	0.05	0.38	0.77	20.00	NA	NA
Som-0	9898	ESP	7.55	14.38	0.22	10.81	36.93	2.61	5.10	-0.12	NA	NA	NA	NA	NA	NA	NA	NA
Tau-0	9899	ESP	6.89	13.96	0.46	15.10	34.74	-3.87	4.92	0.39	47.00	84.00	0.07	0.35	0.29	NA	NA	NA
Urd-1	9901	ESP	6.91	16.29	2.77	11.43	34.74	-0.20	4.17	0.28	NA	NA	NA	NA	NA	NA	NA	NA
Usa-0	9902	ESP	7.58	15.47	1.29	11.43	39.66	4.73	3.61	0.42	NA	NA	0.05	0.44	0.84	2.00	10.00	0.36
Val-0	9903	ESP	7.35	14.70	0.74	14.11	38.86	1.23	6.55	-2.48	NA	NA	NA	NA	NA	NA	NA	NA
Vas-0	9904	ESP	8.89	15.82	0.32	11.68	38.01	2.82	6.28	-2.46	NA	NA	0.07	0.34	0.25	10.00	11.00	-1.16
Mah-6	9906	ESP	6.95	15.15	1.59	17.20	37.11	-3.60	4.37	0.19	NA	NA	0.05	0.36	0.70	NA	NA	NA
ARR-17	9927	FRA	7.27	11.65	-2.23	14.47	36.10	-1.88	4.71	-1.34	NA	NA	0.04	0.50	1.11	6.00	8.00	-0.97
MOU2-25	9931	FRA	8.89	14.04	-1.45	14.87	36.03	-2.36	4.54	0.23	33.33	59.67	NA	NA	NA	NA	NA	NA
WAV-8	9938	FRA	6.01	13.89	1.28	12.96	37.44	0.96	5.62	-2.07	43.50	69.33	0.05	0.56	0.99	NA	NA	NA
Agu-1	9942	ESP	5.74	13.63	1.29	21.58	43.97	-1.12	7.61	-2.93	NA	NA	0.03	0.36	1.13	10.00	8.00	-1.48
Pra-6	9948	ESP	6.57	13.95	0.77	20.78	30.95	-13.35	5.50	-1.53	NA	NA	0.07	0.44	0.46	2.00	7.00	0.00
Qui-0	9949	ESP	8.71	11.94	-3.38	14.99	30.83	-7.67	5.56	-1.01	47.00	90.00	0.06	0.31	0.25	13.00	NA	NA
Vie-0	9950	ESP	7.94	14.47	-0.08	13.26	36.19	-0.59	5.68	-1.87	NA	NA	0.05	0.42	0.81	9.00	8.00	-1.37
Copac-1	10005	ROU	NA	NA	NA	NA	NA	NA	NA	NA	NA	NA	0.06	0.58	0.90	19.00	4.00	-2.81
Petro-1	10017	SRB	NA	NA	NA	NA	NA	NA	NA	NA	NA	NA	0.04	0.42	0.92	4.00	11.00	-0.24
Arb0	18513	MAR	NA	NA	NA	NA	NA	NA	NA	NA	NA	NA	NA	NA	NA	NA	NA	NA
Zin9	18515	MAR	NA	NA	NA	NA	NA	NA	NA	NA	NA	NA	NA	NA	NA	NA	NA	NA
IFr0	22002	MAR	NA	NA	NA	NA	NA	NA	NA	NA	NA	NA	NA	NA	NA	NA	NA	NA
Taz0	22005	MAR	NA	NA	NA	NA	NA	NA	NA	NA	NA	NA	NA	NA	NA	NA	NA	NA
Bab0	22008	MAR	NA	NA	NA	NA	NA	NA	NA	NA	NA	NA	NA	NA	NA	NA	NA	NA
Elh2	35616	MAR	NA	NA	NA	NA	NA	NA	NA	NA	NA	NA	NA	NA	NA	NA	NA	NA
Militärring A2	100048	GER	NA	NA	NA	NA	NA	NA	NA	NA	NA	NA	0.06	0.44	0.69	NA	NA	NA
Militärring B1	100049	GER	NA	NA	NA	NA	NA	NA	NA	NA	NA	NA	0.05	0.49	0.90	NA	NA	NA
Bernhardstr. 110	100050	GER	NA	NA	NA	NA	NA	NA	NA	NA	NA	NA	NA	NA	NA	NA	NA	NA
MilitärringA2	100051	GER	NA	NA	NA	NA	NA	NA	NA	NA	NA	NA	NA	NA	NA	NA	NA	NA
MilitärringB1	100052	GER	NA	NA	NA	NA	NA	NA	NA	NA	NA	NA	NA	NA	NA	NA	NA	NA
Bernhardstr.110	100053	GER	NA	NA	NA	NA	NA	NA	NA	NA	NA	NA	NA	NA	NA	NA	NA	NA
Mol-2	115927	FRA	7.87	13.70	-0.77	13.38	33.05	-3.84	3.35	1.30	41.33	68.33	0.04	NA	NA	NA	NA	NA
All1-2	115930	FRA	6.30	14.07	1.16	18.46	42.54	0.57	4.21	-0.90	NA	NA	NA	NA	NA	NA	NA	NA
All1-4	115932	FRA	7.81	13.88	-0.53	19.12	35.60	-7.03	3.67	0.25	NA	87.00	0.08	0.34	0.05	6.00	10.00	-0.74
All1-5	115934	FRA	6.99	14.82	1.22	14.38	36.63	-1.26	4.97	-1.01	56.00	81.67	0.06	0.29	0.26	NA	NA	NA
All1-8	115936	FRA	7.46	12.39	-1.68	16.46	31.86	-8.10	4.73	-1.27	33.33	51.67	0.06	0.59	1.02	NA	NA	NA
All2-1	115938	FRA	7.92	17.21	2.68	14.95	40.63	2.17	4.47	-1.32	41.00	56.50	0.06	0.25	0.15	NA	NA	NA
All2-4	115940	FRA	7.10	12.22	-1.49	16.71	35.51	-4.71	3.69	0.11	43.00	74.33	0.05	0.24	0.25	NA	NA	NA
All2-5	115942	FRA	6.68	11.28	-2.01	16.66	38.02	-2.15	5.22	-1.76	45.67	73.00	0.03	0.19	0.48	NA	NA	NA
Cam-10	115944	FRA	5.49	12.19	0.09	14.08	35.98	-1.61	5.64	-1.91	39.33	78.33	0.05	0.28	0.32	NA	NA	NA
Cam-11	115946	FRA	6.59	13.41	0.21	10.98	34.65	0.15	4.26	-0.89	38.67	73.67	0.06	0.20	-0.20	NA	NA	NA
Cam-2	115948	FRA	7.02	12.36	-1.27	14.31	38.77	0.95	4.03	-0.55	41.67	83.00	0.08	0.28	-0.06	NA	NA	NA

Cam-6	115950	FRA	5.65	12.58	0.32	16.00	32.92	-6.59	3.97	0.43	42.67	78.33	0.07	0.11	-0.81	NA	NA	NA
Cam-8	115952	FRA	6.13	12.76	0.02	18.50	33.62	-8.39	6.15	-3.14	40.00	66.00	0.03	0.29	0.88	NA	NA	NA
Cla-3	115954	FRA	7.06	12.02	-1.65	14.32	38.06	0.22	3.65	-0.09	NA	NA	0.10	NA	NA	NA	12.00	NA
Cla-5	115956	FRA	6.45	12.39	-0.66	9.91	35.06	1.64	4.12	0.16	NA	NA	0.09	NA	NA	NA	2.00	NA
Cla-6	115958	FRA	7.37	12.41	-1.56	12.45	39.55	3.58	3.99	-0.95	NA	NA	0.08	0.33	0.07	NA	12.00	NA
Cur-10	115960	FRA	8.68	13.71	-1.57	13.15	34.53	-2.13	3.80	-0.25	42.33	69.33	0.06	0.21	-0.15	NA	NA	NA
Cur-2	115962	FRA	7.22	12.63	-1.20	11.73	34.02	-1.22	3.89	0.15	51.67	81.00	NA	NA	NA	NA	NA	NA
Cur-5	115964	FRA	8.15	14.59	-0.17	17.09	42.96	2.36	4.94	-1.13	NA	84.00	0.05	0.46	0.88	21.00	NA	NA
Fet-6	115968	FRA	6.32	12.86	-0.06	15.08	34.52	-4.06	3.17	0.97	NA	NA	0.08	NA	NA	4.00	4.00	-1.25
All2-6	115970	FRA	7.66	12.09	-2.17	15.87	40.20	0.82	4.00	-0.80	40.00	80.33	0.04	0.27	0.58	NA	NA	NA
Lac-2	115972	FRA	7.38	13.42	-0.56	19.43	34.09	-8.85	4.22	0.98	42.67	68.33	0.10	NA	NA	NA	NA	NA
Lac-7	115974	FRA	8.52	14.42	-0.71	12.85	31.59	-4.77	4.44	0.83	36.67	71.67	0.10	0.21	-0.56	NA	NA	NA
Ldv-1	115976	FRA	7.27	13.43	-0.44	15.82	36.62	-2.71	5.01	-0.63	45.33	84.00	0.04	0.29	0.53	NA	NA	NA
Ldv-11	115978	FRA	7.54	14.32	0.18	14.17	35.93	-1.74	4.34	0.67	45.33	NA	0.03	0.27	0.88	NA	NA	NA
Ldv-2	115980	FRA	6.84	14.63	1.18	15.75	38.82	-0.44	5.77	-1.30	48.33	87.00	0.05	0.26	0.25	NA	NA	NA
Ldv-3	115982	FRA	7.93	15.13	0.59	16.60	37.32	-2.80	3.39	1.58	45.33	85.50	0.06	0.13	-0.60	NA	NA	NA
Mib-11	115986	FRA	6.91	11.91	-1.61	9.08	35.58	2.99	4.30	0.50	39.33	65.33	0.08	0.41	0.34	NA	NA	NA
Mib-18	115988	FRA	8.15	13.73	-1.03	12.97	37.64	1.16	3.64	1.45	50.67	NA	0.08	0.21	-0.42	13.00	4.00	-2.43
Mib-3	115990	FRA	6.54	12.00	-1.14	14.62	37.44	-0.69	4.10	0.37	45.33	67.67	0.14	0.18	-1.07	NA	NA	NA
Mib-9	115992	FRA	6.75	12.04	-1.31	13.58	34.64	-2.44	5.11	-0.91	41.33	67.33	0.06	0.35	0.49	NA	NA	NA
Mog-1	115994	FRA	8.34	10.68	-4.27	15.25	31.53	-7.23	4.06	0.98	NA	NA	0.07	0.41	0.43	18.00	4.00	-2.76
Mog-11	115996	FRA	7.12	12.43	-1.29	16.20	36.58	-3.13	5.11	-0.99	37.33	65.00	0.08	0.32	0.10	NA	NA	NA
Mol-12	116000	FRA	7.39	11.42	-2.57	12.63	32.56	-3.58	3.97	0.97	47.00	77.00	NA	NA	NA	NA	NA	NA
Mol-4	116002	FRA	7.54	11.74	-2.40	12.69	33.71	-2.49	4.70	-1.01	48.67	80.67	0.03	0.38	1.30	NA	NA	NA
Par-10	116004	FRA	8.12	14.23	-0.49	12.89	34.58	-1.83	4.03	0.23	38.00	69.33	0.08	0.31	0.03	NA	NA	NA
Par-13	116006	FRA	7.17	12.85	-0.93	13.67	36.97	-0.21	4.36	-0.67	48.33	79.67	0.04	0.15	-0.09	NA	NA	NA
Par-3	116008	FRA	7.34	14.38	0.43	15.25	38.24	-0.52	6.40	-3.20	45.67	71.67	0.08	0.28	-0.05	NA	NA	NA
Par-4	116010	FRA	7.25	13.71	-0.15	16.67	32.84	-7.34	5.70	-1.94	35.67	64.33	0.08	0.37	0.15	NA	5.00	NA
Pyl-1	116012	FRA	NA	17.13	NA	NA	39.88	NA	NA	NA	NA	68.33	0.06	0.15	-0.45	NA	NA	NA
Pyl-3	116014	FRA	7.49	17.66	3.56	18.32	41.68	-0.14	5.99	-2.64	50.50	69.67	0.05	0.35	0.69	NA	NA	NA
Pyl-4	116016	FRA	7.57	16.41	2.24	10.82	36.14	1.81	5.80	-1.36	38.00	67.00	0.04	0.27	0.45	NA	NA	NA
Vou-1	116020	FRA	8.74	14.81	-0.54	17.30	36.82	-3.99	6.22	-2.10	NA	NA	0.05	NA	NA	NA	NA	NA
Vou-10	116022	FRA	5.28	12.28	0.40	20.42	29.33	-14.60	5.30	-0.72	NA	NA	0.02	0.25	0.96	14.00	NA	NA
Vou-6	116024	FRA	8.71	15.15	-0.17	13.60	38.60	1.50	4.93	-1.06	NA	NA	0.05	0.51	0.94	16.00	19.00	-1.08
Vou-9	116026	FRA	8.52	15.57	0.45	13.48	36.18	-0.81	3.90	0.93	NA	NA	0.03	0.22	0.59	NA	16.00	NA
Zdy-62	2000000	CHI	NA	NA	NA	NA	NA	NA	NA	NA	NA	NA	NA	NA	NA	NA	NA	NA
Aqs-11	2189710	CHI	NA	14.53	NA	NA	35.17	NA	NA	NA	NA	61.67	NA	NA	NA	NA	NA	NA
Ayx-42	2189718	CHI	NA	NA	NA	NA	NA	NA	NA	NA	NA	67.00	0.04	0.20	0.24	NA	NA	NA
Jjgs-30	2204161	CHI	8.69	13.63	-1.66	12.76	33.28	-2.99	4.05	-0.41	43.00	48.33	0.06	0.37	0.55	NA	NA	NA
Jjj-32	2204162	CHI	7.66	13.49	-0.77	14.73	33.70	-4.54	4.01	0.46	45.00	53.33	0.06	NA	NA	NA	NA	NA
Zkh-29	2204168	CHI	NA	12.81	NA	NA	34.65	NA	NA	NA	NA	55.67	NA	NA	NA	NA	NA	NA
Zla-62	2204170	CHI	8.98	14.69	-0.90	13.25	33.52	-3.24	3.85	1.36	48.00	77.00	NA	NA	NA	NA	NA	NA
Hwc-61	2204174	CHI	8.06	14.49	-0.18	16.16	32.02	-7.65	4.34	-0.60	45.00	53.67	NA	NA	NA	NA	NA	NA
Cbb-60	2204175	CHI	NA	NA	NA	NA	NA	NA	NA	NA	34.00	41.00	0.06	0.55	0.93	NA	NA	NA
Gwx-11	2204177	CHI	7.26	13.47	-0.39	16.44	31.67	-8.28	4.47	1.05	47.00	47.00	0.08	NA	NA	NA	NA	NA
Smx-34	2204179	CHI	NA	10.56	NA	NA	30.71	NA	NA	NA	NA	48.00	NA	NA	NA	NA	NA	NA
Hnzjj-75	2204239	CHI	NA	NA	NA	NA	NA	NA	NA	NA	NA	71.33	NA	NA	NA	NA	NA	NA
Hyl-40	2204313	CHI	6.87	12.44	-1.04	11.94	30.43	-5.02	3.76	0.65	42.33	58.00	0.03	0.46	1.47	NA	NA	NA

Ygs-39	2204316	CHI	6.84	12.09	NA	16.66	30.84	NA	3.26	NA	51.67	63.67	0.06	0.48	0.72	NA	NA	NA
HNxy-46	2204317	CHI	NA	NA	NA	NA	NA	NA	NA	NA	40.00	44.00	0.04	NA	NA	NA	NA	NA
Xem	2204324	CHI	7.44	11.50	NA	18.43	28.55	NA	4.61	NA	54.00	74.67	0.05	NA	NA	NA	NA	NA
Ahthx-23	6414606	CHI	NA	12.03	NA	NA	34.98	NA	NA	NA	NA	64.50	NA	NA	NA	NA	NA	NA
Hha-21	6414609	CHI	7.41	13.50	-0.51	14.40	34.39	-3.52	4.18	0.78	44.67	55.00	0.04	NA	NA	NA	NA	NA
JSnj-8	6414610	CHI	NA	11.05	NA	NA	32.50	NA	NA	NA	NA	81.00	NA	0.25	NA	NA	3.00	NA

Table 28: Genotypic mean of each genotype in field conditions.

Each row shows the genotypic mean of each accession. The phenotypes are DD (Diameter in December), BO (Bolting in below-ground competition), FS (Final size in above-ground competition), H (Final plant height), FD (Flowering time in above-ground competition) in HD, LD and ID conditions, plus the GXE between conditions.

Genotype	ID	Country	DD HD	DD LD	GXE DD	BO HD	BO LD	GXE BO	FS LD	FS HD	FS ID	GXE FSLD HD	GXE FSL DID	GXE FSH DID	H LD	H HD	H ID	GXE HLD HD	GXE HLD ID	GXE HH DID	FD LD	FD HD	FD ID	GXE FDLD HD	GXE FDLD ID	GXE FDHDID
LDV-46	139	FRA	4.29	6.31	-0.75	156.54	163.15	0.02	4.15	3.90	4.00	NA	NA	NA	5.84	5.64	5.55	NA	NA	NA	184.98	173.43	182.22	NA	NA	NA
Doubravnik7	410	CZE	6.64	12.32	2.91	160.13	162.01	-0.01	NA	NA	NA	NA	NA	NA	NA	NA	NA	NA	NA	NA	NA	NA	NA	NA	NA	NA
Gr-1	430	AUT	5.44	5.02	-3.19	154.90	163.87	0.04	NA	NA	NA	NA	NA	NA	NA	NA	NA	NA	NA	NA	NA	NA	NA	NA	NA	NA
Ale-Stenar-41-1	991	SWE	NA	NA	NA	NA	NA	NA	NA	NA	NA	NA	NA	NA	NA	NA	NA	NA	NA	NA	NA	NA	NA	NA	NA	NA
Ale-Stenar-44-4	992	SWE	NA	NA	NA	NA	NA	NA	NA	NA	NA	NA	NA	NA	NA	NA	NA	NA	NA	NA	NA	NA	NA	NA	NA	NA
Ale-Stenar-56-14	997	SWE	9.91	12.68	NA	165.62	169.01	NA	4.38	3.73	4.27	0.30	-0.03	0.44	5.86	5.10	5.94	NA	-0.37	0.93	190.73	199.32	194.07	-12.00	-6.10	-14.04
Ale-Stenar-64-24	1002	SWE	5.50	6.86	-1.42	173.66	174.89	-0.01	4.46	4.09	3.77	-0.25	0.55	-0.42	5.80	5.71	5.49	-0.46	0.02	-0.13	196.72	201.22	198.90	-14.23	-4.93	-11.10
Brösarp-11-135	1061	SWE	NA	7.81	NA	NA	172.51	NA	4.37	3.98	3.96	0.07	0.27	-0.12	5.89	5.65	5.71	0.28	-0.11	0.15	197.17	197.54	194.81	-19.19	-0.39	-11.52
Brösarp-15-138	1062	SWE	4.00	9.16	2.39	176.60	181.01	0.00	4.04	3.81	3.97	-0.08	-0.07	0.06	5.73	5.37	5.65	0.14	-0.20	0.37	197.50	203.55	200.87	-17.46	-6.13	-11.47
Brösarp-21-140	1063	SWE	5.98	7.92	-0.83	161.91	169.95	0.03	4.18	3.55	4.07	-0.03	-0.04	0.41	6.02	5.66	5.89	0.12	-0.16	0.33	189.86	196.44	194.92	-15.00	-7.82	-10.31
Brösarp-34-145	1066	SWE	8.63	9.82	-1.58	164.37	169.95	0.01	4.26	4.11	3.88	0.21	0.23	-0.32	5.73	NA	5.68	0.33	-0.24	NA	196.54	NA	196.52	-15.23	-2.74	NA
Tos-82-387	1254	SWE	NA	11.34	NA	NA	156.75	NA	4.21	4.02	3.98	-0.06	0.08	-0.14	5.19	NA	5.45	0.25	-0.54	NA	188.08	189.86	188.07	-16.11	-2.75	-10.57
App1-12	5830	SWE	NA	5.73	NA	NA	169.95	NA	3.88	NA	3.79	-0.25	-0.06	NA	5.87	NA	5.47	0.15	0.11	NA	191.96	NA	NA	-14.43	NA	NA
App1-14	5831	SWE	8.23	14.25	3.25	161.80	169.01	0.02	4.33	4.06	3.95	-0.27	0.23	-0.21	NA	5.22	5.90	-0.07	NA	0.78	198.18	203.96	196.60	-13.50	-1.18	-16.14
App1-16	5832	SWE	8.13	13.73	2.83	155.63	157.01	-0.01	4.13	NA	4.24	0.22	-0.26	NA	6.12	NA	5.95	-0.53	-0.12	NA	189.43	NA	188.63	-17.85	-1.97	NA
Dra1-4	5865	SWE	5.93	6.90	-1.80	164.99	170.95	0.02	3.65	3.66	3.17	0.04	0.33	-0.59	5.63	4.86	5.15	-0.06	0.19	0.38	196.95	199.48	201.38	-16.93	-7.19	-6.88
Dra2-1	5867	SWE	6.99	7.21	-2.55	165.37	172.01	0.02	4.18	3.98	4.19	0.33	-0.15	0.11	5.69	5.83	5.79	-0.73	-0.39	0.05	196.31	190.12	205.79	-14.90	-12.24	6.88
DraIV2-9	5907	CZE	4.28	7.32	0.27	161.10	159.87	-0.03	NA	NA	NA	NA	NA	NA	NA	NA	NA	NA	NA	NA	NA	NA	NA	NA	NA	NA
Eden-1	6009	SWE	6.37	5.99	-3.16	155.63	168.39	0.06	4.16	3.66	3.99	-0.07	0.03	0.23	5.72	5.43	5.83	-0.02	-0.40	0.49	190.88	196.20	193.86	-8.91	-5.73	-11.12

Eden-6	6011	SWE	8.34	12.61	1.50	158.55	157.01	-0.03	4.31	4.14	4.19	0.34	-0.03	-0.05	5.96	6.08	6.00	-0.11	-0.32	0.01	190.96	193.27	193.11	-8.13	-4.91	-8.95
Eden-7	6012	SWE	5.73	10.82	2.32	152.69	161.01	0.03	4.21	4.00	4.07	0.10	-0.01	-0.03	NA	5.47	5.78	0.33	NA	0.40	187.95	192.67	193.50	-14.27	-8.31	-7.95
Eds-1	6016	SWE	9.74	12.90	0.39	160.05	165.51	0.01	4.18	4.21	4.20	0.25	-0.16	-0.11	6.15	NA	4.59	-0.26	1.28	NA	190.41	NA	196.54	-19.82	-8.89	NA
Fjä1-2	6019	SWE	5.87	12.04	3.39	162.73	168.51	0.01	4.07	4.24	3.93	0.10	-0.01	-0.40	5.51	5.37	4.95	0.02	0.28	-0.33	188.37	198.52	197.27	-21.07	-11.66	-10.03
Fjä1-5	6020	SWE	6.43	5.21	-3.99	162.31	171.77	0.04	4.21	3.93	NA	0.14	NA	NA	5.62	5.58	NA	0.04	NA	NA	195.48	193.97	NA	-23.73	NA	NA
Fjä2-4	6021	SWE	4.74	8.51	1.00	165.09	167.01	-0.01	4.37	3.88	4.12	0.22	0.11	0.14	5.55	5.48	5.06	0.30	0.20	-0.33	191.58	194.09	196.89	-9.99	-8.07	-5.99
Fly2-1	6023	SWE	7.69	10.27	-0.19	166.49	173.01	0.02	4.37	3.96	4.02	0.19	0.21	-0.04	5.20	NA	5.49	0.02	-0.58	NA	188.83	187.67	188.42	1.96	-2.36	-8.03
Fly2-2	6024	SWE	6.11	8.13	-0.76	168.80	171.01	-0.01	4.12	3.48	3.70	-0.31	0.27	0.12	5.68	NA	5.88	0.31	-0.49	NA	200.71	NA	197.76	NA	0.19	NA
Hov1-10	6035	SWE	5.86	8.04	-0.59	160.48	165.51	0.01	4.26	3.77	3.93	-0.05	0.18	0.06	5.44	5.33	5.67	NA	-0.52	0.43	190.67	192.65	190.69	-20.05	-2.78	-10.74
Hov3-2	6036	SWE	6.94	9.22	-0.49	166.50	172.51	0.02	4.24	3.96	4.07	0.26	0.02	0.02	5.97	5.76	5.60	0.52	0.08	-0.07	191.55	194.57	192.46	-16.60	-3.67	-10.90
Hov3-5	6038	SWE	5.99	11.35	2.59	172.04	173.45	-0.01	4.29	3.88	4.00	-0.10	0.14	0.02	6.03	6.06	6.04	0.24	-0.30	0.08	190.96	196.44	194.73	NA	-6.52	-10.50
Hovdala-2	6039	SWE	5.12	7.30	-0.60	167.11	170.51	0.00	4.50	4.18	4.04	-0.57	0.31	-0.24	5.97	6.03	6.01	NA	-0.33	0.08	186.68	191.47	187.98	-4.20	-4.06	-12.27
Kni-1	6040	SWE	5.87	6.39	-2.25	164.25	167.87	0.00	4.27	3.98	4.17	0.18	-0.04	0.08	6.00	NA	5.65	-0.30	0.07	NA	189.99	200.48	196.05	-27.05	-8.83	-13.21
Lis-3	6041	SWE	5.86	7.20	-1.44	164.38	169.95	0.01	4.42	4.16	3.91	0.00	0.37	-0.36	5.37	5.94	5.77	0.12	-0.68	-0.07	186.27	191.71	191.21	NA	-7.70	-9.28
Nyl-7	6069	SWE	6.72	11.57	2.08	162.78	169.51	0.02	4.29	3.81	NA	0.30	NA	NA	5.75	6.02	NA	0.64	NA	NA	197.49	198.53	NA	-14.91	NA	NA
Omn-5	6071	SWE	5.51	7.33	-0.96	160.70	164.51	0.00	4.20	3.79	3.58	0.31	0.48	-0.31	5.75	5.55	5.44	-0.25	0.02	-0.03	196.29	197.54	195.81	-16.33	-2.27	-10.51
Ömö1-7	6073	SWE	6.25	10.48	1.46	163.78	167.87	0.00	4.18	3.94	3.87	NA	0.16	-0.16	5.40	5.07	5.14	0.87	-0.02	0.16	191.76	196.61	194.73	NA	-5.73	-10.67
Rev-2	6076	SWE	7.65	9.23	-1.19	162.60	167.01	0.01	4.28	4.16	3.98	-0.37	0.15	-0.29	5.78	5.42	NA	NA	NA	NA	193.22	196.27	NA	-11.89	NA	NA
Sparta-1	6085	SWE	6.21	8.09	-0.90	164.17	172.51	0.03	4.28	3.90	3.94	0.38	0.20	-0.06	5.81	NA	4.78	-0.17	0.75	NA	194.34	NA	196.77	-16.45	-5.19	NA
T1000	6090	SWE	5.19	7.42	-0.54	165.72	171.95	0.02	4.17	NA	4.12	0.58	-0.10	NA	5.82	NA	5.95	0.09	-0.42	NA	193.59	NA	196.93	-8.59	-6.10	NA
T1040	6094	SWE	7.65	8.47	-1.96	168.75	174.95	0.02	4.38	3.95	4.10	0.06	0.14	0.05	5.90	5.38	5.85	0.99	-0.23	0.55	192.89	199.94	188.11	-15.56	2.01	-20.61
T1070	6097	SWE	5.92	7.81	-0.88	168.78	172.95	0.00	4.38	4.09	4.17	-0.07	0.07	-0.03	5.94	5.59	5.62	-0.33	0.03	0.12	193.98	199.00	200.52	-16.66	-9.30	-7.26
T1110	6100	SWE	7.91	10.31	-0.37	163.24	170.01	0.02	4.21	4.21	4.04	-0.14	0.02	-0.27	NA	5.83	5.85	-0.03	NA	0.10	205.15	199.18	195.85	-11.95	6.55	-12.12
T1160	6104	SWE	4.74	4.96	-2.56	177.18	180.51	0.00	4.11	4.05	4.05	-0.04	-0.09	-0.10	6.00	5.82	5.95	-0.56	-0.24	0.22	194.28	199.67	196.80	-11.49	-5.29	-11.65
T450	6105	SWE	5.95	8.29	-0.44	165.05	169.01	0.00	4.25	3.52	3.80	0.03	0.30	0.18	5.66	4.67	4.94	-0.08	0.43	0.36	185.94	NA	194.73	-16.13	-11.55	NA
T460	6106	SWE	4.91	4.90	-2.78	167.47	170.45	0.00	4.37	4.09	3.55	0.02	0.68	-0.64	5.81	5.78	5.47	-0.14	0.05	-0.22	191.68	196.23	200.61	-14.10	-11.69	-4.40
T470	6107	SWE	6.81	10.29	0.71	164.68	172.01	0.02	4.39	3.89	4.01	0.09	0.24	0.02	5.63	5.28	5.66	0.14	-0.32	0.47	198.94	197.66	194.88	-16.07	1.30	-11.57
T480	6108	SWE	5.90	6.94	-1.73	161.80	170.01	0.03	4.49	4.11	4.23	-0.04	0.12	0.01	5.73	5.52	5.91	-0.10	-0.46	0.48	187.96	198.60	189.77	-17.30	-4.57	-17.62
T510	6109	SWE	NA	NA	NA	NA	NA	NA	NA	NA	NA	NA	NA	NA	NA	NA	NA	NA	NA	NA	NA	NA	NA	NA	NA	NA
T530	6111	SWE	7.12	8.26	-1.64	163.44	170.01	0.02	4.39	3.99	4.29	0.02	-0.05	0.21	5.68	5.72	5.83	-0.19	-0.44	0.20	193.56	197.92	195.04	-13.95	-4.24	-11.66
T540	6112	SWE	6.55	10.50	1.18	161.70	167.01	0.01	4.39	3.87	4.16	0.26	0.08	0.19	5.29	5.43	5.85	-0.06	-0.84	0.51	189.96	194.81	194.57	-14.73	-7.37	-9.02
T570	6114	SWE	7.41	8.70	-	162.	171.0	0.03	4.01	4.02	3.79	0.25	0.08	-	5.54	5.77	6.03	-	-	0.35	195.	197.	194.4	-18.44	-1.86	-12.20

					1.48	10	1							0.33				0.02	0.78		40	91	9			
T610	6118	SWE	6.70	10.79	1.31	172.13	176.01	0.00	4.17	3.97	3.99	0.10	0.04	-0.09	5.98	5.75	5.84	0.62	-0.15	0.18	194.31	199.82	198.05	-15.19	-6.50	-10.56
T670	6122	SWE	6.38	9.22	0.08	166.45	169.95	0.00	4.01	3.70	4.06	-0.27	-0.19	0.26	5.46	5.28	5.14	-0.32	0.03	-0.05	193.89	200.93	196.81	-7.91	-5.67	-12.92
T710	6125	SWE	NA	7.08	NA	NA	169.77	NA	4.25	3.82	4.04	0.06	0.07	0.12	5.65	4.75	5.32	-0.40	0.04	0.66	191.99	198.51	196.88	-18.37	-7.65	-10.42
T720	6126	SWE	6.60	9.39	0.02	163.99	170.01	0.02	4.45	3.87	4.01	0.30	0.30	0.03	5.69	5.34	5.69	-0.02	-0.29	0.44	198.23	198.40	197.65	-15.35	-2.18	-9.54
T740	6128	SWE	8.88	7.11	-4.54	169.44	179.01	0.03	4.32	4.14	3.77	-0.10	0.40	-0.47	5.53	5.53	4.71	0.27	0.53	-0.73	196.46	200.27	200.97	-11.85	-7.27	-8.09
T780	6131	SWE	6.42	7.44	-1.75	166.80	175.01	0.03	4.03	4.03	3.90	0.18	-0.01	-0.24	5.47	5.73	5.83	-0.03	-0.65	0.19	196.72	199.41	198.83	-19.75	-4.87	-9.36
T790	6132	SWE	5.83	6.70	-1.90	162.66	167.89	0.01	4.36	4.05	4.18	0.11	0.04	0.04	5.75	5.28	5.74	0.16	-0.27	0.55	194.72	202.37	197.84	-16.86	-5.87	-13.32
T800	6133	SWE	6.25	7.13	-1.89	172.90	179.02	0.01	4.18	4.01	4.16	NA	-0.13	0.05	5.77	5.43	5.87	-0.17	-0.39	0.54	193.44	199.36	197.68	NA	-7.00	-10.46
T810	6134	SWE	4.09	4.66	-2.21	168.72	178.51	0.04	4.16	3.94	4.08	0.08	-0.06	0.04	5.66	5.34	5.71	NA	-0.34	0.46	195.94	199.40	196.17	-17.86	-2.98	-12.02
T840	6136	SWE	4.86	5.10	-2.53	162.01	167.51	0.01	4.34	3.88	4.07	0.45	0.13	0.08	6.06	5.53	5.91	-0.15	-0.14	0.47	191.26	194.94	193.78	-15.13	-5.28	-9.95
T860	6138	SWE	4.74	5.73	-1.78	168.61	172.51	0.00	4.07	3.89	3.99	0.15	-0.06	-0.01	6.07	5.63	5.87	-0.02	-0.08	0.33	189.91	194.48	194.14	-13.24	-6.98	-9.13
T880	6140	SWE	4.98	5.78	-1.97	167.60	172.51	0.01	4.32	4.00	3.93	0.16	0.24	-0.18	5.70	5.69	5.56	0.08	-0.14	-0.04	192.56	198.82	197.11	-12.51	-7.30	-10.50
T900	6142	SWE	5.25	6.84	-1.18	159.62	163.27	0.00	4.22	4.01	4.12	-0.22	-0.04	0.01	6.04	5.97	5.96	-0.10	-0.21	0.08	191.00	195.15	191.69	-10.59	-3.45	-12.25
T930	6145	SWE	7.74	10.51	0.00	176.92	180.51	0.00	4.27	4.21	3.75	0.12	0.38	-0.56	5.92	6.08	5.33	NA	0.31	-0.66	195.49	198.10	200.57	-22.00	-7.84	-6.31
T960	6148	SWE	5.20	6.12	-1.85	167.04	173.51	0.02	4.31	3.92	4.08	-0.23	0.08	0.06	5.79	5.86	NA	-0.19	NA	NA	195.28	200.05	NA	-16.49	NA	NA
T980	6150	SWE	4.74	6.08	-1.43	165.86	171.45	0.01	3.99	4.01	3.32	-0.05	0.52	-0.79	5.89	5.48	5.37	-0.02	0.24	-0.02	191.61	197.34	198.53	-19.13	-9.68	-7.60
T990	6151	SWE	5.21	5.39	-2.59	162.90	174.95	0.05	4.30	3.66	4.22	0.03	-0.06	0.46	4.90	4.30	NA	0.11	NA	NA	196.03	195.94	NA	NA	NA	NA
TAA 03	6153	SWE	5.76	8.08	-0.45	163.15	164.39	-0.01	4.13	3.96	3.81	0.21	0.17	-0.24	5.76	5.76	5.78	NA	-0.30	0.11	194.03	198.98	196.72	-24.97	-5.45	-11.05
TAA 04	6154	SWE	7.60	7.57	-2.80	160.70	164.51	0.00	3.92	3.38	3.68	-0.03	0.09	0.20	5.72	5.43	5.72	0.30	-0.28	0.38	192.60	199.14	195.00	-11.49	-5.16	-12.93
TAA 14	6163	SWE	7.82	9.50	-1.09	157.63	164.01	0.02	3.76	3.06	3.66	0.08	-0.05	0.50	6.01	4.82	5.43	-0.24	0.30	0.69	195.18	195.53	196.98	-14.91	-4.56	-7.34
TBÖ 01	6184	SWE	7.28	10.57	0.52	153.12	157.45	0.01	4.27	4.13	4.03	0.20	0.10	-0.20	5.93	NA	5.93	0.15	-0.29	NA	187.23	193.40	190.57	-13.00	-6.10	-11.62
TDr-1	6188	SWE	5.73	10.67	2.17	161.64	158.77	-0.04	4.19	4.12	4.11	0.25	-0.07	-0.11	5.39	5.50	5.59	-1.70	-0.49	0.18	184.28	181.29	177.58	-17.06	3.94	-12.50
TDr-2	6189	SWE	4.58	6.73	-0.62	163.54	173.27	0.04	4.39	3.78	NA	0.07	NA	NA	6.19	4.97	NA	-0.06	NA	NA	180.84	187.33	NA	-16.97	NA	NA
TDr-4	6191	SWE	5.69	6.91	-1.55	157.48	164.87	0.03	4.04	4.05	3.97	-0.07	-0.08	-0.18	NA	5.58	5.79	0.35	NA	0.29	189.01	196.05	191.07	-20.49	-4.82	-13.76
TDr-5	6192	SWE	4.00	4.46	-2.31	166.65	168.51	-0.01	4.20	3.96	3.86	-0.03	0.19	-0.20	6.01	5.84	5.67	-0.13	0.05	-0.08	191.74	193.57	195.02	-15.17	-6.03	-7.34
TDr-7	6193	SWE	5.53	8.74	0.44	158.84	163.51	0.01	4.12	4.06	3.75	0.05	0.22	-0.41	5.79	5.47	5.29	-0.02	0.21	-0.09	191.77	192.43	189.59	-12.89	-0.58	-11.62
TDr-8	6194	SWE	5.27	7.27	-0.77	177.18	183.14	0.01	3.96	3.30	3.26	0.27	0.56	-0.15	6.11	5.12	5.36	-0.30	0.46	0.33	198.59	207.30	206.52	-24.46	-10.69	-9.57
TDr-9	6195	SWE	5.31	7.14	-0.93	163.19	167.83	0.01	4.33	3.66	4.16	0.23	0.02	0.40	5.85	5.13	5.98	-0.15	-0.42	0.95	182.35	194.97	187.72	-13.08	-8.13	-16.03
TDr-13	6198	SWE	6.19	8.03	-0.93	174.75	176.01	-0.01	NA	NA	NA	NA	NA	NA	NA	NA	NA	NA	NA	NA	NA	NA	NA	NA	NA	NA
TDr-16	6201	SWE	NA	NA	NA	NA	NA	NA	NA	NA	NA	NA	NA	NA	NA	NA	NA	NA	NA	NA	NA	NA	NA	NA	NA	NA
TDr-17	6202	SWE	3.94	5.75	-0.97	165.68	171.01	0.01	4.31	4.21	3.89	-0.07	0.27	-0.42	6.03	5.95	5.55	0.19	0.19	-0.30	189.80	196.52	196.98	-16.59	-9.94	-8.32

TDr-18	6203	SWE	5.90	5.81	-2.86	165.11	170.51	0.01	4.23	3.76	3.91	0.21	0.18	0.05	5.89	5.54	5.70	0.31	-0.09	0.25	193.13	194.74	196.13	-16.88	-5.76	-7.40
TEDEN02	6209	SWE	5.98	10.79	2.04	158.65	160.51	-0.01	4.17	3.86	4.13	0.16	-0.10	0.17	5.11	5.31	5.55	0.32	-0.72	0.33	194.73	189.07	192.82	-12.14	-0.85	-5.04
TFÄ 07	6217	SWE	5.39	5.03	-3.13	159.95	165.51	0.01	4.11	NA	3.78	-0.11	0.19	NA	5.95	NA	NA	-0.12	NA	NA	189.96	NA	192.25	-13.67	-5.05	NA
TOM01	6235	SWE	5.27	11.78	3.74	162.49	161.51	-0.03	4.06	3.78	3.78	0.38	0.14	-0.10	6.05	5.70	6.05	-0.07	-0.28	0.43	193.10	198.07	194.41	-13.22	-4.06	-12.45
TOM06	6240	SWE	5.32	7.39	-0.71	159.99	160.01	-0.02	3.79	3.80	3.80	-0.06	-0.15	-0.10	5.72	5.59	5.90	-0.23	-0.47	0.40	190.84	193.73	191.77	-10.34	-3.69	-10.74
Tomega p-2	6242	SWE	NA	NA	NA	NA	NA	NA	NA	NA	NA	NA	NA	NA	NA	NA	NA	NA	NA	NA	NA	NA	NA	NA	NA	NA
TV-10	6258	SWE	NA	NA	NA	NA	NA	NA	NA	NA	NA	NA	NA	NA	NA	NA	NA	NA	NA	NA	NA	NA	NA	NA	NA	NA
TV-22	6268	SWE	6.09	7.01	-1.85	165.72	167.01	-0.01	4.31	4.34	4.16	0.21	0.00	-0.27	5.19	5.53	5.27	-0.61	-0.37	-0.16	188.84	190.80	192.97	-4.54	-6.89	-6.61
TV-38	6284	SWE	NA	NA	NA	NA	NA	NA	NA	NA	NA	NA	NA	NA	NA	NA	NA	NA	NA	NA	NA	NA	NA	NA	NA	NA
Udul 1-11	6296	CZE	5.04	7.79	-0.02	162.24	165.51	0.00	NA	NA	NA	NA	NA	NA	NA	NA	NA	NA	NA	NA	NA	NA	NA	NA	NA	NA
Ull3-4	6413	SWE	NA	NA	NA	NA	NA	NA	NA	NA	NA	NA	NA	NA	NA	NA	NA	NA	NA	NA	NA	NA	NA	NA	NA	NA
Zdrl 1-23	6424	CZE	5.31	5.83	-2.26	161.63	167.51	0.02	NA	NA	NA	NA	NA	NA	NA	NA	NA	NA	NA	NA	NA	NA	NA	NA	NA	NA
Zdrl 2-21	6445	CZE	6.80	8.06	-1.52	147.91	151.95	0.01	NA	NA	NA	NA	NA	NA	NA	NA	NA	NA	NA	NA	NA	NA	NA	NA	NA	NA
Bor-4	6903	CZE	5.81	3.77	-4.82	157.68	164.45	0.02	NA	NA	NA	NA	NA	NA	NA	NA	NA	NA	NA	NA	NA	NA	NA	NA	NA	NA
Ei-2	6915	GER	5.60	5.98	-2.39	157.88	170.51	0.06	4.29	3.82	3.87	-0.03	0.27	-0.05	5.68	5.54	5.74	0.58	-0.35	0.29	185.64	191.94	188.53	-11.71	-5.65	-12.20
LL-0	6933	ESP	4.71	7.02	-0.46	143.59	140.01	-0.05	4.48	4.20	NA	0.26	NA	NA	5.01	5.55	NA	-0.32	NA	NA	168.02	173.41	NA	-16.13	NA	NA
NFA-8	6944	UK	4.75	7.39	-0.13	159.09	150.83	-0.07	NA	NA	NA	NA	NA	NA	NA	NA	NA	NA	NA	NA	NA	NA	NA	NA	NA	NA
Nok-3	6945	NED	5.58	9.78	1.43	165.11	171.01	0.01	NA	NA	NA	NA	NA	NA	NA	NA	NA	NA	NA	NA	NA	NA	NA	NA	NA	NA
Pu2-8	6957	CZE	5.78	5.70	-2.86	152.04	160.51	0.03	NA	NA	NA	NA	NA	NA	NA	NA	NA	NA	NA	NA	NA	NA	NA	NA	NA	NA
Se-0	6961	ESP	6.13	11.70	2.80	141.38	137.51	-0.05	4.63	4.06	4.47	0.03	0.02	0.31	5.33	5.16	5.52	0.55	-0.47	0.45	167.85	171.20	170.48	-14.22	-5.39	-9.50
Tamm-27	6969	FIN	5.93	9.29	0.60	155.57	153.01	-0.04	NA	NA	NA	NA	NA	NA	NA	NA	NA	NA	NA	NA	NA	NA	NA	NA	NA	NA
Ts-1	6970	ESP	5.64	10.32	1.90	143.60	139.01	-0.05	4.53	4.36	NA	0.20	NA	NA	5.41	5.32	NA	-0.39	NA	NA	175.52	172.88	NA	-13.09	NA	NA
Ts-5	6971	ESP	5.48	7.32	-0.93	146.51	142.14	-0.05	4.68	4.10	4.33	0.06	0.21	0.13	5.45	4.93	5.08	-0.18	0.09	0.24	174.21	170.79	168.71	-13.21	2.74	-10.86
Ull2-5	6974	SWE	6.60	6.44	-2.93	160.90	166.89	0.02	4.38	4.03	NA	0.05	NA	NA	5.71	5.77	NA	-1.31	NA	NA	192.76	195.49	NA	-13.43	NA	NA
Ws-2	6981	RUS	4.24	6.92	-0.09	163.40	163.01	-0.02	NA	NA	NA	NA	NA	NA	NA	NA	NA	NA	NA	NA	NA	NA	NA	NA	NA	NA
Wt-5	6982	GER	5.71	7.68	-0.80	160.04	164.89	0.01	4.51	4.01	4.21	0.14	0.16	0.10	5.97	5.75	5.75	-0.67	-0.07	0.09	183.02	191.29	184.76	-3.77	-4.50	-15.32
Ak-1	6987	GER	5.14	6.20	-1.72	151.25	152.01	-0.02	4.21	3.87	3.95	-0.11	0.12	-0.02	5.71	5.48	5.62	-0.09	-0.20	0.24	169.43	178.95	171.50	-8.51	-4.84	-16.23
Alst-1	6989	UK	6.22	6.28	-2.71	157.88	166.51	0.03	NA	NA	NA	NA	NA	NA	NA	NA	NA	NA	NA	NA	NA	NA	NA	NA	NA	NA
Baa-1	7002	NED	5.85	10.84	2.22	NA	155.51	NA	NA	NA	NA	NA	NA	NA	NA	NA	NA	NA	NA	NA	NA	NA	NA	NA	NA	NA
Bs-1	7003	SUI	6.16	9.77	0.84	158.16	160.51	-0.01	NA	NA	NA	NA	NA	NA	NA	NA	NA	NA	NA	NA	NA	NA	NA	NA	NA	NA
Benk-1	7008	NED	5.21	8.96	0.98	163.69	166.01	-0.01	NA	NA	NA	NA	NA	NA	NA	NA	NA	NA	NA	NA	NA	NA	NA	NA	NA	NA
Bd-0	7013	GER	6.52	10.95	1.66	155.50	154.45	-0.03	4.38	3.99	NA	-0.13	NA	NA	5.74	5.24	NA	-0.01	NA	NA	172.63	184.81	NA	-18.39	NA	NA

Bur-0	7058	ESP	7.52	11.37	1.08	155.07	158.33	0.00	NA	NA	NA	NA	NA	NA	NA	NA	NA	NA	NA	NA	NA	NA	NA	NA	NA
Ca-0	7062	GER	6.15	7.21	-1.71	162.32	163.01	-0.02	4.38	3.91	3.67	0.14	0.56	-0.33	5.80	5.58	5.31	0.02	0.20	-0.18	179.31	177.76	192.54	-6.50	-15.99	6.00
En-2	7119	GER	4.94	7.76	0.05	164.17	169.51	0.01	4.28	3.84	3.86	-0.03	0.28	-0.09	5.61	5.11	5.15	NA	0.18	0.13	190.06	176.56	182.82	-9.40	4.49	-2.53
Fr-2	7133	GER	5.08	7.51	-0.34	157.57	164.87	0.03	4.08	4.14	4.06	-0.06	-0.13	-0.18	NA	5.84	NA	0.43	NA	NA	NA	186.47	177.37	-13.21	NA	-17.88
Gie-0	7147	GER	7.56	10.58	0.25	162.41	170.01	0.03	4.20	4.00	4.02	-0.07	0.03	-0.09	5.82	5.10	5.66	-2.85	-0.13	0.65	188.66	197.17	191.33	-15.19	-5.42	-14.63
Gr-5	7158	AUT	6.39	6.13	-3.03	144.61	152.01	0.03	NA	NA	NA	NA	NA	NA	NA	NA	NA	NA	NA	NA	NA	NA	NA	NA	NA	NA
Hau-0	7164	DEN	5.09	9.27	1.41	NA	NA	NA	NA	NA	NA	NA	NA	NA	NA	NA	NA	NA	NA	NA	NA	NA	NA	NA	NA	NA
Hh-0	7169	GER	7.58	8.74	-1.62	163.24	169.95	0.02	4.54	4.03	4.24	NA	0.15	0.10	5.83	5.39	5.67	NA	-0.12	0.37	190.85	195.90	193.11	NA	-5.02	-11.58
Hh-0	7169	GER	7.58	8.74	-1.62	163.24	169.95	0.02	4.54	4.03	4.24	NA	0.15	0.10	5.83	5.39	5.67	NA	-0.12	0.37	190.85	195.90	193.11	NA	-5.02	-11.58
Jm-0	7177	CZE	6.27	4.75	-4.29	161.34	168.51	0.02	NA	NA	NA	NA	NA	NA	NA	NA	NA	NA	NA	NA	NA	NA	NA	NA	NA	NA
Kyoto	7207	JPN	6.14	9.06	0.15	157.75	161.95	0.01	NA	NA	NA	NA	NA	NA	NA	NA	NA	NA	NA	NA	NA	NA	NA	NA	NA	NA
Mnz-0	7244	GER	6.03	7.25	-1.55	159.79	167.51	0.03	4.23	4.08	3.90	-0.03	0.19	-0.29	5.51	NA	5.76	NA	-0.53	NA	180.18	NA	189.63	-10.67	-12.21	NA
Mh-0	7255	POL	6.70	10.49	1.01	157.99	162.45	0.01	NA	NA	NA	NA	NA	NA	NA	NA	NA	NA	NA	NA	NA	NA	NA	NA	NA	NA
Np-0	7268	GER	6.82	14.38	4.79	161.59	162.51	-0.01	4.13	4.45	4.15	0.95	-0.16	-0.40	6.09	6.19	5.68	0.23	0.12	-0.42	186.82	179.48	197.03	NA	-12.97	8.76
Ob-0	7276	GER	5.80	10.28	1.71	164.49	167.01	-0.01	4.39	3.96	4.10	-0.02	0.14	0.04	6.09	5.78	6.01	NA	-0.20	0.32	180.43	195.94	186.20	-13.33	-8.53	-18.52
Oy-0	7288	NOR	5.82	8.92	0.33	156.88	155.01	-0.03	NA	NA	NA	NA	NA	NA	NA	NA	NA	NA	NA	NA	NA	NA	NA	NA	NA	NA
Pt-0	7305	GER	6.78	12.00	2.45	164.13	171.51	0.02	4.48	4.24	4.11	-0.05	0.23	-0.23	6.07	5.24	5.54	0.06	0.25	0.39	177.73	NA	183.81	-14.24	-8.84	NA
Sf-1	7327	ESP	7.56	10.22	-0.11	136.65	139.01	0.00	4.53	3.98	4.24	-0.16	0.15	0.15	5.51	5.56	5.50	-0.16	-0.28	0.03	168.54	171.91	171.16	-9.87	-5.38	-9.53
Sf-2	7328	ESP	6.92	10.57	0.88	135.41	135.89	-0.02	4.49	3.93	4.39	-0.26	-0.05	0.36	5.79	4.73	NA	-0.60	NA	NA	167.53	172.32	169.30	-15.71	-4.53	-11.80
Sp-0	7343	GER	7.91	11.42	0.74	157.37	163.01	0.01	4.34	NA	4.52	-0.39	-0.32	NA	5.95	NA	NA	NA	NA	NA	178.25	NA	170.89	-11.70	4.60	NA
Sten-0	7346	GER	5.73	8.85	0.35	168.66	171.01	-0.01	3.90	4.03	3.89	0.07	-0.14	-0.24	5.85	5.82	5.43	0.46	0.13	-0.30	191.05	191.39	193.59	-12.44	-5.30	-6.59
Sten-0	7346	GER	5.73	8.85	0.35	168.66	171.01	-0.01	3.90	4.03	3.89	0.07	-0.14	-0.24	5.85	5.82	5.43	0.46	0.13	-0.30	191.05	191.39	193.59	-12.44	-5.30	-6.59
Ting-1	7354	SWE	5.43	7.25	-0.95	163.54	162.51	-0.03	4.40	3.77	4.02	0.11	0.24	0.14	5.60	5.32	5.76	-0.09	-0.45	0.53	192.88	197.78	194.12	NA	-4.00	-12.44
Utrecht	7382	NED	6.96	8.51	-1.23	149.23	160.51	0.05	NA	NA	NA	NA	NA	NA	NA	NA	NA	NA	NA	NA	NA	NA	NA	NA	NA	NA
Van-0	7383	CAN	4.29	7.86	0.80	144.17	157.01	0.07	NA	NA	NA	NA	NA	NA	NA	NA	NA	NA	NA	NA	NA	NA	NA	NA	NA	NA
Gy-0	8214	FRA	5.62	6.30	-2.09	150.59	153.95	0.00	4.34	3.52	3.94	NA	0.26	0.32	5.80	4.62	5.57	0.04	-0.05	1.04	179.51	176.55	179.80	NA	-3.05	-5.54
Lis-2	8222	SWE	7.03	9.02	-0.78	163.10	169.01	0.02	4.39	4.09	3.90	NA	0.34	-0.29	5.70	5.83	5.76	NA	-0.34	0.01	190.32	194.34	193.17	NA	-5.60	-9.96
THÖ 03	8227	SWE	6.78	7.32	-2.23	160.67	168.51	0.03	4.02	3.85	3.80	0.39	0.08	-0.15	5.85	5.69	5.83	NA	-0.26	0.23	194.85	199.96	196.79	-14.55	-4.70	-11.96
Brö1-6	8231	SWE	5.23	8.63	0.62	157.66	162.51	0.01	4.25	4.14	3.89	-0.17	0.22	-0.36	5.56	5.93	5.74	-0.02	-0.46	-0.10	193.54	193.94	198.53	-10.01	-7.75	-4.20
Gul1-2	8234	SWE	6.75	11.96	2.45	162.79	168.01	0.01	4.04	3.84	4.13	0.08	-0.23	0.19	5.65	5.54	5.53	-0.83	-0.16	0.08	194.84	194.78	192.54	-22.73	-0.46	-11.03
Kävlinge-1	8237	SWE	6.11	9.05	0.17	164.66	169.51	0.01	4.38	4.11	4.03	NA	0.20	-0.18	5.67	5.62	5.64	0.54	-0.26	0.11	191.19	195.77	193.70	NA	-5.27	-10.86
Kulture	8240	SWE	5.09	7.04	-	160.	161.5	-	4.19	3.93	4.09	0.14	-	0.07	5.86	5.53	5.69	NA	-	0.26	191.	193.	188.8	-21.21	-0.25	-13.85

n-1					0.83	61	1	0.01					0.05						0.12		40	95	9			
Liarum	8241	SWE	5.82	9.82	1.22	163.69	170.01	0.02	4.31	3.97	4.06	0.05	0.11	-0.02	5.89	5.79	5.91	0.25	-0.31	0.21	191.80	196.33	193.54	-12.80	-4.50	-11.57
Lillö-1	8242	SWE	4.92	8.68	0.99	163.50	167.51	0.00	4.33	4.12	4.01	0.17	0.18	-0.22	5.76	5.75	5.61	0.65	-0.14	-0.05	187.80	193.55	195.46	-18.78	-10.43	-6.88
San-2	8247	SWE	5.43	11.32	3.11	165.12	167.01	-0.01	4.34	4.07	3.91	-0.17	0.28	-0.26	6.01	5.88	5.74	0.55	-0.02	-0.04	191.00	193.41	192.79	-5.52	-4.54	-9.41
Vimmerby	8249	SWE	8.35	11.22	0.10	156.05	162.01	0.02	4.11	3.60	3.83	0.64	0.13	0.13	5.84	5.67	5.97	-0.19	-0.42	0.40	189.00	192.18	193.06	-10.00	-6.82	-7.91
Bå1-2	8256	SWE	5.86	11.00	2.37	159.68	164.51	0.01	4.21	3.72	4.12	0.12	-0.06	0.30	6.09	5.27	5.98	0.81	-0.18	0.80	189.41	196.30	189.82	-8.93	-3.17	-15.27
Bå5-1	8259	SWE	5.91	8.80	0.11	163.60	162.51	-0.03	4.40	4.05	4.16	-0.09	0.10	0.00	5.20	5.33	5.74	-0.16	-0.82	0.50	195.10	198.74	195.43	-10.00	-3.09	-12.10
Bla-1	8264	ESP	5.86	8.95	0.32	148.57	152.01	0.00	4.19	4.21	4.39	0.20	-0.35	0.08	5.46	5.66	NA	-0.15	NA	NA	174.41	170.78	NA	-26.65	NA	NA
Dra3-1	8283	SWE	NA	NA	NA	NA	NA	NA	NA	NA	NA	NA	NA	NA	NA	NA	NA	NA	NA	NA	NA	NA	NA	NA	NA	NA
Hov4-1	8306	SWE	7.03	10.12	0.31	176.16	178.95	0.00	4.33	4.03	3.93	0.19	0.26	-0.20	5.81	5.64	5.63	0.69	-0.11	0.08	196.54	203.36	199.79	-18.80	-6.01	-12.36
Hovdala-6	8307	SWE	8.27	11.95	0.90	161.06	167.51	0.02	4.28	3.73	4.05	NA	0.08	0.22	6.02	5.55	5.94	-0.14	-0.20	0.47	188.47	192.27	190.73	NA	-5.02	-10.33
Lis-1	8326	SWE	6.88	12.16	2.51	163.25	164.01	-0.02	4.33	4.18	3.93	0.15	0.26	-0.36	5.76	5.60	5.86	NA	-0.38	0.35	197.52	197.83	189.23	-15.20	5.53	-17.38
Lund	8335	SWE	4.80	9.17	1.59	175.83	176.95	-0.01	4.10	3.67	4.03	0.16	-0.08	0.26	5.65	5.30	5.87	0.65	-0.50	0.66	196.41	204.61	198.87	-24.37	-5.22	-14.53
Mir-0	8337	ITA	NA	NA	NA	NA	NA	NA	NA	NA	NA	NA	NA	NA	NA	NA	NA	NA	NA	NA	NA	NA	NA	NA	NA	NA
Ost-0	8351	SWE	6.56	7.92	-1.41	154.16	163.51	0.04	4.38	4.03	4.04	-0.04	0.19	-0.09	5.60	5.58	5.66	-0.21	-0.34	0.18	190.20	195.51	191.02	-16.19	-3.58	-13.28
Rev-1	8369	SWE	5.70	9.20	0.72	166.62	168.45	-0.01	4.22	NA	3.99	0.24	0.09	NA	5.21	NA	5.64	1.22	-0.72	NA	192.68	NA	188.65	-14.29	1.27	NA
Sanna-2	8376	SWE	6.15	8.39	-0.53	164.81	163.01	-0.03	4.27	3.94	4.12	-0.09	0.00	0.08	5.98	5.93	5.44	0.02	0.25	-0.40	188.85	195.17	191.51	-10.97	-5.42	-12.44
Sr:5	8386	SWE	7.03	7.89	-1.91	152.00	159.01	0.02	4.57	3.88	4.04	0.09	0.39	0.06	5.34	5.17	NA	-0.02	NA	NA	190.99	194.57	NA	-6.47	NA	NA
St-0	8387	SWE	6.96	8.91	-0.82	152.17	159.95	0.03	NA	NA	NA	NA	NA	NA	NA	NA	NA	NA	NA	NA	NA	NA	NA	NA	NA	NA
Kelsterbach-4	8420	GER	5.59	8.43	0.07	161.06	159.51	-0.03	4.20	3.80	3.84	0.05	0.21	-0.06	5.92	5.65	5.71	0.66	-0.07	0.15	184.66	186.35	188.20	-10.53	-6.30	-6.94
Fjä1-1	8422	SWE	5.87	8.81	0.16	168.67	173.45	0.01	4.38	3.97	4.17	0.32	0.06	0.10	5.61	5.51	5.67	NA	-0.35	0.25	198.71	199.67	197.71	-11.40	-1.76	-10.75
Ull1-1	8426	SWE	6.01	7.89	-0.90	162.17	167.01	0.01	4.41	4.38	3.87	0.07	0.39	-0.61	5.69	NA	5.52	-0.17	-0.11	NA	173.30	172.34	175.81	-12.57	-5.27	-5.31
Vinslöv	9057	SWE	5.93	8.03	-0.68	161.63	169.51	0.03	4.33	3.97	4.08	0.34	0.11	0.01	5.61	5.60	5.90	0.24	-0.58	0.39	184.42	194.87	193.47	-17.36	-11.80	-10.19
Böt 1	9339	SWE	5.10	8.19	0.32	166.29	174.51	0.03	4.00	3.99	3.70	-0.04	0.16	-0.39	6.10	5.92	5.62	-0.16	0.20	-0.21	194.56	199.50	195.83	-10.97	-4.04	-12.46
EdJ 2	9363	SWE	5.55	10.13	1.81	160.28	162.01	-0.01	4.12	3.92	3.95	0.12	0.02	-0.07	5.50	5.20	5.16	0.01	0.05	0.06	196.44	204.03	198.98	-13.32	-5.29	-13.84
EkS 2	9369	SWE	6.58	13.15	3.80	159.66	158.39	-0.03	4.36	4.08	4.06	0.09	0.15	-0.12	5.27	NA	5.65	0.55	-0.67	NA	187.18	NA	188.33	-12.37	-3.91	NA
FlyA 3	9380	SWE	5.94	10.27	1.56	159.23	163.51	0.01	4.25	3.79	3.94	-0.05	0.16	0.05	6.09	5.59	5.99	-0.41	-0.19	0.49	183.04	196.46	193.26	-12.13	-12.98	-11.99
Grön 12	9386	SWE	5.36	10.56	2.43	159.72	166.01	0.02	4.14	3.92	3.92	-0.02	0.07	-0.10	5.94	5.99	5.84	-0.51	-0.19	-0.06	198.35	198.30	196.81	-9.94	-1.22	-10.27
Grön 14	9388	SWE	5.09	9.00	1.13	156.16	160.51	0.01	4.21	3.89	4.12	0.17	-0.06	0.13	6.04	5.70	5.76	-0.37	0.00	0.15	193.35	196.71	196.24	-4.89	-5.65	-9.26
Hal-1	9395	SWE	4.94	5.55	-2.17	162.41	170.01	0.03	4.38	3.94	4.13	0.10	0.10	0.09	4.34	5.85	5.97	-0.15	-1.91	0.20	196.29	197.75	196.81	-7.70	-3.28	-9.72
Hamm-1	9399	SWE	7.60	7.55	-2.82	163.56	172.01	0.03	4.44	3.94	4.24	-0.17	0.06	0.19	5.67	5.54	5.93	-0.21	-0.54	0.48	193.54	199.06	193.40	-3.77	-2.62	-14.45
HolA-1-1	9404	SWE	5.30	12.57	4.50	161.61	165.51	0.00	4.37	4.06	4.08	-0.04	0.15	-0.08	5.85	5.31	5.86	NA	-0.30	0.64	192.52	197.94	192.67	-12.20	-2.91	-14.05

HolA-1-2	9405	SWE	6.40	12.59	3.42	161.24	161.01	-0.02	4.25	4.08	4.06	0.31	0.05	-0.11	5.87	5.80	5.87	-0.10	-0.29	0.16	190.02	198.96	192.19	-16.44	-4.93	-15.55
HolA-2-2	9407	SWE	5.24	7.56	-0.45	162.72	168.51	0.01	4.34	4.12	4.00	-0.01	0.19	-0.22	5.73	5.55	5.40	0.49	0.04	-0.06	189.92	193.54	191.99	-8.96	-4.83	-10.34
Kal-1	9408	SWE	5.56	5.47	-2.86	166.54	171.51	0.01	4.23	3.93	4.15	-0.04	-0.07	0.12	5.73	5.84	5.63	0.21	-0.18	-0.12	193.56	194.91	195.56	-10.94	-4.75	-8.14
Kia-1	9409	SWE	6.58	7.69	-1.66	167.75	172.51	0.01	4.34	3.82	3.79	0.01	0.40	-0.13	5.49	5.45	5.18	-0.04	0.02	-0.18	182.94	195.85	191.23	-15.79	-11.05	-13.41
Lan-1	9421	SWE	6.82	8.24	-1.35	165.68	170.01	0.01	4.26	3.79	4.10	0.15	0.02	0.21	5.71	5.32	5.78	0.10	-0.35	0.54	197.99	199.52	196.69	-8.73	-1.46	-11.62
Puk-1	9436	SWE	6.54	14.21	4.90	166.60	170.01	0.00	4.13	3.96	NA	0.08	NA	NA	5.92	5.42	NA	0.75	NA	NA	194.60	199.64	NA	-15.03	NA	NA
Puk-2	9437	SWE	NA	NA	NA	NA	NA	NA	NA	NA	NA	NA	NA	NA	NA	NA	NA	NA	NA	NA	NA	NA	NA	NA	NA	NA
Ste-2	9453	SWE	4.72	10.47	2.97	165.70	163.01	-0.04	4.27	3.82	4.05	0.07	0.08	0.13	5.91	5.39	5.27	-0.09	0.35	-0.03	189.36	194.70	191.53	-6.92	-4.93	-11.96
Ste-3	9454	SWE	5.14	14.29	6.38	166.60	171.01	0.01	4.37	3.97	3.99	-0.13	0.24	-0.08	5.65	5.58	5.57	-0.13	-0.21	0.09	193.33	193.93	187.47	-13.91	3.11	-15.25
Tur-4	9470	SWE	6.57	8.06	-1.29	166.79	173.01	0.02	4.20	4.06	3.92	-0.11	0.13	-0.24	5.95	5.83	5.60	-0.44	0.06	-0.13	195.23	197.36	199.24	-8.50	-6.77	-6.91
Yst-1	9481	SWE	NA	NA	NA	NA	NA	NA	NA	NA	NA	NA	NA	NA	NA	NA	NA	NA	NA	NA	NA	NA	NA	NA	NA	NA
IP-Alo-0	9506	POR	8.48	12.17	0.92	147.18	145.51	-0.03	NA	NA	NA	NA	NA	NA	NA	NA	NA	NA	NA	NA	NA	NA	NA	NA	NA	NA
IP-All-0	9517	ESP	7.36	13.61	3.48	131.63	134.89	0.00	4.53	3.91	4.18	-0.19	0.21	0.17	5.02	5.06	NA	-0.29	NA	NA	171.90	173.57	169.85	-15.06	-0.71	-12.51
IP-Ang-0	9519	ESP	6.54	7.70	-1.61	141.72	140.51	-0.03	4.42	4.24	4.06	0.18	0.22	-0.28	4.81	5.23	5.62	0.18	-1.09	0.48	172.15	170.95	174.96	-7.34	-5.56	-4.78
IP-Ara-4	9520	ESP	NA	NA	NA	NA	NA	NA	NA	NA	NA	NA	NA	NA	NA	NA	NA	NA	NA	NA	NA	NA	NA	NA	NA	NA
IP-Bar-1	9521	ESP	5.59	10.48	2.12	149.73	149.01	-0.03	4.55	4.10	4.08	0.30	0.32	-0.12	5.82	5.53	5.38	0.72	0.15	-0.05	184.98	177.97	175.33	-11.95	6.88	-11.42
IP-Ber-0	9524	ESP	7.14	12.92	3.00	155.57	156.45	-0.01	4.66	4.07	3.85	-0.24	0.66	-0.32	NA	5.28	4.92	NA	NA	-0.27	184.99	187.45	183.84	-1.25	-1.61	-12.40
IP-Bis-0	9525	ESP	6.31	10.83	1.74	163.79	167.45	0.00	4.50	4.06	4.21	-0.07	0.14	0.05	6.01	5.76	5.98	-0.35	-0.25	0.31	190.67	196.01	193.26	-5.56	-5.35	-11.53
IP-Cab-3	9526	ESP	9.04	7.09	-4.72	134.68	147.95	0.07	4.40	4.44	4.39	0.03	-0.14	-0.15	5.29	4.51	5.54	-0.69	-0.53	1.12	179.12	170.64	171.16	-11.01	5.20	-8.27
IP-Cad-0	9527	ESP	NA	NA	NA	NA	NA	NA	NA	NA	NA	NA	NA	NA	NA	NA	NA	NA	NA	NA	NA	NA	NA	NA	NA	NA
IP-Cal-0	9528	ESP	7.76	14.26	3.72	154.38	156.51	-0.01	4.28	4.07	3.43	-0.11	0.71	-0.74	5.44	5.56	4.84	0.00	0.32	-0.64	188.87	189.03	185.06	-12.75	1.05	-12.76
IP-Cdc-3	9531	ESP	8.48	11.24	-0.01	150.34	157.01	0.02	4.54	4.03	3.88	0.05	0.51	-0.25	5.91	5.16	5.52	-0.36	0.10	0.45	183.14	187.72	184.74	-15.12	-4.36	-11.77
IP-Cdo-0	9532	ESP	6.13	11.98	3.08	147.86	140.77	-0.07	4.60	4.32	4.44	-0.09	0.02	0.02	4.98	5.18	5.45	0.44	-0.76	0.37	168.25	170.93	169.17	-9.54	-3.67	-10.55
IP-Cmo-3	9534	ESP	NA	NA	NA	NA	NA	NA	NA	NA	NA	NA	NA	NA	NA	NA	NA	NA	NA	NA	NA	NA	NA	NA	NA	NA
IP-Coc-1	9535	ESP	8.34	9.09	-2.02	155.17	161.39	0.02	4.42	3.97	NA	0.31	NA	NA	5.45	5.44	NA	0.11	NA	NA	186.42	187.96	NA	-12.97	NA	NA
IP-Deh-1	9539	ESP	6.36	10.69	1.56	145.17	146.01	-0.01	4.61	4.30	4.26	0.16	0.21	-0.14	4.46	5.58	5.30	0.76	-1.12	-0.19	170.05	171.71	170.02	-13.33	-2.73	-10.48
IP-Elb-0	9540	ESP	5.45	7.26	-0.97	160.68	161.01	-0.02	4.52	4.22	4.37	-0.04	0.01	0.05	4.75	5.22	5.22	-0.21	-0.76	0.09	186.48	188.36	186.66	-12.88	-2.94	-10.48
IP-Hor-0	9547	ESP	6.32	10.13	1.04	153.09	155.39	-0.01	4.53	4.14	4.23	0.01	0.15	-0.01	5.60	5.49	5.55	0.22	-0.24	0.15	182.37	174.59	180.78	-12.86	-1.16	-2.61
IP-Hoy-0	9548	ESP	NA	NA	NA	NA	NA	NA	NA	NA	NA	NA	NA	NA	NA	NA	NA	NA	NA	NA	NA	NA	NA	NA	NA	NA
IP-Jim-1	9551	ESP	5.78	6.81	-1.74	154.12	154.45	-0.02	4.49	4.36	3.91	0.28	0.44	-0.55	5.90	5.71	5.57	NA	0.04	-0.05	190.50	187.46	187.79	-15.71	-0.05	-8.46
IP-Lab-7	9552	ESP	NA	NA	NA	NA	NA	NA	NA	NA	NA	NA	NA	NA	NA	NA	NA	NA	NA	NA	NA	NA	NA	NA	NA	NA
IP-Ldd-0	9553	ESP	NA	NA	NA	NA	NA	NA	NA	NA	NA	NA	NA	NA	NA	NA	NA	NA	NA	NA	NA	NA	NA	NA	NA	NA

IP-Men-2	9556	ESP	7.78	10.01	-0.54	147.69	146.77	-0.03	4.17	4.05	3.55	-0.07	0.47	-0.60	5.33	5.11	4.51	-0.08	0.53	-0.51	173.07	179.91	169.55	-17.55	0.76	-19.15
IP-Moa-0	9557	ESP	5.27	8.69	0.64	166.44	170.45	0.00	4.28	3.89	3.82	0.07	0.32	-0.18	5.09	NA	5.53	-0.31	-0.72	NA	202.40	197.36	194.65	NA	4.99	-11.49
IP-Moc-11	9558	ESP	4.83	8.43	0.83	162.57	160.45	-0.03	4.19	3.98	3.94	-0.17	0.11	-0.14	5.86	5.24	5.73	NA	-0.16	0.59	185.29	183.15	179.78	-14.02	2.76	-12.16
IP-Mun-0	9561	ESP	6.39	8.71	-0.45	160.24	164.51	0.01	4.30	4.11	4.13	-0.16	0.03	-0.08	2.72	5.38	5.41	-0.44	-2.98	0.13	194.67	196.34	192.59	-4.72	-0.67	-12.54
IP-Mur-0	9562	ESP	7.53	11.58	1.28	154.51	156.01	-0.01	4.46	4.29	4.25	NA	0.07	-0.14	NA	5.56	4.28	0.11	NA	-1.19	184.64	188.28	186.85	NA	-4.97	-10.21
IP-Nog-17	9564	ESP	8.97	9.61	-2.13	163.40	171.77	0.03	4.40	NA	4.00	0.15	0.26	NA	5.87	NA	5.68	NA	-0.10	NA	200.43	NA	196.80	-8.94	0.87	NA
IP-Orb-10	9565	ESP	7.83	9.22	-1.38	149.00	154.01	0.01	4.25	4.03	3.65	-0.28	0.46	-0.49	6.11	5.68	4.63	0.94	1.19	-0.96	187.60	186.73	184.72	-16.27	0.12	-10.79
IP-Pal-0	9567	ESP	7.50	13.69	3.42	165.47	169.39	0.00	4.54	3.35	4.16	0.08	0.24	0.71	6.14	NA	5.91	-1.09	-0.06	NA	197.10	NA	195.64	-0.71	-1.29	NA
IP-Pan-0	9568	ESP	8.38	11.84	0.69	158.76	160.01	-0.01	4.47	4.24	4.23	0.30	0.09	-0.11	5.93	5.68	5.76	-1.01	-0.11	0.17	189.87	191.66	191.53	-15.21	-4.42	-8.91
IP-Pds-1	9569	ESP	9.25	11.03	-0.99	151.69	160.01	0.03	4.50	4.30	4.18	NA	0.18	-0.23	5.58	5.54	5.49	NA	-0.20	0.04	188.06	190.76	189.40	NA	-4.10	-10.15
IP-Rds-0	9573	ESP	5.55	9.59	1.26	146.90	138.01	-0.08	4.51	4.42	3.69	NA	0.67	-0.83	4.96	5.36	4.97	NA	-0.29	-0.30	173.22	171.55	170.05	NA	0.41	-10.28
IP-Ria-0	9577	ESP	7.94	12.18	1.47	161.54	169.51	0.03	4.42	4.43	4.11	NA	0.17	-0.42	5.78	NA	5.02	NA	0.47	NA	189.80	193.96	193.82	NA	-6.79	-8.92
IP-Sac-0	9578	ESP	7.10	9.30	-0.58	147.57	155.01	0.03	3.51	3.66	3.29	NA	0.08	-0.47	5.78	5.12	4.96	NA	0.54	-0.07	183.93	184.08	181.62	NA	-0.45	-11.25
IP-Scm-0	9580	ESP	5.76	10.64	2.11	152.83	149.51	-0.04	4.47	4.15	4.19	NA	0.14	-0.06	5.56	5.45	5.45	NA	-0.18	0.09	169.10	169.99	174.74	NA	-8.41	-4.04
IP-Sdv-3	9581	ESP	NA	NA	NA	NA	NA	NA	NA	NA	NA	NA	NA	NA	NA	NA	NA	NA	NA	NA	NA	NA	NA	NA	NA	NA
IP-Ses-0	9582	ESP	NA	NA	NA	NA	NA	NA	NA	NA	NA	NA	NA	NA	NA	NA	NA	NA	NA	NA	NA	NA	NA	NA	NA	NA
IP-Stp-0	9584	ESP	7.60	12.65	2.28	168.17	174.01	0.01	4.36	4.01	4.06	NA	0.16	-0.05	6.04	5.81	5.65	NA	0.10	-0.07	197.19	NA	204.07	NA	-9.64	NA
IP-Svi-0	9585	ESP	6.88	10.04	0.38	130.44	136.51	0.03	4.49	NA	4.14	0.19	0.20	NA	5.29	NA	5.79	NA	-0.78	NA	168.36	NA	171.19	-18.65	-5.59	NA
IP-Tam-0	9586	ESP	7.10	7.47	-2.40	162.69	173.45	0.04	4.28	NA	3.87	0.09	0.26	NA	5.55	NA	4.98	0.30	0.28	NA	196.00	NA	194.95	-15.75	-1.71	NA
IP-Tdc-0	9587	ESP	6.34	11.37	2.26	161.59	164.51	0.00	4.40	3.77	4.06	0.15	0.20	0.19	5.51	5.34	5.58	0.23	-0.35	0.33	190.97	193.97	190.86	-17.42	-2.66	-11.89
IP-Tol-7	9588	ESP	NA	NA	NA	NA	NA	NA	NA	NA	NA	NA	NA	NA	NA	NA	NA	NA	NA	NA	NA	NA	NA	NA	NA	NA
IP-Tor-1	9589	ESP	9.00	11.96	0.19	156.10	161.95	0.02	4.17	4.10	4.16	-0.10	-0.13	-0.04	5.94	6.58	5.44	NA	0.21	-1.04	189.62	188.09	186.77	-14.82	0.10	-10.11
IP-Vad-0	9591	ESP	8.77	10.14	-1.41	144.93	153.01	0.03	4.62	4.30	4.24	0.20	0.24	-0.16	5.80	5.06	2.23	-0.13	3.28	-2.74	170.16	181.34	NA	-24.27	NA	NA
IP-Vae-2	9592	ESP	6.21	13.25	4.27	154.49	152.21	-0.04	NA	NA	NA	NA	NA	NA	NA	NA	NA	NA	NA	NA	NA	NA	NA	NA	NA	NA
IP-Vaz-0	9593	ESP	NA	14.25	NA	NA	169.45	NA	4.53	NA	4.16	0.14	0.23	NA	5.89	NA	4.79	0.19	0.81	NA	193.57	NA	195.37	-11.87	-4.56	NA
IP-Vdm-0	9594	ESP	8.08	13.49	2.64	157.73	166.01	0.03	4.43	4.04	4.00	0.30	0.29	-0.14	6.00	5.56	5.75	0.04	-0.03	0.28	190.34	200.01	194.81	-14.38	-7.22	-13.99
IP-Vdt-0	9595	ESP	8.19	11.25	0.29	154.48	167.51	0.06	4.39	4.09	4.16	0.13	0.09	-0.03	5.69	4.85	5.79	NA	-0.38	1.03	186.38	187.64	185.91	-12.97	-2.28	-10.51
IP-Ver-5	9596	ESP	8.02	12.02	1.23	137.36	141.89	0.01	4.61	4.20	4.10	-0.11	0.37	-0.20	5.36	4.61	4.40	0.07	0.68	-0.13	168.42	175.66	169.77	-16.33	-4.11	-14.68
IP-Vig-1	9597	ESP	7.93	12.61	1.91	157.18	160.45	0.00	4.48	4.40	4.40	0.20	-0.07	-0.10	5.69	5.69	5.89	-0.13	-0.48	0.29	186.79	180.76	177.33	-17.53	6.70	-12.22
IP-Vin-0	9599	ESP	NA	16.46	NA	NA	170.79	NA	4.53	3.65	3.96	0.49	0.43	0.21	5.58	4.57	5.89	-0.12	-0.60	1.41	191.47	189.92	189.12	-13.25	-0.41	-9.58
IP-Voz-0	9601	ESP	NA	8.78	NA	NA	152.45	NA	4.34	3.97	4.26	-0.23	-0.07	0.19	5.65	5.62	5.74	-1.58	-0.38	0.22	186.88	184.26	180.50	-3.69	3.62	-12.55
IP-Vpa-	9602	ESP	8.24	7.90	-	152.	157.9	0.02	4.52	4.36	4.18	-0.11	0.19	-	5.72	5.68	4.17	-	1.27	-	176.	174.	176.1	-12.14	-2.71	-7.29

1					3.11	11	5							0.29				0.06		1.43	19	64	4			
Toc-1	9739	ROU	8.45	12.18	0.96	154.06	159.45	0.01	NA	NA	NA	NA	NA	NA	NA	NA	NA	NA	NA	NA	NA	NA	NA	NA	NA	NA
Staro-2	9756	SRB	NA	10.12	NA	NA	161.65	NA	NA	NA	NA	NA	NA	NA	NA	NA	NA	NA	NA	NA	NA	NA	NA	NA	NA	NA
Fell3-7	9776	GER	6.31	8.42	-0.66	155.51	168.01	0.06	4.36	3.92	3.87	0.09	0.34	-0.15	6.09	5.21	NA	-0.24	NA	NA	180.91	196.02	184.49	-17.13	-6.34	-20.32
Bach-7	9778	GER	5.33	6.90	-1.20	161.13	169.89	0.03	4.29	3.85	4.23	0.13	-0.09	0.28	5.72	5.66	NA	0.27	NA	NA	180.68	187.94	183.24	-12.37	-5.31	-13.49
Erg2-6	9784	GER	5.92	5.75	-2.94	162.49	167.89	0.01	4.53	NA	4.15	0.30	0.23	NA	6.00	NA	6.15	0.14	-0.43	NA	172.26	NA	186.97	-13.64	-17.48	NA
Wank-2	9795	GER	6.79	8.93	-0.63	158.26	161.39	0.00	4.36	3.97	4.14	-0.14	0.08	0.07	6.04	5.20	5.26	0.18	0.49	0.16	174.68	178.33	176.10	-9.89	-4.19	-11.01
Obe1-15	9804	GER	6.81	8.72	-0.87	162.56	170.01	0.02	4.45	4.05	4.32	-0.08	-0.01	0.17	5.77	5.78	6.13	0.30	-0.64	0.44	173.87	186.69	183.29	-16.16	-12.19	-12.18
Schl-7	9807	GER	6.27	8.49	-0.54	159.80	165.51	0.01	4.28	4.07	3.93	-0.23	0.20	-0.24	5.58	4.16	5.79	-0.01	-0.49	1.71	185.31	189.96	188.56	-14.10	-6.00	-10.19
Amu-0	9819	ESP	NA	NA	NA	NA	NA	NA	NA	NA	NA	NA	NA	NA	NA	NA	NA	NA	NA	NA	NA	NA	NA	NA	NA	NA
Are-0	9820	ESP	7.75	10.24	-0.27	140.73	144.45	0.01	4.52	4.04	4.23	0.12	0.14	0.10	5.61	5.39	5.72	0.29	-0.40	0.42	168.07	170.81	169.67	-8.47	-4.36	-9.93
Aru-0	9821	ESP	7.35	13.36	3.23	154.03	154.39	-0.02	4.20	4.04	3.88	-0.09	0.17	-0.26	5.58	5.41	5.17	-0.57	0.13	-0.15	188.19	187.62	184.76	-14.10	0.67	-11.64
Aul-0	9822	ESP	5.08	8.87	1.03	157.52	155.27	-0.03	4.43	4.09	4.29	0.06	-0.01	0.10	5.66	4.81	NA	1.70	NA	NA	182.78	177.70	171.51	-12.40	8.51	-14.98
Bes-5	9824	ESP	NA	NA	NA	NA	NA	NA	NA	NA	NA	NA	NA	NA	NA	NA	NA	NA	NA	NA	NA	NA	NA	NA	NA	NA
Boa-0	9825	ESP	6.44	10.23	1.02	144.74	147.51	0.00	4.63	4.33	4.48	-0.22	0.01	0.05	NA	3.83	5.90	0.20	NA	2.16	170.03	169.01	170.64	-14.33	-3.37	-7.16
Bor-0	9826	ESP	7.72	10.39	-0.10	156.15	151.39	-0.05	4.67	4.11	4.22	0.12	0.31	0.01	4.93	4.91	5.39	0.22	-0.75	0.57	173.89	173.75	169.96	-16.55	1.17	-12.58
Cha-0	9833	ESP	NA	NA	NA	NA	NA	NA	4.35	4.04	4.13	-0.18	0.08	-0.01	5.77	5.33	5.60	-0.14	-0.11	0.36	171.54	172.56	169.95	-16.10	-1.17	-11.40
IP-Cha-0	9833	ESP	NA	NA	NA	NA	NA	NA	4.35	4.04	4.13	-0.18	0.08	-0.01	5.77	5.33	5.60	-0.14	-0.11	0.36	171.54	172.56	169.95	-16.10	-1.17	-11.40
Cho-0	9834	ESP	8.09	15.25	4.39	156.04	154.21	-0.03	4.63	4.04	3.96	0.24	0.53	-0.18	5.21	5.18	5.27	-0.20	-0.35	0.19	174.58	180.39	177.22	-8.93	-5.41	-11.95
Cir-0	9835	ESP	5.99	7.81	-0.96	157.37	159.27	-0.01	4.42	4.21	4.21	0.04	0.06	-0.10	5.64	5.44	5.65	0.31	-0.30	0.31	173.00	172.43	175.71	-11.86	-5.47	-5.50
Cod-0	9836	ESP	8.50	9.59	-1.68	151.92	164.02	0.06	4.44	4.07	4.36	0.20	-0.06	0.18	5.68	4.94	NA	-0.15	NA	NA	186.05	187.83	187.21	-17.96	-3.92	-9.41
Cot-0	9838	ESP	5.97	12.49	3.75	142.99	137.51	-0.06	4.39	4.05	4.16	0.03	0.08	0.01	5.37	5.59	5.53	0.23	-0.44	0.03	169.90	170.73	169.55	-14.05	-2.41	-9.96
Coy-0	9839	ESP	NA	NA	NA	NA	NA	NA	NA	NA	NA	NA	NA	NA	NA	NA	NA	NA	NA	NA	NA	NA	NA	NA	NA	NA
Dar-0	9840	ESP	NA	NA	NA	NA	NA	NA	4.01	3.81	3.62	-0.15	0.24	-0.29	5.22	5.54	5.21	0.32	-0.27	-0.24	187.20	187.78	188.37	-16.03	-3.93	-8.20
Ees-0	9841	ESP	NA	14.26	NA	NA	149.45	NA	4.54	4.32	4.24	-0.07	0.15	-0.17	5.38	5.55	5.61	0.35	-0.52	0.16	174.25	172.65	171.72	-9.34	-0.22	-9.72
Elp-0	9843	ESP	7.61	10.28	-0.11	144.69	146.14	-0.01	4.55	4.14	4.24	0.30	0.17	0.00	5.39	5.35	5.23	-0.08	-0.13	-0.02	178.19	171.53	169.25	-16.67	6.19	-11.07
Esn-2	9844	ESP	NA	12.08	NA	NA	146.27	NA	4.41	4.07	4.17	-0.33	0.10	0.00	5.59	5.61	5.47	-0.06	-0.16	-0.05	175.59	171.74	172.29	-9.52	0.54	-8.24
Evs-0	9845	ESP	7.77	9.02	-1.53	142.84	156.39	0.07	4.53	4.45	4.67	0.11	-0.29	0.12	5.59	NA	5.99	0.26	-0.69	NA	178.30	170.52	167.77	-8.81	7.77	-11.54
Ezc-2	9846	ESP	8.62	7.23	-4.17	153.03	167.83	0.07	4.47	4.27	4.24	0.43	0.09	-0.13	5.79	5.70	5.42	0.01	0.08	-0.19	192.42	193.08	189.94	-15.20	-0.28	-11.92
Gud-3	9849	ESP	NA	NA	NA	NA	NA	NA	NA	NA	NA	NA	NA	NA	NA	NA	NA	NA	NA	NA	NA	NA	NA	NA	NA	NA
Hec-0	9850	ESP	NA	NA	NA	NA	NA	NA	NA	NA	NA	NA	NA	NA	NA	NA	NA	NA	NA	NA	NA	NA	NA	NA	NA	NA
Hue-3	9851	ESP	9.44	13.49	1.28	160.22	166.51	0.02	4.61	4.05	4.13	-0.13	0.33	-0.02	5.99	5.31	5.71	0.13	-0.01	0.49	191.72	196.61	194.81	-14.83	-5.84	-10.60
Ini-0	9852	ESP	7.09	11.65	1.78	157.58	152.51	-0.05	4.36	4.12	4.14	0.19	0.08	-0.08	5.46	5.06	NA	-0.11	NA	NA	177.47	174.89	171.26	-14.06	3.45	-12.41

Lam-0	9855	ESP	NA	10.89	NA	NA	145.83	NA	4.35	4.14	3.96	0.09	0.24	-0.28	5.89	5.74	5.62	0.50	-0.01	-0.03	171.70	171.10	168.87	-11.98	0.07	-11.01
Lch-0	9856	ESP	7.62	9.49	-0.90	152.78	152.01	-0.03	4.41	4.15	4.16	0.13	0.11	-0.09	5.87	5.57	5.68	-0.46	-0.10	0.20	168.22	172.47	168.95	-15.68	-3.48	-12.30
Leg-0	9857	ESP	5.97	8.29	-0.45	160.38	153.87	-0.06	4.57	4.17	4.07	-0.28	0.36	-0.21	5.87	4.93	3.47	0.08	2.12	-1.37	174.32	171.50	178.04	-16.54	-6.48	-2.24
Loz-0	9858	ESP	6.15	4.72	-4.20	165.32	178.75	0.06	4.45	4.12	4.25	-0.14	0.06	0.03	5.70	5.59	5.59	NA	-0.18	0.09	190.73	194.22	193.20	-18.60	-5.23	-9.80
Lro-0	9859	ESP	NA	NA	NA	NA	NA	NA	4.25	3.93	4.16	0.15	-0.06	0.13	5.78	5.72	5.52	NA	-0.02	-0.11	177.38	172.75	170.45	-12.73	4.17	-11.09
Lum-0	9860	ESP	8.66	10.83	-0.60	156.38	165.01	0.03	4.29	4.17	4.28	-0.23	-0.14	0.01	5.63	5.88	5.88	0.32	-0.53	0.09	186.53	188.89	181.32	-1.30	2.44	-16.35
Mac-0	9861	ESP	7.92	13.29	2.60	150.17	153.45	0.00	4.48	4.35	4.20	0.08	0.14	-0.26	5.44	5.54	5.49	0.14	-0.33	0.04	179.39	176.35	177.76	-13.92	-1.13	-7.37
Mat-0	9864	ESP	9.48	12.83	0.58	139.05	137.45	-0.03	4.15	4.10	4.37	0.20	-0.37	0.18	5.27	4.90	5.63	0.31	-0.64	0.82	167.01	170.53	169.51	-22.75	-5.26	-9.81
Mie-1	9867	ESP	7.15	9.55	-0.37	162.50	170.87	0.03	4.35	3.93	3.99	0.19	0.21	-0.04	5.90	4.99	5.62	0.44	0.00	0.72	191.23	187.03	184.59	-13.91	3.88	-11.22
Moe-0	9868	ESP	NA	9.16	NA	NA	156.87	NA	4.40	3.86	4.15	0.33	0.11	0.19	5.46	NA	5.03	-0.39	0.15	NA	171.92	172.33	170.67	-16.70	-1.51	-10.45
Moz-0	9870	ESP	NA	NA	NA	NA	NA	NA	NA	NA	NA	NA	NA	NA	NA	NA	NA	NA	NA	NA	NA	NA	NA	NA	NA	NA
Oja-0	9874	ESP	8.18	13.02	2.07	140.75	143.01	0.00	4.43	4.43	4.16	0.43	0.13	-0.37	5.39	5.55	5.36	0.57	-0.26	-0.09	182.63	172.34	172.30	-19.19	7.57	-8.82
Pad-0	9876	ESP	NA	NA	NA	NA	NA	NA	4.39	4.21	4.31	0.17	-0.07	0.00	4.77	5.26	5.68	1.24	-1.20	0.51	176.88	170.90	167.47	-20.18	6.65	-12.22
Pdl-0	9877	ESP	NA	NA	NA	NA	NA	NA	NA	NA	NA	NA	NA	NA	NA	NA	NA	NA	NA	NA	NA	NA	NA	NA	NA	NA
Pee-0	9878	ESP	10.48	12.45	-0.80	147.56	150.39	0.00	4.30	4.02	NA	0.10	NA	NA	4.98	4.78	NA	-0.08	NA	NA	177.30	176.76	NA	-15.26	NA	NA
Pie-0	9881	ESP	6.65	7.37	-2.05	155.03	161.01	0.02	4.48	4.35	4.58	-0.07	-0.24	0.13	5.48	5.64	5.59	-0.35	-0.40	0.04	171.03	172.23	169.84	NA	-1.57	-11.18
Piq-0	9883	ESP	6.07	10.24	1.41	151.63	157.51	0.02	4.52	4.23	3.88	-0.30	0.50	-0.45	5.69	5.05	5.11	NA	0.30	0.14	171.49	175.07	181.84	-17.74	-13.11	-2.01
Pru-0	9886	ESP	7.08	10.60	0.75	159.06	155.51	-0.04	4.25	4.09	4.11	0.04	-0.01	-0.08	5.75	5.45	5.72	-0.48	-0.26	0.37	186.09	184.08	182.73	-7.25	0.61	-10.14
Pva-1	9888	ESP	NA	8.62	NA	NA	152.27	NA	4.53	3.98	4.34	-0.11	0.05	0.26	6.05	5.10	5.36	0.35	0.40	0.35	170.20	171.63	169.63	NA	-2.19	-10.79
Rib-1	9890	ESP	6.59	10.76	1.39	158.10	159.51	-0.01	4.44	4.03	4.02	-0.29	0.27	-0.11	5.69	5.71	5.82	NA	-0.42	0.21	190.60	192.38	190.13	-11.23	-2.29	-11.04
Sal-0	9891	ESP	NA	NA	NA	NA	NA	NA	NA	NA	NA	NA	NA	NA	NA	NA	NA	NA	NA	NA	NA	NA	NA	NA	NA	NA
Sam-0	9892	ESP	7.13	11.22	1.32	160.43	163.27	0.00	4.38	4.18	3.85	0.22	0.39	-0.43	5.92	5.50	4.79	-0.08	0.84	-0.62	190.24	191.57	190.25	-14.55	-2.77	-10.11
Sfb-6	9895	ESP	7.16	8.86	-1.08	148.13	148.01	-0.02	4.46	4.20	4.17	-0.21	0.15	-0.14	NA	5.53	3.87	-0.70	NA	-1.57	169.94	171.26	170.43	-9.18	-3.25	-9.62
Smt-1	9897	ESP	8.03	6.70	-4.10	151.10	158.87	0.03	4.56	4.03	4.16	NA	0.25	0.03	5.34	5.22	5.19	0.03	-0.14	0.06	178.36	182.53	178.74	NA	-3.14	-12.57
Som-0	9898	ESP	NA	NA	NA	NA	NA	NA	NA	NA	NA	NA	NA	NA	NA	NA	NA	NA	NA	NA	NA	NA	NA	NA	NA	NA
Tau-0	9899	ESP	6.86	10.64	1.01	162.72	167.51	0.01	4.28	4.10	4.09	0.02	0.05	-0.12	5.48	5.60	5.59	0.05	-0.40	0.08	181.02	187.03	188.10	-14.07	-9.84	-7.71
Urd-1	9901	ESP	NA	NA	NA	NA	NA	NA	NA	NA	NA	NA	NA	NA	NA	NA	NA	NA	NA	NA	NA	NA	NA	NA	NA	NA
Usa-0	9902	ESP	4.96	11.50	3.77	157.06	150.95	-0.06	4.55	4.24	3.95	0.00	0.46	-0.39	NA	4.75	4.87	0.64	NA	0.21	NA	181.16	183.45	-20.72	NA	-6.49
Val-0	9903	ESP	NA	NA	NA	NA	NA	NA	NA	NA	NA	NA	NA	NA	NA	NA	NA	NA	NA	NA	NA	NA	NA	NA	NA	NA
Vas-0	9904	ESP	8.91	9.92	-1.77	152.42	155.71	0.00	4.21	4.13	4.01	0.01	0.05	-0.22	5.59	5.84	5.90	0.30	-0.59	0.15	189.81	192.29	189.18	NA	-2.13	-11.89
Mah-6	9906	ESP	6.17	8.13	-0.81	134.22	138.89	0.01	4.29	4.20	4.00	0.00	0.15	-0.31	5.98	5.67	5.57	NA	0.12	-0.01	178.45	171.63	170.76	-14.81	4.93	-9.65
ARR-17	9927	FRA	6.31	10.95	1.88	149.72	151.51	-0.01	NA	NA	NA	NA	NA	NA	NA	NA	NA	NA	NA	NA	NA	NA	NA	NA	NA	NA
MOU2-25	9931	FRA	NA	NA	NA	NA	NA	NA	NA	NA	NA	NA	NA	NA	NA	NA	NA	NA	NA	NA	NA	NA	NA	NA	NA	NA

WAV-8	9938	FRA	5.44	8.53	0.32	150.20	149.01	-0.03	4.33	NA	4.27	1.08	-0.09	NA	5.35	NA	5.22	NA	-0.16	NA	177.98	NA	174.72	NA	0.50	NA
Agu-1	9942	ESP	4.73	6.81	-0.70	158.44	161.01	0.00	4.46	4.07	4.19	0.04	0.13	0.02	5.64	4.50	5.76	-0.16	-0.40	1.34	189.63	187.02	184.75	-22.19	2.12	-11.06
Pra-6	9948	ESP	5.75	9.23	0.71	160.31	158.95	-0.03	3.99	4.02	3.99	-0.16	-0.14	-0.14	4.44	5.33	5.20	-0.14	-1.04	-0.04	185.38	190.11	180.77	-15.22	1.85	-18.12
Qui-0	9949	ESP	6.38	8.46	-0.69	150.20	155.51	0.01	4.40	4.07	3.99	-0.04	0.26	-0.19	4.71	5.53	5.45	0.12	-1.02	0.01	188.32	177.48	178.88	-9.82	6.68	-7.39
Vie-0	9950	ESP	6.08	7.81	-1.03	158.87	160.51	-0.01	4.45	3.90	3.81	-0.26	0.49	-0.19	NA	5.59	NA	0.07	NA	NA	191.14	194.80	188.54	-10.68	-0.15	-15.05
Copac-1	10005	ROU	6.89	7.79	-1.88	158.01	163.51	0.01	NA	NA	NA	NA	NA	NA	NA	NA	NA	NA	NA	NA	NA	NA	NA	NA	NA	NA
Petro-1	10017	SRB	7.65	8.49	-1.93	156.88	157.51	-0.02	NA	NA	NA	NA	NA	NA	NA	NA	NA	NA	NA	NA	NA	NA	NA	NA	NA	NA
Arb0	18513	MAR	NA	NA	NA	NA	NA	NA	4.49	NA	NA	0.07	NA	NA	4.98	NA	NA	-0.18	NA	NA	167.28	NA	NA	-17.80	NA	NA
Zin9	18515	MAR	NA	NA	NA	NA	NA	NA	4.14	NA	NA	-0.03	NA	NA	3.60	NA	NA	-0.12	NA	NA	177.57	NA	NA	-15.69	NA	NA
IFr0	22002	MAR	NA	NA	NA	NA	NA	NA	4.37	NA	NA	0.39	NA	NA	4.67	NA	NA	0.41	NA	NA	196.21	NA	NA	-11.46	NA	NA
Taz0	22005	MAR	NA	NA	NA	NA	NA	NA	4.44	NA	NA	-0.07	NA	NA	5.46	NA	NA	-0.19	NA	NA	185.21	NA	NA	-16.50	NA	NA
Bab0	22008	MAR	NA	NA	NA	NA	NA	NA	4.28	NA	NA	0.29	NA	NA	5.67	NA	NA	0.10	NA	NA	185.58	NA	NA	-18.09	NA	NA
Elh2	35616	MAR	NA	NA	NA	NA	NA	NA	4.60	NA	NA	0.03	NA	NA	5.29	NA	NA	NA	NA	NA	181.19	NA	NA	-16.51	NA	NA
Militärring A2	100048	GER	6.47	8.94	-0.30	159.11	160.95	-0.01	NA	NA	NA	NA	NA	NA	NA	NA	NA	NA	NA	NA	NA	NA	NA	NA	NA	NA
Militärring B1	100049	GER	6.79	9.16	-0.40	155.80	163.01	0.02	NA	NA	NA	NA	NA	NA	NA	NA	NA	NA	NA	NA	NA	NA	NA	NA	NA	NA
Bernhardstr.110	100050	GER	NA	11.70	NA	NA	167.27	NA	NA	NA	NA	NA	NA	NA	NA	NA	NA	NA	NA	NA	NA	NA	NA	NA	NA	NA
MilitärringA2	100051	GER	NA	NA	NA	NA	NA	NA	4.41	3.73	4.06	0.19	0.20	0.23	5.72	4.28	5.23	0.71	0.21	1.03	179.19	186.83	182.16	-18.07	-5.73	-13.46
MilitärringB1	100052	GER	NA	NA	NA	NA	NA	NA	4.44	4.03	4.14	0.33	0.16	0.00	5.45	5.33	5.66	0.15	-0.50	0.42	178.93	187.56	180.00	-11.71	-3.83	-16.34
Bernhardstr.110	100053	GER	NA	NA	NA	NA	NA	NA	4.33	3.99	3.93	-0.07	0.25	-0.16	5.45	5.61	5.68	-0.20	-0.51	0.16	185.32	189.04	189.25	-15.36	-6.68	-8.58
Mol-2	115927	FRA	6.40	9.63	0.46	146.11	144.87	-0.03	4.42	4.06	4.04	NA	0.24	-0.12	5.98	5.78	5.85	NA	-0.15	0.16	179.73	176.99	175.33	NA	1.64	-10.44
All1-2	115930	FRA	5.39	9.58	1.42	153.99	151.65	-0.04	4.19	3.76	4.23	-0.19	-0.18	0.37	5.90	5.41	6.10	-0.36	-0.48	0.78	177.97	185.08	183.22	-14.15	-8.01	-10.65
All1-4	115932	FRA	6.34	9.46	0.34	150.06	155.51	0.02	4.26	3.93	3.96	0.41	0.16	-0.07	5.79	5.36	5.74	0.56	-0.24	0.47	180.79	184.99	182.78	-20.13	-4.75	-11.00
All1-5	115934	FRA	NA	NA	NA	NA	NA	NA	4.30	3.90	4.03	0.12	0.12	0.03	4.76	NA	5.54	-0.11	-1.06	NA	184.06	189.93	186.37	-16.04	-5.07	-12.35
All1-8	115936	FRA	5.07	6.60	-1.25	149.55	156.01	0.02	4.28	4.14	NA	0.15	NA	NA	5.56	5.49	NA	0.04	NA	NA	168.88	172.15	NA	-11.91	NA	NA
All2-1	115938	FRA	6.58	8.78	-0.57	145.23	152.39	0.03	4.49	4.05	4.25	-0.01	0.09	0.11	5.78	5.40	5.69	0.17	-0.19	0.38	170.48	183.20	174.46	-17.60	-6.74	-17.53
All2-4	115940	FRA	5.50	6.75	-1.52	157.49	159.89	-0.01	4.34	3.95	4.09	0.38	0.11	0.04	5.21	4.97	5.48	0.17	-0.56	0.60	177.00	177.33	178.92	-18.13	-4.68	-7.19
All2-5	115942	FRA	4.46	5.30	-1.93	157.61	165.45	0.03	4.37	3.82	4.00	-0.09	0.22	0.07	5.41	NA	5.44	NA	-0.32	NA	179.91	182.75	183.10	NA	-5.95	-8.43
Cam-10	115944	FRA	4.84	5.09	-2.52	157.07	154.01	-0.04	4.30	4.17	3.92	NA	0.23	-0.35	5.63	5.56	4.95	NA	0.40	-0.53	174.55	179.33	177.57	NA	-5.78	-10.55
Cam-11	115946	FRA	6.01	7.36	-1.42	148.10	152.51	0.01	4.39	3.95	3.92	0.02	0.33	-0.14	5.55	5.48	5.34	NA	-0.07	-0.05	174.07	180.05	173.76	-17.32	-2.44	-15.08
Cam-2	115948	FRA	5.94	8.59	-0.12	149.50	149.45	-0.02	4.33	3.60	4.09	NA	0.10	0.39	3.70	5.09	5.52	NA	-2.10	0.52	180.51	182.22	174.34	NA	3.41	-16.66
Cam-6	115950	FRA	5.59	9.89	1.53	148.45	144.83	-0.04	4.11	4.09	4.06	-0.26	-0.10	-0.13	5.69	5.56	5.46	0.57	-0.05	-0.01	182.20	174.35	173.08	-14.07	6.36	-10.06

Cam-8	115952	FRA	6.77	5.80	-3.74	144.03	149.95	0.02	4.29	4.16	4.06	-0.04	0.09	-0.20	5.69	5.73	5.65	-0.34	-0.25	0.01	184.69	185.28	177.78	-5.35	4.14	-16.29
Cla-3	115954	FRA	3.11	4.64	-1.24	158.16	162.65	0.01	3.91	3.57	4.03	0.25	-0.26	0.35	5.73	5.26	5.91	0.09	-0.47	0.74	186.28	191.86	187.37	-16.86	-3.85	-13.27
Cla-5	115956	FRA	5.88	7.68	-0.97	NA	150.21	NA	NA	NA	NA	NA	NA	NA	NA	NA	NA	NA	NA	NA	NA	NA	NA	NA	NA	NA
Cla-6	115958	FRA	6.65	6.39	-3.03	147.61	152.71	0.01	4.24	3.87	4.06	-0.08	0.03	0.10	5.76	5.42	5.21	-0.31	0.27	-0.13	184.44	185.27	186.85	-13.86	-5.17	-7.21
Cur-10	115960	FRA	5.10	7.45	-0.42	152.57	154.51	-0.01	4.48	3.93	4.18	-0.04	0.15	0.15	5.66	5.29	NA	NA	NA	NA	174.85	176.95	170.98	-16.27	1.11	-14.76
Cur-2	115962	FRA	6.10	5.44	-3.43	151.11	158.89	0.03	3.75	3.64	3.60	-0.27	0.00	-0.15	5.77	5.28	5.41	NA	0.07	0.23	186.24	184.59	186.32	NA	-2.84	-7.05
Cur-5	115964	FRA	6.75	5.43	-4.09	159.15	165.01	0.02	4.39	4.23	3.81	-0.42	0.43	-0.51	5.91	5.73	5.09	-0.06	0.53	-0.54	180.01	184.63	187.72	-21.69	-10.47	-5.69
Fet-6	115968	FRA	6.20	5.64	-3.34	164.32	169.75	0.01	4.04	4.02	NA	0.03	NA	NA	6.01	5.52	NA	-0.16	NA	NA	188.19	190.74	NA	-10.03	NA	NA
All2-6	115970	FRA	5.03	7.35	-0.45	158.30	162.45	0.01	4.29	3.91	3.98	-0.06	0.17	-0.04	5.50	5.24	5.67	NA	-0.45	0.53	178.62	180.05	178.90	-13.32	-3.04	-9.93
Lac-2	115972	FRA	6.48	6.27	-2.98	152.65	164.39	0.05	4.39	4.03	4.20	0.25	0.05	0.07	5.20	5.57	5.47	-0.13	-0.56	-0.01	182.06	178.99	170.82	-14.06	8.49	-16.96
Lac-7	115974	FRA	5.67	5.92	-2.52	149.04	158.45	0.04	4.23	4.07	4.04	0.16	0.04	-0.13	5.84	3.94	5.94	NA	-0.38	2.08	184.15	186.70	182.48	-10.39	-1.09	-13.01
Ldv-1	115976	FRA	7.17	6.32	-3.62	159.31	164.01	0.01	4.35	4.04	4.05	0.40	0.15	-0.09	5.87	5.48	5.30	NA	0.29	-0.08	189.72	190.58	191.50	NA	-4.54	-7.86
Ldv-11	115978	FRA	6.57	7.51	-1.84	159.88	162.51	0.00	4.07	4.04	3.91	0.24	0.01	-0.23	5.94	5.53	5.71	-0.08	-0.06	0.28	190.05	192.83	188.52	-13.52	-1.22	-13.10
Ldv-2	115980	FRA	7.16	9.25	-0.68	158.43	160.45	-0.01	4.40	4.03	3.95	0.03	0.30	-0.18	5.59	5.53	5.71	0.01	-0.41	0.27	187.88	192.88	189.76	-14.57	-4.64	-11.91
Ldv-3	115982	FRA	7.41	11.70	1.52	157.28	161.15	0.00	4.15	4.09	3.88	0.16	0.13	-0.32	5.73	5.74	5.59	-0.22	-0.15	-0.05	189.69	194.25	190.70	-17.02	-3.77	-12.33
Mib-11	115986	FRA	4.71	6.11	-1.37	152.90	147.95	-0.05	4.16	3.68	3.97	0.07	0.05	0.19	5.63	5.13	5.60	-0.25	-0.25	0.56	176.16	173.54	170.13	-16.34	3.27	-12.20
Mib-18	115988	FRA	4.08	4.51	-2.34	158.98	160.89	-0.01	4.30	4.01	3.89	0.04	0.27	-0.22	5.85	5.80	5.29	NA	0.27	-0.42	189.22	189.54	189.31	-22.04	-2.85	-9.02
Mib-3	115990	FRA	NA	7.10	NA	NA	155.65	NA	4.12	3.66	3.72	0.01	0.25	-0.05	5.58	5.16	5.26	-0.76	0.03	0.19	175.52	181.94	174.18	-16.98	-1.42	-16.54
Mib-9	115992	FRA	5.84	8.53	-0.08	143.03	151.83	0.04	4.08	3.81	4.03	0.24	-0.10	0.13	5.66	5.15	5.74	-0.47	-0.36	0.68	174.31	176.82	172.87	-12.59	-1.33	-12.73
Mog-1	115994	FRA	5.16	NA	NA	167.76	NA	NA	4.23	4.14	4.02	0.17	0.07	-0.22	5.97	5.43	5.68	0.00	0.00	0.35	189.89	194.37	194.27	-12.79	-7.14	-8.89
Mog-11	115996	FRA	4.99	6.12	-1.64	152.66	154.77	-0.01	4.28	4.11	3.86	0.00	0.28	-0.35	5.46	5.35	5.27	0.13	-0.09	0.01	182.42	180.22	189.12	-16.40	-9.46	0.12
Mol-12	116000	FRA	6.79	6.74	-2.83	157.59	157.95	-0.02	3.86	3.94	4.00	0.14	-0.29	-0.04	5.94	5.48	5.95	NA	-0.30	0.56	182.93	180.90	171.54	NA	8.63	-18.15
Mol-4	116002	FRA	7.53	11.27	0.97	154.69	153.51	-0.03	4.18	3.51	4.03	0.18	0.01	0.42	5.80	5.48	5.81	0.32	-0.30	0.43	185.16	188.82	182.62	-18.60	-0.21	-14.99
Par-10	116004	FRA	5.27	4.34	-3.69	155.30	164.15	0.04	4.23	4.12	4.06	0.04	0.03	-0.16	5.63	5.55	5.55	0.15	-0.21	0.09	187.10	190.38	176.88	-16.57	7.46	-22.29
Par-13	116006	FRA	5.26	6.03	-2.00	159.56	163.45	0.00	4.37	3.94	3.88	-0.25	0.35	-0.16	5.75	5.05	5.72	NA	-0.26	0.76	187.55	190.07	186.72	-5.58	-1.92	-12.14
Par-3	116008	FRA	5.66	6.69	-1.74	151.03	159.01	0.03	4.45	4.12	4.10	-0.19	0.21	-0.12	5.40	5.66	5.67	-0.01	-0.56	0.10	177.58	178.01	182.73	-16.94	-7.91	-4.07
Par-4	116010	FRA	4.87	5.00	-2.64	159.56	166.39	0.02	4.26	3.89	4.01	0.48	0.11	0.02	5.93	5.66	5.74	0.79	-0.09	0.17	182.84	186.97	186.98	NA	-6.90	-8.78
Pyl-1	116012	FRA	NA	7.58	NA	NA	156.15	NA	4.30	4.34	3.95	0.04	0.20	-0.49	5.55	NA	5.18	-0.17	0.08	NA	174.48	179.47	182.06	-16.10	-10.35	-6.20
Pyl-3	116014	FRA	5.56	6.76	-1.57	146.06	151.51	0.02	4.25	4.15	4.14	0.26	-0.03	-0.11	5.95	NA	5.54	0.16	0.13	NA	186.28	193.34	188.53	-10.27	-5.01	-13.59
Pyl-4	116016	FRA	7.35	13.41	3.28	146.13	144.51	-0.03	4.47	4.08	4.32	0.14	0.01	0.14	5.79	5.28	5.72	0.01	-0.21	0.54	177.02	178.21	170.79	-22.19	3.47	-16.20
Vou-1	116020	FRA	6.53	7.55	-1.75	158.43	164.45	0.02	4.38	4.06	3.91	0.27	0.33	-0.25	6.12	5.61	NA	-0.33	NA	NA	191.76	194.13	195.01	-16.39	-6.01	-7.91

Vou-10	116022	FRA	7.33	7.87	-2.23	158.51	169.51	0.05	4.12	3.67	3.74	-0.25	0.24	-0.04	5.89	5.25	5.23	-0.43	0.38	0.06	185.94	197.15	194.47	-14.06	-11.29	-11.46
Vou-6	116024	FRA	7.85	13.21	2.58	155.57	158.45	0.00	4.35	3.92	4.31	-0.05	-0.10	0.29	5.53	5.73	6.06	0.04	-0.81	0.42	190.89	193.26	190.11	-17.05	-1.98	-11.93
Vou-9	116026	FRA	7.06	9.98	0.15	158.91	160.83	-0.01	4.50	3.93	4.14	0.07	0.22	0.11	5.98	5.21	5.66	-0.02	0.04	0.53	190.44	195.59	196.76	-18.59	-9.08	-7.62
Zdy-62	2000000	CHI	NA	NA	NA	NA	NA	NA	3.73	3.55	3.83	NA	-0.24	0.17	5.55	NA	5.53	-0.39	-0.27	NA	186.14	NA	186.54	NA	-3.15	NA
Aqs-11	2189710	CHI	NA	NA	NA	NA	NA	NA	4.10	4.15	4.03	0.14	-0.07	-0.23	5.36	5.64	5.33	-0.27	-0.26	-0.23	178.67	184.86	184.43	-16.31	-8.52	-9.22
Ayx-42	2189718	CHI	7.13	7.30	-2.60	162.52	166.45	0.00	4.36	4.08	3.97	-0.27	0.25	-0.21	5.69	5.15	5.33	0.21	0.07	0.28	187.02	182.72	186.78	-17.28	-2.53	-4.72
Jjgs-30	2204161	CHI	9.77	15.76	3.22	NA	139.89	NA	4.52	4.38	4.41	0.45	-0.03	-0.07	5.18	NA	4.95	0.99	-0.05	NA	165.85	NA	170.11	-11.90	-7.01	NA
Jjj-32	2204162	CHI	6.51	8.21	-1.07	NA	159.71	NA	4.36	4.40	3.77	-0.10	0.44	-0.73	5.52	5.41	4.86	NA	0.38	-0.46	185.98	185.66	188.89	-17.72	-5.67	-5.55
Zkh-29	2204168	CHI	NA	NA	NA	NA	NA	NA	4.61	4.14	4.17	-0.18	0.29	-0.07	4.29	4.79	4.81	-0.31	-0.81	0.11	172.91	175.91	174.51	-8.55	-4.36	-10.19
Zla-62	2204170	CHI	NA	NA	NA	NA	NA	NA	4.29	4.26	3.93	0.37	0.21	-0.43	5.14	4.92	5.28	1.02	-0.43	0.45	189.59	187.22	186.32	-18.04	0.51	-9.69
Hwc-61	2204174	CHI	NA	12.90	NA	NA	150.33	NA	4.44	NA	4.33	-0.26	-0.03	NA	NA	NA	NA	NA	NA	NA	186.40	NA	171.15	-18.59	12.49	NA
Cbb-60	2204175	CHI	10.25	13.76	0.74	NA	NA	NA	NA	NA	4.40	NA	NA	NA	NA	NA	6.10	NA	NA	NA	NA	NA	195.11	NA	NA	NA
Gwx-11	2204177	CHI	10.39	11.76	-1.41	149.28	152.71	0.00	4.52	4.26	4.12	-0.01	0.26	-0.24	5.47	5.23	NA	NA	NA	NA	170.00	172.53	166.98	-13.37	0.27	-14.34
Smx-34	2204179	CHI	7.55	11.88	1.56	141.84	138.33	-0.05	4.45	4.20	4.26	-0.19	0.05	-0.05	5.55	4.72	NA	-0.03	NA	NA	168.71	177.88	170.04	-12.20	-4.09	-16.62
Hnzjj-75	2204239	CHI	NA	NA	NA	NA	NA	NA	4.39	4.13	4.27	0.41	-0.03	0.04	5.22	4.72	NA	0.12	NA	NA	191.41	NA	NA	-20.26	NA	NA
Hyl-40	2204313	CHI	7.40	11.05	0.88	152.83	151.02	-0.03	4.53	4.28	4.29	0.42	0.09	-0.08	NA	5.32	5.47	0.80	NA	0.24	169.20	172.46	171.32	-24.16	-4.88	-9.93
Ygs-39	2204316	CHI	7.24	8.56	-1.46	NA	149.02	NA	4.59	3.26	4.19	-0.15	0.25	0.83	4.92	NA	NA	0.52	NA	NA	170.51	NA	170.67	-18.26	-2.92	NA
HNxy-46	2204317	CHI	7.46	9.79	-0.45	148.81	157.51	0.04	4.23	3.95	4.17	0.23	-0.09	0.12	5.26	5.22	4.90	-0.11	0.07	-0.23	175.13	185.78	170.13	-13.16	2.25	-24.44
Xem	2204324	CHI	6.46	8.52	-0.71	NA	NA	NA	3.82	3.74	3.81	0.07	-0.13	-0.03	6.07	6.01	6.37	0.16	-0.59	0.45	192.45	196.12	193.06	-5.89	-3.36	-11.85
Ahthx-23	6414606	CHI	NA	NA	NA	NA	NA	NA	4.15	3.94	4.07	0.34	-0.07	0.03	5.58	5.27	5.59	0.10	-0.29	0.40	189.49	187.77	191.42	-14.00	-4.69	-5.13
Hha-21	6414609	CHI	NA	NA	NA	NA	NA	NA	4.31	4.32	NA	0.19	NA	NA	5.32	5.06	NA	NA	NA	NA	181.30	180.43	NA	-16.89	NA	NA
JSnj-8	6414610	CHI	NA	NA	NA	NA	NA	NA	4.16	3.62	3.95	-0.29	0.06	0.23	NA	4.69	5.85	0.06	NA	1.25	189.46	189.91	190.01	-3.07	-3.31	-8.69

Table 29: Pairwise comparisons of phenotypes for each trait and treatment.

The mean difference between traits is given with Z- and p-value from a GLHT of a glm(parameter~population).

Trait	Treatment	Population 1	Population 2	Mean_Difference	Z-value	P-value
FS	HL	Northern Europe	China	-0.230	-0.790	0.852
		Spain	China	0.602	2.185	0.120
		Western Europe	China	-0.350	-1.089	0.685
		Spain	Northern Europe	0.832	5.167	**<0.001**
		Western Europe	Northern Europe	-0.120	-0.519	0.952
		Western Europe	Spain	-0.952	-4.509	**<0.001**
FS	LL	Northern Europe	China	0.301	0.730	0.880

		Spain	China	1.583	4.102	**<0.001**
		Western Europe	China	0.572	1.241	0.589
		Spain	Northern Europe	1.282	5.117	**<0.001**
		Western Europe	Northern Europe	0.271	0.763	0.866
		Western Europe	Spain	-1.011	-3.125	**0.009**
FS	GXE	Northern Europe	China	0.371	0.792	0.851
		Spain	China	0.815	1.834	0.245
		Western Europe	China	0.627	1.218	0.601
		Spain	Northern Europe	0.445	1.762	0.279
		Western Europe	Northern Europe	0.256	0.708	0.888
		Western Europe	Spain	-0.188	-0.570	0.938
t50	HL	Northern Europe	China	-1.157	-1.446	0.456
		Spain	China	0.200	0.260	0.993
		Western Europe	China	-0.267	-0.297	0.990
		Spain	Northern Europe	1.378	3.061	**0.011**
		Western Europe	Northern Europe	0.911	1.408	0.480
		Western Europe	Spain	-0.467	-0.791	0.852
t50	LL	Northern Europe	China	1.197	1.622	0.355
		Spain	China	2.866	4.154	**<0.001**
		Western Europe	China	2.915	3.540	**0.002**
		Spain	Northern Europe	1.670	3.727	**0.001**
		Western Europe	Northern Europe	1.719	2.708	**0.032**
		Western Europe	Spain	0.049	0.084	1.000
t50	GXE	Northern Europe	China	2.486	2.296	0.093
		Spain	China	2.826	2.748	**0.028**
		Western Europe	China	3.159	2.654	**0.037**
		Spain	Northern Europe	0.339	0.581	0.934
		Western Europe	Northern Europe	0.673	0.804	0.845
		Western Europe	Spain	0.334	0.436	0.971
Slope	HL	Northern Europe	China	0.538	1.625	0.351
		Spain	China	0.802	2.562	**0.047**
		Western Europe	China	0.372	1.017	0.729
		Spain	Northern Europe	0.264	1.444	0.458
		Western Europe	Northern Europe	-0.166	-0.632	0.918
		Western Europe	Spain	-0.430	-1.793	0.264
Slope	LL	Northern Europe	China	-0.092	-0.480	0.962
		Spain	China	-0.315	-1.751	0.287
		Western Europe	China	-0.375	-1.749	0.288
		Spain	Northern Europe	-0.222	-1.906	0.216
		Western Europe	Northern Europe	-0.283	-1.711	0.307
		Western Europe	Spain	-0.060	-0.401	0.977

Slope	GXE	Northern Europe	China	-0.712	-1.808	0.257
		Spain	China	-1.206	-3.224	**0.006**
		Western Europe	China	-0.830	-1.917	0.210
		Spain	Northern Europe	-0.494	-2.326	0.086
		Western Europe	Northern Europe	-0.118	-0.387	0.979
		Western Europe	Spain	0.376	1.352	0.515
Diameter	Field	Northern Europe	China	-1.347	-1.742	0.288
		Spain	China	-0.196	-0.264	0.993
		Western Europe	China	-3.284	-3.975	**<0.001**
		Spain	Northern Europe	1.151	2.929	**0.016**
		Western Europe	Northern Europe	-1.937	-3.635	**0.002**
		Western Europe	Spain	-3.088	-6.314	**<0.001**

Table 30: Testing the accuracy of polygenic trait predictions.

A. Polygenic scores were computed based on the phenotypic measurements for two replicates, and correlated with the phenotype observed for the third replicate. Correlation was tested with a Spearman rank correlation test Rho. SNP Nr: number of SNPs associated with each trait at p<10E-4.
B. SNPs associated with the phenotype at sub-significant level improve significantly the phenotype prediction but random SNPs show that population structure plays an important role. Rho_associated shows the correlation between polygenic score and the genotypic values. Based on 1000 random samples of an equal number of SNPs, a distribution of random Z-scores was computed and compared to the Spearman correlation of the prediction of associated variants to the input phenotypes (Rho_associated). The distributions of Spearman correlations of the 1000 random sets is described with the median (Rho_random_median), 95th-quantile (Rho_random_95quantile) and the maximal Rho (Rho_random_max). The correlation obtained with random SNP set is also often significant at p<0.05 (Percentage_significant), but the maximum correlation coefficient (Rho_random_max) is always markedly lower than the one obtained with sub-significant SNPs (Rho_associated).

A.						
Phenotype	SNP Nr	Rho	P-value			
FSHL	22	0.48	1.67E-11			
t50HL	32	0.23	0.0021			
SLHL	25	0.28	0.0002			
FSLL	32	0.57	<2.2E-16			
t50LL	37	0.38	2.01E-7			
SLLL	27	0.25	0.0008			
B.						
Phenotype	SNP Nr	Rho_associated	Rho_random_median	Rho_random_95quantile	Rho_random_max	Percentage_significant
	GWAS output, p<10-4	Correlation polygenic score/genotypic	Median correlation coefficient polygenic	95th percentile of the distribution of correlation	Maximum correlation coefficient	Percentage of significant correlation

		value	score/genotypic value for random sets of SNPs	coefficients between polygenic score and genotypic value for random sets of SNPs	polygenic score/genotypic value for random sets of SNPs	between polygenic score based on random SNPs and genotypic value
FSHL	27	0.793 (<2.2E-16)	0.37	0.5	0.56	98.5
FSLL	34	0.781 (<2.2E-16)	0.41	0.52	0.57	99.7
FSGXE	46	0.749 (<2.2E-16)	0.36	0.45	0.53	99.9
t50HL	47	0.794 (<2.2E-16)	0.43	0.52	0.59	100
t50LL	26	0.854 (<2.2E-16)	0.36	0.46	0.52	99.6
t50GXE	14	0.614 (<2.2E-16)	0.17	0.27	0.4	69.8
SLHL	28	0.847 (<2.2E-16)	0.34	0.42	0.5	99.9
SLLL	35	0.759 (<2.2E-16)	0.37	0.44	0.52	100
SLGXE	19	0.644 (<2.2E-16)	0.25	0.34	0.44	93.3

Table 31: Correlation between traits in HD and LD in controlled conditions.

Pearson correlation between the traits in the upper triangle. P-value (corrected for multiple testing with FDR) in the lower triangle. The abbreviations are: HD = High density, LD= Low density, HL= Hypocotyl length, BM= Biomass after 39 days, BO= Bolting time until vernalization, BV= Bolting time of vernalized plants, FN= Fruit number.

	HLHD	BMHD	BOHD	BVHD	FNHD	HLLD	BMLD	BOLD	BVLD	FNLD	GXEBM
HLHD		0.021	0.039	0.083	-0.162	0.794	0.115	0.049	-0.145	-0.076	0.064
BMHD	0.830		-0.217	-0.059	0.266	-0.094	0.062	-0.280	-0.036	0.045	-0.658
BOHD	0.799	0.028		0.088	-0.096	0.059	-0.075	0.799	0.154	-0.145	0.118
BVHD	0.557	0.702	0.946		0.050	0.090	-0.028	-0.011	-0.384	0.343	0.004
FNHD	0.142	0.007	0.493	0.917		-0.216	-0.281	-0.136	-0.644	0.383	-0.391
HLLD	2.01E-70	0.178	0.659	0.517	0.036		0.143	0.081	-0.155	-0.062	0.189
BMLD	0.117	0.458	0.582	0.879	0.007	0.040		-0.034	-0.153	-0.090	0.665
BOLD	0.743	0.004	8.29E-29	0.985	0.281	0.518	0.830		NA	-0.244	0.175
BVLD	0.134	0.799	0.799	0.001	0.026	0.103	0.147	NA		-0.348	-0.185
FNLD	0.563	0.768	0.288	0.128	0.002	0.655	0.517	0.049	0.061		-0.236
GXEBM	0.447	4.21E-35	0.325	0.984	7.46E-05	0.005	3.85E-36	0.126	0.064	0.032	

Table 32: Correlation between traits in HD and LD in the 1st field experiment.

Pearson correlation between the traits in the upper triangle. P-value (corrected for multiple testing with FDR) in the lower triangle. The abbreviations are: HD = High density, LD= Low density, DD= Diameter in December, BO= Bolting time, GE= Germination rate, DM= Maximum Diameter, SR= Survival rate.

	DDHD	BOHD	GEHD	DMHD	SRHD	DDLD	BOLD	GELD	DMLD	SRLD	GXEDD
DDHD		-0.270	-0.227	0.940	-0.166	0.568	-0.177	-0.001	0.530	0.005	0.057
BOHD	3.39E-06		0.153	-0.215	0.080	-0.176	0.903	0.139	-0.116	0.001	-0.046
GEHD	1.01E-04	0.012		-0.160	0.201	0.000	0.101	0.415	0.025	0.022	0.144

DMHD	2.42E-147	2.89E-04	0.008		-0.119	0.560	-0.120	0.048	0.521	-0.028	0.085
SRHD	0.005	0.213	0.001	0.053		-0.160	0.143	0.413	-0.141	0.531	-0.024
DDLD	1.05E-27	0.003	0.996	9.08E-27	0.006		-0.281	0.005	0.948	0.049	0.857
BOLD	0.003	9.30E-113	0.106	0.053	0.016	5.37E-07		0.166	-0.222	0.035	-0.237
GELD	0.996	0.024	5.19E-14	0.470	1.29E-14	0.950	0.004		0.016	0.071	0.069
DMLD	1.29E-23	0.064	0.727	1.01E-22	0.017	2.76E-163	1.05E-04	0.823		0.087	0.813
SRLD	0.958	0.994	0.754	0.692	7.09E-26	0.442	0.597	0.255	0.159		0.116
GXEDD	0.387	0.491	0.018	0.184	0.737	1.73E-90	5.30E-05	0.279	3.65E-74	0.060	

Table 33: Correlation between traits in LD, ID and HD in the 2st field experiment.

Pearson correlation between the traits in the upper triangle. P-value (corrected for multiple testing with FDR) in the lower triangle. The abbreviations are: LD= Low density, ID= Intermediate density, HD = High density, FH= Flowering Height, FD= Flowering time in days, H= Final Plant Height, BR= Number of Branches, SI= Number of Siliques, FS= Final Size, T5= t50, GXEFSLH= GxE for FS between LD and HD, GXEFSLI= GxE for FS between LD and ID, GXEFSHI= GxE for FS between HD and ID.

	FHLD	FDLD	HLD	BRLD	SILD	FSLD	T5LD	FHHD	FDHD	HHD	BRHD	SIHD	FSHD	T5HD	FHID	FDID	HID	BRID	SIID	FSID	T5ID	GXEFSLH	GXEFSLI	GXEFSHI
FHLD		**-0.133**	**-0.352**	-0.041	0.057	**0.134**	0.014	**0.553**	**-0.208**	-0.106	0.067	0.061	0.081	-0.046	**0.532**	**-0.169**	**-0.167**	0.100	0.069	0.082	-0.037	-0.003	0.042	-0.011
FDLD	0.050		**0.236**	-0.057	0.093	**-0.404**	**-0.220**	-0.075	**0.879**	**0.297**	-0.024	0.121	**-0.296**	**-0.221**	-0.067	**0.881**	**0.277**	**-0.234**	**-0.246**	**-0.371**	**-0.257**	0.072	0.013	-0.060
HLD	2.07E-09	1.44E-04		**0.144**	**0.265**	**-0.181**	-0.108	**-0.151**	**0.282**	**0.267**	**-0.173**	0.045	-0.139	-0.105	-0.048	**0.315**	**0.180**	**-0.149**	-0.039	**-0.167**	-0.091	0.014	0.001	-0.043
BRLD	0.653	0.502	0.034		**0.213**	0.092	0.000	0.080	-0.049	-0.093	0.018	-0.025	0.033	**0.237**	0.100	-0.037	-0.067	**0.226**	0.132	0.003	-0.028	-0.022	0.088	-0.025
SILD	0.499	0.220	1.45E-05	0.001		-0.026	-0.027	0.071	0.054	0.000	0.008	0.033	**0.149**	-0.015	0.073	0.128	0.059	0.131	0.271	-0.051	-0.140	0.031	0.030	**-0.180**
FSLD	0.048	8.81E-13	0.005	0.224	0.789		0.027	0.049	**-0.385**	**-0.166**	0.003	-0.087	**0.452**	0.047	0.047	**-0.383**	**-0.168**	0.122	0.064	**0.556**	0.047	-0.038	**0.376**	0.072
T5LD	0.891	3.25E-04	0.141	0.997	0.776	0.768		0.016	**-0.307**	**-0.228**	-0.091	-0.053	0.064	**0.445**	0.034	**-0.245**	**-0.183**	-0.072	-0.088	-0.096	**0.478**	0.030	0.128	-0.133
FHHD	1.28E-22	0.366	0.036	0.341	0.415	0.591	0.881		-0.130	**-0.280**	0.007	0.045	-0.122	-0.034	**0.465**	**-0.147**	**-0.184**	0.135	0.033	0.081	0.023	0.018	-0.044	**0.169**
FDHD	0.002	3.38E-90	1.17E-05	0.598	0.555	1.58E-10	7.07E-07	0.074		**0.280**	-0.090	0.132	**-0.390**	**-0.244**	**-0.151**	**0.915**	**0.300**	**-0.237**	**-0.197**	**-0.363**	**-0.304**	0.042	0.025	0.011
HHD	0.175	3.02E-06	5.05E-05	0.262	0.998	0.017	0.001	1.31E-05	1.34E-05		**0.231**	**0.451**	**0.152**	**-0.167**	-0.068	**0.320**	**0.233**	-0.091	0.002	-0.098	**-0.274**	0.032	-0.057	**-0.235**
BRHD	0.440	0.818	0.015	0.873	0.941	0.980	0.259	0.946	0.272	4.34E-04		**0.332**	**0.249**	-0.011	-0.065	-0.048	-0.036	0.108	0.084	0.068	-0.082	0.037	-0.079	-0.173
SIHD	0.495	0.110	0.642	0.809	0.748	0.285	0.557	0.633	0.075	4.52E-14	1.01E-07		-0.043	-0.073	0.093	0.140	-0.034	-0.023	0.007	**-0.155**	**-0.243**	0.078	0.083	-0.101
FSHD	0.307	1.18E-06	0.052	0.733	0.035	2.94E-15	0.441	0.099	8.42E-11	0.033	1.24E-04	0.647		**0.327**	0.066	**-0.291**	**-0.243**	0.073	-0.043	**0.362**	0.043	0.017	0.049	-0.594
T5HD	0.610	4.75E-04	0.169	2.21E-04	0.890	0.593	8.91E-15	0.721	1.31E-04	0.017	0.920	0.390	4.40E-08		0.020	**-0.219**	**-0.273**	0.008	**-0.129**	-0.068	**0.435**	-0.018	0.119	-0.339
FHID	3.83E-21	0.426	0.609	0.205	0.392	0.607	0.716	1.59E-14	0.038	0.453	0.481	0.267	0.444	0.853		**-0.140**	**-0.412**	0.060	-0.111	-0.088	**-0.077**	-0.056	0.144	-0.121
FDID	0.013	8.03E-93	4.93E-07	0.699	0.087	1.22E-10	1.03E-04	0.045	1.56E-103	9.76E-07	0.622	0.065	3.86E-06	0.001	0.046		**0.229**	**-0.279**	**-0.283**	**-0.414**	**-0.259**	0.107	0.091	-0.091
HID	0.017	1.48E-05	0.011	0.457	0.522	0.016	0.008	0.010	5.59E-06	0.001	0.733	0.748	2.69E-04	2.87E-05	1.15E-11	0.001		0.126	**0.449**	0.140	**-0.226**	0.091	-0.320	0.339
BRID	0.206	3.71E-04	0.043	0.001	0.087	0.107	0.403	0.082	0.001	0.302	0.197	0.839	0.402	0.946	0.499	1.31E-05	0.092		**0.621**	**0.343**	-0.130	0.075	-0.258	0.231
SIID	0.428	1.72E-04	0.690	0.081	3.92E-05	0.469	0.280	0.749	0.006	0.986	0.349	0.948	0.656	0.091	0.152	9.82E-06	6.48E-14	3.98E-29		**0.431**	**-0.189**	0.134	-0.413	0.421
FSID	0.302	3.35E-10	0.015	0.982	0.571	3.53E-24	0.206	0.339	4.98E-09	0.230	0.448	0.035	2.07E-09	0.420	0.261	1.84E-12	0.054	3.16E-08	8.63E-13		0.069	0.095	-0.562	0.535

T5ID	0.685	3.30E-05	0.250	0.777	0.051	0.599	3.19E-17	0.829	1.73E-06	3.17E-05	0.340	2.87E-04	0.641	1.54E-13	0.348	3.54E-05	0.001	0.081	0.006	0.402		-0.041	-0.029	0.013
GXEF SLH	0.980	0.379	0.895	0.835	0.752	0.674	0.753	0.873	0.667	0.751	0.715	0.373	0.877	0.871	0.542	0.175	0.284	0.396	0.083	0.230	0.665		-0.151	0.070
GXEF SLI	0.642	0.898	0.990	0.271	0.758	1.81E-10	0.071	0.645	0.808	0.539	0.360	0.335	0.587	0.108	0.040	0.245	3.51E-07	7.03E-05	1.25E-11	1.04E-24	0.758	0.034		-0.526
GXEF SHI	0.919	0.494	0.648	0.805	0.010	0.392	0.066	0.016	0.918	4.77E-04	0.015	0.215	4.71E-27	3.01E-08	0.108	0.258	9.52E-08	0.001	1.05E-11	4.23E-21	0.900	0.425	2.36E-20	

Table 34: GWAS genes in proximity to significantly associated SNPs in the competition experiments.

All genes within +-10kb around signficantly associated SNPs (p< 1E-8). Information on the GWAS input Trait, the associated SNP (Chromosome, Base Pair, Effect size & p-value), number of genes in proximity. Gene identifier, Gene name and described function from Tair10 (arabidopis.org).

Trait	Chr	Base pair	Effect size	P-value	Gene Nr	Gene Identifier	Gene name	Gene name full	Function
Height LD	4	8763510	0.5196	4.45E-09	1	AT4G15330	CYP705A1	CYTOCHROME P450, FAMILY 705, SUBFAMILY A, POLYPEPTIDE 1	NA
					2	AT4G15340	PEN1	PENTACYCLIC TRITERPENE SYNTHASE 1	Encodes a protein that catalyzes the production of the tricyclic triterpene arabidiol when expressed in yeast.
					3	AT4G15345	CYP702A4P	CYTOCHROME P450, FAMILY 702, SUBFAMILY A, POLYPEPTIDE 4 PSEUDOGENE	NA
					4	AT4G15350	CYP705A2	CYTOCHROME P450, FAMILY 705, SUBFAMILY A, POLYPEPTIDE 2	NA
					5	AT4G15360	CYP705A3	CYTOCHROME P450, FAMILY 705, SUBFAMILY A, POLYPEPTIDE 3	NA
					6	AT4G15370	PEN2	PENTACYCLIC TRITERPENE SYNTHASE 2	Encodes an oxidosqualene cyclase that primarily produces the tetracyclic triterpene baruol in vitro and when expressed in yeast. It can also make 22 other minor triterpenoid products with varying numbers of rings.
	4	10957505	0.5811	7.59E-09	1	AT4G20270	BAM3	BARELY ANY MERISTEM 3	Encodes a CLAVATA1-related receptor kinase-like protein required for both shoot and flower meristem function. It has a broad expression pattern and is involved in vascular strand development in the leaf, control of leaf shape, size and symmetry, male gametophyte development and ovule specification and function. The mRNA is cell-to-cell mobile.
					2	AT4G20280	TAF11	TBP-ASSOCIATED FACTOR 11	Encodes TAF11, a putative TBP-associated factor.
					3	AT4G20290	NA	NA	NA
					4	AT4G20300	NA	NA	NA
					5	AT4G20310	S2P	SITE 2 PROTEASE	Encodes a Golgi-localized protease that can cleave the transcription factors bZIP17 and bZIP28 that are translocated from the ER through the Golgi so that the transcription factors can be released to translocate into the nucleus.
	3	15524080	0.6180278	8.86E-09	1	AT3G43600	AAO2	ALDEHYDE OXIDASE 2	Encodes an aldehyde oxidase. AAO2 does not appear to act on abscisic aldehyde in vitro but it is possible that it may function in abscisic acid biosynthesis when the activity

									of At2g27150 (AAO3), the primary abscisic aldehyde oxidase, is lost.
					2	AT3G43610	NA	NA	NA
					3	AT3G43620	NA	NA	transposable element gene
					4	AT3G43622	NA	NA	transposable element gene
					5	AT3G43623	NA	NA	obsolete
					6	AT3G43625	NA	NA	transposable element gene
Height ID	1	7067725	0.8332	5.03E-12	1	AT1G20375	MIR394A	MICRORNA394A	Encodes a microRNA that targets one member of the F-box family. […] MicroRNAs can negatively regulate gene expression by attenuating translation or by directing mRNA cleavage. […] It is involved in the regulation of leaf morphology.
					2	AT1G20380	POQR	PROLYL-OLIGOPEPTIDASE ASSOCIATED WITH QUANTITATIVE RESISTANCE	Putative prolyl oligopeptidase, associated with quantitive disease resistance to S. sclerotiorum.
					3	AT1G20390	NA	NA	transposable element gene
					4	AT1G20400	NA	NA	NA
					5	AT1G20405	NA	NA	NA
	4	6325703	0.7769	2.22E-10	1	AT4G10120	SPS4F	SUCROSE PHOSPHATE SYNTHASE 4F	Encodes a protein with putative sucrose-phosphate synthase activity.
					2	AT4G10130	NA	NA	DNAJ heat shock N-terminal domain-containing protein
					3	AT4G10140	NA	NA	transmembrane protein
					4	AT4G10150	ATL07	ARABIDOPSIS TÃ³XICOS EN LEVADURA 7	NA
					5	AT4G10160	ATL59	ARABIDOPSIS TÃ³XICOS EN LEVADURA 59	NA
	3	7637722	0.7138	6.66E-09	1	AT3G21660	NA	NA	NA
					2	AT3G21670	ATNPF6.4	NRT1/ PTR FAMILY 6.4	NA
					3	AT3G21680	NA	NA	NA
					4	AT3G21690	NA	NA	NA
					5	AT3G21700	SGP2	NA	Monomeric G protein. Expressed in root epidermal cells that are destined to become atrichoblasts. Also expressed during pollen development and in the pollen tube tip.
					6	AT3G21710	VUP1	VASCULAR-RELATED UNKNOWN PROTEIN 1	NA
Height GxE LD-ID	4	8770638-8771298 (5 SNPs)	0.8524	1.08E-09	1	AT4G15340	PEN1	PENTACYCLIC TRITERPENE SYNTHASE 1	Encodes a protein that catalyzes the production of the tricyclic triterpene arabidiol when expressed in yeast.
					2	AT4G15345	CYP702A4P	CYTOCHROME P450, FAMILY 702, SUBFAMILY A, POLYPEPTIDE 4 PSEUDOGENE	NA
					3	AT4G15350	CYP705A2	CYTOCHROME P450, FAMILY 705, SUBFAMILY A, POLYPEPTIDE 2	NA
					4	AT4G15360	CYP705A3	CYTOCHROME P450, FAMILY 705, SUBFAMILY A, POLYPEPTIDE 3	NA

					5	AT4G15370	PEN2	PENTACYCLIC TRITERPENE SYNTHASE 2	Encodes an oxidosqualene cyclase that primarily produces the tetracyclic triterpene baruol in vitro and when expressed in yeast. It can also make 22 other minor triterpenoid products with varying numbers of rings.

Table 35: GO-enrichment of genes in LD (within 10kb) to SNPs with p < 0.008 (based on permutation) in a GWAS for the respective trait.

Shown are terms with an enrichment < 0.001. GO.ID and term give information on the enriched GO term. Annotated states all genes that are in the term, Significant is the number of genes that are associated in the input data set and Expected the number of genes that are expected to be enriched by chance. The resultFisher gives the Fisher score for enrichment. We only report GO terms with >5 genes in them. Abbreviations: High light (HL), low light (LL), GxE (Genome-Environment interaction between LL and HL), Final size (FS), slope (SL), low density (LD), high density (HD), intermediate density (ID), GxELH (Genome-Environment interaction between LD and HD), GxELI (Genome-Environment interaction between LD and ID), GxEHI (Genome-Environment interaction between HD and ID), height (H), diameter (D), biomass (B). Trait and environment are combined into single abbreviations, e.g. FSHL is FS in HL conditions

Trait	GO.ID	Term	Annotated	Significant	Expected	resultFisher
FSHL						
	GO:0009612	response to mechanical stimulus	17	11	3.55	0.0007
	GO:0010584	pollen exine formation	346	10	3.33	0.0016
	GO:0070206	protein trimerization	277	2	0.11	0.0032
	GO:0080164	regulation of nitric oxide metabolic process	170	2	0.11	0.0032
FSLL						
	GO:0009873	ethylene-activated signaling pathway	125	21	8.83	0.0002
	GO:0009880	embryonic pattern specification	46	10	3.25	0.0012
	GO:0010200	response to chitin	421	46	29.74	0.0022
	GO:0006354	DNA-templated transcription, elongation	59	11	4.17	0.0025
	GO:0098813	nuclear chromosome segregation	189	24	13.35	0.0038
	GO:0009651	response to salt stress	780	75	55.1	0.0039
	GO:0048825	cotyledon development	90	14	6.36	0.0041
	GO:0006606	protein import into nucleus	101	15	7.13	0.0048
	GO:0009926	auxin polar transport	102	15	7.21	0.0053
	GO:0032880	regulation of protein localization	48	9	3.39	0.0058
	GO:0000278	mitotic cell cycle	403	42	28.47	0.0075
	GO:0006468	protein phosphorylation	715	68	50.51	0.0075
	GO:0043086	negative regulation of catalytic activity	59	10	4.17	0.0079
	GO:0016070	RNA metabolic process	3044	253	215.03	0.0079
GxEFS						
	GO:0009641	shade avoidance	17	6	1.45	0.0020
	GO:0007389	pattern specification process	346	45	29.45	0.0028
	GO:0031348	negative regulation of defense response	277	37	23.57	0.0041
	GO:0010014	meristem initiation	170	25	14.47	0.0050
t50HL						

	GO:0010413	glucuronoxylan metabolic process	182	25	13.62	0.0023
	GO:0045492	xylan biosynthetic process	183	25	13.7	0.0025
t50LL						
	GO:0010196	nonphotochemical quenching	7	3	0.35	0.0039
	GO:0009069	serine family amino acid metabolic process	254	23	12.83	0.0050
	GO:0015976	carbon utilization	8	3	0.4	0.0059
GxEt50						
	GO:0080027	response to herbivore	7	3	0.37	0.0043
	GO:0002679	respiratory burst involved in defense response	121	14	6.36	0.0045
SLHL						
	GO:0010389	regulation of G2/M transition of mitotic cell cycle	64	11	3.41	0.0005
	GO:0006346	methylation-dependent chromatin silencing	120	16	6.39	0.0006
	GO:0006591	ornithine metabolic process	5	3	0.27	0.0014
	GO:0051225	spindle assembly	46	8	2.45	0.0027
	GO:0016556	mRNA modification	115	14	6.12	0.0032
	GO:0051567	histone H3-K9 methylation	183	19	9.74	0.0042
	GO:0034284	response to monosaccharide	173	18	9.21	0.0051
	GO:0009250	glucan biosynthetic process	288	26	15.33	0.0061
	GO:0035725	sodium ion transmembrane transport	42	7	2.24	0.0062
	GO:0006260	DNA replication	304	27	16.18	0.0066
	GO:0018119	peptidyl-cysteine S-nitrosylation	15	4	0.8	0.0068
	GO:1902531	regulation of intracellular signal transduction	33	6	1.76	0.0072
SLLL						
	GO:0034220	ion transmembrane transport	210	27	16.09	0.0056
	GO:0015672	monovalent inorganic cation transport	200	26	15.33	0.0056
	GO:0009168	purine ribonucleoside monophosphate biosynthetic process	212	27	16.25	0.0064
GxESL						
	GO:0009612	response to mechanical stimulus	63	12	3.58	0.0002
	GO:0010033	response to organic substance	2716	189	154.41	0.0023
	GO:0009845	seed germination	236	24	13.42	0.0043
	GO:0043622	cortical microtubule organization	20	5	1.14	0.0045
	GO:0009793	embryo development ending in seed dormancy	576	48	32.75	0.0052
	GO:0030422	production of siRNA involved in RNA interference	139	16	7.9	0.0056
	GO:1901700	response to oxygen-containing compound	2351	161	133.66	0.0065
	GO:0035196	production of miRNAs involved in gene silencing	129	15	7.33	0.0066
	GO:0034976	response to endoplasmic reticulum stress	354	32	20.13	0.0066
	GO:0007154	cell communication	1976	138	112.34	0.0093
	GO:0010389	regulation of G2/M transition of mitotic cell cycle	64	9	3.64	0.0099
DENSITY						
FSLD						
	GO:0008202	steroid metabolic process	244	34	19.83	0.0014

	GO:0048440	carpel development	257	33	20.89	0.0060
	GO:0006869	lipid transport	153	22	12.44	0.0062
FSHD						
	GO:0009910	negative regulation of flower development	46	10	3.63	0.0027
	GO:1901615	organic hydroxy compound metabolic process	758	81	59.74	0.0031
	GO:2000280	regulation of root development	33	8	2.6	0.0034
	GO:0009785	blue light signaling pathway	16	5	1.26	0.0063
	GO:0018401	peptidyl-proline hydroxylation to 4-hydroxy-L-proloine	11	4	0.87	0.0081
	GO:0010506	regulation of autophagy	6	3	0.47	0.0082
	GO:1900424	regulation of defense response to bacterium	6	3	0.47	0.0082
	GO:0071486	cellular response to high light intensity	6	3	0.47	0.0082
FSID						
	GO:0006952	defense response	1597	150	120.69	0.0029
	GO:0009606	tropism	166	23	12.55	0.0034
	GO:0080134	regulation of response to stress	571	59	43.15	0.0089
FSGxELH						
	GO:0009699	phenylpropanoid biosynthetic process	139	27	12.29	7.7E-05
	GO:0018401	peptidyl-proline hydroxylation to 4-hydroxy-L-proloine	11	5	0.97	0.0016
	GO:0006952	defense response	1597	183	141.25	0.0051
	GO:0048629	trichome patterning	5	3	0.44	0.0060
	GO:0002218	activation of innate immune response	34	8	3.01	0.0083
	GO:0009814	defense response, incompatible interaction	537	64	47.5	0.0087
FSGxELI						
	GO:0009970	cellular response to sulfate starvation	12	5	0.89	0.0011
	GO:0009451	RNA modification	325	40	24.17	0.0012
	GO:0009617	response to bacterium	580	62	43.13	0.0025
	GO:0006809	nitric oxide biosynthetic process	5	3	0.37	0.0037
	GO:0009395	phospholipid catabolic process	6	3	0.45	0.0069
	GO:0006108	malate metabolic process	6	3	0.45	0.0069
	GO:0006952	defense response	1597	144	118.76	0.0082
FSGxEHI						
	GO:0006071	glycerol metabolic process	18	7	1.72	0.0009
	GO:0019745	pentacyclic triterpenoid biosynthetic process	41	11	3.92	0.0013
	GO:0019375	galactolipid biosynthetic process	99	18	9.47	0.0056
	GO:0051262	protein tetramerization	5	3	0.48	0.0075
HLD						
	GO:0009809	lignin biosynthetic process	52	13	4.85	0.0008
	GO:0010582	floral meristem determinacy	15	6	1.4	0.0016
	GO:0009870	defense response signaling pathway, resistance gene-dependent	15	6	1.4	0.0016
	GO:0046777	protein autophosphorylation	147	25	13.7	0.0023

	GO:0015802	basic amino acid transport	27	8	2.52	0.0025
	GO:0015696	ammonium transport	31	8	2.89	0.0063
	GO:0002679	respiratory burst involved in defense response	121	20	11.28	0.0082
HHD						
	GO:0006857	oligopeptide transport	112	20	8.87	0.0005
	GO:0009684	indoleacetic acid biosynthetic process	109	19	8.63	0.0009
	GO:0006744	ubiquinone biosynthetic process	23	7	1.82	0.0015
	GO:0009624	response to nematode	80	14	6.33	0.0038
	GO:0045597	positive regulation of cell differentiation	5	3	0.4	0.0044
	GO:0008361	regulation of cell size	57	11	4.51	0.0046
	GO:0090558	plant epidermis development	671	72	53.11	0.0051
	GO:0010252	auxin homeostasis	22	6	1.74	0.0060
	GO:0009825	multidimensional cell growth	111	17	8.79	0.0063
	GO:0006605	protein targeting	751	78	59.45	0.0081
	GO:0006952	defense response	1597	152	126.41	0.0089
HID						
	GO:0080028	nitrile biosynthetic process	5	4	0.41	0.0002
	GO:0009643	photosynthetic acclimation	6	4	0.49	0.0006
	GO:0010026	trichome differentiation	169	24	13.85	0.0057
	GO:0044273	sulfur compound catabolic process	22	6	1.8	0.0071
	GO:0072348	sulfur compound transport	16	5	1.31	0.0075
HGxELH						
	GO:0006265	DNA topological change	13	6	1.01	0.0002
	GO:0006952	defense response	1597	169	123.86	0.0007
	GO:0045087	innate immune response	866	89	67.17	0.0038
	GO:0000184	nuclear-transcribed mRNA catabolic process	5	3	0.39	0.0041
	GO:0051645	Golgi localization	44	9	3.41	0.0059
	GO:0051646	mitochondrion localization	44	9	3.41	0.0059
	GO:0060151	peroxisome localization	44	9	3.41	0.0059
	GO:0009556	microsporogenesis	53	10	4.11	0.0069
HGxELI						
	GO:0010218	response to far red light	99	18	7.21	0.0003
	GO:0009631	cold acclimation	33	8	2.4	0.0021
	GO:0006863	purine nucleobase transport	124	17	9.04	0.0086
	GO:0016106	sesquiterpenoid biosynthetic process	42	8	3.06	0.0099
HGxEHI						
	GO:0010583	response to cyclopentenone	146	12	4.85	0.0035
	GO:0009631	cold acclimation	33	5	1.1	0.0044
	GO:0006536	glutamate metabolic process	12	3	0.4	0.0064
DLD						
	GO:0009807	lignan biosynthetic process	16	5	1.35	0.0084

	GO:0045038	protein import into chloroplast thylakoid membrane	6	3	0.51	0.0099
DHD						
	GO:0006813	potassium ion transport	42	10	3.25	0.0011
	GO:0030865	cortical cytoskeleton organization	24	7	1.85	0.0017
	GO:0000226	microtubule cytoskeleton organization	243	31	18.78	0.0040
	GO:0080028	nitrile biosynthetic process	5	3	0.39	0.0041
DGxELH						
	GO:0009637	response to blue light	128	21	10.45	0.0016
	GO:0006508	proteolysis	885	95	72.24	0.0035
	GO:0010218	response to far red light	99	16	8.08	0.0063
	GO:0009807	lignan biosynthetic process	16	5	1.31	0.0073
	GO:0048445	carpel morphogenesis	36	8	2.94	0.0074
	GO:0034620	cellular response to unfolded protein	184	25	15.02	0.0081
	GO:0045038	protein import into chloroplast thylakoid membrane	6	3	0.49	0.0090
	GO:0019408	dolichol biosynthetic process	17	5	1.39	0.0097
BHD						
	GO:0006817	phosphate ion transport	26	7	2.12	0.0039
	GO:0000070	mitotic sister chromatid segregation	6	3	0.49	0.0089
	GO:0055075	potassium ion homeostasis	11	4	0.9	0.0091
	GO:0009095	aromatic amino acid family biosynthetic process, prephenate pathway	11	4	0.9	0.0091
BLD						
	GO:0006468	protein phosphorylation	715	94	68.08	0.0008
	GO:0042343	indole glucosinolate metabolic process	14	6	1.33	0.0011
	GO:0042446	hormone biosynthetic process	747	92	71.13	0.0061
	GO:0046189	phenol-containing compound biosynthetic process	221	33	21.04	0.0063
	GO:0046794	transport of virus	9	4	0.86	0.0069
	GO:0043244	regulation of protein complex disassembly	14	5	1.33	0.0075
	GO:0009627	systemic acquired resistance	446	58	42.47	0.0091
	GO:0072511	divalent inorganic cation transport	211	31	20.09	0.0099
BGxELH						
	GO:0009269	response to desiccation	38	9	2.85	0.0017
	GO:0051053	negative regulation of DNA metabolic process	15	5	1.13	0.0038

Table 36: Loadings of the climate PCAs for Figure 23.

The input variables for the respective PCA are in the column Climatic_variable and the loading for PC1 and PC2 are in the following columns. The PCAs were performed with data within the projected growing season (PCA_growing_season, 185 unique locations), for bioclimatic variables related to temperature (PCA_temperature, 180 unique locations) and bioclimatic variables related to precipitation (PCA_precipitation, 180 unique locations).

PCA	Climatic_variable	Loading_PC1	Loading_PC2
PCA_growing_season	Nr_Growing months	0.02	-0.05
PCA_growing_season	T_GS	0.03	-0.03
PCA_growing_season	SWC_GS	0.46	0.88
PCA_growing_season	Water vapor_GS	0	0
PCA_growing_season	Wind_GS	0	0.04
PCA_growing_season	Rain_GS	0.88	-0.46
PCA_temperature	Bioclim1_T_Annual	0.02	-0.25
PCA_temperature	Bioclim2_Diurnal_Range	0	-0.14
PCA_temperature	Bioclim3_Isothermality	-0.03	-0.36
PCA_temperature	Bioclim4_T_Seasonality	1	0
PCA_temperature	Bioclim5_MaxT_Wrmst_Month	0.03	-0.33
PCA_temperature	Bioclim_MinT_Cldst_Month	0	-0.19
PCA_temperature	Bioclim7_T_Ann_Range	0.03	-0.15
PCA_temperature	Bioclim8_T_Wettest_Qtr	0.04	-0.08
PCA_temperature	Bioclim9_T_Driest_Qtr	-0.02	-0.7
PCA_temperature	Bioclim10_T_Wrmst_Qtr	0.03	-0.25
PCA_temperature	Bioclim11_T_Cldst_Qtr	0	-0.25
PCA_precipitation	Bioclim12_Ann_Precip	0.86	0.14
PCA_precipitation	Bioclim13_P_Wettest_Month	0.14	-0.08
PCA_precipitation	Bioclim14_P_Driest_Month	0.02	0.02
PCA_precipitation	Bioclim15_P_Seasonality	0.01	-0.04
PCA_precipitation	Bioclim16_P_Wettest_Qtr	0.37	-0.14
PCA_precipitation	Bioclim17_P_Driest_Qtr	0.07	0.09
PCA_precipitation	Bioclim18_P_Wrmst_Qtr	0.25	-0.68
PCA_precipitation	Bioclim19_P_Cldst_Qtr	0.17	0.69

Table 37: GO-enrichment of differentially expressed genes between mutants of light-signaling genes.

Shown are terms with an enrichment < 0.0008. GO.ID and term give information on the enriched GO term. Ann. states all genes that are in the term, Sign. is the number of genes that are associated in the input data set and Exp. the number of genes that are expected to be enriched by chance. The Fisher gives the Fisher score for enrichment. We only report GO terms with >5 genes in them. HLN: 161 genes; CN: 3600 genes; CD: 4551 genes; LLN: 3158 genes

Nr	Set	GO.ID	Term	Ann.	Sign.	Exp.	Fisher
	HLN						
1		GO:0006354	DNA-templated transcription, elongation	112	12	0.97	2.2E-10
2		GO:0042542	response to hydrogen peroxide	166	10	1.44	1.8E-06
3		GO:0009644	response to high light intensity	197	9	1.71	5.4E-05

4		GO:0010193	response to ozone	34	4	0.29	0.00020
5		GO:0019684	photosynthesis, light reaction	306	12	2.65	0.00025
6		GO:0009627	systemic acquired resistance	425	12	3.68	0.00032
7		GO:0006457	protein folding	251	9	2.18	0.00034
8		GO:0009751	response to salicylic acid	434	12	3.76	0.00039
9		GO:0007623	circadian rhythm	163	7	1.41	0.00054
10		GO:0009408	response to heat	258	10	2.24	0.00108
11		GO:0009769	photosynthesis, light harvesting in photosystem II	6	2	0.05	0.00109
12		GO:0055074	calcium ion homeostasis	27	3	0.23	0.00160
13		GO:0009684	indoleacetic acid biosynthetic process	99	5	0.86	0.00169
14		GO:0034976	response to endoplasmic reticulum stress	329	9	2.85	0.00226
15		GO:0006268	DNA unwinding involved in DNA replication	9	2	0.08	0.00258
16		GO:0010167	response to nitrate	112	5	0.97	0.00289
17		GO:0006569	tryptophan catabolic process	70	4	0.61	0.00317
18		GO:0019430	removal of superoxide radicals	10	2	0.09	0.00320
19		GO:0006468	protein phosphorylation	643	13	5.57	0.00382
20		GO:0010310	regulation of hydrogen peroxide metabolic process	176	6	1.53	0.00430
21		GO:0055062	phosphate ion homeostasis	12	2	0.1	0.00465
22		GO:0015977	carbon fixation	13	2	0.11	0.00546
23		GO:0000103	sulfate assimilation	14	2	0.12	0.00634
24		GO:0006071	glycerol metabolic process	14	2	0.12	0.00634
25		GO:0006873	cellular ion homeostasis	197	6	1.71	0.00738
	HLD						
		not enough samples					
	CN						
1		GO:0009853	photorespiration	157	68	31.65	3.2E-11
2		GO:0010264	myo-inositol hexakisphosphate biosynthethic process	61	33	12.3	4.5E-09
3		GO:0010075	regulation of meristem growth	154	61	31.05	2.1E-08
4		GO:0006412	translation	472	146	95.17	1.2E-06
5		GO:0007169	transmembrane receptor protein tyrosine kinase signaling pathway	103	42	20.77	1.3E-06
6		GO:0009651	response to salt stress	737	196	148.6	9.2E-06
7		GO:0019344	cysteine biosynthetic process	205	67	41.33	1.5E-05
8		GO:0008283	cell proliferation	245	77	49.4	1.8E-05
9		GO:0046686	response to cadmium ion	455	126	91.74	5.5E-05
10		GO:0006084	acetyl-CoA metabolic process	85	33	17.14	5.6E-05
11		GO:0009269	response to desiccation	36	18	7.26	6.1E-05
12		GO:0009744	response to sucrose	196	62	39.52	9.1E-05
13		GO:0006414	translational elongation	31	16	6.25	9.6E-05
14		GO:0009828	plant-type cell wall loosening	20	12	4.03	0.00011

15		GO:0010089	xylem development	54	23	10.89	0.00014
16		GO:0009735	response to cytokinin	223	68	44.96	0.00015
17		GO:0009753	response to jasmonic acid	438	118	88.31	0.00031
18		GO:0006096	glycolytic process	192	59	38.71	0.00032
19		GO:0009739	response to gibberellin	122	45	24.6	0.00037
20		GO:0055072	iron ion homeostasis	61	24	12.3	0.00044
21		GO:0007623	circadian rhythm	163	51	32.86	0.00049
22		GO:0016572	histone phosphorylation	62	24	12.5	0.00059
23		GO:0009695	jasmonic acid biosynthetic process	125	41	25.2	0.00059
24		GO:0042254	ribosome biogenesis	331	95	66.74	0.00097
25		GO:0010583	response to cyclopentenone	128	41	25.81	0.00100
26		GO:0016126	sterol biosynthetic process	156	48	31.45	0.00106
27		GO:0080167	response to karrikin	117	38	23.59	0.00113
28		GO:0046364	monosaccharide biosynthetic process	169	51	34.07	0.00122
29		GO:0010043	response to zinc ion	41	17	8.27	0.00149
30		GO:0042364	water-soluble vitamin biosynthetic process	38	18	7.66	0.00187
31		GO:0006633	fatty acid biosynthetic process	137	42	27.62	0.00226
32		GO:0097237	cellular response to toxic substance	14	8	2.82	0.00252
33		GO:0009813	flavonoid biosynthetic process	191	55	38.51	0.00260
34		GO:0009750	response to fructose	138	42	27.82	0.00263
35		GO:0080129	proteasome core complex assembly	126	39	25.4	0.00264
36		GO:0006817	phosphate ion transport	17	9	3.43	0.00272
37		GO:0006553	lysine metabolic process	9	6	1.81	0.00319
38		GO:0001510	RNA methylation	172	50	34.68	0.00320
39		GO:0016132	brassinosteroid biosynthetic process	93	30	18.75	0.00398
40		GO:0051567	histone H3-K9 methylation	178	51	35.89	0.00405
41		GO:0006972	hyperosmotic response	237	65	47.78	0.00411
42		GO:0010017	red or far-red light signaling pathway	41	16	8.27	0.00422
43		GO:0042274	ribosomal small subunit biogenesis	18	9	3.63	0.00448
44		GO:0000911	cytokinesis by cell plate formation	200	56	40.32	0.00462
45		GO:0019722	calcium-mediated signaling	45	17	9.07	0.00478
46		GO:0010067	procambium histogenesis	7	5	1.41	0.00484
47		GO:0015996	chlorophyll catabolic process	56	20	11.29	0.00490
48		GO:0006952	defense response	1420	324	286.31	0.00523
49		GO:0009737	response to abscisic acid	562	138	113.31	0.00550
50		GO:0051225	spindle assembly	46	17	9.27	0.00619
51		GO:0009723	response to ethylene	319	83	64.32	0.00621
52		GO:0072525	pyridine-containing compound biosynthetic process	211	68	42.54	0.00667
53		GO:0009755	hormone-mediated signaling pathway	670	161	135.09	0.00690
54		GO:0080170	hydrogen peroxide transmembrane transport	5	4	1.01	0.00692
55		GO:0006021	inositol biosynthetic process	5	4	1.01	0.00692

56		GO:0009260	ribonucleotide biosynthetic process	359	106	72.38	0.00705
57		GO:0009821	alkaloid biosynthetic process	13	7	2.62	0.00731
58		GO:0006551	leucine metabolic process	13	7	2.62	0.00731
59		GO:0071370	cellular response to gibberellin stimulus	58	20	11.69	0.00764
60		GO:1901606	alpha-amino acid catabolic process	150	43	30.24	0.00776
61		GO:0009825	multidimensional cell growth	97	30	19.56	0.00780
	CD						
1		GO:0009220	pyrimidine ribonucleotide biosynthetic process	133	89	34.7	4.7E-23
2		GO:0006412	translation	472	237	123.15	2.5E-22
3		GO:0006612	protein targeting to membrane	368	180	96.02	1.9E-21
4		GO:0010363	regulation of plant-type hypersensitive response	365	178	95.24	4.8E-21
5		GO:0010200	response to chitin	399	187	104.11	1.2E-19
6		GO:0031348	negative regulation of defense response	271	140	70.71	1.3E-19
7		GO:0009697	salicylic acid biosynthetic process	205	114	53.49	1.9E-19
8		GO:0009627	systemic acquired resistance	425	220	110.89	5.0E-17
9		GO:0050832	defense response to fungus	329	155	85.84	9.8E-17
10		GO:0009862	systemic acquired resistance, salicylic acid mediated signaling pathway	237	118	61.84	3.3E-15
11		GO:0051567	histone H3-K9 methylation	178	94	46.44	2.2E-14
12		GO:0043069	negative regulation of programmed cell death	163	88	42.53	2.7E-14
13		GO:0002679	respiratory burst involved in defense response	117	67	30.53	8.3E-13
14		GO:0006275	regulation of DNA replication	132	72	34.44	3.1E-12
15		GO:0000911	cytokinesis by cell plate formation	200	97	52.18	6.8E-12
16		GO:0006606	protein import into nucleus	100	58	26.09	1.4E-11
17		GO:0010389	regulation of G2/M transition of mitotic cell cycle	63	42	16.44	1.6E-11
18		GO:0000165	MAPK cascade	215	101	56.1	2.8E-11
19		GO:0009867	jasmonic acid mediated signaling pathway	269	119	70.19	6.6E-11
20		GO:0030968	endoplasmic reticulum unfolded protein response	164	81	42.79	1.2E-10
21		GO:0042254	ribosome biogenesis	331	147	86.36	5.0E-10
22		GO:0006270	DNA replication initiation	64	39	16.7	4.3E-09
23		GO:0051225	spindle assembly	46	31	12	5.0E-09
24		GO:0008283	cell proliferation	245	104	63.93	1.6E-08
25		GO:0034976	response to endoplasmic reticulum stress	329	156	85.84	3.4E-08
26		GO:0009723	response to ethylene	319	127	83.23	4.4E-08
27		GO:0010310	regulation of hydrogen peroxide metabolic process	176	79	45.92	4.8E-08
28		GO:0006984	ER-nucleus signaling pathway	15	14	3.91	7.6E-08
29		GO:0002237	response to molecule of bacterial origin	93	48	24.27	1.3E-07
30		GO:0009664	plant-type cell wall organization	205	95	53.49	1.4E-07
31		GO:0042742	defense response to bacterium	384	150	100.19	1.5E-07
32		GO:0009165	nucleotide biosynthetic process	458	210	119.5	1.1E-06
33		GO:0009625	response to insect	43	26	11.22	2.0E-06

34		GO:0009611	response to wounding	304	116	79.32	2.1E-06
35		GO:0006306	DNA methylation	175	74	45.66	2.1E-06
36		GO:0009595	detection of biotic stimulus	102	48	26.61	4.0E-06
37		GO:0016572	histone phosphorylation	62	33	16.18	4.8E-06
38		GO:0043900	regulation of multi-organism process	123	55	32.09	5.8E-06
39		GO:0009828	plant-type cell wall loosening	20	15	5.22	6.7E-06
40		GO:0006499	N-terminal protein myristoylation	145	62	37.83	9.0E-06
41		GO:0006084	acetyl-CoA metabolic process	85	41	22.18	9.3E-06
42		GO:0006418	tRNA aminoacylation for protein translation	44	25	11.48	1.5E-05
43		GO:0009963	positive regulation of flavonoid biosynthesis	101	46	26.35	1.8E-05
44		GO:0010075	regulation of meristem growth	154	64	40.18	2.0E-05
45		GO:0010583	response to cyclopentenone	128	55	33.4	2.4E-05
46		GO:0006406	mRNA export from nucleus	61	31	15.92	3.1E-05
47		GO:0010167	response to nitrate	112	49	29.22	3.7E-05
48		GO:0007000	nucleolus organization	22	15	5.74	4.2E-05
49		GO:0006399	tRNA metabolic process	106	56	27.66	4.3E-05
50		GO:0009738	abscisic acid-activated signaling pathway	229	87	59.75	4.6E-05
51		GO:0009863	salicylic acid mediated signaling pathway	334	161	87.15	5.1E-05
52		GO:0042545	cell wall modification	160	72	41.75	6.2E-05
53		GO:0006164	purine nucleotide biosynthetic process	260	95	67.84	0.00012
54		GO:0010286	heat acclimation	79	36	20.61	0.00014
55		GO:0009753	response to jasmonic acid	438	184	114.28	0.00018
56		GO:0009718	anthocyanin-containing compound biosynthetic process	52	26	13.57	0.00019
57		GO:0006569	tryptophan catabolic process	70	32	18.26	0.00030
58		GO:0000028	ribosomal small subunit assembly	6	6	1.57	0.00031
59		GO:0009414	response to water deprivation	386	131	100.72	0.00032
60		GO:0009814	defense response to other organism	515	258	134.37	0.00033
61		GO:0048451	petal formation	59	28	15.39	0.00033
62		GO:0048453	sepal formation	59	28	15.39	0.00033
63		GO:0045036	protein targeting to chloroplast	65	30	16.96	0.00038
64		GO:0010260	animal organ senescence	28	16	7.31	0.00048
65		GO:0009089	lysine biosynthetic process via diaminopimelate	8	7	2.09	0.00051
66		GO:0006865	amino acid transport	221	80	57.66	0.00054
67		GO:0006414	translational elongation	31	17	8.09	0.00062
68		GO:0006364	rRNA processing	242	94	63.14	0.00082
69		GO:0052542	defense response by callose deposition	59	27	15.39	0.00085
70		GO:0009617	response to bacterium	545	218	142.2	0.00091
71		GO:0000478	endonucleolytic cleavage involved in rRNA processing	17	11	4.44	0.00092
72		GO:0009612	response to mechanical stimulus	60	27	15.66	0.00117
73		GO:0052033	pathogen-associated molecular pattern dependent induction by symbiont of host innate immune response	5	5	1.3	0.00121

74		GO:0006914	autophagy	69	30	18	0.00127
75		GO:0009684	indoleacetic acid biosynthetic process	99	40	25.83	0.00128
76		GO:0015706	nitrate transport	119	46	31.05	0.00173
77		GO:0006268	DNA unwinding involved in DNA replication	9	7	2.35	0.00176
78		GO:0009651	response to salt stress	737	227	192.3	0.00186
79		GO:0046686	response to cadmium ion	455	146	118.72	0.00218
80		GO:0009957	epidermal cell fate specification	14	9	3.65	0.00296
81		GO:0035556	intracellular signal transduction	454	182	118.46	0.00300
82		GO:0007169	transmembrane receptor protein tyrosine kinase signaling pathway	103	40	26.87	0.00303
83		GO:0006972	hyperosmotic response	237	81	61.84	0.00329
84		GO:0009658	chloroplast organization	234	80	61.06	0.00344
85		GO:0009620	response to fungus	464	204	121.07	0.00373
86		GO:0009646	response to absence of light	33	16	8.61	0.00470
87		GO:0006952	defense response	1420	583	370.51	0.00482
88		GO:0009909	regulation of flower development	319	104	83.23	0.00519
89		GO:0000462	maturation of SSU-rRNA from tricistronic...	8	6	2.09	0.00532
90		GO:0006949	syncytium formation	20	11	5.22	0.00560
91		GO:0009073	aromatic amino acid family biosynthetic process	103	39	26.87	0.00562
92		GO:0042274	ribosomal small subunit biogenesis	18	15	4.7	0.00562
93		GO:0009831	plant-type cell wall modification involved in multidimensional cell growth	15	9	3.91	0.00569
94		GO:0006413	translational initiation	48	21	12.52	0.00596
95		GO:0046785	microtubule polymerization	69	28	18	0.00598
96		GO:0007568	aging	132	55	34.44	0.00650
97		GO:0009751	response to salicylic acid	434	198	113.24	0.00744
98		GO:0009682	induced systemic resistance	18	10	4.7	0.00748
99		GO:0009693	ethylene biosynthetic process	108	40	28.18	0.00782
100		GO:0019319	hexose biosynthetic process	157	55	40.96	0.00793
	LLN						
1		GO:0019344	cysteine biosynthetic process	205	75	35.69	3.3E-11
2		GO:0010264	myo-inositol hexakisphosphate biosynthetic process	61	33	10.62	8.6E-11
3		GO:0000023	maltose metabolic process	150	59	26.12	1.5E-10
4		GO:0019252	starch biosynthetic process	187	68	32.56	3.7E-10
5		GO:0043481	anthocyanin accumulation in tissues in response to UV light	98	43	17.06	8.6E-10
6		GO:0009825	multidimensional cell growth	97	44	16.89	6.9E-08
7		GO:0010304	PSII associated light-harvesting complex II catabolic process	27	17	4.7	1.7E-07
8		GO:0035304	regulation of protein dephosphorylation	139	49	24.2	3.1E-07
9		GO:0015996	chlorophyll catabolic process	56	26	9.75	4.8E-07
10		GO:0009862	systemic acquired resistance, salicylic acid mediated signaling pathway	237	72	41.26	5.7E-07

11		GO:0010310	regulation of hydrogen peroxide metabolic process	176	57	30.64	8.9E-07
12		GO:0031348	negative regulation of defense response	271	79	47.18	1.0E-06
13		GO:0000165	MAPK cascade	215	66	37.43	1.1E-06
14		GO:0007020	microtubule nucleation	66	28	11.49	1.7E-06
15		GO:0009965	leaf morphogenesis	196	60	34.13	3.7E-06
16		GO:0010218	response to far red light	96	35	16.71	6.2E-06
17		GO:0008361	regulation of cell size	53	23	9.23	8.9E-06
18		GO:0042744	hydrogen peroxide catabolic process	71	28	12.36	9.3E-06
19		GO:0010207	photosystem II assembly	169	52	29.42	1.4E-05
20		GO:0009739	response to gibberellin	122	40	21.24	2.6E-05
21		GO:0043085	positive regulation of catalytic activity	114	38	19.85	2.7E-05
22		GO:0016556	mRNA modification	114	38	19.85	2.7E-05
23		GO:0009926	auxin polar transport	86	34	14.97	3.5E-05
24		GO:0009867	jasmonic acid mediated signaling pathway	269	73	46.83	4.0E-05
25		GO:0009617	response to bacterium	545	130	94.89	6.2E-05
26		GO:0048767	root hair elongation	161	48	28.03	7.0E-05
27		GO:0030003	cellular cation homeostasis	191	54	33.25	0.00012
28		GO:0010189	vitamin E biosynthetic process	7	6	1.22	0.00017
29		GO:0006098	pentose-phosphate shunt	181	51	31.51	0.00021
30		GO:0009932	cell tip growth	182	51	31.69	0.00024
31		GO:0009697	salicylic acid biosynthetic process	205	56	35.69	0.00025
32		GO:0019761	glucosinolate biosynthetic process	169	48	29.42	0.00025
33		GO:0009831	plant-type cell wall modification involved in multidimensional cell growth	15	9	2.61	0.00026
34		GO:0000038	very long-chain fatty acid metabolic process	45	18	7.83	0.00029
35		GO:0009741	response to brassinosteroid	97	31	16.89	0.00034
36		GO:0080167	response to karrikin	117	35	20.37	0.00059
37		GO:0009828	plant-type cell wall loosening	20	10	3.48	0.00085
38		GO:0009595	detection of biotic stimulus	102	31	17.76	0.00089
39		GO:0009746	response to hexose	161	44	28.03	0.00108
40		GO:0010114	response to red light	99	30	17.24	0.00112
41		GO:0009637	response to blue light	121	35	21.07	0.00116
42		GO:0042335	cuticle development	42	16	7.31	0.00117
43		GO:0019684	photosynthesis, light reaction	306	90	53.28	0.00144
44		GO:0010363	regulation of plant-type hypersensitive response	365	86	63.55	0.00152
45		GO:0015979	photosynthesis	400	118	69.64	0.00171
46		GO:0016132	brassinosteroid biosynthetic process	93	28	16.19	0.00180
47		GO:0009409	response to cold	556	123	96.8	0.00216
48		GO:0071482	cellular response to light stimulus	73	23	12.71	0.00233
49		GO:0009646	response to absence of light	33	13	5.75	0.00234
50		GO:0010155	regulation of proton transport	74	23	12.88	0.00283

51		GO:0070838	divalent metal ion transport	198	56	34.47	0.00288
52		GO:0006766	vitamin metabolic process	94	35	16.37	0.00293
53		GO:0009072	aromatic amino acid family metabolic process	232	57	40.39	0.00342
54		GO:0031408	oxylipin biosynthetic process	20	9	3.48	0.00384
55		GO:0009108	coenzyme biosynthetic process	327	76	56.93	0.00399
56		GO:0006812	cation transport	565	147	98.37	0.00402
57		GO:0007169	transmembrane receptor protein tyrosine signaling pathway	103	29	17.93	0.00450
58		GO:0009641	shade avoidance	17	8	2.96	0.00457
59		GO:0016051	carbohydrate biosynthetic process	745	192	129.71	0.00470
60		GO:0006546	glycine catabolic process	52	17	9.05	0.00545
61		GO:0009269	response to desiccation	36	13	6.27	0.00566
62		GO:0052325	cell wall pectin biosynthetic process	11	6	1.92	0.00575
63		GO:0010817	regulation of hormone levels	822	213	143.12	0.00586
64		GO:0016126	sterol biosynthetic process	156	40	27.16	0.00602
65		GO:0006612	protein targeting to membrane	368	83	64.07	0.00628
66		GO:0016117	carotenoid biosynthetic process	101	28	17.58	0.00653
67		GO:0006816	calcium ion transport	115	31	20.02	0.00681
68		GO:0005976	polysaccharide metabolic process	588	163	102.38	0.00694
69		GO:0010540	basipetal auxin transport	18	8	3.13	0.00698
70		GO:0006833	water transport	134	35	23.33	0.00720
71		GO:0006732	coenzyme metabolic process	565	141	98.37	0.00747
72		GO:0007623	circadian rhythm	163	41	28.38	0.00775